AD NUMBER

ADB020636

LIMITATION CHANGES

TO:

Approved for public release; distribution is unlimited.

FROM:

Distribution authorized to U.S. Gov't. agencies only; Test and Evaluation; AUG 1976. Other requests shall be referred to Air Force Armament Lab., Eglin AFB, FL 32542.

AUTHORITY

AFATL ltr 1 Oct 1980

AFATL-TR-76-94
VOLUME I

MIDCOURSE GUIDANCE STUDY FOR TACTICAL GUIDED WEAPONS

VOLUME I: SURVEY AND ANALYSIS

BOOZ, ALLEN AND HAMILTON INC.
4733 BETHESDA AVENUE
BETHESDA, MARYLAND 20014

AUGUST 1976

FINAL REPORT: SEPTEMBER 1975 - MAY 1976

AIR FORCE ARMAMENT LABORATORY
AIR FORCE SYSTEMS COMMAND • UNITED STATES AIR FORCE
EGLIN AIR FORCE BASE, FLORIDA

UNCLASSIFIED

SECURITY CLASSIFICATION OF THIS PAGE (When Data Entered)

REPORT DOCUMENTATION PAGE	READ INSTRUCTIONS BEFORE COMPLETING FORM
1. REPORT NUMBER: AFATL-TR-76-94-Volume I-1	2. GOVT ACCESSION NO.	3. RECIPIENT'S CATALOG NUMBER
4. TITLE (and Subtitle): MIDCOURSE GUIDANCE STUDY FOR TACTICAL GUIDED WEAPONS. Volume I. Survey and Analysis.	5. TYPE OF REPORT & PERIOD COVERED: Final Report, 15 September 1975-8 May 1976.
	6. PERFORMING ORG. REPORT NUMBER
7. AUTHOR(s): T.S. Stanton	8. CONTRACT OR GRANT NUMBER(s): F08635-76-C-0034
9. PERFORMING ORGANIZATION NAME AND ADDRESS: Booz, Allen & Hamilton, Inc. 4733 Bethesda Avenue Bethesda, Maryland 20014	10. PROGRAM ELEMENT, PROJECT, TASK AREA & WORK UNIT NUMBERS: Project No 2568 Task No: 01 Work Unit No: 002
11. CONTROLLING OFFICE NAME AND ADDRESS: Air Force Armament Laboratory Armament Development and Test Center Eglin Air Force Base, Florida 32542	12. REPORT DATE: August 1976
	13. NUMBER OF PAGES: 237
14. MONITORING AGENCY NAME & ADDRESS (if different from Controlling Office): 246p.	15. SECURITY CLASS. (of this report): UNCLASSIFIED
	15a. DECLASSIFICATION/DOWNGRADING SCHEDULE

16. DISTRIBUTION STATEMENT (of this Report)

Distribution limited to U.S. Government agencies only; this report documents test and evaluation; distribution limitation applied August 1976. Other requests for this document must be referred to the Air Force Armament Laboratory (DLMA), Eglin Air Force Base, Florida 32542.

17. DISTRIBUTION STATEMENT (of the abstract entered in Block 20, if different from Report)

18. SUPPLEMENTARY NOTES

Available in DDC.

19. KEY WORDS (Continue on reverse side if necessary and identify by block number)

Midcourse Guidance Methodology
Air Launch Weapon Alignment
Air Launch Weapon Aiding Mechanization

20. ABSTRACT (Continue on reverse side if necessary and identify by block number)

This development addresses midcourse guidance problems of air-to-surface weapons. It emphasizes methodology for guidance law selection, prelaunch alignment of the missile, and postlaunch update. The development involved both survey and analysis. The survey portion of the study resulted in the evaluation of inertial sensors, RF sensors, and discrete update procedures. The analysis portion of the study resulted in the definition of a guidance law, a comparison of several alignment techniques and update techniques.

DD FORM 1 JAN 73 1473 EDITION OF 1 NOV 65 IS OBSOLETE

UNCLASSIFIED

SECURITY CLASSIFICATION OF THIS PAGE (When Data Entered)

PREFACE

This report documents the work accomplished by Booz, Allen & Hamilton, Inc., 4733 Bethesda Avenue, Bethesda, Maryland 20014, under Contract Number F08635-76-C-0034 with the Air Force Armament Laboratory, Armament Development and Test Center, Eglin Air Force Base, Florida. Captain John Wiles (DLMA) managed the program for the Armament Laboratory. This effort was begun on 15 September 1975 and was completed on 8 May 1976.

This report consists of two volumes. Volume I, Survey and Analysis, is unclassified. Volume II, Survey and Analysis (Appendices), is classified CONFIDENTIAL. This is Volume I.

This technical report has been reviewed and is approved for publication.

FOR THE COMMANDER:

CLIFFORD H. ALLEN, JR., Colonel, USAF
Chief, Guided Weapons Division

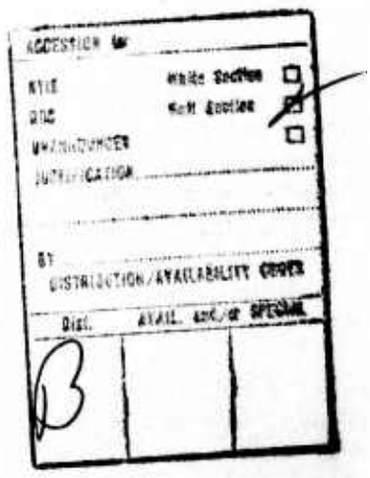

SUMMARY

The objective of the effort was to provide engineering services for the development of methods that can be used to study and analyze midcourse inertial navigation and guidance schemes for conventional air-to-surface guided weapons.

The study involved four major task areas: (1) Guidance Law Survey; (2) Guidance Law Methodology; (3) Inertial Measurement Unit Initialization and Alignment; and (4) Aided Inertial Navigation.

The baseline guidance system for the study was constrained by the following specifications:

- Cost: $10,000
- Gyroscope Drift Rate: 1/2 to 1 degree/hour
- Accelerometer Bias: 200 μg (2×10^{-4}g)
- Flight Time: 10 minutes
- System Accuracy: 3,000 feet.

The required 3,000-foot accuracy could be achieved by any practical combination of inertial and auxiliary sensors within the cost constraint.

The Air Force Baseline Guided Weapon (AFBGW) series was considered the basic application for the methods and concepts that were investigated. To apply the methods and concepts that were developed in the survey to a realistic system, a generic attack weapon designated AFBGW was defined. The AFBGW system contains elements of several existing programs, including the GBU-15 and the Radiometric Area Correlation Guidance (RACG). A generalized weapon concept was assumed because the main thrust of the study was to develop principles rather than to become involved in an ongoing program.

The AFBGW is based on a modular MK-84 glide bomb concept with cruciform (short range) and planar wing (long range) options. Configuration, mass, inertia, aerodynamic, and stability coefficients are similar to the GBU-15 cruciform wing (CW) and planar wing (PW) missiles.

The results of the survey showed that there are ample systems to address the inertial requirement. However, system

costs of off-the-shelf equipment are about 75 percent above the baseline. The prognosis is considered good for an aided or pure inertial system that can meet the baseline specifications. It would require a full production base (2,000 to 6,000) and a tailoring of requirements to the AFBGW mission.

The guidance law portion of the study indicated that many diverse approaches can be used to steer the missile to its target. An acceleration autopilot with the range-adaptive guidance law was investigated, and results indicated that the AFBGW short-range baseline autopilot could be compensated for effective transit flight, and that improved transit flexibility could be achieved by varying autopilot gain constants. (The term "transit" in this context refers to the midcourse phase of flight during which the AFBGW is guided from launch point to terminal acquisition area. Transit guidance requirements are relatively moderate when compared to air intercept guidance requirements.)

The alignment phase involved the comparison of gyrocompassing (using auxiliary aircraft-mounted sensors), multiple discrete alignment, and parameter transfer. Bases for comparison included alignment accuracy, speed, flexibility, and support requirements. The results indicated the following order of preference: (1) parameter transfer; (2) multiple discrete fixes; and (3) gyrocompassing. Gyrocompassing was considered a poor choice because of awkwardness of mechanization and because of the extended time required to align the system.

The aiding portion of the study involved the review of discrete methods of update during midcourse flight. It also included the investigation of sensors that could be used for continuous update (Doppler Radar, Global Positioning Satellite, Passive RF, Distance Measuring Equipment, and Air Data Computation). The study included a review of methods of combining diverse update information with inertially-derived navigation data. Both conventional and optical approaches were considered. The study indicated a need to develop data on the error processes of inertial and continuous auxiliary update sensors to allow evaluation of their potential from an engineering rather than a mathematical point of view.

In general, the study indicated that the aided inertial approach was a viable alternative to the Distance Measuring Equipment midcourse guidance, which is presently in use. Pure inertial, discretely aided inertial, and continuously aided inertial concepts are all competitive. However, selected continuously aided approaches seem to have unique potential.

(The Reverse of This Page is Blank.)

TABLE OF CONTENTS

TABLE OF CONTENTS (CONTINUED)

TABLE OF CONTENTS (CONTINUED)

TABLE OF CONTENTS (CONTINUED)

TABLE OF CONTENTS (CONCLUDED)

LIST OF FIGURES

LIST OF FIGURES (CONTINUED)

LIST OF FIGURES (CONTINUED)

LIST OF FIGURES (CONCLUDED)

LIST OF TABLES

LIST OF TABLES (CONTINUED)

LIST OF TABLES (CONCLUDED)

SECTION I

INTRODUCTION

The purpose of this study was to provide engineering support for the analysis of inertially guided weapons. The study involved a survey and an analysis.

The survey was intended to produce information on equipment, software, and methods of analysis necessary to analyze the Air Force Baseline Guided Weapon (AFBGW).

The analytical work included guidance law methodology characteristics, inertial navigation error analysis, comparative analysis of alignment techniques, and aiding concept comparisons.

It was considered essential at the outset of the study that the work be applicable to tactical Air Force weapons that will be in inventory prior to 1985. Emphasis was placed on the Air Force Baseline Guided Weapon/short range (AFBGW/SR) and the Air Force Baseline Guided Weapon/long range (AFBGW/LR).

Specific midcourse performance and cost goals were postulated at the outset of the study. The study concerned itself with aided strapdown inertial platforms and components that would navigate within 3,000 feet after 10 minutes of flight. Emphasis was placed on gyroscopes with a drift rate of 0.5 to 1.0 degree/hour and on accelerometers with a 200 μ g (2×10^{-4} g) bias. A $10,000 cost goal was placed on the inertial measurement unit (IMU) (excluding navigation computer). The study objectives included the definition of systems that could meet the above cost and performance objectives. Effort was made to provide sufficient detail to support cost/performance tradeoffs in subsequent study efforts.

The baseline systems used for this study assume the generic AFBGW weapon with the Radiometric Area Correlation Guidance (RACG) system. The RACG sensor is designated as the baseline midcourse guidance sensor for the purpose of this study. It may be used at any point in the midcourse phase of flight for discrete updates.

The AFBGW aero and guidance configuration is derived from current Air Force glide weapon concepts. The AFBGW weapons provide the baseline configuration with time of flight constraints. The accuracy objective of the system is based upon the acquisition requirement of the RACG fixtaking process.

Although the RACG system is essentially a midcourse guidance system, it can be used as a terminal sensor.

One objective of the study was to define alternative missile navigation arrangements within the $10,000 cost goal. Three generic alternatives were emphasized in this context: (1) an all-inertial capability that would produce a 3,000-foot accuracy; (2) a RACG/inertial capability that would produce a 3,000-foot accuracy by discrete updating; and (3) a velocity/inertial capability that would produce a 3,000-foot accuracy by conventional or synergistic mechanization.

The flow of the study is shown in Figure 1. The survey portion of the study was conducted through literature review, correspondence, telephone discussion, and on-site conferences. This part of the study accounted for the first three months of effort and resulted in the accumulation of the major portion of the information required in the subsequent analytical effort.

In the subsequent analytical phases, some new information requirements were identified; these resulted in an iterative effect in the flow of the work.

Emphasis in the analytical effort was on compiling performance and cost data for strapdown inertial platform and sensors.

The guidance law methodology phase involved error analysis, formulation of guidance laws, and trajectory analysis. In the error analysis effort, error expressions were tabulated for major AFBGW sources. Position, attitude, and velocity error expressions were developed for the major forcing functions. The guidance law formulations were based on root locus analysis, and they applied typical autopilot and airframe data received from Rockwell. The trajectory analysis dealt with course correction methods that could reduce energy expenditure to a reasonable level.

The alignment study compared three approaches: gyrocompassing, discrete fixtaking, and velocity matching. It involved a quantitative comparison of representative techniques developed and applied over the past 10 years. About 20 government and corporate sources are represented in this study.

The aiding phase of the study included the identification of equipment and techniques for deriving navigation data independently from the inertial navigation system. It also

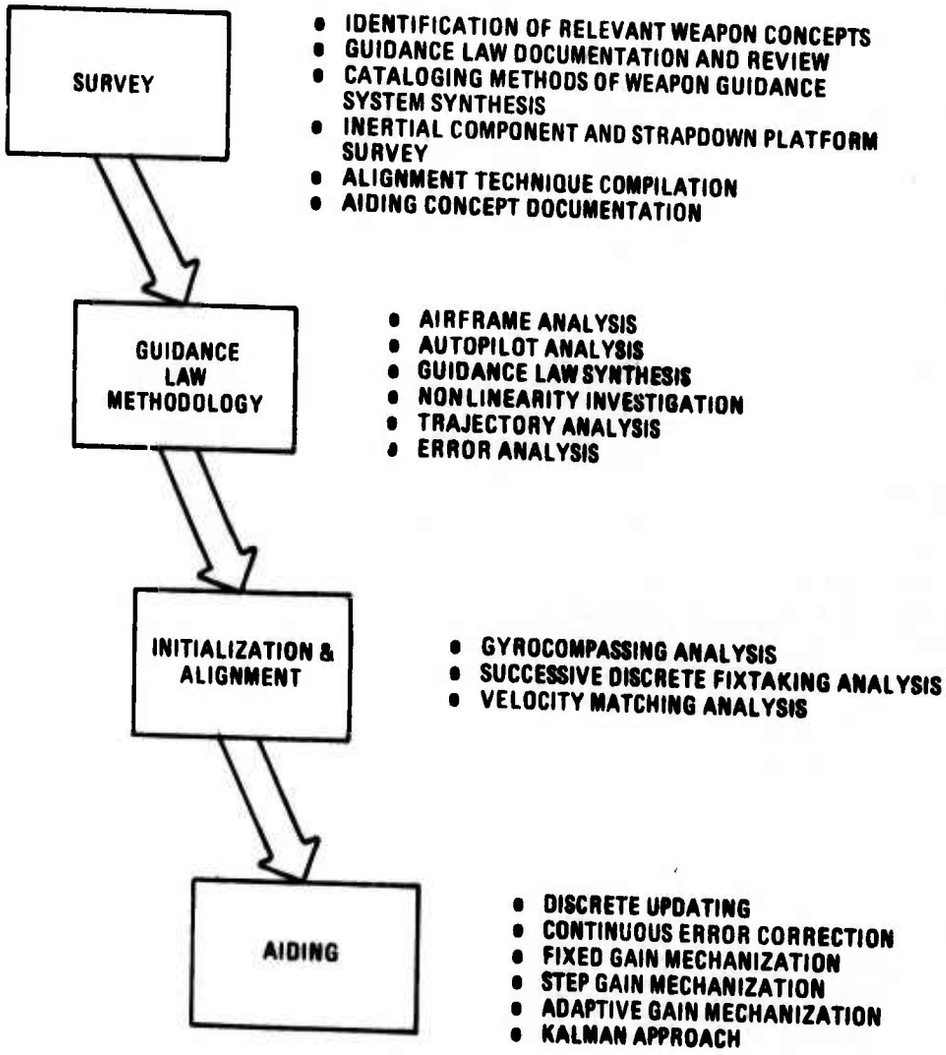

Figure 1. Sequence of Tasks in the Air Force Baseline Guided Weapon Midcourse Guidance Study

included the comparative analysis of techniques for combining inertially derived information and independently derived navigation data. The general relationship between the Statement of Work and the activities reported in this document are given in Table 1.

The data sources in this report were of four types: (1) the project monitor; (2) other Air Force and Navy agencies who are actively engaged in GBU-15, RACG, and parallel or related weapons and concepts; (3) contractors engaged in the work associated with GBU-15 and RACG; and (4) contractors who are developing concepts and systems whose application to GBU-15 and RACG can materially benefit the effort. Many of these sources are summarized in Section II, Survey and Results.

Many of the results, conclusions, and recommendations of this study have broad application beyond the limits of the generalized example weapon concept. The guidance law methodology is particularly applicable to air-to-air missiles. The navigation error formulations can serve as a quick reference for all cruise applications. The alignment comparisons are universally applicable, and the aiding comparisons could serve as a starting point for an engineering approach to navigation by optimal-state estimation.

TABLE 1. RELATIONSHIP BETWEEN STATEMENT OF WORK AND STUDY ACTIVITIES

ACTIVITY	RATIONALE FOR INITIATION	REPORT REFERENCE
Identification of Relevant Weapon Concepts	Statement of Work 4.1a	Section V
Guidance Law Documentation and Review	Statement of Work 4.1	Section II
Inertial Component and Strapdown Platform Survey	Statement of Work 4.2, 4.2c, and 3.0 (General Cost/ Performance Optimization of Midcourse Guidance)	Section II Section III
Alignment Technique Compilation	Statement of Work 4.3	Section II Section VI
Aiding Concept Documentation	Statement of Work 4.4	Section II Section VIII
Error Analyses	Statement of Work 4.2c	Section V
Airframe Analysis and Autopilot Analysis	Statement of Work 4.2b	Section IV
Guidance Law Synthesis	Statement of Work 4.2b	Section IV
Nonlinearity Investigation (Autopilot)	Statement of Work 4.2b	Section IV
Trajectory Analysis	Statement of Work 4.2d	Section IV
Gyrocompass Analysis	Statement of Work 4.3	Section VI
Successive Discrete Fixtaking Analysis (Alignment)	Statement of Work 4.3	Section VI

TABLE 1. RELATIONSHIP BETWEEN STATEMENT OF WORK AND STUDY ACTIVITIES (CONCLUDED)

ACTIVITY	RATIONALE FOR INITIATION	REPORT REFERENCE
Velocity Matching Analysis (Alignment)	Statement of Work 4.3	Section VI
Discrete Updating	Statement of Work 4.4	Section VII Section VIII
Continuous Error Correction	Statement of Work 3.0 (General Cost/Performance Optimization of Midcourse Guidance)	Section VII Section VIII
Fixed Gain Mechanization	Statement of Work 4.4	Section VIII
Step Gain Mechanization	Statement of Work 4.4	Section VIII
Adaptive Gain Mechanization	Statement of Work 4.4	Section VIII
Kalman Approach	Statement of Work 4.4	Section VIII

SECTION II

SURVEY AND RESULTS

The purpose of conducting this survey was to compile a body of current information on guidance laws, inertial sensors, updating techniques, alignment, and aiding. The initial concept of the survey was limited to guidance law considerations. However, during the course of the investigation, the spectrum of guidance concepts uncovered required that the scope be expanded to:

- Weapon guidance concepts
- Cruise missile guidance law review
- Weapon guidance system synthesis
- Inertial component and platform technology
- Alignment concepts
- Aiding concepts.

Similarly, the investigation initially focused on glide weapons and on Radiometric Area Correlation Guidance (RACG) since the Air Force has concentrated resources in this area, but it was expanded to include data on other weapon and guidance systems.

A literature search (Reference 1) was conducted prior to beginning the survey to establish the state-of-the-art; relevant documents are contained in the References portion of this report. This review formed the basis for selecting candidate corporate and laboratory sources for subsequent telephone and personal interviews. Corporations contacted, their qualifications, and the types of data obtained are listed in Table 2.

This section describes the results obtained in the survey for each of the areas defined in the first paragraph, concluding with a summary of results of how they are used in the subsequent analysis.

(The Reverse of This Page is Blank.)

TABLE 2. TYPICAL SUR

Company	Project Relationship	Supporting Activities
Aerospace	GPS-IMU integration studies impact on FCCM requirements for missileborne receiver configuration	Supporting design, tradeoffs, and a cation analysis for GPS/inertial systems
Boeing	SRAM guidance system integration; implementation of virtual target steering guidance for flexibility in midcourse steering and good steering command response; Kalman filter development and evaluation (Subcontractor: Kearfott)	SRAM/B-52 development, USAF C Missile development; navigation s tem development and integration; port of in-flight alignment and ca tion investigations; development a optimization of guidance and cont software
Celesco	GBU-15 development	None indicated
Delco	Developed a series of Kalman mechanizations for GBU-15 type weapons; digital simulation to assess performance; gyro calibration of missileborne equipment to aircraft platform	Leading commercial inertial navig system developer; background in sor calibration and compensation Carousel; specialization in mech tion and estimation software
E-Systems, Inc.	Conceived a follow-on terrain elevation correlation system for use with GBU-15; strives for autopilot quality capability inertial sensors and low cost; developed and captive-tested a Cruise Missile guidance system	Originator of the terrain elevation relation concept; adapted the con to many aerospace applications; ly qualified to analyze the streng and weaknesses of the terrain el tion correlation and follow-on ap proaches
Hamilton Standard	Alternative midcourse guidance system equipment; computer software module for RACG IMU	Inertial systems for a broad spect of aircraft, missiles, and space vehicles
Honeywell	Developer of ATIGS based on the ring laser gyro with a 0.5 to 1.0 deg/hr performance potential GEANS	Active in the development of inert components and platforms for a defense missiles and spacecraft pioneer in the field of strapdown mechanizations and laser gyros; veloper of airborne navigation c puters and software

ATIGS Advanced Tactical Inertial Guidance System
IMU Inertial measuring unit
GPS Global Position Satellite
GEANS Gimballed Electrostatic Gyro Aircraft Navigation

TYPICAL SURVEY RESULTS

ing Activities	Data Supplied	Contact
a, tradeoffs, and appli- for GPS/inertial	Report and supplementary data on GPS/inertial systems (i.e., antijamming margin of an IMU/computer-aided global navigation system); emphasis on aircraft user, but has missile application	P. P. Yeh, Satellite Navigation System Directorate
lopment, USAF Cruise ment; navigation sys- t and integration; sup- alignment and calibra- ons; development and guidance and control	SRAM inertial navigation and guidance data; simulation analysis results for the Kalman filter used with the SRAM missile; guidance and control system data for SRAM; virtual target steering description	C. A. Lindblad, SRAM Systems Management J. Jobe, SRAM Configuration M. Lobbia, SRAM Guidance and Control
	GBU-15/PW data, including configuration, weight and balance, component, physical parameters, stability derivatives, and autopilot	W. Goehley, Project Management R. Benton, Aerodynamics Specialist
cial inertial navigation er; background in sen- and compensation; lalization in mechaniza- tion software	Results of the mechanization study; application of Delco compensation techniques to the GBU-15; Delco synthesis methodology for alignment and aiding	G. Quinn, System Development Manager T. Wolf, Inertial Mechanizations for Tactical Systems
terrain elevation cor- t; adapted the concept ace applications; unique- nalyze the strengths of the terrain eleva- and follow-on ap-	Two documents were supplied to Booz, Allen by E-Systems: one described the application of terrain elevation correlation to the GBU-15 system (cost, performance, packaging data, and software concepts were included); the other described a new concept for use with GBU-15	K. Sturdavant J. Warren
for a broad spectrum siles, and space	Description of the HS-3030 IMU and the Mini-RIGs 30 strapdown rate-integrating gyro; system characteristics, specifications, and gyro technology	E. J. Herzlich, G&C Marketing Manager R. Baum, System Integration R. Angelillo, Guidance Technology
elopment of inertial platforms for aircraft s and spacecraft; ield of strapdown and laser gyros; de- orne navigation com- ware	Material on the ring laser and ATIGS; conventional gyro, platform, accelerometer, and computed data relating to performance, cost, support and availability; alignment technique data; system mechanization data	R. Schiedenhelm B. Browne C.D. Talbot

(The reverse of this page is blank)

TABLE 2. TYPICAL SURVEY RE

Company	Project Relationship	Supporting Activities
Hughes	Digital autopilot for GBU-15/PW Maverick missile system	Harm and Brazo; IR imaging seeke laser guidance
IBM Federal System	Management of the Harpoon IMU integration; strapdown mechanization with a performance level at the 1 deg/hr level; monolithic (read only) memory computer for navigation processing; first system in production status with capability between inertial and autopilot and corresponding cost saving	Application of digital processing to ertial mechanization; investigatio performance and requirements fo suboptimal systen s as compared full Kalman filter systems
Kearfott	Constructing small aircraft equipment for the Joint DME/TOA Glide Weapon (RNWDS have been used to identify this equipment); active in low-cost strapdown innovation (TIGS proposed to DLMM); major software contractor for inertial navigation systems; extensive capability in aiding mechanization, alignment, and calibration	One of the top developers and supp of aircraft inertial navigation sy producing first-, second-, and th generation equipment; specialist the area of system design and int tion; top quality gyro developer a supplier (Gyroflex)
Lear Siegler (Grand Rapids)	Harpoon IMU gyro supplier	Autopilot development
Litton	Gyro development leader; ongoing development of components that can contribute to **AFBGW** capability; history of successful mechanization synthesis; ongoing Cruise Missile guidance system development program	Leading aircraft platform and gyr veloper; synthesis of scores of m anizations for aircraft and missi applications; major contributor t state-of-the-art of inertial com- ponents

ARIS Airborne Range Instrumentation System
EOGB Electro-Optical Glide Bomb
SOM Standoff Missile
TIGS Tactical Inertial Guidance System

PICAL SURVEY RESULTS (CONTINUED)

orting Activities	Data Supplied	Contact
izo; IR imaging seeker; ce	Maverick reports; GBU-15/PW digital autopilot description	H. Maurer, Missile Systems Management C. Bauer, IR Imaging Systems
digital processing to inization; investigation of and requirements for ystems as compared to filter systems	Harpoon IMU configuration data; program data; cost data; performance specifications; and test results	J. Heiss
developers and suppliers ertial navigation systems, st-, second-, and third- uipment; specialists in ystem design and integra- lty gyro developer and oflex)	Description of the RNWDS concept and equipment; description of TIGS approach; comparison of aircraft equipment for selected missions; assessment of the impact of aircraft hardware and software on alignment initialization and calibration	B. Danik, Director of the System Engineering Analysis Section Edwin Solov, Leader of the Tactical Missile Weapon Delivery Group W. Payne, Business Development M. Greenberg, RNWDS effort
opment	Dynamic performance analysis; functional description of sensors and systems; instrument design; support application data	G. Proctor, System Integration R. Gray, Gyro Technology
ft platform and gyro de- hesis of scores of mech- aircraft and missile major contributor to the rt of inertial com-	History of gyro development including performance, producibility, reducibility, reliability, packaging, cost, and maintainability; methodology for system synthesis; review of requirements for GBU-15, SOM, Condor-X, EOGB; cost objectives for GBU-15; Litton interpretation—Cruise Missile status; ARIS	S. R. Richardson, Business Development J. S. Lipman, Manager, Systems Engineering J. R. Huddle, Manager, Systems Analysis S. Wyse, Gyro Technology R. Anthald, Cruise Missile J. M. Peterson, Manager, Missile Systems Requirements

(The reverse of this page is blank)

TABLE 2. TYPICAL SURVEY

Company	Project Relationship	Supporting Activities
Lockheed	RACGS prime contractor; responsible for integration of the radiometric-inertial weapon guidance concept	Operational deployment of stando weapons; radiometry—its stren limitatio ; critical radiometri tial tradeoffs and requirements tional environment in West Ger
Mitre	Coordination and support of ARPA in GPS studies for midcourse guidance of standoff weapons	Strapdown investigations for glid weapons
Naval Weapons Center	Supporting an Independent Microwave Radiometric Seeker Program (MICRAD); DME Homing System (Joint Navy/USAF Program); Advanced Tactical Inertial Guidance System (ATIGS)	Broad weapon guidance capabilit ical disciplines include radiom standoff glide weapon guidance; tial components; microwave an and components; simulation an analysis
Northrop	Experience with torpedo targets employing 1 deg/hr gyro systems; experience with floated spherical platforms (possible future alternative to strapdown approach)	Major developer of aircraft iner navigation equipment; design-t for conventional (gimballed) in navigation platforms
Rockwell	Prime contractor for GBU-15/CW; prime contractor for Condor (Columbus Division); development of strapdown gyros and strapdown guidance platforms; active in the MICRON and GEANS efforts (Autonetics Division)	Supplier of the AN/AJN16 for th navigation computers; termina ance systems defense; suppres missile design, laser imaging tems; Hellfire, Hobo, Road Ru and Condor guidance

MICRON Micro navigator (Rockwell designation and product)

PICAL SURVEY RESULTS (CONTINUED)

rting Activities	Data Supplied	Contact
loyment of standoff ometry—its strengths and itical radiometric/iner- and requirements; opera- ment in West Germany	East German scenario; data requirements for a radiometric missile guidance system; microwave radiometry performance and support data; RACGS inertial navigation system description; radiometric-inertial cost data	G. Clearly, Operational Role of Standoff Weapons L. Goe, Radiometric-Inertial Guidance Tradeoffs J. B. Rarich, Radiometric-Inertial Guidance Manager J. Matsunaga, RACGS Technology J. Dodd, Program Manager, Lockheed RACGS Program
tigations for glide	GPS workshop results and report; qualitative concepts on GPS support requirements; tradeoff considerations concerning satellite network density, ECCM, data denial periods, weapon equipment, etc.	John Burgess, Principal Investigator for ARPA GPS Effort
idance capability; crit- include radiometry, weapon guidance; iner- ; microwave antennas ; simulation and	MICRAD description; significant differences between MICRAD and RACGS; ATIGS test data; standoff DME guidance approach	Claud Launch, John Owens, and Bob Moore, Radiometric Tracking Program J. Hopper, MICRAD Mechanizations and Applications
of aircraft inertial pment; design-to-cost l (gimballed) inertial orms	History of use of strapdown inertial platforms of 1 deg/hr quality; data on the Flip System; indication of alternative low-cost approaches	T. Noble, Torpedo Targets Management (Ventura Division) J. D. McClanahan, C-5 Program Manager (Electronics Division)
N/AJN16 for the F111; puters; terminal guid- efense; suppression laser imaging sys- Hobo, Road Runner, dance	Description of GBU-15/CW, including configuration, weight and balance, physical, stability, and autopilot data; inertial sensor development data; mechanization synthesis approach; auxiliary (update/aiding) sensor data	P. Verona, GBU-15 Project Manager T. V. Murphy, Missile Systems Engineering Management M. Longo, Condor Program R. E. Mediatore, Advanced Engineering G. W. Sargent, Manager ESG Strapdown Systems

(The reverse of this page is blank)

TABLE 2. TYPICAL SURVEY RE

Company	Project Relationship	Supporting Activities
SAMSO	Development of generalized GPS receiver model to assess integration requirements; evaluation of the impact of electronics requirements on the user set	Justification of low-cost strapdown systems for GPS application
Sperry	Development of a ring laser gyro system; emphasis on low-cost, producibility, reliability and maintainability; development of a D-Gain update system for optimal estimation with minimum computation requirements	Extensive activity in laser gyro ar with NASA, MICOM, Navy, Mart and Holloman AFB; concentrated ground in aided inertial mechani tions step gain optimal systems/ Gain optimal systems; SINS; cali tion of inertial sensors
TASC	Evaluation of GPS tactical missile guidance	Broad spectrum of studies relatin missile inertial guidance, initial tion, updating, mechanization, a software

SINS Shipboard Inertial Navigation System

PICAL SURVEY RESULTS (CONCLUDED)

orting Activities	Data Supplied	Contact
f low-cost strapdown GPS application	Guidelines for establishing inertial requirements for GPS systems; role of 0.5 to 1.0 deg/hr strapdown system for GPS systems; synergistic operation through INS rather than IMU deployment	Capt. John Thau, GPS Battlefield Application Specialist
vity in laser gyro area MICOM, Navy, Martin, n AFB; concentrated back- led inertial mechaniza- in optimal systems/D- systems; SINS; calibra- al sensors	Laser gyro configuration, performance, mechanization, production, yield, reliability, and maintainability data; step gain effectiveness and requirements data; tradeoff results for selected levels of optimal filter sophistication; laser gyro contract history; Program Oscar	R. Benzinger, Corporate Executive Staff E. Levinson, Department Head, Advanced Inertial Systems
m of studies relating to tial guidance, initializa- g, mechanization, and	GPS tactical guidance evaluation; aided inertial Cruise Missile analysis; Kalman tutorial data; Kalman filter in transfer alignment	Don Van Der Sloop, Project Leader, GPS Missile Guidance

(The reverse of this page is blank)

WEAPON GUIDANCE CONCEPTS

To derive maximum benefit from the experience of recently developed equipment, several weapon guidance concepts were examined. The types of systems examined are shown in Table 3. The system that most directly relates to the Air Force Baseline Guided Weapon (AFBGW) is the Relative Navigation Weapon Delivery System (RNWDS) now under development at the Naval Weapons Center. Such systems as Condor, Shrike, and Maverick are less applicable because they lack a comparable midcourse flight phase. Harpoon and Standard Arm represent performance levels similar to the AFBGW requirements, but differences in target and deployment criteria preclude direct technology application. The Short-Range Attack Missile (SRAM) and Cruise Missile are included because each employs guidance methods that can be adapted to the AFBGW situation. The high cost of these systems should be emphasized as a limiting factor. The Cruise Missile will use an LN-30 series platform with a price ranging from $90,000 to $100,000. The guidance and navigation software are of more interest in these cases than are the inertial systems.

The SRAM virtual target steering approach offers a flexible method of programming the missile trajectory without affecting the response of the missile. The technique results from a desire to incorporate a very simple guidance law with the application of previously developed pitch and yaw loop elements. Application of the virtual target steering approach to the AFBGW may not be desirable since the simplicity and economy of a directly synthesized guidance law may be overriding goals (Reference 2).

The Harpoon system combines an effective terminal guidance active radar with a strapdown midcourse guidance platform. Harpoon has several features that apply to the AFBGW concept. However, the cost of the Harpoon system exceeds the AFBGW goals (Reference 3). Lower cost is required without serious degradation in performance from the Harpoon datum. Higher yield and a greater production base may represent a partial solution.

Condor and Maverick are oriented to terminal guidance sensors; consequently, there is very little application to the RACG situation. They were investigated in this study as a source of low-cost inertial sensor performance data (Reference 4).

The Cruise Missile is of interest primarily for the application of terrain elevation correlation to midcourse

(The Reverse of This Page is Blank.)

TABLE 3. GENERIC WEAPON SYSTE

Weapon System	Platform Approach	Gyros	Acce
SRAM	Four-gimbal platform, all-attitude operation; 5-in. diameter x 6-in. length; 1 nm/hr; 2 ft/sec; 1.33 mrad	Gyroflex; 2-axis gyro; 0.01 deg/hr; flexure suspension	10^{-4}g acc 0.1% sc one sing axis acc 1 cu in. unit
Harpoon	Strapdown integrated autopilot and platform; 12-in. cylinder; 6-in. height; 25 lb	Rate-integrating gyros; single axis; first-generation fluid suspension; 10 deg/hr absolute value; possible use of 1.0 deg/hr	Q-Flex 2
Maverick	Orthogonal triad of low-cost gyros and accelerometers 13x5.3x5.4 in.; 15 lb	Supergyro; subminiature rate gyro; 0.2 percent linearity; full scale to quarter scale	SUPERGE
Cruise Missile	Four-gimbal platform, all-attitude operation; third-generation system (SKN-2400 LN-30 series equipment)	Floated two-degree-of-freedom gas-bearing gyros; 0.5 deg/hr random drift; 0.5 deg/hr day-to-day repeatability	10^{-4}g acc Litton 20 rebalanc
RNWDS	Attitude and heading reference unit; Walleye guidance unit	1 deg/min; 2 lb; 2.5-in. diameter x 4.5 in.; 60-deg pitch/yaw; 170-deg roll freedom	Threshold 0.02 g (i voltage c readout

RNWDS Relative Navigation Weapon Delivery System (subsequently named JAWS also designates a DME system similar to ALSS being developed at Nav

SRAM Short-Range Attack Missile.

C WEAPON SYSTEM GUIDANCE CONCEPTS

	Accelerometers	Computer	Remarks
	10^{-4}g accelerometer bias; 0.1% scale factor error; one single-axis, one 2-axis accelerometer; 1 cu in. envelope for each unit	2048 words of memory (8 bits); 24 μsec add time; 5 lb; 138 cu in.; 45.5 w	Autopilot with rate gyros also provided; 5-min pre-launch cycle
); lera- ; alue; eg/hr	Q-Flex 2 x 10^{-3}g bias	3-5 μsec add; memory: 8000 words (monolithic) read only; 32 cu in.; 1.1 lb; 21 w	—
ıre nt to	SUPERGEE	Pulse width modulator	—
t- g ndom -to-	10^{-4}g accelerometer — Litton 200; digital pulse rebalance	Litton 728 — 32000 words of storage; computer provides all-guidance autopilot	15-min/transfer alignment; autopilot with rate gyros also provided; APN-194 computer; radar altimeter
ın. 60-deg roll	Threshold sensitivity of 0.02 g (indicated by 1% voltage change); analog readout	Analog servoamplifier mechanization	5-min gyro spinup

ently named JAWS [Joint Air Weapon System]);
developed at Naval Weapons Center.

(The reverse of this page is blank)

update. Schemes have been developed to use discrete fixes for velocity update without a high penalty in computer requirements. E-Systems, Inc., has developed extensive data on the application of this and successor concepts to the AFBGW. This is discussed further in Section VIII.

The RNWDS concept relates to this study because it is similar to the Advanced Location Strike System (ALSS), and it is austere with regard to guidance software and inertial sensors. The mechanization employs a basic Walleye guidance package with a Hobo receiver and transponder.

CRUISE MISSILE GUIDANCE LAW REVIEW

The term "guidance law" has been applied to many aspects of the missile guidance process. The guidelines of this study specified a broad approach to the guidance process, including sensor characteristics, error signal processing, and autopilot. Therefore, the guidance law review, which forms an important part of the survey, considers synthesis of kinematic loop compensation. The relation between this function and the total missile guidance process is shown in Figure 2, which illustrates the proportional guidance approach. The guidance law block could contain any acceptable error processing function.

The more important guidance laws reviewed during the study are shown in Table 4. These laws apply to cruise missile systems only. The survey excludes guidance laws developed primarily for space and ballistic missile applications, such as Q-guidance, delta guidance, explicit guidance, numerical integration guidance, linear tangent guidance, and parameter optimization guidance. Although many of these concepts could be adapted to the cruise missile situation, they are cumbersome and demand data processing resources on the missile.

Adaptive proportional systems are emphasized in the analysis, and their advantages are evaluated by linearized analysis. This type of processing is advantageous in situations where autopilot parameters have been frozen and the stability regime is confined. Also important to effective missile response is compensation for discontinuities in line-of-sight (σ) indication. The use of a concept such as virtual target steering can obviate the need for adaptive proportional guidance.

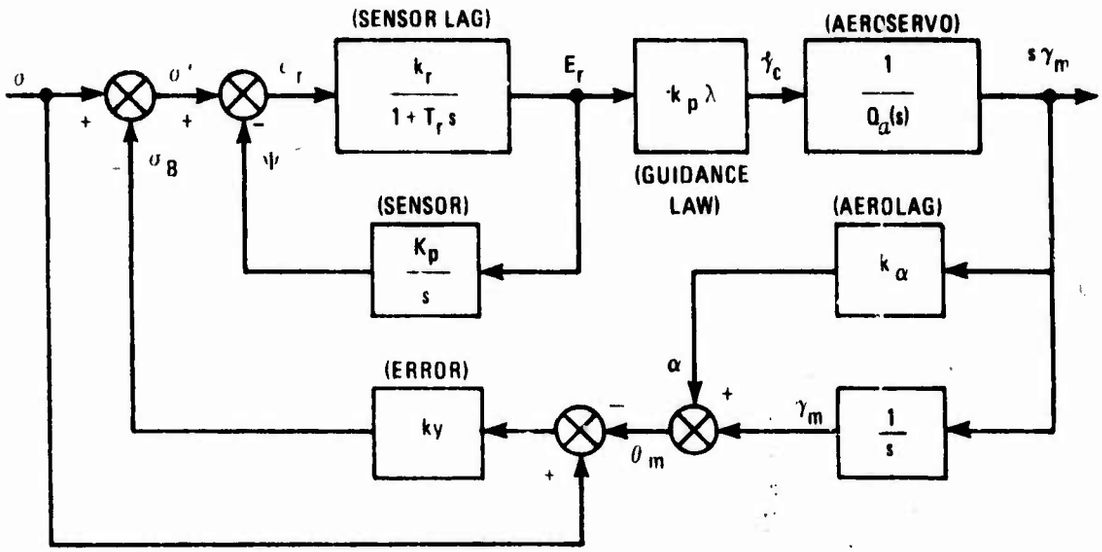

ϵ_r = MEASURED ERROR IN SEEKER ORIENTATION
E_r = MEASURED OFFSET IN MISSILE ORIENTATION
ψ = SENSOR SERVO ANGULAR RESPONSE
σ_B = BORESIGHT ERROR OF SENSOR
γ_m = FLIGHT PATH ANGLE OF MISSILE
θ_m = MISSILE BODY ROTATION ANGLE
k_r = SENSOR GAIN (SEEKER)
k_y = RADOME BORESIGHT ERROR SLOPE
α = ANGLE OF ATTACK
T_r = SEEKER TIME CONSTANT
k_p = GUIDANCE LAW GAIN CONSTANT
λ = CONVERSION FACTOR (E_r to $\dot{\gamma}_c$)
$Q_a(s)$ = AEROSERVO TRANSFER FUNCTION
k_α = ANGLE OF ATTACK LEAD PARAMETER
K_p = SENSOR FEEDBACK GAIN (SEEKER)
σ = LINE OF SIGHT ANGLE (TRUE)
σ' = LINE OF SIGHT ANGLE (DISTORTED)
$\dot{\gamma}_c$ = COMMANDED ANGULAR RATE

Note: DOT ABOVE A VARIABLE INDICATES $\frac{d}{dt}$;
s DESIGNATES DIFFERENTIATION, $\frac{1}{s}$ INDICATES INTEGRATION

Figure 2. Linearized Sensor Controlled Proportional Guidance

TABLE 4. GENERIC GUI

Guidance Law	Applications	Reference	Comment
Line-of-Sight	CONDOR - Midcourse Data Link Tracking	Mr. Donald Smith - Rockwell	Uses "Data Link" tracking - pilot provides steering com mands in midcourse phase
	Bullpup	Navy Missile Systems Reports - NAVPERS 10785A - P327)	Pilot tracks missile flare to target
Pure Pursuit	SHRIKE (Velocity pursuit)	Mr. Nall - Texas Instruments	Velocity pursuit - error sig referenced to velocity vect rather than body axis
	Standard Arm	Mr. R. Katzman General Dynamics	Transition
Deviated Pursuit (Lead Pursuit)	SCRAM	Boeing Documents	
	Standard Arm	Mr. R. Katzman General Dynamics	Initial Midcourse
Constant Bearing (Intercept)	Cruise Missile	Boeing Document No. 2-6003-7500-047 Page 37	
Proportional	Standard Arm	Mr. R. Katzman General Dynamics	Terminal Phase
	HARPOON	HARPOON Weapon System McDonnell Douglas Doc- ument No. E0796 Page 3-3	Common midcourse and terminal
	MAVERICK	MAVERICK Missile - Hughes Document No. MAV 8364-1 Page 13-3	Common midcourse and terminal
	CONDOR (Terminal)	Mr. Donald Smith Rockwell	After terminal acquisition proportional guidance is used
Adaptive Proportional	Conceptual		

ϕ = Deviation of missile from an arbitrarily fixed path
ξ = Arbitrary angular constant
ψ = Deviation of missile from previously selected heading
r = Range to target
σ = Target line-of-sight angle

GENERIC GUIDANCE LAWS

Comment	Mathematical Description	Principal Characteristics and Potential Application
ta Link" tracking - ovides steering com- n midcourse phase ks missile flare to	$\dot{\gamma}_c = k\phi$	Designed for remote control of a missile; requires a knowledge of both target and missile position; assumes a minimal capability in terms of missileborne equipment; may be considered obsolescent
ursuit - error signal ed to velocity vector han body axis n	$\dot{\gamma}_c = k\sigma$	A utility guidance approach; missile must function autonomously and perform simple conversion operations; adapted from air-to-air systems to employ available hardware
dcourse	$\dot{\gamma}_c = k(\sigma + \xi)$	Implies some a priori knowledge of relative rates of missile and target; particularly useful where high relative rates are anticipated of a predetermined magnitude
	$\dot{\gamma}_c = k(\psi)r$	Requires estimate of range rate, which may be available from missile inertial sensors in slow-moving target situations; reduces load factor in terminal phase of flight
Phase nidcourse and	$\dot{\gamma}_c = k\dot{\sigma}$	Operates on angular rate rather than angular displacement; provides a better dynamic response in a high angular rate situation; $\dot{\sigma}$ data must be derived and is usually "noisy"
nidcourse and		
inal acquisition onal guidance is		
	$\dot{\gamma}_c = k(r, \dot{r}) \cdot \sigma + l(r, \dot{r})\dot{\sigma}$	Approximates a full intercept solution; the functions k and l are empirically derived and are associated with a given approach situation

(The reverse of this page is blank)

WEAPON GUIDANCE SYSTEM SYNTHESIS

Discussions were held with Litton Industries, Kearfott, Northrop, IBM, Sperry, and Boeing Aircraft to review weapon cruise guidance system mechanization. As Table 5 illustrates, current systems have wide range application and employ a broad spectrum of sensors. Their sophistication and computer memory requirements also vary greatly.

Many compromises are used by major software developers to reduce computer requirements while retaining the advantages of the Kalman filter approach that is described in the introduction. The results of the interviews indicated that it is possible to approximate a Kalman filter through use of a step gain filter having low computational requirements. For example, whereas computer memory is considered to limit a full Kalman filter to a maximum of 10 state variables for cruise missile applications, a 23 state variable filter was mechanized with a 5-second update cycle requiring 10,000 operations/second and 800 words of memory. Although this arrangement reduces the guidance system computer memory requirement, it requires a large ground computer operation and is relatively sensitive to changes in system statistics.

Kalman filter operations also have been used for prelaunch alignment and calibration. Prelaunch calibration involves a critical operational tradeoff between operational flexibility and component cost, generally allowing less expensive instruments, since the effect of day-to-day gyroscope drift is eliminated, leaving only random gyroscope drift. Prelaunch calibration is conveniently implemented using a Kalman mechanization with the computational load allocated to the aircraft.

In the synthesis of weapon guidance systems, the following steps are employed with some variations due to system complexity and application:

1. Error model development
2. Determination of system potential
3. Performance/requirements tradeoffs
4. Evaluation by simulation.

Step 1 uses a linearized approximation of the sensor measurement and computational processes. Step 2 includes the use of covariance analysis to establish the ideal

TABLE 5. SELECTED CRUISE GUIDANCE MECHANIZATIONS

System	Developer	Applications	Sensors	Mechanization	Approximate Digital Computer Word Memory Impact
Classified	Litton	Demonstration aircraft	Stellar, doppler, and inertial	16-state Kalman	4300
LRPA	Litton	Antisubmarine warfare	LORAN, Omega, and doppler	16-state Kalman	4300
A-7	Kearfott	Attack aircraft	Doppler, inertial, and Omega	4-state Kalman	460
Tactical Aircraft	Litton	General	Doppler and LORAN	11-state Kalman	2300
Many Navy Systems	Litton	CAINS	Multiple types	5 Maximum likelihood	660
B-52	Boeing/ Kearfott	Strategic operations	Position fix, doppler radar, and altimeter	14-state Kalman	3400
Experimental	Litton	Antijam system for GPS	Global position satellite	18-state Kalman	5250
C-5	Northrop	Cargo aircraft	Doppler/radio position	23-state Kalman	7300

CAINS Carrier Aircraft Inertial Navigation System

performance of the system. The results of these two steps of the synthesis process indicate the effects of major system error sources on relevant system outputs as well as the behavior of optional feedback correction gains. This leads directly to Step 3 of the synthesis process which determines whether a full Kalman mechanization is needed or whether compromises are possible (i.e., step gain or suboptimal filter). Step 4 provides actual simulation of the navigation process using appropriate models of software, flight hardware, error process, and environment. This process accounts for the effects of all modeled nonlinearities and reflects a system unit error response for each independent error source. This is necessary for the construction of a cost-effective error budget. It also provides an opportunity for iterating both system requirements and error budget to reduce complexity and cost within the performance constraints.

INERTIAL COMPONENT AND PLATFORM TECHNOLOGY

Discussions of inertial components and platform technology disclosed interest on the part of inertial equipment manufacturers for a 0.5 to 1.0 degree/hour gyroscope in the $1,000 to $2,000 price region. Discussions with laboratories and contractors indicate that rate-integrating gyroscopes (RIGs) are now available, rate gyroscopes are being adapted, and tuned rotor two-degree-of-freedom gyroscopes may become available shortly for this application. Figure 3 shows representative cost and performance for state-of-the-art RIGs. All meet the AFBGW cost and performance requirements, indicating that a technology base now exists to realize the AFBGW cost and performance goals. No implications can be drawn regarding the relative cost effectiveness of the indicated gyroscopes, as apparent differences in cost effectiveness may result from differences in definition of terms, calibration constraint assumptions, and cost model. A comparison of gyroscopes can be made only on the basis of rigid specifications.

In the course of the survey, effort was made to establish a requirement for this level of performance in terms of military utility across a broad spectrum of applications. This was done to establish a production base that would justify a projected system cost at the $10,000 to $15,000 level for a guidance system with a 1.0 degree/hour gyroscope. However, many situations were found where updating concepts required a 0.5 to 1.0 degree/hour performance level. Further study is needed to establish the 1.0 degree/hour requirement across a sufficiently broad range of AFBGW versions and applications to support a recommendation for a development program.

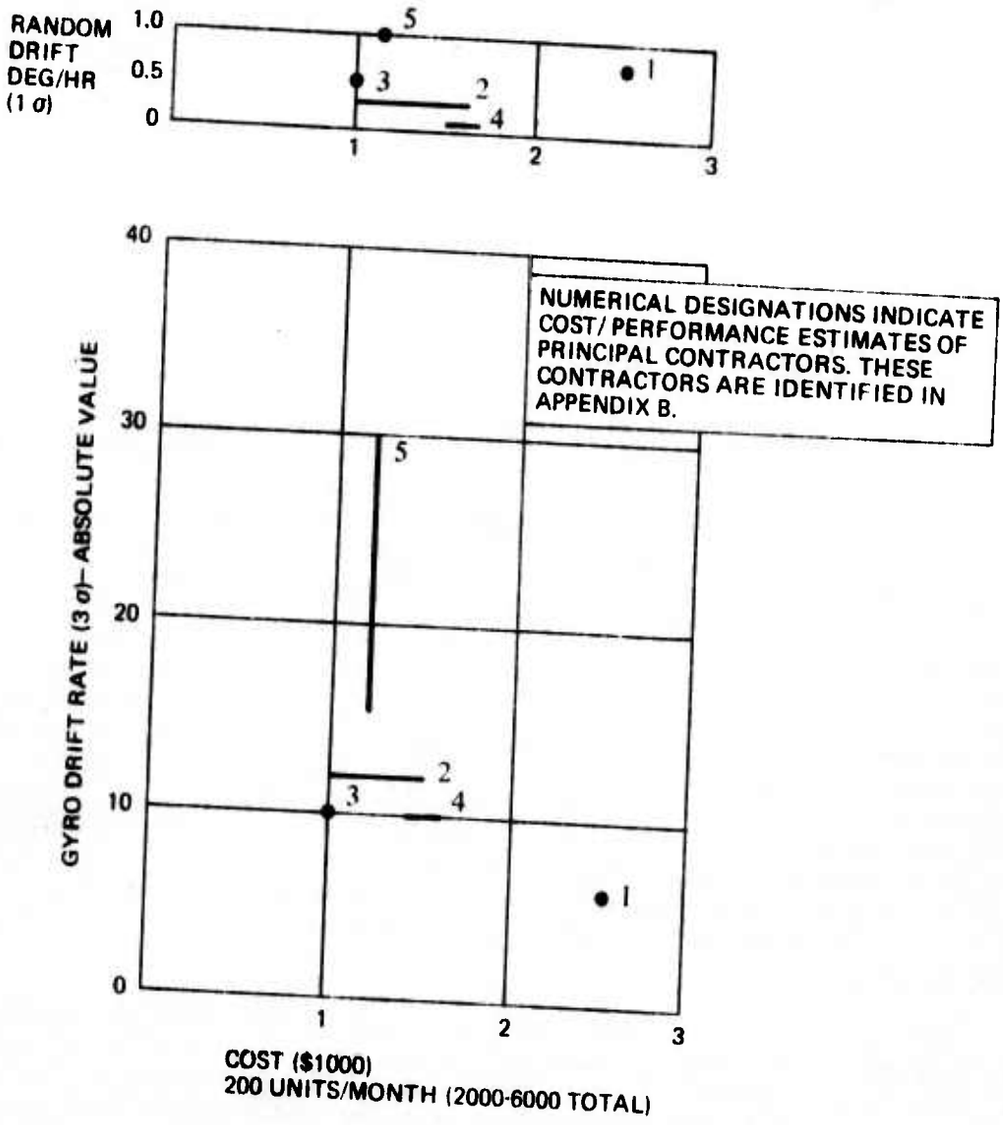

Figure 3. Gyroscope Performance (1 Degree/Hour at $1,000 to $2,000)

During the survey, many gyroscope and platform approaches were examined including laser gyroscope concepts, a new low-cost flexure gyroscope, alternative strapdown configurations, and computational approaches. The tradeoffs between hardware performance, software concepts, alignment techniques, and cost are complex; however, where critical AFBGW issues arose, the appropriate tradeoff considerations were addressed. These are developed in Section V.

ALIGNMENT CONCEPTS

Alignment, broadly speaking, also includes initialization, calibration, and leveling, as well as azimuth alignment. Although azimuth alignment is not usually critical in short duration flights, errors in azimuth above 2 miliradians do contribute significantly to the error budget. For this reason, azimuth alignment remains an important issue.

The generic alignment concepts which were initially considered are gyrocompassing, parameter matching, and parameter transfer. Gyrocompassing was not recommended because it requires a great investment in missileborne sensors. Parameter matching compares position, velocity, and acceleration between missile and aircraft. Parameter transfer of alignment may be accomplished by direct transmission of data from aircraft to missile but requires instrumentation of the launch aircraft. Postlaunch alignment is related to parameter transfer but is a much more complicated process. Typical alignment issues are summarized in Table 6. The data indicate that a tradeoff is necessary between sequential fix alignments, which allocate requirements to the missile, and maneuver alignments, which allocate requirements to the aircraft. The first alternative has disadvantages in that a disposable system may be costly. The second limits the use of the missile to aircraft equipped with high quality platforms. Methods of discrete alignment were also analyzed; however, their limited operational experience precludes their applicability to this study.

Initialization is perhaps more critical than alignment. Recent operating experience indicates that initial velocity and position requirements are too stringent to be met by utility aircraft equipment after several hours of flight.

Calibration can be accomplished by comparing the gyroscope drift of the missile sensor to that of the aircraft master inertial navigator. Alternative approaches include modulation of the spin motor and rotation of the instruments.

TABLE 6. TYPICAL ALIGNMENT ISSUES

Approach	Organization	Developer	Advantages	Limitations
Classical Velocity Matching	General application	Many	Unsophisticated approach	Large programs Fixed maneuvers
Acceleration Measurement Input to Kalman Filter	TASC	Sutherland	Speed and operational advantages over velocity systems	Large memory requirement for missile system
Acceleration Matching Input to Kalman Filter Aligns Strapdown to Gimballed Platform	TASC	Fagan	Minimum computational requirements	Long duration lateral turns requirement Quality aircraft equipment
Acceleration Matching Kalman—Wing-Mounted Missile Frror Reduction	Honeywell	Schultz	Acceptable accuracy for wing-mounted case	Restrictions on aircraft maneuvers Quality aircraft equipment
Acceleration and Angular Rate Matching Kalman Filter	Honeywell	Schultz	High-speed maneuver flexibility	Requires two parameters
Sequential In-Air Fix for In-Air Alignment with Kalman Filter	E-Systems, Inc. LMSD NAFI NWC	Many	Adequate accuracy Not dependent on aircraft equipment	Protracted alignment process Missileborne processing requirement Quality missileborne sensors
Continuous In-Air Fix for In-Air Alignment with Conventional Processing	Many	Many	Quick alignment Reduced missileborne equipment and processing requirement	ECM susceptibility

Several methods of calibrating gyroscopes investigated in the survey indicate calibration to be particularly attractive for the AFBGW, since the effective gyroscope drift rate of a platform can often be reduced by a factor of 3 to 5 in a relatively short period of time.

Leveling can be performed by using the missile's inertial sensors and the aircraft velocity reference.

UPDATE CONCEPTS

Typical update concepts, as shown in Table 7, can be categorized as discrete or continuous systems. Continuous systems generally provide prime velocity as well as position data. Discrete systems (terrain elevation correlation, midcourse radiometric fixes and scene matching) require multiple high precision fixes to derive velocity information. They do not depend on supporting equipment but require considerable external data.

All the continuous and discrete concepts can meet RACG midcourse guidance accuracy objectives if the inertial sensor requirements listed in the table are met. A critical issue was found to be electronic countermeasures (ECM). Low-cost versions of the continuous systems can be highly effective in a clear environment, although many lack capability in an intense ECM situation. The following paragraphs summarize the strengths and weaknesses of selected tabular entries.

In general, the Global Position Satellite (GPS) is an attractive possibility. Areas of uncertainty involve the projected initial operational capability (IOC) dates of the space equipment and the counter-countermeasures effectiveness of the missileborne equipment.

The use of the RACG midcourse approach would avoid many of the ECM and support equipment problems. However, the system would require a unique data package for each update area, and the approach flight would be constrained by this factor. The impact of these considerations on the practical military role of this concept requires further study. Similar restrictions exist for the midcourse terrain elevation correlation fix concept and the scene matching approach.

The Distance Measuring Equipment/Time of Arrival (DME/TOA) concept—the Advanced Location Strike System—implies a greater military control over the target area than do other approaches. Sensitive to ECM, it is dependent upon the freedom of action of one or more support aircraft. It is also

TABLE 7. TYPICAL UPDATE CONCEPTS

Concept	ECM Susceptibility	Missileborne Equipment	Geographic Limitations	Inertial Sensor Requirements	Operational Flexibility	External Equipment	Data Source
GPS	High	Receiver	Depends on status	Depends on status and CCM operations requirement — 1 deg/hr probable	Excellent with adequate satellite network	Satellite and ground equipment	None required
Terrain Elevation Correlation	Low	Altimeter and computer	Some terrain constraints	Could work with autopilot sensors	Good but needs demonstration in this role	None	Defense Map Agency
RACG Midcourse Radiometric Fixes	Low	Radiometer and computer	Some environmental limitations	4 to 10 deg/hr probable	Good	None	Defense Map Agency
DME/TOA	High	Receiver transponder	None	Could work with autopilot sensors	Good	Aircraft must triangulate on target and missile	None required
LORAN	Moderate	Receiver	Significant	0.1 deg/hr required	Not worldwide	Ground stations	None required
Omega	Low	Receiver	Questionable	0.1 deg/hr required to ensure reacquisition	Good	Ground stations	None required
Doppler Radar	Low	Transceiver	None	Needs 2 mrad external heading reference	Good	None	None required
Scene Matching	Low	Optical sensor and correlator	Questionable	1 deg/hr probable	Data problem	None	Undetermined

low cost and compatible with autopilot grade gyroscope equipment, having modest missileborne radio frequency system requirements.

Doppler radar has been extensively applied in the past as a cost-effective source of velocity data. It is applicable primarily to aircraft but is adaptable for missileborne applications. It is self-contained, inexpensive, and relatively immune to countermeasures.

The radio navigation systems (LORAN and Omega) can provide position update within their spheres of operation. Although stationary LORAN transmitters are limited to developed areas of the world, quickly deployed stations may also be used. The possible need for an aircraft in the operation depends on the approach geometry, accuracy achievement, and ground systems deployment effectiveness. It is unlikely that Omega will meet RACG accuracy requirements world-wide; consequently, a relay arrangement may be required to implement a differential Omega operation.

SUMMARY

The preceding discussion presents the information developed during the survey portion of the study and outlines the types of sources used. A methodology is presented for synthesizing weapon guidance systems which incorporate the large body of experience accumulated in Kalman filter development. Selected cruise guidance mechanizations are listed with their applications, sensors, and computer memory requirements.

Weapon guidance concepts are examined, and existing systems are evaluated for their application to the AFBGW. The RNWDS concept is of particular interest because of its austerity with regard to guidance software and inertial sensors.

Alignment concepts, including initialization, calibration, and leveling, are reviewed, and their advantages and limitations indicated. Aiding concepts are also categorized by concept, ECM susceptibility, requirements, and limitations. Several likely systems are noted which meet AFBGW requirements.

The study of inertial component and platform technology indicates that rate-integrating gyroscopes are available, rate gyroscopes are being adapted, and tuned rotor two-degree-of-freedom gyroscopes may be available shortly. Cost and

performance for state-of-the-art rate-integrating gyroscopes are presented, and tradeoffs are addressed.

A review of guidance laws presents the characteristics and applications of generic laws pertaining to cruise missiles. Adaptive proportional systems are shown to be well-adapted for glide weapon use.

SECTION III

INERTIAL SYSTEMS

An inertial system consists of gyroscopic sensors, stabilization hardware, a mechanization computer and software, and preflight support equipment and software. Gyroscopic sensors, the major elements in achieving mission accuracy, are emphasized in this discussion. A distinction is sometimes made between inertial grade gyroscopic sensors and body-mounted gyroscopic sensors. For the purpose of this discussion, all gyroscopic sensors are considered inertial sensors.

This section reviews available inertial equipment that can be adapted for air-to-surface cruise missiles, including prototype and conceptual strapdown inertial measuring units (IMUs) as well as components that can be adapted to alternative strapdown IMU concepts. Existing inertial platforms and gyroscopes are described, and their accuracy is discussed.

The navigation accuracy of inertial systems varies from 0.01 degree/hour (1 nautical mile/hour) to 0.25 degree/second. Of interest for this study are those in the 0.1- to 5.0-degree/hour range; the 0.1-degree/hour system provides an accuracy for the AFBGW (long range) of about 1,000 feet, while the 5.0-degree/hour system allows 3,000-foot accuracy for the short-range version. (Navigation accuracy is related to flight duration for the two AFBGW versions.) A target cost for the AFBGW/RACG guidance system is $10,000.

MISSILE SYSTEMS

Three systems are presented as a baseline for examining AFBGW inertial guidance candidates: the SRAM system, the Harpoon system, and the RNWDS (DME/TOA), a Navy system similar to the Advanced Location Strike System (ALSS).

The SRAM system employs computer techniques, particularly the virtual target steering system, which are applicable to the AFBGW. It has an aircraft quality inertial platform, the SKN-89, which is used on the A-7 and is capable of 2 nautical miles/hour performance.

The Harpoon guidance system is included because it is the first application of a strapdown system to a major tactical missile procurement. It consists of three Lear Siegler 1903 gyroscopes, three Sundstrand accelerometers, and a navigation

computer, with a specified gyroscope drift rate of 1 degree/hour (calibrated). This translates to an accuracy for the AFBGW (long range) of 10,000 feet and of 600 feet for the short-range version. The 1904 gyroscope can be substituted online for the 1903 to improve accuracy to 0.2 degree/hour, translating to 2,000 feet and 120 feet, respectively, for the long-range and short-range versions. With the 1904 gyroscope, the system easily meets AFBGW accuracy goals.

A typical cost distribution example can be applied to Harpoon as follows:

Lear Siegler (1903 gyroscopes/2 x 10^{-3}g)	$ 7,500	(3 x $2,500)
Sundstrand Q-Flex Accelerometer	$ 1,500	(3 x $500) (2 x 10^{-3}g)
System Mechanization	$ 6,000	
Computer	$10,000	(8,000 words read-only selectable memory and 3 μ sec add)
Operational Support	$ 5,000	
	$30,000	

The IMU cost of the Harpoon is about $15,000 for the system and $3,000 for test calibration and field support (a total of $18,000), and the production price is estimated at $30,000 with the computer and $20,000 without the computer—considerably above the AFBGW cost goal.

The RNWDS (DME/TOA), as shown in Figure 4, is a typical rate sensor derived system; it has autopilot gyroscopic capability and employs autopilot sensors. The RNWDS gyroscopic equipment can make only a limited contribution to midcourse guidance, because it requires continuous input from the DME/TOA navigation equipment. It is capable of independent operation for only a fraction of a minute. The total cost of all gyroscopic sensors for the system is estimated at $2,000.

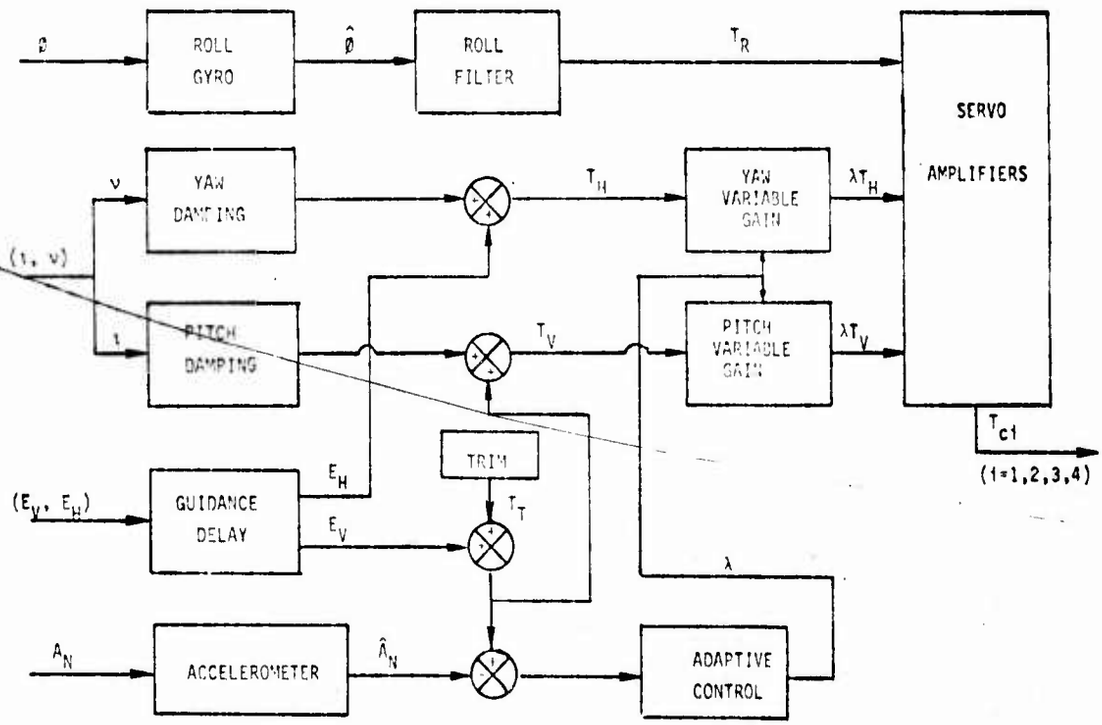

ϕ	Pitch	λ	Conditioning Gain
$\hat{\phi}$	Indicated Pitch Orientation	E_V	Error, Vertical Plane
T_R	Roll Torquing Signal	E_H	Error, Horizontal Plane
v	Yaw	T_T	Trim Torque
z	Pitch	A_N	Normal Acceleration
T_H	Torquing Signal Horizontal Plane	$\hat{A}_N$	Indicated Acceleration
T_V	Torquing Signal Vertical Plane	T_{ci}	Control Actuator Commanded Torque

Figure 4. Relative Navigation Weapon Delivery System (DME/TOA) Control Section Simulation

These costs indicate that Harpoon is above the price goal of the AFBGW ($10,000 without computer) and that RNWDS is substantially below the performance goal of the AFBGW (1 degree/hour). Therefore, adaptation of equipment whose performance and cost lie between those of the Harpoon and RNWDS is desired.

TYPES OF PLATFORMS

Table 8 indicates the types of platforms that have been actively promoted by major inertial equipment producers. A review of the tables indicates that the price and quality that have been emphasized are somewhat higher than the AFBGW objectives. Note that Harpoon is the only system for which estimated cost is available, and production run is now in progress. Consequently, Harpoon cost figures are exact, while other cost figures may vary by a factor of 2 or more.

The accuracy of these systems is based on observed error propagation at 42 minutes divided by 0.7. The geometry of this estimate is shown in Figure 5. The method is used extensively in quoting performance of platforms for long-term applications. Since many of the platforms discussed in Table 8 are to be adapted from long-term application, it is essential to be able to relate this data to the short-term missile situation.

Nautical mile per hour performance figures are given by:

$$\Delta P = 100 \times \delta$$

where δ is gyroscope drift rate (in degrees/hour), and ΔP is position error (in nautical miles).

Applied to missile systems, this formula gives large nautical mile/hour error results (1 degree/hour = 100 nautical mile/hour). However, the actual error is well below this value since operation is confined to 0.1 to 0.2 hour (see Figure 23).

Error figures are presented for both the short-range and long-range missions in Table 8. The state-of-the-art is represented by Harpoon, which achieves an accuracy of 11,300 feet for the long-range mission. A Lear Siegler platform using the same gyroscope also achieves this accuracy. The Hamilton Standard HS-3030, the Bendix SDI-900-2, and a system using the Honeywell GG1111 operate in this performance range or better.

TABLE 8. SELECTED STRAPDOWN MISSILE GUIDANCE SYSTEMS REPRESENTING DIVERSE APPLICATIONS

Parameter	Manufacturer of System				
	Bendix (1)		Hamilton Standard (2)		
	SDI-920	SDI-900-2	HS-2020	HS-3030	HS-4040
Error Accumulation*	5 nm/hr (Page 1-2)	5-10 nm/hr (Page 7-2)	1 nm/hr (CEP)+ (Page 29-31)	30 nm/hr (Page 36)	100 nm/hr (Page 44)
Gyro	LG-60 SDF	LDGR-100 SDF (rate)	DILAG	Mini-RIG 30 (rate integ.)	Super gyros (rate)
Drift Rate	0.1 deg/hr (Page 3-4)	0.1 deg/hr* (Page 7-2)		0.5 deg/hr (30)+	30 deg/hr (1σ)
Accelerometer	LB-50 PIA	FH-300 Flex Hinge	Sundstrand QA-1100	Sundstrand QA-1100	SUPERGEE
Computer	BDX-920	BDX-900	CMOS parallel processor	CMOS parallel processor	CMOS parallel processor
Size (in.)	8 x 8 x 12	10 x 10 x 15	7.5 x 7.6 x 15	7.5 x 7.6 x 15	13 x 5.3 x 5.4
Weight (lb)	18.4	35	30	25	15
Power (w)	157	250	150	60-200	60-200
Status	Prototype	Preproduction	Development	Used on space systems	30,000 per year for Maverick
Application	Heavy lift helicopter	MK-30 torpedo CH-47 helicopter	Aircraft, missile	Aircraft and missile	Missile
Type	Strapdown	Strapdown	Strapdown	Strapdown	Strapdown
SR Error (ft) (2σ)	120	120	10	200	Drift too large to quote meaningful error
LR Error (ft) (2 r)	2000	2000	163	3300	

+ Designates parameter used in calculating **LR and SR error.**
* Errors not designated as to standard deviation are 1σ errors.

(1) Bendix brochure material—SD1920 strapdown inertial navigation system Bendix Corporation—Guidance Systems Division, Teterboro, N.J.
(2) Hamilton Standard Inertial Products ESP 7502, January 15, 1972

TABLE 8. SELECTED STRAPDOWN MISSILE GUIDANCE SYSTEMS REPRESENTING DIVERSE APPLICATIONS (CONCLUDED)

Parameter	Manufacturer of System			
	IBM	Litton	Singer Kearfott	Honeywell
	Harpoon MGU	LP80	TIGS	XO
Position Error Accumulation	6 nm/hr**	3-5 nm/hr**	6 nm/hr**	10 nm/hr**
Gyro	LS 1903 H. F. 1.7 deg/hr (3σ)	Tuned rotor	Fluidic or gyro flex	GG-1300
Accelerometer	Sundstrand Q-Flex	Miniature	KFT 2401	Sundstrand Q-Flex
Computer	IBM 8000 ROS 3.5 μsec add	Advanced	SKC-3000	Magic 362
Size (in.)	12 dia x 6 long	7.6 x 7.5 x 12	10 x 8 x 12	10 x 10 x 15
Weight (lb)	25.4	18	12	50
Power (w)	127	100	200	200
Cost (dollars)	30,000+ Can be delivered from inventory)	20,000◇ (Development goal)	23,000 (Development goal)	20,000◇ (Development goal)
Status	Production	Concept	Concept	Prototype
Application	Harpoon	Aircraft	Aircraft	Missile
Type	Strapdown	Strapdown	Strapdown	Strapdown
SR Error (ft) (2σ)	68	36-60	72	164
LR Error (ft) (2σ)	11,300	600-1000	1200	2000

(1) Harpoon Weapon System — McDonell Douglas Astronautics Company—East, MDC E0796, 14 May 1973, (Page 2-7). (Quantitative data was transmitted informally by Jerry Hiess of IBM Corp.)

\+ Estimated offering price of hardware that can be delivered out of inventory today—single unit.

◇ Cost goal for future development—depends upon successful engineering development and sufficient volume (2000-6000) for large scale production.

** Parameter used in calculating LR and SR error.

ROS Read-only selectable

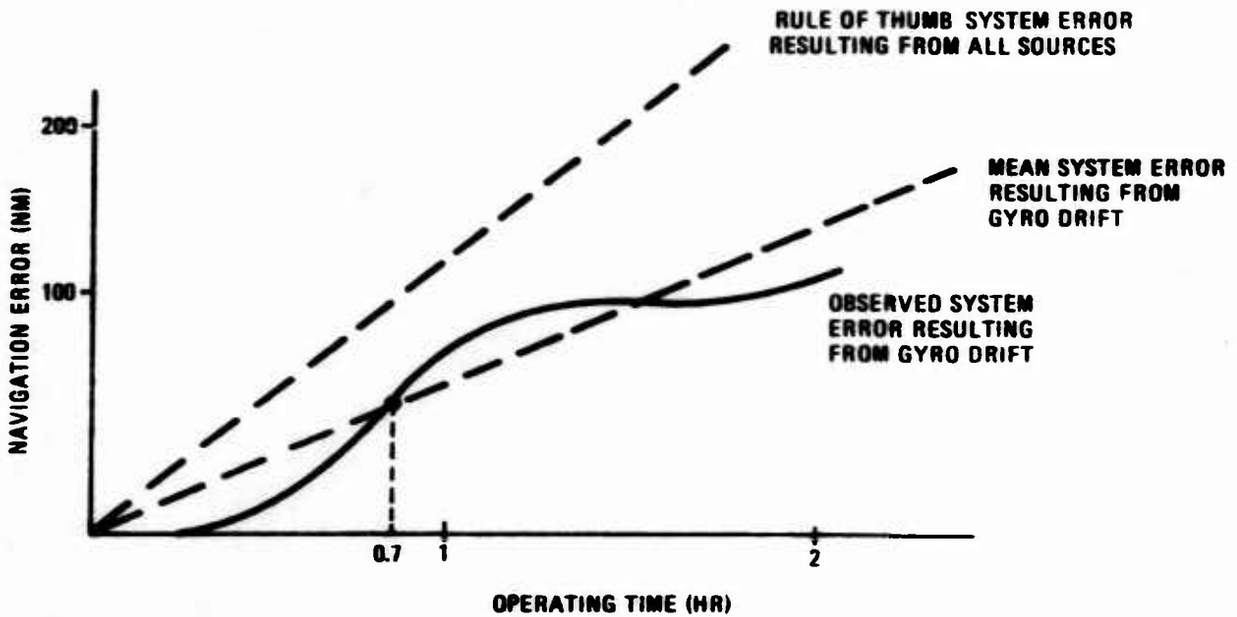

Figure 5. Rule of Thumb Estimation Procedure*

* These curves are based on equations contained in Table 23, Error Performance Equations.

All the contractors include computer data in their system estimates; consequently, size, weight, power, and cost data are presented on a total system basis—including IMU and computer. Table 9 shows some alternative computer options that are available. Typical packaging goals for these systems are 500 cubic inches, 20 pounds, and 100 watts for a fully computerized mechanization. Computer technology is changing rapidly, and current indications are that the costs shown will be reduced significantly in the near future.

APPLICABLE GYROSCOPES

Types of Gyroscopes

Gyroscopes are the primary components of inertial platforms and fall into two major classes: electromechanical gyroscopes and optical effect gyroscopes. Table 10 lists types of gyroscopes currently available. Electromechanical gyroscopes may be categorized by many design criteria, but single-degree-of-freedom and two-degree-of-freedom is a prime differentiation. This report emphasizes single-degree-of-freedom instruments as most applicable for the AFBGW cost requirements. Tuned rotor gyroscopes are not emphasized in this discussion because they have not yet demonstrated adequate low-cost potential for this application.

Rate gyroscopes and rate-integrating gyroscopes are both single-degree-of-freedom instruments. Rate gyroscopes evolved from spring-constrained attitude reference systems. In the past, the spring pickoff and rebalance arrangement have been subject to nonlinearities (generally caused by temperature variation) and cross-coupling. Recent improvements using closed-loop feedback rebalance techniques now permit performance levels approaching AFBGW requirements.

Rate-integrating gyroscopes originated in aircraft navigation and space applications. They employ feedback techniques to rebalance the torque generated by rotation about an input axis. The angular displacement can be measured by determining the current required to balance the torquer circuit. Higher quality rate-integrating gyroscopes have a ball-bearing suspension, whereas lower performance instruments have a jewel and pivot suspension. Maximum allowable angular rates for vehicles on which rate-integrating gyroscopes are mounted range from 275 to 573 degrees/second. All gyroscopes in this discussion have been used for tactical missile guidance or can be adapted to this application. Instruments

TABLE 9. TYPICAL MISSILE COM

Missile Computer Configurations for 1975-1985	Features	Functions	Interface Electronics Modules	Weight (lb)	Volume (cu in.)	Po (W
Magic 4016(LSI)	N-MOS CPU Small memory LSI Small I/O	Navigation Guidance Control Target preset	A/D-D/A Analog multiplexer Discrete	5.0 6.0	200 240	
Magic 362(Core)	Bipolar CPU Medium-size memory Core Medium I/O	Navigation Guidance Control Autostabilization Terminal seeker	A/D-D/A Analog multiplexer Discrete Digital	15.7 17.9	280 360	1(
Magic 4032 (Core/LSI)	N-MOS CPU Medium-size memory Core (LSI scratch) Medium I/O	Navigation Guidance Control Area correlation	A/D-D/A Analog multiplexer Discrete Correlator	16.0 18.3	280 360	
Magic 362 FP (Core)	Bipolar CPU Large memory Core Large I/O	Navigation Guidance Control Autostabilization Area correlation Terminal guidance	A/D-D/A Analog multiplexer Discrete Correlator Digital	19.5 22.0	400 520	
Magic 362 FP (LSI)	Bipolar CPU Large memory LSI Large I/O	Navigation Guidance Control Autostabilization Area correlation Terminal guidance	A/D-D/A Analog multiplexer Discrete Correlator Digital	13.0 15.0	280 320	
Average value				14.8	325	

* Cost distribution (percent)

Power Supply	11
Processor	9
Memory	45
Interface	15
Structure	9
Test	11

AL MISSILE COMPUTER CONFIGURATIONS

Volume (cu in.)	Power (w)	Program Memory Size	Scratch Memory Size	Instruction Word Size (bits)	Data Word Size (bits)	Execution Time (μsec)		Equivalent Operations (1000/sec) (75% Add; 25% Mul.)
200	20	2,048(LSI)	256(LSI)	16	16	Add	2.1	320
						Mul.	6.1	
240	25	4,096(LSI)	1,024(LSI)					
280	100	6,144(Core)	2,048(Core)	16	16	Add	2.9	250
						Mul.	7.3	
360	110	12,288(Core)	4,096(Core)					
280	50	8,192(Core)	2,048(LSI)	16	32	Add	3.5	145
						Mul.	17.0	
360	70	16,384(Core)	4,096(LSI)					
400	130	12,288(Core)	4,096(Core)	32/16	16/32	Add	2.9	300
						Mul.	4.6	
520	140	16,384(Core)	16,384(Core)					
280	80	12,288(LSI)	4,096(LSI)	32/16	16/32	Add	1.0	600
						Mul.	3.7	
320	100	16,384(LSI)	16,384(LSI)					
325	82.5							

(The reverse of this page is blank)

TABLE 10. TYPES OF GYROSCOPES

Type	Cost-Effective Performance Range (deg/hr)	Estimated Cost Range (dollars)	Status	Size (cu in.)	Maximum Rate (radians/sec)	Angular Quantization (mrad)
Wide Angle Gas-Bearing Gyro*	0.2-1.0	1000-5000	Advanced Development	20.0	0.05	350
Tuned Rotor Gyro*	0.005-1.0	2000-10,000	15-year production history for inertial grade instrument; low-cost strapdown version in development	1.5	0.5	3
Rate Gyro+	0.1-80	300-2000	30-year production history	2.0	1.0	5
Rate-Integrating Gyro+	0.001-10	1000-90,000	20-year production history	2.0	1.0	5
Magnetic Resonance Gyro+	0.01	5000	Exploratory Development	25.0	1.0	5
Wide Angle Electrostatic Gyro*	0.01	5000	Advanced Development	3.0	0.5	100

* Two degrees of freedom
\+ Single degree of freedom

vary in volume from 4 to 12 cubic inches and have a 0.5- to 1.5-pound weight variation. Several contractors produce instruments in the degree-per-minute category (i.e., Timex and Humphrey). These are designed for low-accuracy applications (where drift rate can be 0.1 degree/second or 360 degrees/hour) and, therefore, are unsuited to AFBGW applications discussed in this study.

Optical effect or laser gyroscopes measure angular rates by comparing differences in frequency of two counterrotating light beams. There are several variants of the laser gyroscope concept due to variations in design policy, methods of solving design problems, and development strategies. For example, as shown in Figure 6, the GG-1300 is a single-block, fully evacuated dithered unit, whereas the SLG-15 is a modular unit in which each element shown is placed in the assembly as a component. The characteristics of the two systems are given in Table 11.

Gyroscope Performance

Gyroscopes are the major contributors to navigation error; the parameter recognized as a measure of gyroscope performance is gyroscope drift rate. For a given nominal sensor drift rate, a wide variation in system position accuracy can result from differences in flight time, calibration time, and the desired probability of terminal acquisition. Flight time affects performance in that errors are proportional to the cube of this parameter, while prolonged calibration time can reduce the drift rate itself to one-tenth of its original value (Reference 6). Probability of adequate midcourse guidance depends upon the level of confidence of achieving performance goals. At least 95 percent probability (2σ) is desirable to provide adequate terminal acquisition. These three parameters must be accurately stipulated before drift rate can be related to performance. Table 12 illustrates a typical relationship for a 1-degree/hour gyroscope (Reference 5).

Table 12 shows that a system using a nominal 1 degree/hour gyroscope (absolute value) produces a 60-foot error in a 4-minute flight if it is calibrated for 60 minutes and if a 1σ standard deviation is acceptable. Using the same gyroscope with no calibration for a 10-minute flight gives an error of 30,000 feet (5 nautical miles) if a 3σ standard deviation (99.7 percent probability of achieving nominal performance) is desired. Thus, calibration can dramatically improve the performance of a system; a calibrated 1 degree/hour system

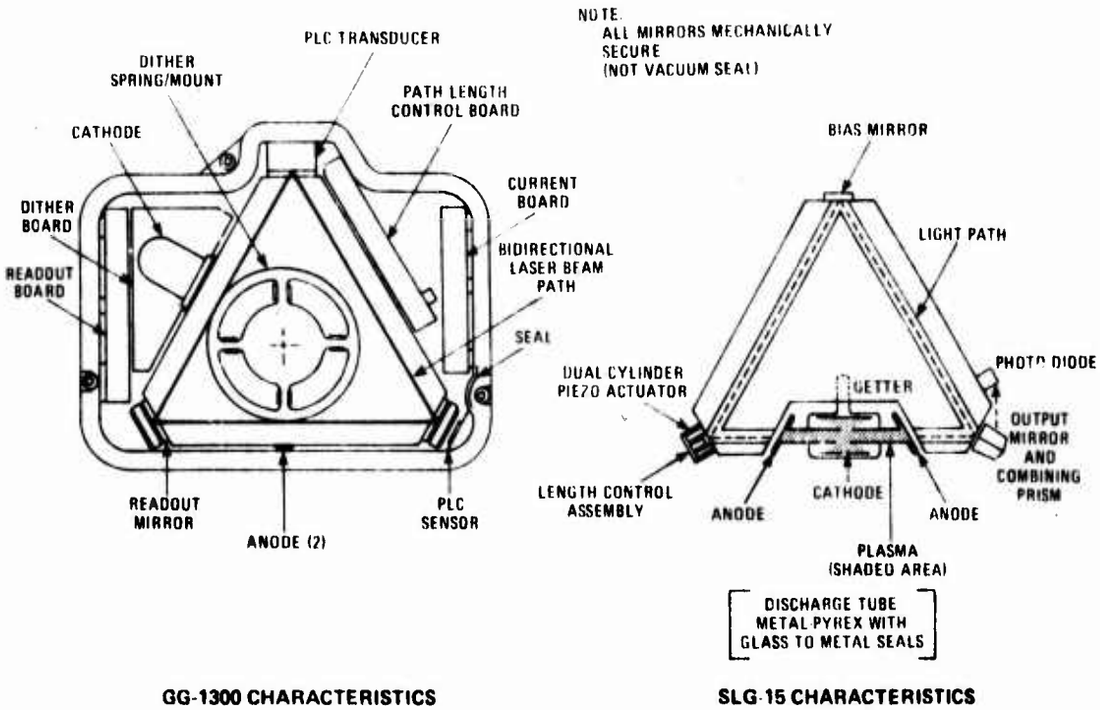

Figure 6. Laser Gyroscope Approaches

TABLE 11. RING LASER GYROSCOPE CONCEPTS

HONEYWELL

PARAMETER	GG-1300 SPECIFICATION	GG-1300 AVERAGE OF ITEMS DELIVERED (10)	GG-1328 SPECIFICATION
Drift Rate (degree/hour)	0.12	0.0106	0.10
Random Drift (degree/hour)	0.02	0.0082	Not Applicable
Response Time (second)	100	Not Applicable	Not Applicable
Scale Factor Accuracy (ppm)	250	106	Not Applicable
Scale Factor Linearity (ppm)	Not Applicable	18	Not Applicable

SPERRY

PARAMETER	SLG-15 SPECIFICATION	SLG-7 SPECIFICATION
Drift Rate, Turn-On (degree/hour)	1.0	3.3
White Noise, Random Drift (degree/$\sqrt{\text{hour}}$)	0.3	0.2
Calibration Time (minute)	15	15
Markovian, Random Drift (degree/hour)	0.1	Not Applicable
Scale Factor Stability (ppm)	100	160

TABLE 12. AFBGW PLATFORM* POSITION ACCURACY VERSUS SELECTED OPERATIONAL CONSTRAINTS (Position Accuracy in Feet)

STANDARD DEVIATION OF MIDCOURSE GUIDANCE (PROBABILITY OF ADEQUATE MIDCOURSE GUIDANCE) (percent)	4-MINUTE FLIGHT (SHORT RANGE)			10-MINUTE FLIGHT (LONG RANGE)		
	CALIBRATION TIME (minutes)					
	DEAD START	10	60	DEAD START	10	60
1σ (62)	600	200	60	10,000	3,000	1,000
2σ (95)	1,200	400	120	20,000	6,000	2,000
3σ (99.7)	1,800	600	180	30,000	9,000	3,000

* 1 degree/hour gyroscope.

can adequately perform the long-range mission, but an uncalibrated 1-degree/hour system is adequate only for the short-range mission. The disadvantage of calibration is that it requires a master inertial navigator in the aircraft that restricts the use of weapons, creates logistic problems, and reduces operational flexibility.

Tables 13 and 14 describe gyroscopes that operate at the 1-degree/hour level without calibration and at the 0.2-degree/hour with calibration. Tables 15 and 16 describe gyroscopes that operate at approximately 10 degrees/hour without calibration and at approximately 1 degree/hour with full calibration. Tables 17 and 18 describe the types of gyroscopes that may be used with the doppler radar (GPS) or other continuous update processes.

Gyroscope manufacturers whose products were found to be particularly applicable to the AFBGW include Lear Siegler, Honeywell, Hamilton Standard, and Northrop. These companies are actually pursuing development and production at the 1- to 3-degree/hour performance range and in the $1,000 to $3,000 instrument cost range.

The short-range accuracy objective can probably be met with a 3-degree/hour gyroscope; however, the long-range needs a 0.15-degree/hour (1σ) gyroscope.

TABLE 13. AFBGW GYROSCOPE PERFORMANCE AND DESIGN— HIGH-PERFORMANCE/HIGH-COST CATEGORY

Parameter	Lear Siegler 1904	Honeywell GG1111-AL-01	Hamilton Standard RI-1010	Northrop GI-G6-G
Performance				
Absolute Value (Turn-on)*	1-2 deg/hr (3σ)	1.0 deg/hr (1σ)	5.0 deg/hr (3σ)	.75 deg.hr (3σ)
Best Performance and Random Drift+	< 0.1 deg/hr (1σ)	.02 deg/hr (1σ)	0.01 deg/hr (1σ)	0.03 deg/hr (1σ)
g-Sensitive Drift	3 deg/hr/g(1σ, major)	5 deg/hr/g (3σ major)	.02 deg/hr/g(1σ)	
g^2-Sensitive Drift	<0.1 deg/hr/g^2(1σ,minor)	.1 deg/hr/g^2	0.06 deg/hr/g(1σ, minor)	
Torquer Scale Factor Linearity	0.02%	0.01%	0.027%	0.02%
Instrument Characteristics				
Type	RIG	RIG	RIG	RIG
Design Objective	Address moderate accuracy tactical weapon applications	Dynamic space environment (applicable to GBU-15)	High accuracy	Inertial quality
Navigation Parameter Measured	Angular rate	Angular rate	Angle	Angular rate
Design Features				
Spin Motor	High momentum Improved bearings	48.000 rpm 48,000 gm cm^2/sec	Hysteresis Synchronous	NA
Pickoff	Moving coil	Moving coil	Moving coil	Microsyn
Torquer	Permanent magnet	Moving coil permanent magnet	Permanent Magnet Samarium Cobalt	Moving coil permanent magnet
Suspension	Ball bearing	Ball bearing gimbal suspension - floated	Ball bearing pivot	Gas bearing
Drift Trim	Circuit bias	Compensation Micro vernier Balance pan Temperature	NA	NA

* Uncalibrated
\+ Calibrated
NA Not available

TABLE 14. AFBGW GYROSCOPE PHYSICAL AND COST DATA— HIGH-PERFORMANCE/HIGH-COST CATEGORY

Parameter	Lear Siegler 1904	Honeywell GG1111-AL-01	Hamilton Standard RI-1010	Northrop GI-G6-G
Angular Rate Limits	400 deg/sec	70 deg/sec	400 deg/sec	300 deg/sec
Temperature and Vibration	Normal Operating: -15° C to -71° C Storage: -65° C to 95° C Vibration: 10 g	NA	-20° to 250° F-storage 160° F-operating 45 g vibration	-65 to 140 deg F (with heater) tested at 50 g sin & 2 g rms; ultimate to be determined
Status—Concept, Captive Demonstration, Missile Flights, and Other Uses	Demonstrated	Released for production	Production	Pilot fabrication
Applications	Precise missile guidance	Space shuttle	In-house system Drone HRI Space telescope (Germany)	Precise missile guidance
Production History	Four tested	95% commonality between GG1111-AL-01 and LC	Several in use	Technology demonstrated Pavetack - flight proven
Size, Shape, and Weight Power	1.59-in. diameter x 3.32-in. length; 0.57 lb; 2.5 w	1.3-in. diameter x 2.5-in. length flange mount	2.5-in. diameter x 3.3-in. length; 1.5 lb	1-in. diameter x 2.25-in. length; 0.22 lb

NA Not available

TABLE 15. AFBGW GYROSCOPE PERFORMANCE AND DESIGN—M

Parameter	Lear Siegler 1903	Honeywell GG1111 LC-04
Performance		
Absolute Value (Turn-on)*	6 deg/hr (3σ)	12 deg/hr (3σ)
Best Performance and Random Drift	0.7 deg/hr (1σ)	0.3 deg/hr (1σ) (Much lower value possible)
g-Sensitive Drift	$\pm$ 10°/hr/g	18 deg/hr/g (3σ)
g^2-Sensitive Drift	0.5°/hr/g^2	.3 deg/hr/g^2
Torquer Scale Factor Linearity	NA	0.1 % at 120 deg/sec
Instrument Characteristics		
Type	RIG	RIG
Design Objective	Moderate duration Moderate accuracy	A/C attitude and heading reference Tactical missiles
Navigation Parameter Measured	Angular rate	Angular rate
Design Features		
Spin Motor	Synchronous hysteresis 26V, 800Hz, 2 phase	Synchronous hysteres 14,000 gm cm^2/sec
Pickoff	Moving coil	Moving coil
Torquer	Permanent Magnet	Moving coil permanent magnet
Suspension	Jewel and pivot	Ball bearing gimbal suspension-floated
Drift Trim	Circuit bias	Compensation Micro vernier Balance pan g-sensitive Temperature

* Calibrated

NA Not available

E AND DESIGN—MODERATE-PERFORMANCE/MODERATE-COST CATEGORY

	Honeywell GG1111 LC-04	Hamilton Standard Mini-RIG 30	Northrop GI-G6-S	Northrop GI-G6-B
	eg/hr (3σ)	10 deg/hr (3σ)	15-30 deg/hr (3σ)	10 deg/hr (3σ)
	g/hr (1σ) uch lower value ssible)	0.5 deg/hr (3σ)	1.0 deg/hr (1σ)	0.1 deg/hr (1σ)
	/hr/g (3σ)	10 deg/hr/g(1σ, major)	5-10 deg/hr/g (1σ major)	2 deg/hr/g(1σ, major)
	g/hr/g^2	0.3 deg/hr/g^2 (1σ, major)	0.5 deg/hr/g^2 (1σ major),	.2 deg/hr/g^2(1σ, major)
	% at 120 deg/sec	0.1%	0.1%	0.05%
		RIG	RIG	RIG
	attitude and head- reference ical missiles	Low-cost tactical weapon guidance	Stabil. or guidance gyro Tactical missile Reduced cost/perform	Aircraft missile Stabil. or guidance gyro Higher cost/perform
	lar rate	Angle	Angular rate	Angular rate
	hronous hysteresis 00 gm /sec	Hysteresis Synchronous Angular momentum= 30,000 gm cm^2/sec	Synchronous hysteresis	Synchronous hysteresis
	ng coil	Microsyn	Microsyn	Microsyn
	ng coil manent magnet	Permanent magnet	Moving coil permanent magnet	Moving coil permanent magnet
	bearing gimbal pension-floated	Nominally floated ball bearing	Partially-floated ball bearing	Fully-floated ball bearing
	pensation ro vernier ance pan ensitive nperature	Temperature compensated	NA	NA

(The reverse of this page is blank)

TABLE 16. AFGBW GYROSCOPE PHYSICAL AND COST DATA — MODERATE-PERFORMANCE/MODERATE-COST CATEGORY

Parameter	Lear Siegler 1903	Honeywell GI111 LC	Hamilton Standard Mini-RIG 30	Northrop GI-G6-S	Northrop GI-G6-B
Angular Rate Limit	275 deg/sec	to 400 deg/sec	140 deg/sec	300 deg/sec	200 deg/sec
Status	Production	Production	Production	Production	Production
Applications	Harpoon Penguin Jumbo Air combat maneuver range	Harpoon F14, F15, Pave Strike MK-73, Tow Cobra	Torpedo Tactical missiles GBI-15/ALCM	HARPOON SEEKER F-14 and A7 FLIR Phoenix	HARPOON Guidance B-1 Att/Hdg Ref Syst. SM-2 SAM-D Tomahawk
Production History	15,000 flown	>2000 built		Hughes	MDAC E
User	IBM McDonnell Cubic Corp.	Hughes Aircraft Co. Texas Instruments Westinghouse General Electric	U.S. Navy and USAF Contractors Lockheed	Texas Instrument	Rockwell G.D. Pomona Raytheon
Size, Shape, Weight, and Power	1.59-in. diameter x 3.32-in. length; 0.57 lb; 2.5 w	1.3-in diameter x 2.5-in. length flange mount	1.00-in. diameter x 2.25-in. length	1.00-in. diameter x 2.25-in. length	1.00-in. diameter x 2.25-in. length

NA Not available

TABLE 17. AFBGW PERFORMANCE AND DESIGN—LOW PERFORMANCE/LOW-COST CATEGORY

Parameter	Lear Siegler 1902	Hamilton Standard Super Gyro	Northrop GI-G6-E
Performance			
Absolute Value (Turn-on)	80-100 deg/hr (3σ)	100-200 deg/hr (3σ)—estimate	40 deg/hr (3σ)
Best Performance and Random Drift	15 deg/hr (1σ)	30 deg/hr(1σ)—estimate	2 deg/hr (1σ)
g-Sensitive Drift		NA	8-15 deg/hr/g (1σ)
g^2-Sensitive Drift	$5^{\circ}/hr/g^2$	NA	2 deg/hr/g^2 (1σ)
Torquer Scale Factor Linearity	0.5%	NA	0.25%
Instrument Characteristics			
Type	RIG	Rate gyro	RIG
Design Objective	Low-accuracy tactical weapon	Tactical weapon	Mid-course guidance, seeker/antennae Stabilization
Navigation Parameter Measured	Angular rate	Angular rate	Angular rate
Design Features			
Spin Motor	Hysteresis	NA	Moderate speed
Pickoff	Moving coil	Double balance Differential transformer	Microsyn
Torquer	Permanent magnet	NA	Moving coil permanent magnet
Suspension	Jewel and pivot	Uniplex suspension	Partially floated ball bearing
Drift Trim	Circuit bias	None	None

* Uncalibrated
\+ Calibrated
NA Not available

TABLE 18. AFBGW GYROSCOPE PHYSICAL AND COST DATA—
LOW PERFORMANCE/LOW-COST CATEGORY

Parameter	Lear Siegler 1302	Hamilton Standard Super Gyro	Northrop GI-G6-E
Physical Constraints			
Angular Rate Data	275 deg/sec	500 deg/sec	400 deg/sec
Temperature and Vibration	-40 deg C to 71 deg C 10 g-rms, 20-1500 Hz	65 to 225 deg F/15g to 2000 Hz	-50°F to +200°F 30 g RMS, 20-2000 Hz
Shock	20 g, 11 millisec	NA	100G, 11 MS , half size
Status			
Concept, Captive Demonstration, Missile Flights, and Other Uses	Concept	Production rated	Production rated
Applications	Low-cost missile guidance	Low-cost missile guidance	Chaparral Harpoon Seeker Stabil.
Production History	Preproduction	Maverick and many other missiles	2400 in operation
Physical Characteristics			
Size, Shape, Weight, and Power	1.5-in. diameter x 3.0-in. length (approximate)	.437-in. diameter x 1.5-in. length; 0.20 lb	1.0-in. diameter x 2.25-in. length; 0.22 lb

NA Not available

Litton, Kearfott, Teledyne, Autonetics, and Delco are not now emphasizing the low-cost gyroscope field, but are primarily interested in the 0.01-degree/hour (1σ) random drift performance range. It has not been demonstrated whether they will produce 0.2-degree/hour (1σ) random drift instruments at the $10,000 level.

If a 10-minute calibration is assumed, GI-G6-B, LS1903, or GG1111LC are adequate for the 4-minute mission. This means that an improved rate gyroscope in a cost range from $700 to $1,000 can be adapted to the short-range situation. A $5,000 platform will be possible under these circumstances. Conversely, the long-range situation requires a more sophisticated rate integrating concept that is associated with gyroscopes that sell for $3,000 and more.

In general, the LS1904, the GG1111-AL-01, and the GI-6G-G represent instruments that can, with calibration, perform the long-range mission. These gyroscopes are compatible with a platform cost objective of $25,000 to $30,000 for quantities of 2,000 to 6,000 gyroscopes.

SUMMARY

The preceding discussion presents the results of an industry investigation of the inertial platforms and gyroscopes that apply to the AFBGW. There are a variety of sources of platforms that meet AFBGW accuracy requirements; however, their cost is approximately 75 percent above the $10,000 goal if currently available equipment is used.

Three sources of data were used in the inertial equipment investigation: (1) descriptions of existing missile guidance hardware for air-to-surface weapons; (2) descriptions of existing and conceptual strapdown platforms; and (3) descriptions of gyroscopes.

Multiple sources exist for the procurement of AFBGW instruments, and the prognosis is good for achieving the general cost/performance parameters required for the AFBGW. These parameters may be achieved by design-to-cost effort that reflects the specific requirements of the AFBGW and the 2,000 to 6,000 gyroscope volume objective of the program.

SECTION IV

GUIDANCE LAW METHODOLOGY

This section develops a methodology for determining tactical weapon guidance laws and includes the detailed step-by-step synthesis of two AFBGW guidance laws. The activities involved in this effort are shown in Figure 7. In the first phase, AFBGW characteristics are defined; in the second phase, AFBGW transit dynamics are analyzed.

The term transit dynamics refers to the manner in which the missile is directed from its launch point to the terminal acquisition area. The term implies a relatively stationary interceptor/target situation. The autopilot used in this section is based on glide weapon concepts that have been applied in the past. However, the data used in this section is not identical to any concept now applied to an actual weapon system. A generalized autopilot configuration was employed because the main thrust of the study was to develop principles rather than to become involved in an ongoing program. An acceleration autopilot was employed to address the requirement of the Statement of Work.

The two phases of the effort constitute a classical linear analysis of the acceleration loop. The first phase deals with the stipulated AFBGW equipment and involves the conversion of parameters to a form that can be used in the second phase of the analysis. The second phase deals with guidance law synthesis and the effect of nonlinearities on the guidance law formulations and system performance. The interrelation of the two phases is shown in Figure 8.

In detail, Figure 8 shows the relationship among airframe transfer function definition, autopilot transfer function determination, and transit dynamics evaluation. In Phase 1, the airframe transfer function is first determined from the stability derivatives and mass properties of the vehicle. The airframe transfer function is then used in the calculation of the autopilot transfer function, which is the objective of Phase 1.

In Phase 2, the performance of several guidance laws is analyzed. This requires the use of the autopilot transfer function that was derived in Phase 1. It also requires the use of flight parameters—speed and range.

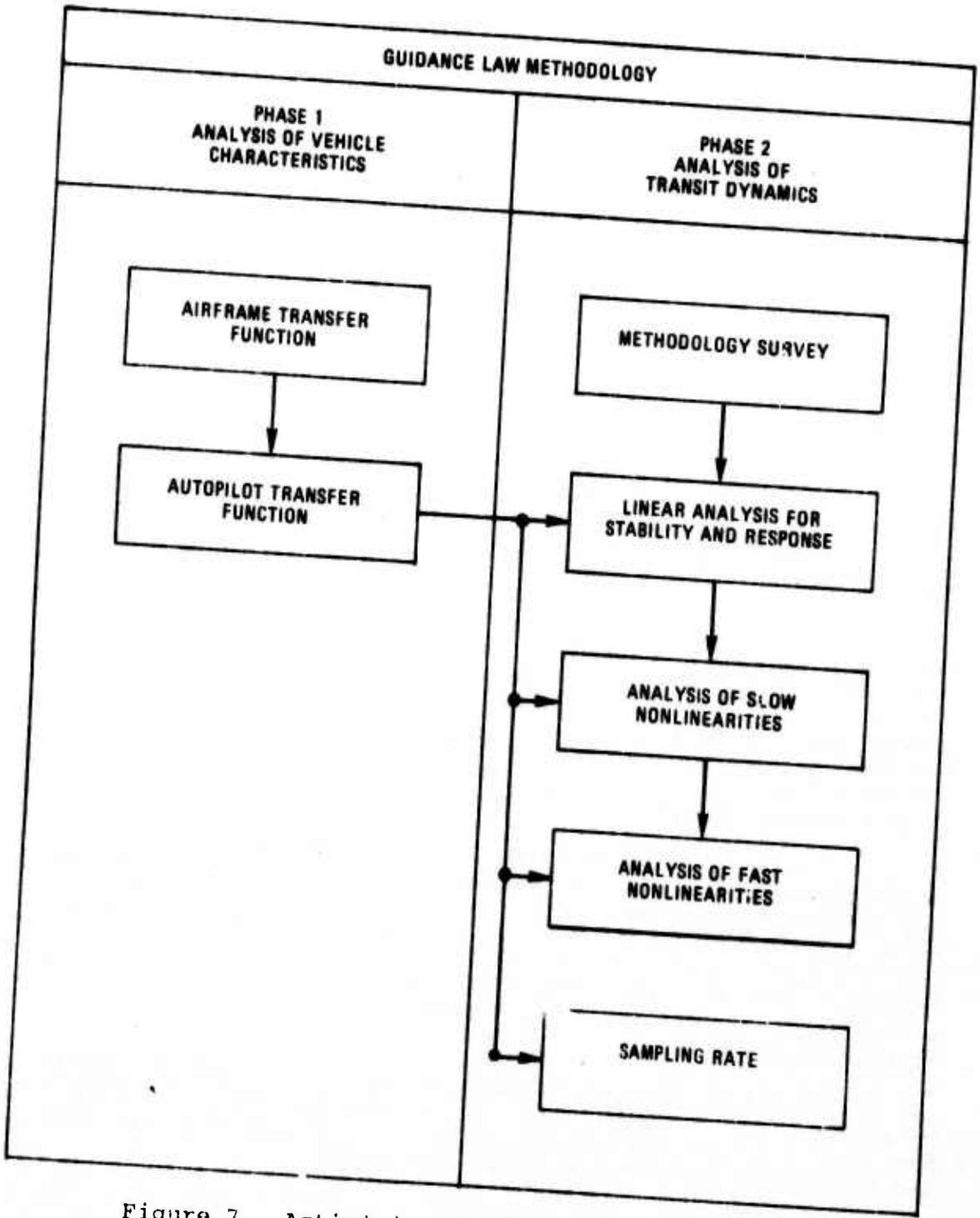

Figure 7. Activities Involved in Guidance Law Methodology Definition

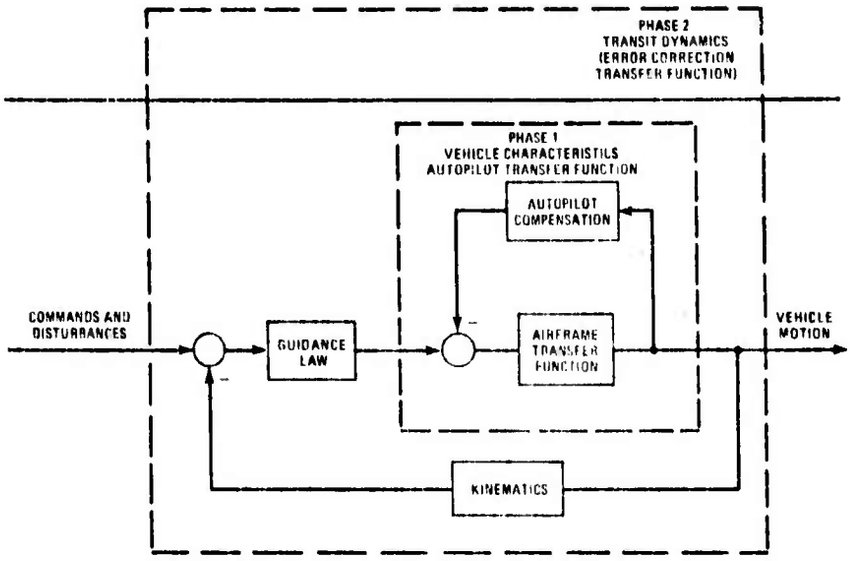

Figure 8. Relationship Between Analysis of Vehicle Characteristics and Transit Dynamics

In Phase 3, the relationship between navigation error and vehicle range is investigated.

ANALYSIS OF VEHICLE CHARACTERISTICS—THE AIRFRAME TRANSFER FUNCTION

The airframe normal acceleration open loop transfer functions are of standard form and are evaluated by use of the mass properties listed in Appendix D, Volume II, and by using stability derivatives derived by classical methods.

The transfer functions are taken from Missile Configuration Design (Reference 7) and are as follows. Pitch or yaw rate open loop transfer function:

$$\frac{\dot{\theta}}{\delta} = \frac{ls^2 - is + c}{s^2 - es - h}$$

where l is $m_{\dot{\delta}}$, i is $f_\delta m_{\dot{\alpha}} - m_\delta - f_\alpha m_{\dot{\delta}}$, c is $f_\alpha m_\delta - f_\delta m_\alpha$, e is $m_{\dot{\alpha}} - f_\alpha + m_{\dot{\theta}}$, and h is $m_\alpha + m_{\dot{\theta}} f_\alpha$. Normal acceleration transfer function (Reference 7):

$$\frac{n}{\delta} = \frac{V\dot{\gamma}}{g\delta} = \frac{V}{g}\left[\frac{as^2 - bs + c}{s^2 - es - h}\right]$$

where a is f_δ and b is $f_\delta m_{\dot{\theta}} + f_\delta m_{\dot{\alpha}} - f_\alpha m_{\dot{\delta}}$. The values that are applied to the equations are given in Tables 19, 20, and 21. The values used in these tables were supplied by Rockwell (Reference 8).

The final calculation for θ/δ and n/δ are given in the lower portion of Table 21. The latter expression was simplified to the following form:

$$\frac{n}{\delta} = -\frac{V}{g}\left\{\frac{K}{s^2 + 2\zeta\omega s + \omega^2}\right\}$$

$$\frac{n}{\delta} = -\frac{V}{g}\left\{\frac{2.885}{s^2 + 2(2.212)(0.07961) + (2.212)^2}\right\}$$

This expression was used in the subsection that follows in calculating the autopilot acceleration loop transfer function.

ANALYSIS OF VEHICLE CHARACTERISTICS—THE AUTOPILOT TRANSFER FUNCTION

This subsection demonstrates the development of the transfer function for the acceleration loop of the autopilot portion of the AFBGW short-range missile control system and is representative of the general autopilot arrangement shown in Figure 9. The airframe transfer function that was developed in the previous section is applied to the block designated "aero." The other transfer functions shown are generalized from Figure B-2 (Appendix B, Volume II) and represent the hard-wired portion of the AFBGW short-range system. The feedback loops (1 and 2) represent the inputs received from rate gyroscope and accelerometer, respectively. The numerical designations of the blocks in this figure correspond to the numerical designations of Figure B-2. The letter designations on the summing junctions also correspond to the letter designations in the summing junctions of Figure B-2. The algebraic reduction of the network is described in the following equations. The general procedure used for the process is

TABLE 19. MASS AND AERODYNAMIC PARAMETERS

SYMBOL	UNITS	SIGNIFICANCE	VALUE	SOURCE
q	$\frac{\text{slug}}{\text{foot/second}^2}$	Dynamic pressure	298	$\frac{1}{2}\rho V^2$
ρ	slug	Density at altitude	5.83×10^{-4}	40,000-foot altitude
S	foot^2	Reference area	1.776	$\frac{\pi}{4} d^2$
d	foot	Diameter	1.5	Appendix B
V	foot/second	Velocity	950	Appendix B
m	slug	Mass	77.6	$\frac{2,500}{32.2}$
W	pound	Weight	2,500	Appendix B
I_{yy}	slug/foot^2	Inertia	670	Appendix B

TABLE 20. STABILITY DERIVATIVES

Symbols				Values		
Parameter	Coefficient	Factor	Factor	Coefficient (Degrees)	Coefficient (Radians)	Parameter Value
f_α	C_{N_α}	$\frac{qS}{mV}$	0.00717	+0.366	+20.97	+ 0.150
f_δ	C_{N_δ}	$\frac{qS}{mV}$	0.00717	+0.147	+ 8.42	+ 0.0603
m_α	C_{m_α}	$\frac{qSd}{I}$	1.134	-0.072	- 4.12	- 4.87
m_δ	C_{m_δ}	$\frac{qSd}{I}$	1.134	-0.314	-17.9	-21.19
$m_{\dot\alpha}$	$C_{m_{\dot\alpha}}$	$\frac{qSd^2}{2VI}$	0.825×10^{-3}	-0.58/sec	-33.23/sec	- 0.0274
$m_{\dot\delta}$	$C_{m_{\dot\delta}}$	$\frac{qSd^2}{2VI}$	0.825×10^{-3}	0	–	0
$m_{\dot\vartheta}$	$C_{m_{\dot\vartheta}}$	$\frac{qSd^2}{2VI}$	0.825×10^{-3}	-3.78/sec	-216/sec	- 0.1782

Required Products

$f_\delta m_{\dot\vartheta}$ = (+0.0603)(-0.1782) = -0.01074

$f_\delta m_{\dot\alpha}$ = (+0.0603)(-0.0274) = -0.001652

$f_\alpha m_{\dot\vartheta}$ = (+0.150)(-0.1782) = -0.02673

$f_\alpha m_\delta$ = (+0.150)(-21.19) = -3.179

$f_\delta m_\alpha$ = (+0.0603)(-4.87) = -0.2937

$f_\delta m_{\dot\delta}$ = (+0.0603)(0) = 0

$f_\alpha m_{\dot\delta}$ = (+0.150)(0) = 0

TABLE 21. TRANSFER FUNCTION COEFFICIENTS

Coefficient	Equation	Substitution	Value
a	f_δ		+ 0.0603
b	$f_\delta m_{\dot\zeta} + f_\delta m_{\dot\alpha} - f_\alpha m_{\dot\delta}$	-0.01074 - 0.001652 - 0	- 0.01239
c	$f_\alpha m_\delta - f_\delta m_\alpha$	-3.179 - (-0.2937)	- 2.885
e	$m_{\dot\alpha} - f_\alpha + m_{\dot\zeta}$	-0.0274 - (+0.150) + (-0.1782)	- 0.3556
h	$m_\alpha + m_{\dot\zeta} f_\alpha$	-(4.87) + (-0.02673)	- 4.896
i	$f_\delta m_{\dot\alpha} - m_\delta - f_\alpha m_{\dot\delta}$	-0.001652 - (-21.19) - 0	+21.19
l	$m_{\dot\delta}$		0

$$\frac{\dot\zeta}{\delta} = \frac{-21.19s - 2.885}{s^2 + 0.3556s + 4.896}$$

$$\frac{n}{\delta} = \frac{V}{g}\left[\frac{0.0603s^2 + -0.01239s - 2.885}{s^2 + 0.3556s + 4.896}\right]$$

$$\frac{\dot\alpha}{\delta} = \frac{ls^2 - is + c}{s^2 - es - h}$$

$$\frac{n}{\delta} = \frac{V\dot\gamma}{g\delta} = \frac{V}{g}\left[\frac{as^2 - bs + c}{s^2 - es - h}\right]$$

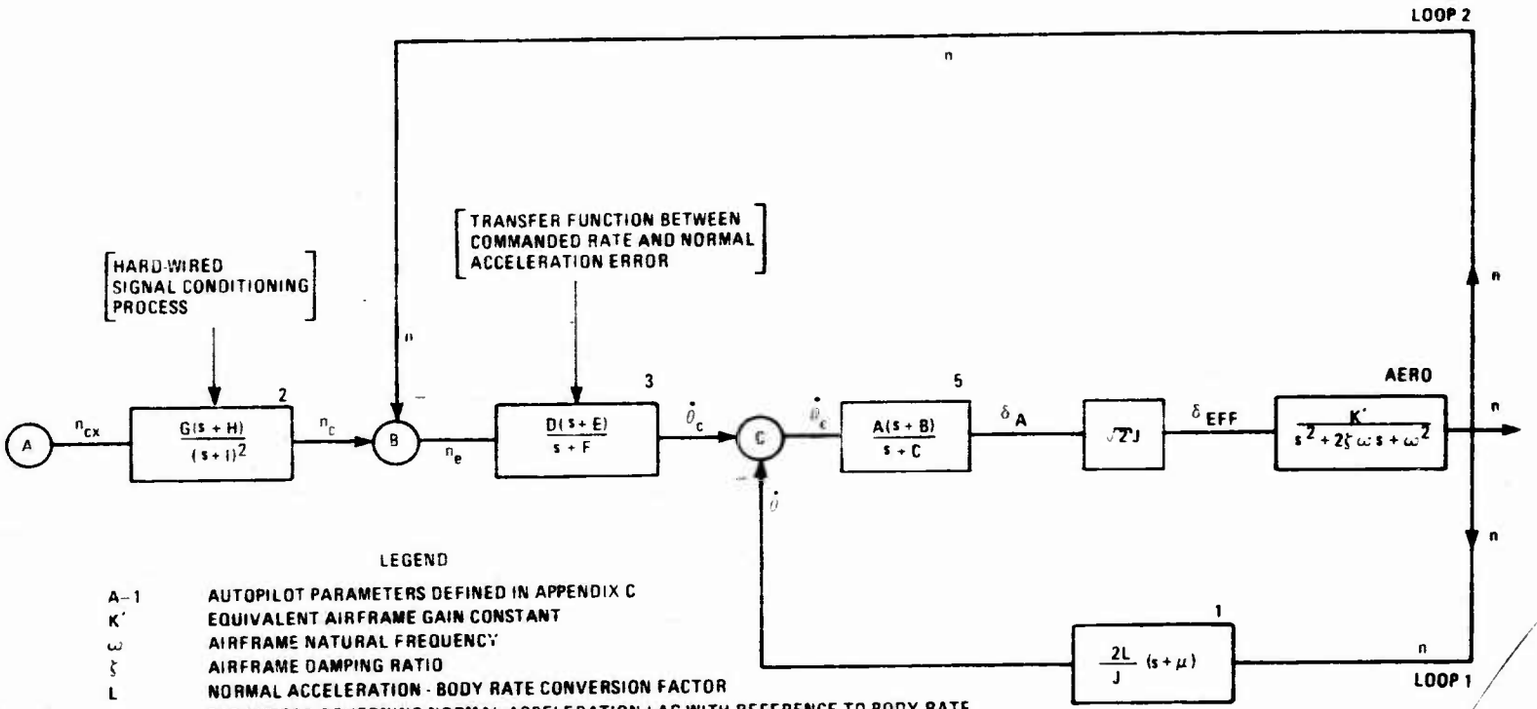

LEGEND

A–1	AUTOPILOT PARAMETERS DEFINED IN APPENDIX C
K'	EQUIVALENT AIRFRAME GAIN CONSTANT
ω	AIRFRAME NATURAL FREQUENCY
ζ	AIRFRAME DAMPING RATIO
L	NORMAL ACCELERATION - BODY RATE CONVERSION FACTOR
μ	PARAMETER GOVERNING NORMAL ACCELERATION LAG WITH REFERENCE TO BODY RATE
J	RADIAN TO DEGREE CONVERSION FACTOR
n_{cx}	EXTERNALLY COMMANDED NORMAL ACCELERATION
n_c	CONDITIONED EXTERNALLY COMMANDED ACCELERATION
n	MISSILE NORMAL ACCELERATION
n_e	DIFFERENCE BETWEEN n_c AND n
$\dot{\theta}_c$	EQUIVALENT COMMANDED ANGULAR RATE
$\dot{\theta}$	MISSILE ANGULAR RATE
$\theta\epsilon$	DIFFERENCE BETWEEN θ_c AND θ
δ_{EFF}	EFFECTIVE CONTROL SURFACE
δ_A	ACTUAL CONTROL SURFACE DEFLECTION (DEG)

Figure 9. Autopilot Normal Acceleration Loop Arrangement

shown in Figure 10, Item 6 of which was used extensively in this instance. (A more comprehensive table is given in Reference 9.)

The first step in the reduction of the loop in Figure 9 to algebraic form is to reduce Loop 1 to transfer function forms. To do this, Item 6 in Figure 10 is applied. The applicable formula is:

$$\frac{n}{\dot{\theta}_C} = G_3 = \frac{K_1 G_1}{1 + (K_1 G_1)(K_2 G_2)}$$

Equating K_1 and K_2 to 1 and substituting N_1/D_1 for G_1, the expression becomes:

$$G_3 = \frac{N_1}{D_1 + N_1 G_2}$$

where N_1 is the numerator of the product of all elements from summing junctions C through the block labeled "aero," D_1 is the denominator of the product of all elements from summing junction C through the block labeled "aero," G_2 is the transfer function of block 1, and G_3 is the transfer function of the complete Loop 1. Therefore:

$$D_1 = (s^2 + 2\omega\zeta s + \omega^2)(s + C) = s^3 + (2\omega\zeta + C)\, s^2 + (\omega^2 + 2\zeta\omega C)\, s + \omega^2 C$$

$$N_1 = \sqrt{2}\, J \cdot A \cdot K'(s + B), \text{ where } K' = \frac{V}{g} K$$

$$G_2 = 2\, \frac{L}{J}\, (s + \mu)$$

As a result, Loop 1 reduces to algebraic form as follows:

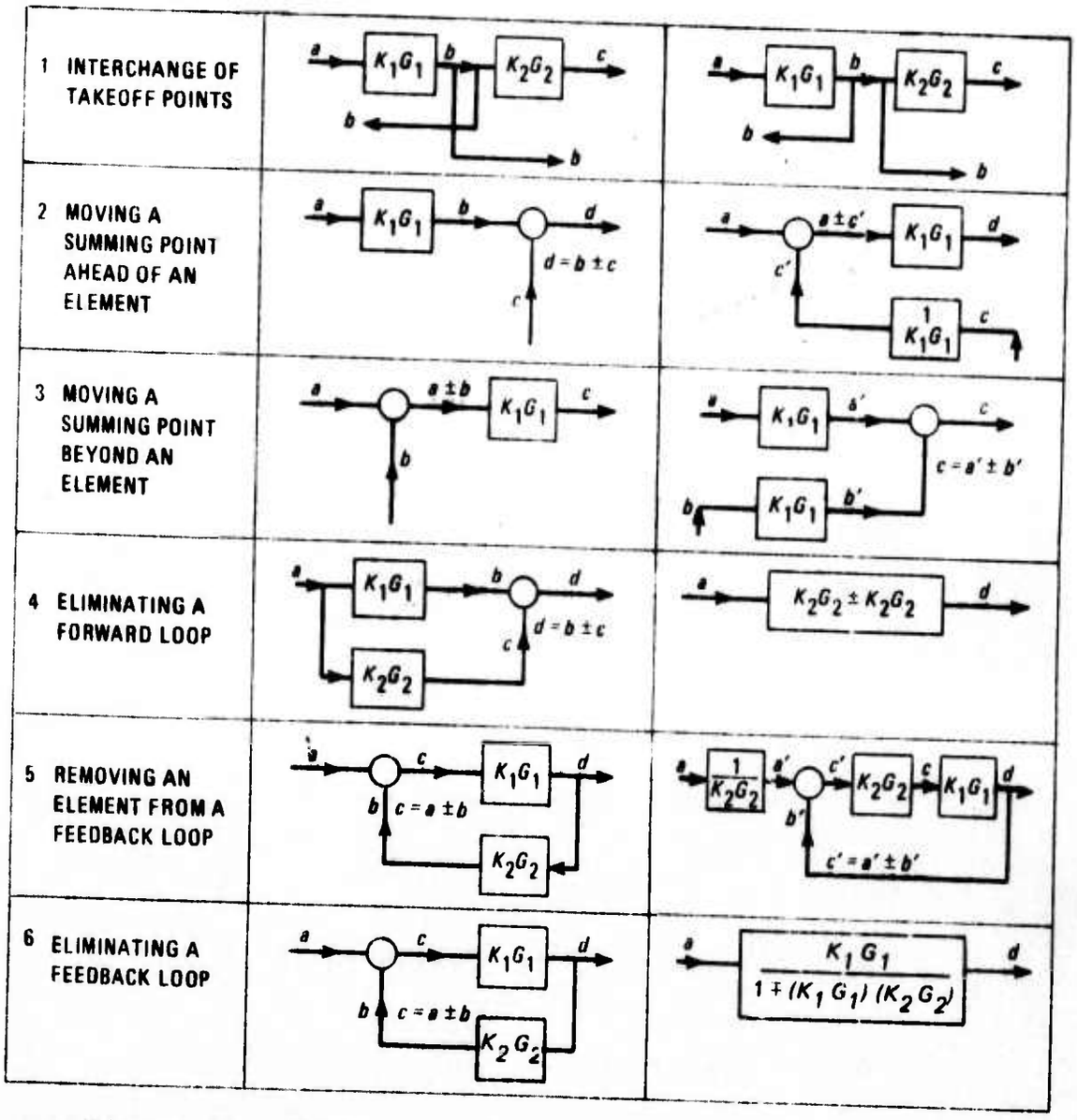

Figure 10. Techniques for Reduction of Block Diagram Elements to Transfer Function Form

$$G_3 = \frac{n}{\dot{\theta}_C} = \frac{N_1}{D_1 + N_1 G_2}$$

$$= \frac{\sqrt{2} \cdot J \cdot AK'(s+B)}{\left\{s^3 + (2\omega\zeta + C)s^2 + (\omega^2 + 2\zeta\omega C)s + \omega^2 C\right\} + \left\{2\sqrt{2}\, AK'L(s+B)(s+\mu)\right\}}$$

This further reduces to:

$$G_3 = \frac{n}{\dot{\theta}_C} = \frac{\sqrt{2} \cdot J \cdot AK'(s+B)}{s^3 + (2\omega\zeta + C + 2\sqrt{2}\, AK'L)s^2 + (\omega^2 + 2\zeta\omega C + 2\sqrt{2}\, AK'L(B+\mu))s + (\omega^2 C + 2\sqrt{2}\, ABLK'\mu)}$$

The diagram of Figure 9 can now be reduced to the following equivalent diagram in which G_3 is substituted for the expression just derived:

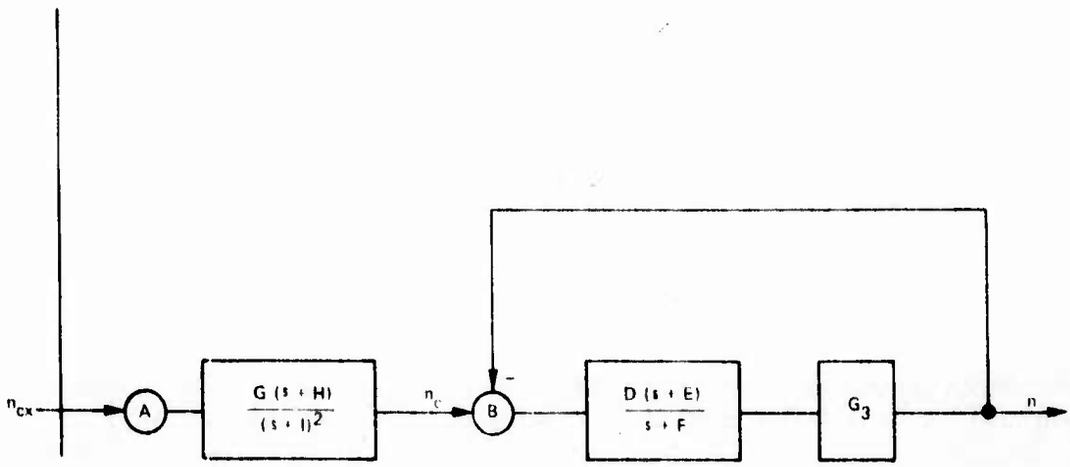

For convenience in algebraic operation, the following substitutions are made:

$$Z_3 = 1$$

$$Z_2 = 2\zeta\omega + C + 2\sqrt{2}\, AK'L$$

$$Z_1 = \omega^2 + 2\zeta\omega C + 2\sqrt{2}\,AK'L\langle B + \mu\rangle$$

$$Z_0 = \omega^2 C + 2\sqrt{2}\,ABLK'\mu$$

and the expression for G_3 now becomes:

$$G_3 = \frac{n}{\dot{\theta}_c}\left\{\frac{\sqrt{2}\,JAK\,(s + B)}{Z_3 s^3 + Z_2 s^2 + Z_1 s + Z_0}\right\}$$

The process used for eliminating Loop 1 in Figure 9 is now repeated to eliminate Loop 2 in Figure 9. The applicable formula is:

$$G_4 = \frac{n}{n_c} = \frac{N_2}{D_2 + N_2}$$

The following is the calculation for D_2:

$$D_2 = \left(Z_3 s^3 + Z_2 s^2 + Z_1 s + Z_0\right)(s+F)$$

$$= Z_3 s^4 + \left(Z_2 + Z_3 F\right)s^3 + \left(Z_1 + Z_2 F\right)s^2 + \left(Z_0 + Z_1 F\right) + Z_0 F$$

Substitution of variables are now made for conciseness of algebraic expression, and the coefficients of D_2 become:

$$Y_4 = Z_3 = 1$$

$$Y_3 = Z_2 + Z_3 F = 2\zeta\omega + C + 2\sqrt{2}\,AK'L + F$$

$$Y_2 = Z_1 + Z_2 F$$

$$= \omega^2 + 2\zeta\omega C + 2\sqrt{2}\,AK'L\langle B + \mu\rangle + \left\{2\zeta\omega + C + 2\sqrt{2}\,AK'L\right\}F$$

$$Y_1 = \left(Z_0 + Z_1\right)F$$

$$= \omega^2 C + 2\sqrt{2}\,ABLK'\mu + \left\{\omega^2 + 2\zeta\omega C + 2\sqrt{2}\,AK'L\langle B + \mu\rangle\right\}F$$

$$Y_0 = \{\omega^2 C + 2\sqrt{2}\ ABLK'\mu\}F$$

The elements to be applied to the formula are now summarized, and the transfer function for Loop 2 is now given:

$$N_2 = \sqrt{2} \cdot J \cdot ADK'(s + B)(s + E)$$

$$D_2 = Y_4 s^4 + Y_3 s^3 + Y_2 s^2 + Y_1 s + Y_0$$

$$G_4 = \frac{n}{n_c} = \frac{N_2}{D_2 + N_2}$$

Therefore:

$$G_4 = \frac{n}{n_c}$$

$$= \frac{\sqrt{2} \cdot J \cdot A\ DK'(s+B)(s+E)}{Y_4 s^4 + Y_3 s^3 + Y_2 s^2 + Y_1 s + Y_0 + \sqrt{2} \cdot J \cdot A\ DK'(s+B)(s+E)}$$

The above denominator is now expanded:

$$Y_4 s^4 + Y_3 s^3 + \left[\sqrt{2} \cdot J \cdot ADK' + Y_2\right] s^2 + \left[\sqrt{2} \cdot J \cdot ADK' <B+E> + Y_1\right] s$$
$$\left[\sqrt{2} \cdot J \cdot ADK' BE + Y_0\right]$$

Substitutions are again made for conciseness and ease of future applications of the formula:

$$X_4 = Y_4 = 1$$

$$X_3 = Y_3 = 2\zeta\omega + C + 2\sqrt{2}\ AK'L + F$$

$$X_2 = Y_2 + \sqrt{2} \cdot J \cdot ADK' = \omega^2 + 2\zeta\omega C$$
$$+ 2\sqrt{2}\ AK'L<B+\mu> + \{2\zeta\omega + C + 2\sqrt{2}\ AK'L\}F + \sqrt{2} \cdot J \cdot ADK'$$

$$X_1 = Y_1 + \sqrt{2}\cdot J\cdot ADK'\langle B + E\rangle$$

$$= \omega^2 C + 2\sqrt{2}\, ABLK'\mu + \left\{\omega^2 + 2\zeta\omega C + 2\sqrt{2}\, AK'L\langle B + \mu\rangle\right\}F$$

$$+ \sqrt{2}\cdot JADK'\langle B + E\rangle$$

$$X_0 = Y_0 + \sqrt{2}\cdot JADK'BE$$

$$= \left\{\omega^2 C + 2\sqrt{2}\, ABLK'\mu\right\}F + \sqrt{2}\cdot J\cdot ADK'BE$$

$$G_4 = \frac{n}{n_c} = \frac{\sqrt{2}\cdot J\cdot A\ DK'(s + B)(s + E)}{s^4 + X_3s^3 + X_2s^2 + X_1s_1 + X_0}$$

The above expression is equivalent to the portion of the network in Figure 9 to the right of summing junction B.

The total autopilot in Figure 9 is given by the following equation:

$$\frac{n}{n_{cx}} = G_4 \cdot \frac{G(s + H)}{(s + I)^2}$$

Therefore:

$$\frac{n}{n_{cx}} = \frac{2\cdot J\cdot ADGK'(s + H)(s + B)(s + E)}{(s + I)^2\left(s^4 + X_3S^3 + X_2s^2 + X_1S + X_0\right)}$$

The availability of the above formula is absolutely essential in the investigation of the stability and response of the autopilot. With the above expression in hand, it is possible to determine how the autopilot will behave in the kinematic loop (see Figure 8). To perform the analysis, the following parametric values are applied to the previous equation:

$K' = \frac{V}{q} K = 85.05$

$\omega = 2.212$

$\zeta = 0.07461$

$\mu = 0.14$

} Obtained from Airframe Data

$A = 0.14$

$B = 10$

$C = 4$

$D = 8$

$E = 4$

$F = 8$

$G = 19.6$

$H = 2.5$

$I = 7$

$J = 57.3$

$L = 0.242$

} Obtained from Figure B-2, Appendix B, Volume II

The terms K', ω, ζ, and μ are taken from the airframe analysis that was conducted in the previous subsection. The upper case letter values (A through I) are obtained from Figure B-2 (Appendix B, Volume II). J is the degree-to-radian conversion factor.

Once reduced to numerical terms, the expression for the autopilot is:

$$\frac{n}{n_{cx}} = \frac{(s + 2.5)(s + 4)(s + 10)(s + 40)}{(s + 7)^2(s + 0.5)(s + 8.05)\left[(s + 5.75)^2 + 7.25\right]}$$

The above expression contains three real roots and two complex roots. The complex roots result from the factor $[(s + 5.75)^2 + 7.25^2]$ and can be expressed in the following form:

$$s + 5.75 \pm 7.25j$$

This form indicates that there are conjugate roots with a real value of -5.75 and an imaginary value of +7.25j and -7.25j. The complex pair can also be expressed in the following form:

$$s^2 + 2\zeta\omega s + \omega^2$$

The corresponding values of the damping rates, ζ, and the natural frequence, ω, are 0.65 and 9.2, respectively, when the form $s^2 + 2\zeta\omega s + \omega^2$ is applied to $[(s + 5.75)^2 + 7.25^2]$. In a system where $[(s + 5.75)^2 + 7.25^2]$ is dominant, the time constant $\doteq 1/\omega$ is 0.108 second, and the response to a step function is characterized by an overshoot of approximately 10 percent. Time constant and overshoot performance are covered in Reference 8 (pages 20-40, Figure 14).

The expression for n/n_{cx} will be used as an input to the following subsection, where analysis will be performed to define the required guidance law for adequate missile course-keeping and course correction.

ANALYSIS OF VEHICLE CHARACTERISTICS—AUTOPILOT GAIN VARIATIONS

The remainder of this subsection will examine the impact of variation of the autopilot gains. There are two reasons for this examination. The first is to make sure that slight variations in the airframe and autopilot parameters do not materially affect the guidance law selection methodology. The second is to determine whether slight variations in the autopilot and airframe parameters could lead to improvements in this overall performance of the guidance system.

In the following discussion, the root locus method is used to examine the variations in autopilot and airframe parameters that relate to Figure 9. Excellent explanations of these methods may be found in both Grabbe (Reference 9)

and Truxal (Reference 10); in essence, the root locus consists of a plot of the movement of the roots of the closed loop of the transfer function as the loop gain is increased. The following performance characteristics are associated with the geometry of these plots:

- If the root is to the left of the imaginary axis (a), then the system is stable.
- The reciprocal of the real part of the root (σ value) approximates the effective time constant of the system.
- A system whose dominant root has a real value (σ) that exceeds the imaginary value (j) usually exhibits good response characteristics.

The open loop transfer function includes the elements within Loop 1 and is given by the following expression:

$$\frac{\dot{\theta}}{\dot{\theta}_{\epsilon}} = \frac{\sqrt{2} \cdot J \cdot A \cdot (s + B)(K')(2L)(s + \mu)}{J\,(s + C)(s^2 + 2\zeta\omega s + \omega^2)}$$

From the general form for the closed loop transfer function, G(s)/1 + G(s)H(s), the general expression for G(s)H(s) is:

$$G(s)H(s) = \frac{\bar{K}\,(s + s_1)(s + s_3)(s + s_5) \cdots (s + s_{an+1})}{(s + s_2)(s + s_4)(s + s_6) \cdots (s + s_{2n})}$$

The loop gain is given as:

$$\bar{\bar{K}}, \text{ loop gain, } = \frac{\bar{K}\,(s_1)(s_3)(s_5) \cdots (s_{2n+1})}{(s_2)(s_4)(s_6) \cdots s_{2n}}$$

$$\therefore G(s)H(s) = \bar{\bar{K}}\,\frac{\left(\frac{s}{s_1} + 1\right)\left(\frac{s}{s_3} + 1\right) \cdots \left(\frac{s}{s_{2n+1}} + 1\right)}{\left(\frac{s}{s_2} + 1\right)\left(\frac{s}{s_4} + 1\right) \cdots \left(\frac{s}{s_{2n}} + 1\right)}$$

and when $\bar{\bar{K}} = 0$, the system is an open loop. For the inner pitch loop:

$$\bar{\bar{K}} = \frac{\sqrt{2}\, J \cdot A \cdot K' \cdot 2L}{J} \quad \frac{B \cdot \mu}{C\omega^2} = K \frac{B\mu}{C\omega^2} = \bar{K} \cdot \frac{10 \times 0.14}{4 \times (2.212)^2} \quad \bar{\bar{K}} = \frac{\bar{K}}{13.97}$$

If the baseline values mentioned in the previous subsection are entered in the equation, the following transfer function results:

$$\frac{\dot{\theta}}{\dot{\theta}_\epsilon} = \frac{1}{13.97} \bar{K} \left\{ \frac{(s + 10)(s + 0.14)}{(s + 4)\left(s^2 + 2 \cdot 0.07961\ 2.212 \cdot s + 2.212^2\right)} \right\}$$

Figure 11 is a root locus of this simplified pitch loop (inner loop of Figure 9).

The system has a real root at $\sigma = -4$, complex roots at $(-0.16 + 2.2j)$, a zero at $\sigma = -0.14$, and a zero at $\sigma = 10$. The complex roots combined with the zero at 0.14 represent the angular rate response of the airframe to a control surface deflection. The open loop system has a damping ratio of 0.075 and a time constant of 6 seconds for the settling envelope and 0.5 second for this initial peak.[a]

Variations in loop gain are obtained by varying $\bar{K}$, which is achieved by changing electromechanical gains in the electronic equipment on the missile.

Using the data previously defined to match the autopilot data with that in Appendix B, Figure B-2, Volume II:

$$\bar{K} = \sqrt{2} \cdot (0.14)(85.05)(2)(0.249) = 8.2$$

Note, therefore, in Figure 11, that as $\bar{K}$ is increased from 0, the location of the open roots, roots r_1 and r_2, moves along path (a) until at $\bar{K} \doteq 8.2$ the autopilot in Appendix B is represented. This occurs at $r_1 = 6.065$.

---

[a] The significance of root locus time constants and their relationship to system responses is discussed in Reference 9, pages 22-05.

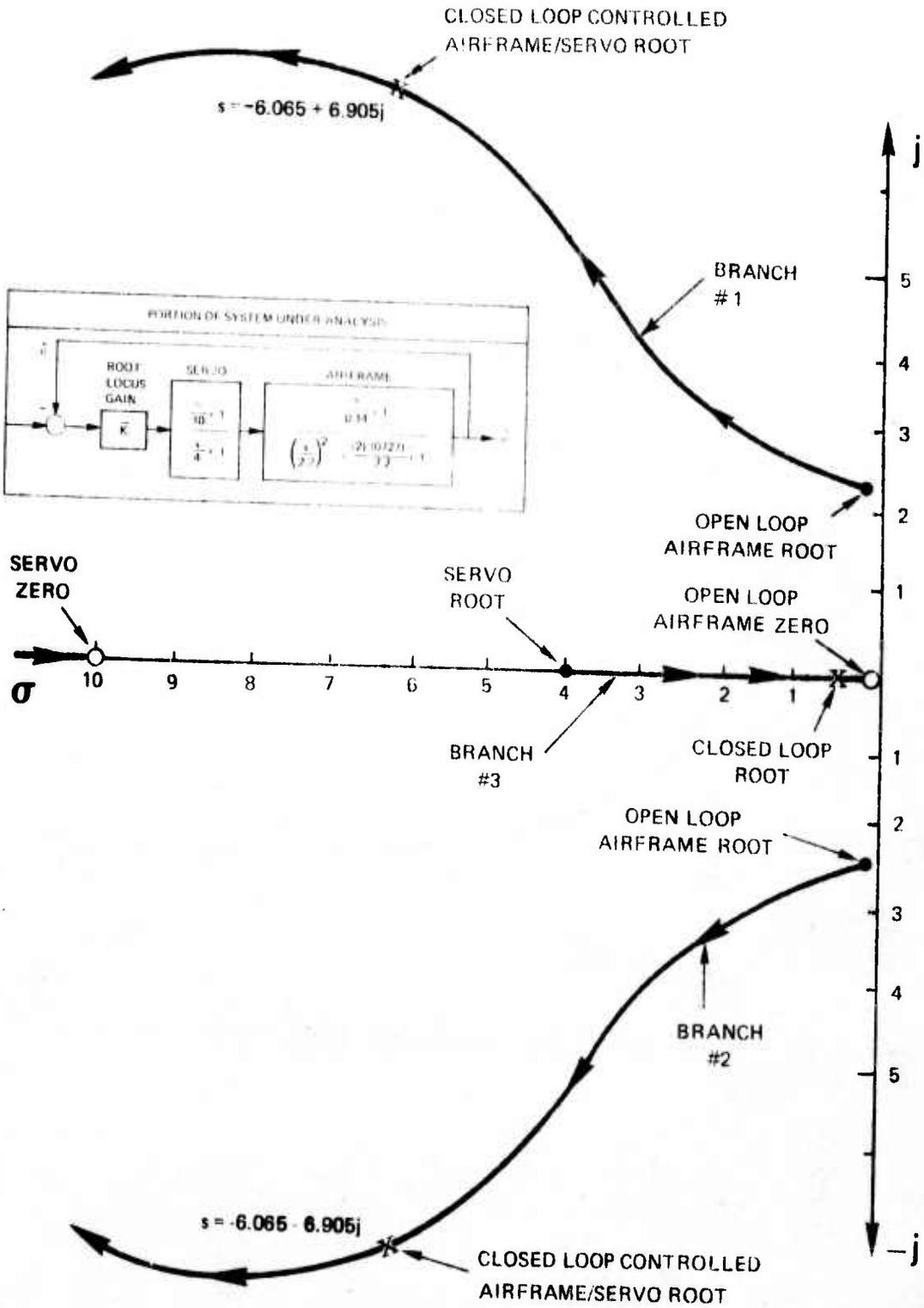

Figure 11a. Root Locus for Simplified Pitch Loop

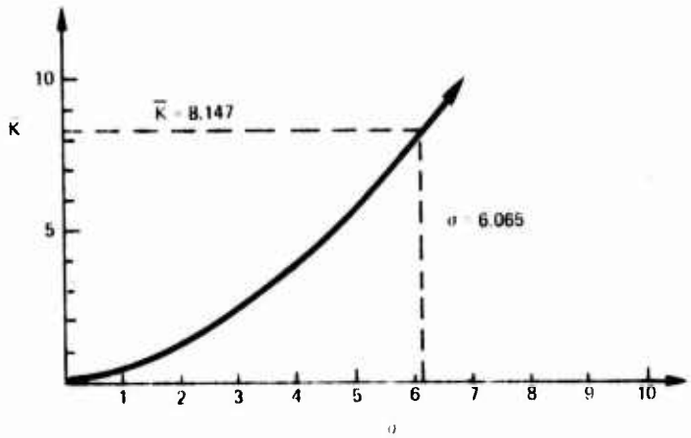

Figure 11b. K Versus σ for Branches 1 and 2

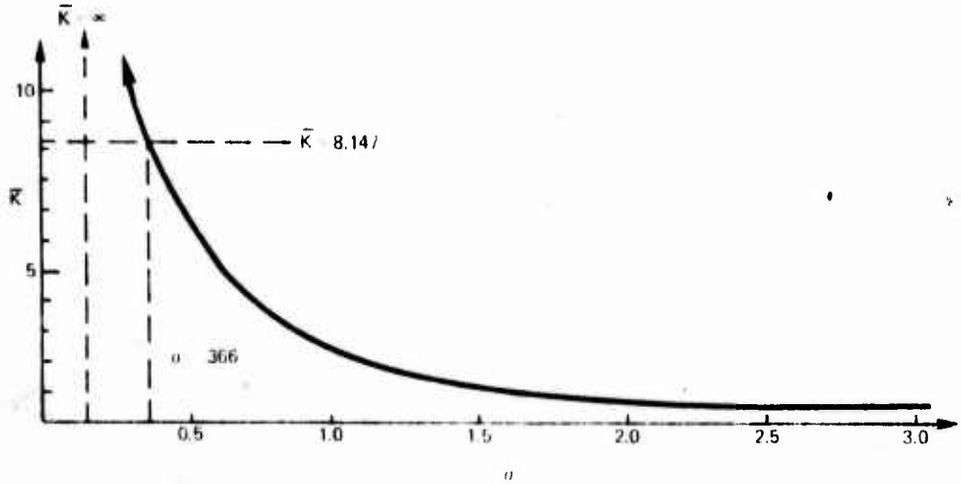

Figure 11c. K Versus σ for Branch 3

Note from Figure 11a that the Rockwell airframe transfer function is:

$$\frac{\dot{\theta}}{\delta_C} = \frac{\frac{s}{0.14} + 1}{\left(\frac{s}{2.2}\right)^2 + \frac{(2)(0.0727)s}{2.2} + 1}$$

the Rockwell open loop airframe transfer function is:

$$\frac{\dot{\theta}}{\dot{\theta}_c} = (\bar{K}) \left\{ \frac{\frac{s}{10} + 1}{\frac{s}{4} + 1} \right\} \cdot \left\{ \frac{\frac{s}{0.14} + 1}{\left(\frac{s}{2.2}\right)^2 + \frac{(2)(0.0727)s}{2.2} + 1} \right\}$$

$$\bar{K} = 8.147$$

the Rockwell airframe/servo transfer function is:

$$\frac{\dot{\theta}}{\dot{\theta}_c} = (22) \left\{ \frac{(s + 10)(s + 0.14)}{(s + 0.366)\left[(s + 6.065)^2 + 6.905^2\right]} \right\}$$

In the selection of an acceptable transfer function by variation of $\bar{K}$, as in Figure 11, a certain degree of compromise is involved. For example, it is desirable to move r_1 as far out as possible while keeping r_3 away from the origin, since as $\sigma(r_3)$ increases, the system damping ratio increases. Such a compromise has been attained at $\bar{K} = 8.147$ where the airframe has the following transfer function:

$$\frac{\dot{\theta}}{\dot{\theta}_\epsilon} = \frac{(0.295)(s + 0.14)(s + 10)}{(s + 0.366)\left[(s + 6.065)^2 + 6.905^2\right]}$$

This value can be checked by referring to the equation for G_3, which corresponds to the closed loop transfer function of the pitch loop:

$$G_3 = \frac{n}{\dot{\theta}_c} = \frac{2\sqrt{2}\ J \cdot A \cdot K(s + B)}{Z_3 s^3 + Z_2 s^2 + Z_1 s_1 + Z_0}$$

When the Z_i values are calculated, as indicated earlier, and placed in the equation, the denominator for the baseline autopilot becomes:

$$G_3 = \frac{n}{\dot{\theta}_c} \left\{ \frac{2\sqrt{2}\ J \cdot A \cdot K(s + B)}{s^3 + 12.5\ s^2 + 88.72\ s + 30.94} \right\}$$

Although the numerators of these transfer functions differ, the denominators are the same and serve as a check on the accuracy of the calculations to this point.

The preceding equation for θ/θ_c gives a time constant of 2.73 seconds and a damping ratio of 0.65 (8 percent overshoot in response to a control surface command).

Figure 12 is a root locus of the acceleration loop (Loop 2). The roots and zeros from Figure 12 are added to those in block 3 of Figure B-2. (The zero at 40 was found to have a negligible effect on the aspects of performance being reviewed here and was consequently omitted from these calculations.) When the loop is closed (summing point B of Figure B-2), the roots move as indicated (Reference 9). The gains that correspond to real root values are shown on the attached gain curves.

ANALYSIS OF TRANSIT DYNAMICS

This subsection presents the results of the guidance law definition methodology effort. This effort employed the survey information to assess practices in guidance law definition, followed by a linear analysis phase in which a portion of the methodology is demonstrated. This demonstration employs data developed in the previous subsection.

Figure B-2 indicates a K value of 2.5, giving the following closed loop transfer function:

$$\frac{n}{n_c} = \frac{(s + 10)(s + 4)(s + 40)}{(s + 8.12)\left[(s + 5.75)^2 + 7.25^2\right](s + 0.68)}$$

The resulting transfer function of the system differs little from that of the open loop. The time constant is reduced 1.5 seconds, and the damping ratio is 0.64.

The primary variables applied to this analysis are line-of-sight (LOS), LOS rate, and LOS acceleration. This was done to make the concept compatible with the terminal guidance mode. LOS and its derivatives, used in the midcourse guidance phase, will be derived from offset reference data. As is indicated in Figure 13, division by R′ will produce the desired synthetic LOS data.

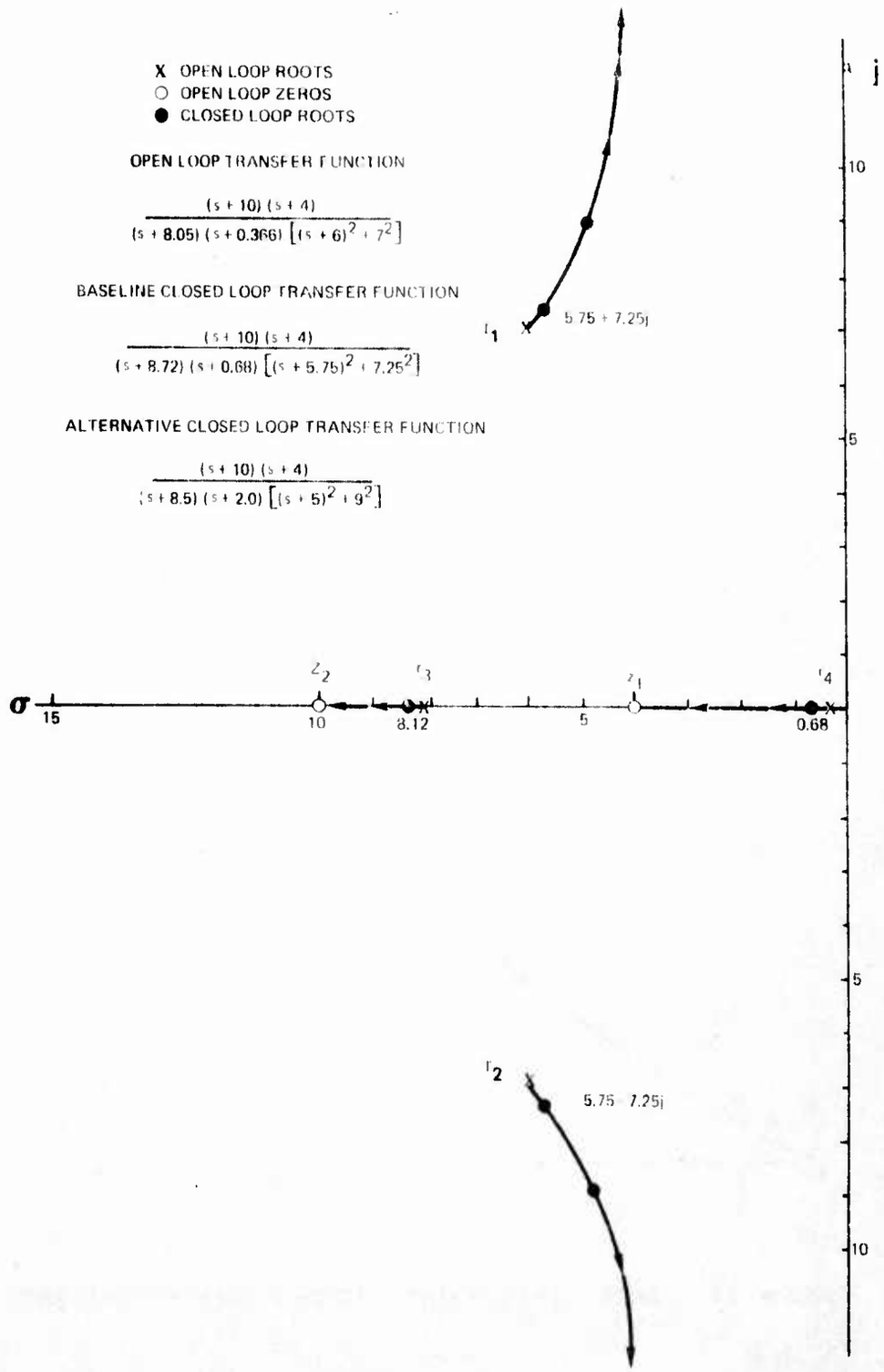

Figure 12. Acceleration Loop Root Locus

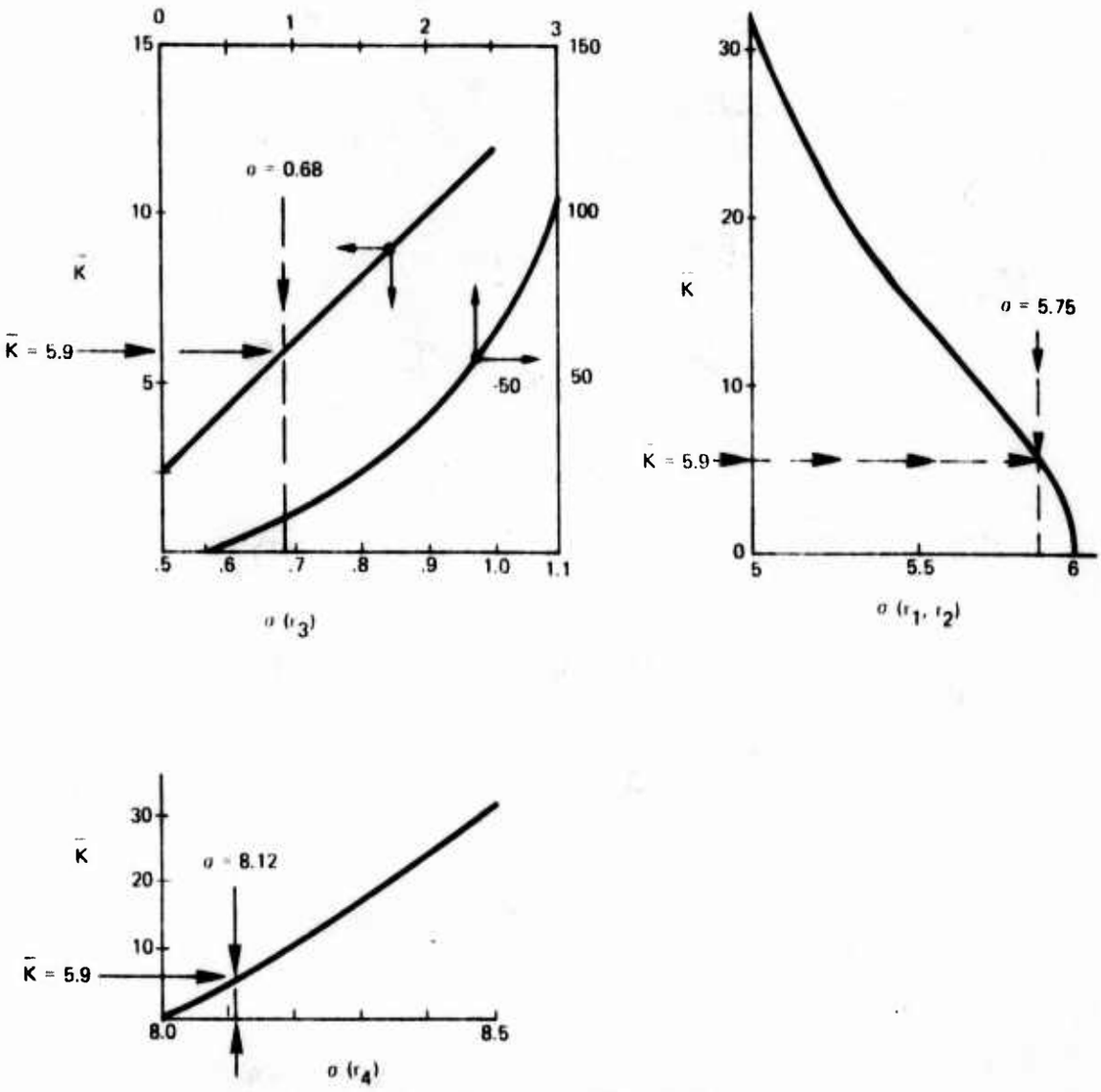

Figure 12. Acceleration Loop Root Locus (Concluded)

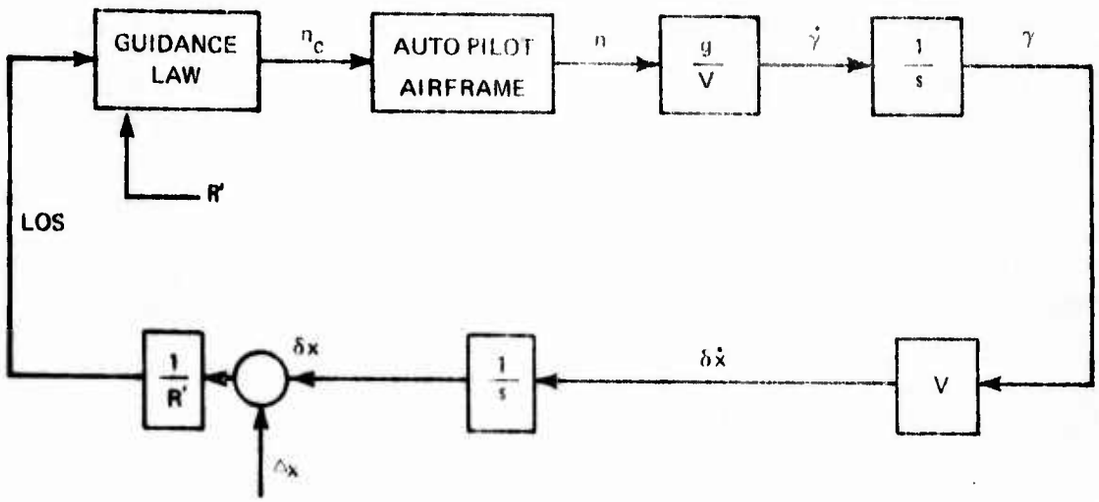

n_c	COMMANDED ACCELERATION
n	ACCELERATION
$\gamma, \dot{\gamma}$	DIRECTION OF MOTION AND TIME DERIVATIVE
$\delta x, \delta \dot{x}$	POSITIONED OFFSET (MISS) AND TIME DERIVATIVE
LOS	LINE OF SIGHT ERROR
Δx	CHANGE IN FLIGHT PATH
g	GRAVITATIONAL CONSTANT
V	MISSILE VELOCITY
R'	RANGE TO TARGET
$\dot{R}'$	TARGET RANGE RATE

Figure 13. AFBGW Kinematic Loop

The relationship of the guidance law, the material developed in the previous subsection, and flight kinematics is shown in Figure 13.

The diagram illustrates the response of the missile to distrubances and corrective commands. Disturbances (lateral motions of target or missile) enter the loop at the summing junction. The missile interprets them as angular offsets. The guidance law converts them to acceleration commands (n_c). The autopilot and airframe convert these to a flight path turning rate ($\dot{\gamma}$). This results in a variation of the missile flight path (γ), and ultimately a correction of the aimpoint (δx).

The central issue of guidance law may be summarized in the following question: "How does one define a guidance law so that the above steps occur in an orderly and controlled manner?" The material that has been developed in this section provides a basis for addressing this question in terms that relate specifically to AFBGW. This subsection is devoted to developing two alternative guidance laws that satisfy this question.

ANALYSIS OF TRANSIT DYNAMICS—METHODOLOGY SURVEY

During the survey, an attempt was made to assess the status of guidance system design practice and to evaluate results. Performance records of actual guidance mechanizations involving missile systems that employ strapdown sensors were unavailable because of their proprietary nature. Space and terrestrial systems were reviewed, however, that gave some indication of the types of problems that may be encountered in design and operation. The approach used in guidance law synthesis was found to be fairly uniform for all applications reviewed. The following sequence shows representative guidance law synthesis methodology:

1.* Reduction of the guidance loop to literal form in three major axes.

2.* Root locus analysis.

---

* These items are demonstrated subsequently in this section. The remaining six items are normally part of an in-depth engineering design and are beyond the scope of this study.

3.* Bode plot, Nyquist, Nichols analysis for special features.

4.* Describing function and phase plane analysis to account for fast nonlinearities (nonlinearities that cannot be compensated by gain variation in real time).

5. Reduction of cross-coupling loops to literal form and application of Steps 2 to 4.

6. Approximation of major loops with second-order systems and setting of the computation rate at 10 times the effective time constant of the equivalent system.

7. Optimization of the system for the disturbances it will experience.

8. Performance analysis.

9. Simulation in increasing degrees of freedom.

10. Hybrid simulation that includes hardware.

The preceding comments relate to linear systems and their control. Nonlinear techniques were also reviewed, and their application was found appropriate under the following conditions: (1) the vehicle and its control system have a combined frequency response that exceeds the disturbance spectrum cutoff by a factor of five or more; and (2) extensive resources are available for the simulation and test associated with the experimental verification of stability and response. Since the above conditions seem to impose stringent constraints on program resources and operational flexibility, this study emphasized linear synthesis by root locus procedure.

In general, the configuration defined by root locus analysis constitutes an upper performance limit for any system. Cross-coupling, nonlinearities, and system dead zones tend to cause instability. Gains set to give equivalent damping ratios of 0.1 to 0.25 in Step 2 above often result in instability in Steps 9 or 10.

---

* These items are demonstrated subsequently in this section. The remaining six items are normally part of an in-depth engineering design and are beyond the scope of this study.

The data rate for a digital system may be safely set at 10 times the equivalent second-order system or 10 times the highest lead term, whichever is greater. A ratio of 10:1 approximates a continuous system with sufficient fidelity to obviate Step 7, above. Ratios between 5 and 10 often result in the need for close examination of the sample data aspects of the system. When the ratio drops to 3, system performance is usually marginal.

Of the systems reviewed in which substantive performance data were obtained, one of the most interesting was the MARK 30 target torpedo. The system employs three rate gyroscopes with a velocity sensor in the dead reckoning mode. It employs an inertial reference to close the vertical accelerometer loop. The system employs a second-order Runge-Kutta direction cosine algorithm. The system was designed for an Omega update, but this feature has not been implemented.

The following general rules of thumb were advocated by system designers who were interviewed:

- Maintain a minimum time constant of $\tau = 0.5$ for Mach 0.6 to 1.6 missiles to keep dynamic lag from contributing to terminal error.
- Maintain a 30-degree positive phase margin in the rigid body linear analysis to assure adequate margin when nonlinearities and body bending modes are examined.
- Maintain a 6-db position gain margin for the same reasons.
- Keep overshoot in response to a step input below 25 percent—damping ratios (ζ) greater than 0.4 (see Figures 14 and 15).

ANALYSIS OF TRANSIT DYNAMICS—LINEAR ANALYSIS FOR STABILITY

This subsection first develops the effect of alternative guidance laws on the performance of the guidance loop, using the transfer function previously defined to be compatible with the current AFBGW autopilot. This is followed by an examination of the effect of varying the feedback gains of the autopilot.

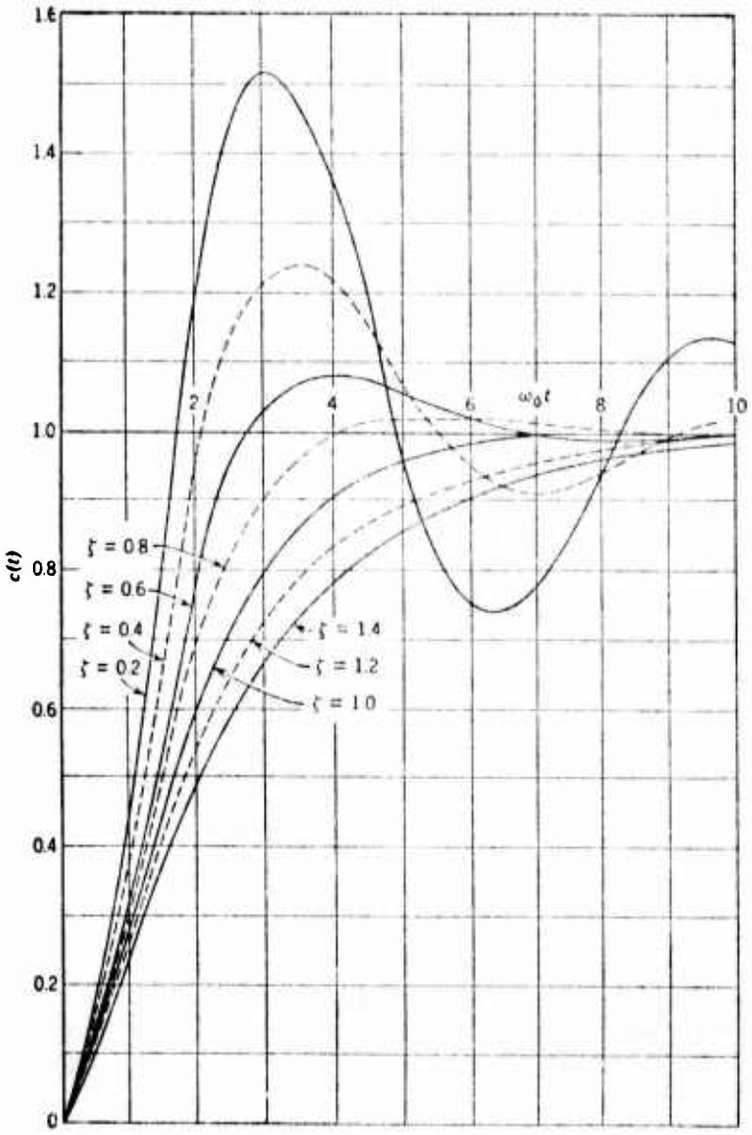

Figure 14. Relationship Between Damping Ratio (ζ) and Time Response for $G(s) = K(s^2 + 2\zeta\omega s + \omega^2)$ (References 10, Pages 20-40)

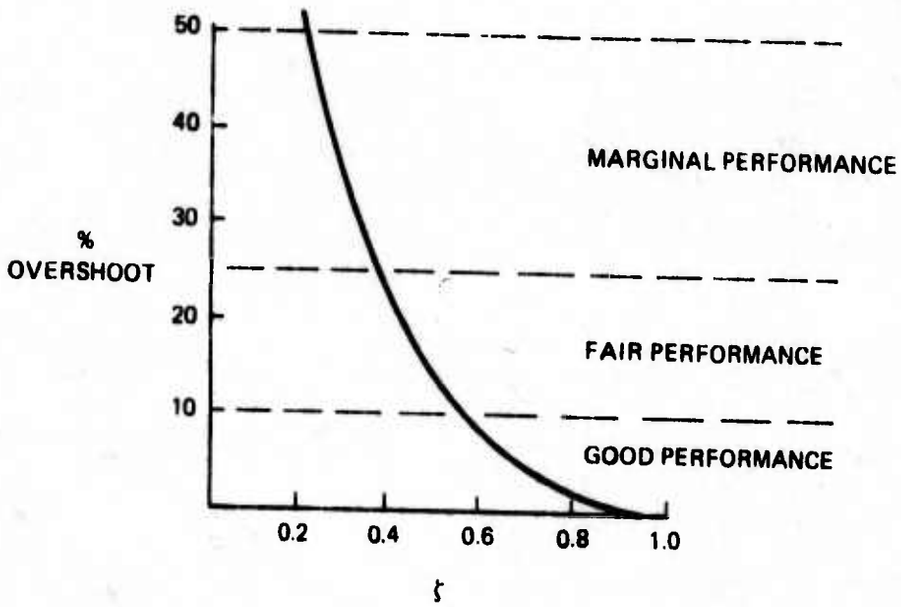

Figure 15. Overshoot Versus Damping Ratio (ζ) for Step Function Response of Systems of the Form $G(s) = K(-s^2 + 2\zeta\omega s + \omega^2)$ (Reference 10, Pages 20-40)

Guidance Law Derivation Using the Baseline Autopilot

Referring to Figure 13, the problem of guidance law derivation may be reduced to a feedback compensation exercise. The guidance law is of the form $n_c = f(LOS)$, where f(LOS) can be of the form $k''s^2 + k's + k$. It is desired to close the kinematic loop around the δx output so that the errors in the system can be cancelled. This can be done by introducing a gain k in the loop. The observed position error indication δx is then nulled by a signal proportional to the uncorrected error. However, with practical autopilots, it is very difficult to maintain a stable system with LOS error feedback (Reference 11).

The problem is illustrated in Figure 16. The missile control system, corresponding to Figure 9, is placed in the autopilot/airframe box of the kinematic loop of Figure 13. All of the roots of the transfer functions within the loop are plotted on Figure 16.

The roots at the origin, r_3, and r_4, result from the kinematics of the loop of Figure 13 (q/v, 1/s, V, 1/s). The roots at -8.12 (r_8) and $-5.75 \pm 7.25j$ (r_1, r_2) are a part of the airframe/autopilot transfer function that was displayed in Figure 12. The roots at -7 (r_6, r_7) are also a part of the autopilot. Autopilot zeros occur at -2.5, -4.0, -10 (Z_1, Z_2, Z_3) and at 40 (not shown).

The above roots are the open loop roots or roots for $K = 0$. (The significance of $\bar{K}$ is discussed in detail in the subsection Vehicle Characteristics—Autopilot Gain Variations. As $\bar{K}$ is increased in value, a locus path occurs to the right of the ω axis. This is indicative of unconditional instability (Reference 8, pages 21-46). One method of correcting this instability is to introduce lead in the form of LOS rate feedback. In supplying angular rate feedback (LOS rate feedback), there are two conditions that must be met. The LOS rate must be an observable physical quantity, and it must be of adequate quality (sufficient signal-to-noise ratio). Angular rate must be observable as a physical phenomenon, and it must be sufficiently noise free to provide accurate performance.

An observable signal of quality is provided, and a guidance law of the type $(\dot{LOS})K'$ may be introduced; the result is shown in Figure 17. There are two problems with the system represented by Figure 17. First, since it is a pure $(\dot{LOS})$ system, K' has some finite value, and K is equal to zero, there will be some finite angular error, which will grow as the flight proceeds. To correct this problem would require

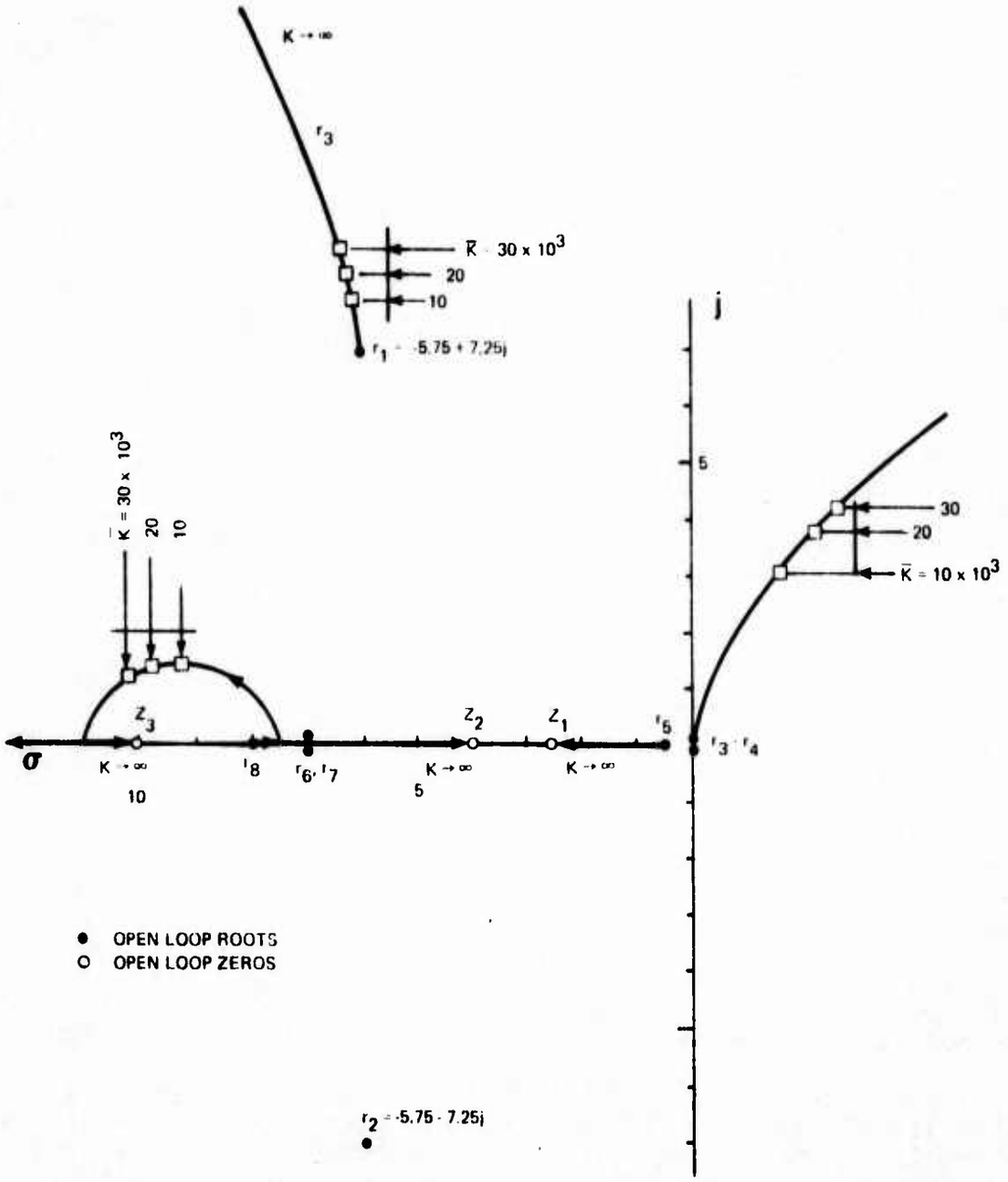

Figure 16. Root Locus for Line-of-Sight Feedback—Acceleration Autopilot

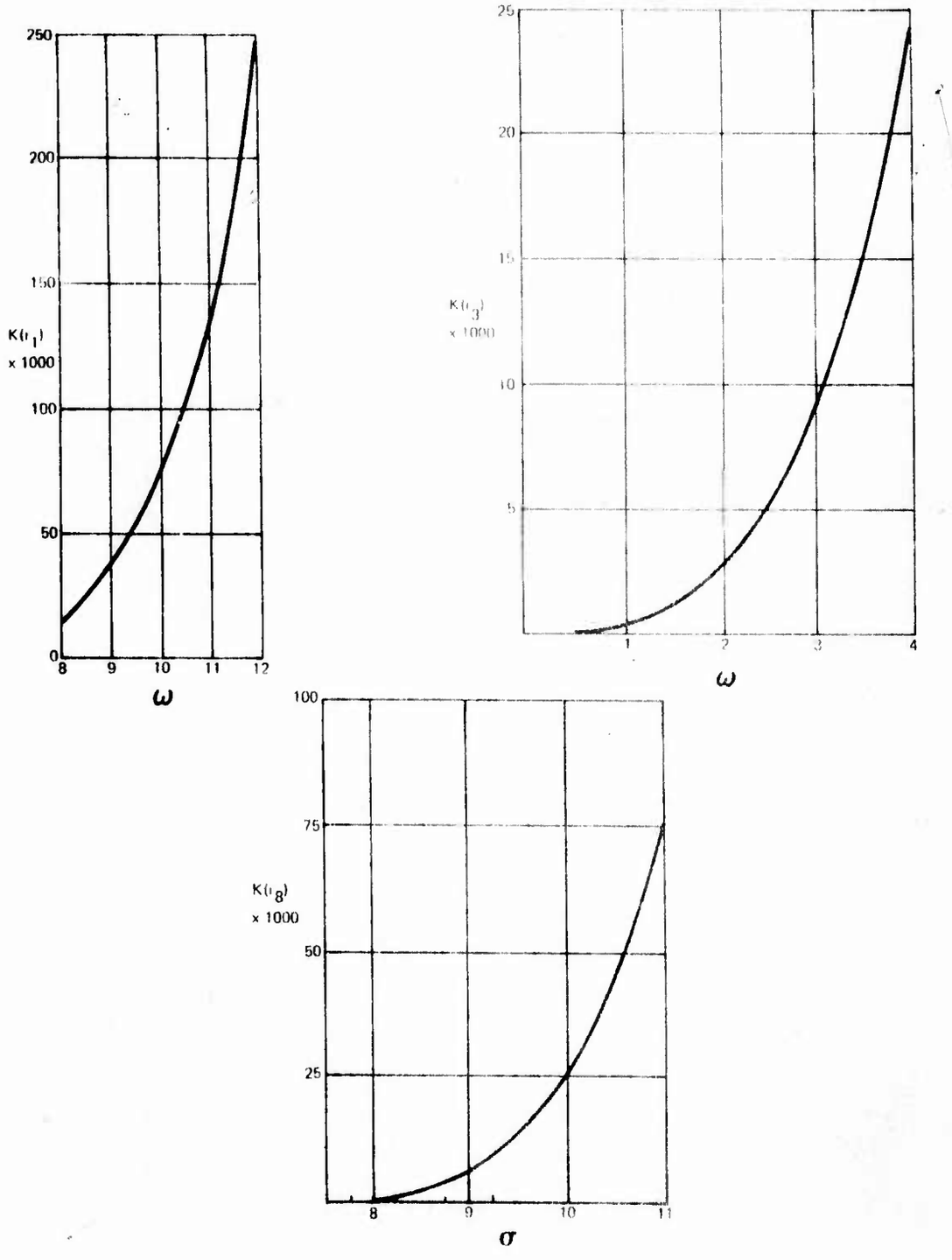

Figure 16. Root Locus for Line-of-Sight Feedback—Acceleration Autopilot (Concluded)

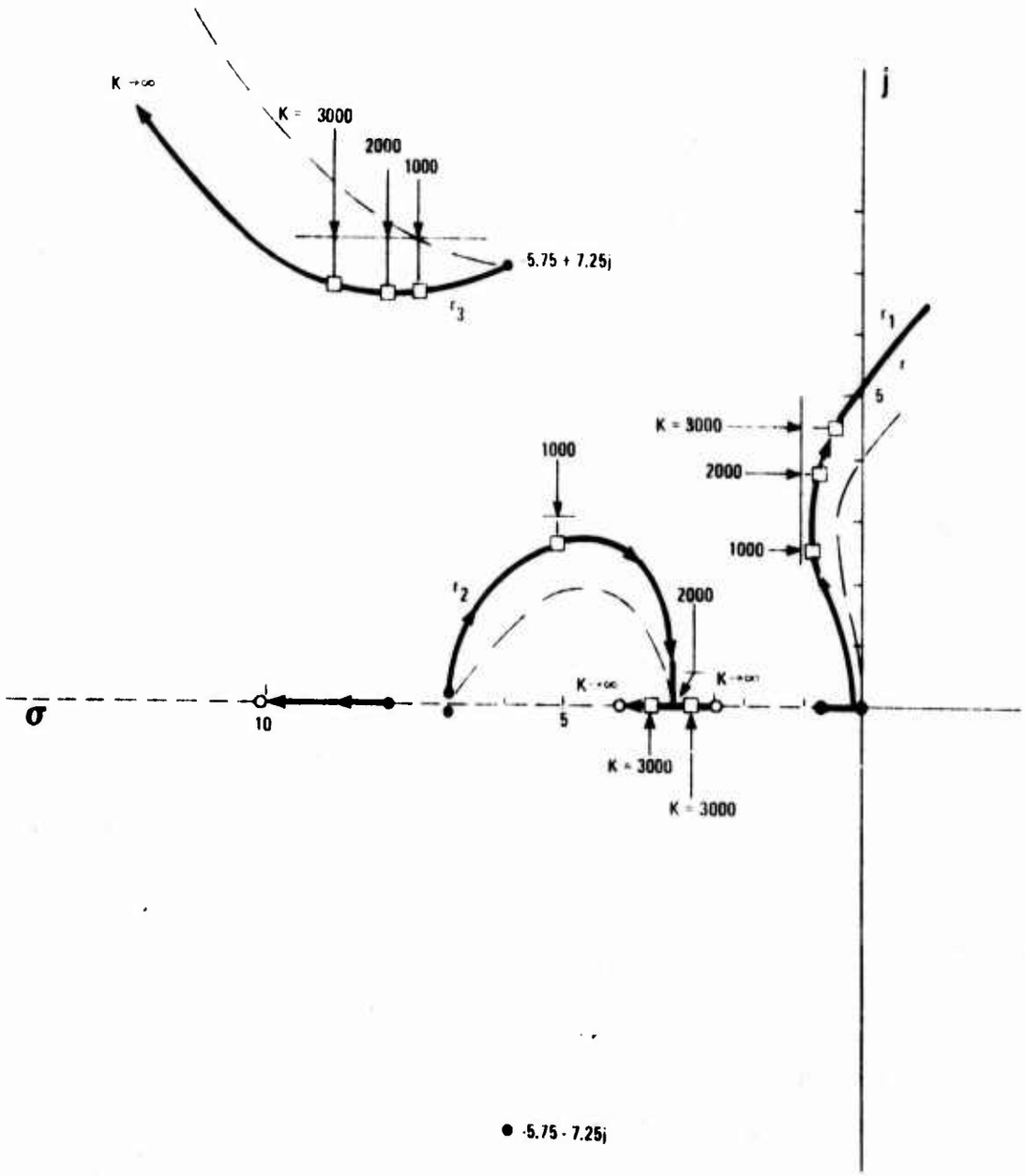

Figure 17. Root Locus for Angular Rate Compensation—Initial Autopilot

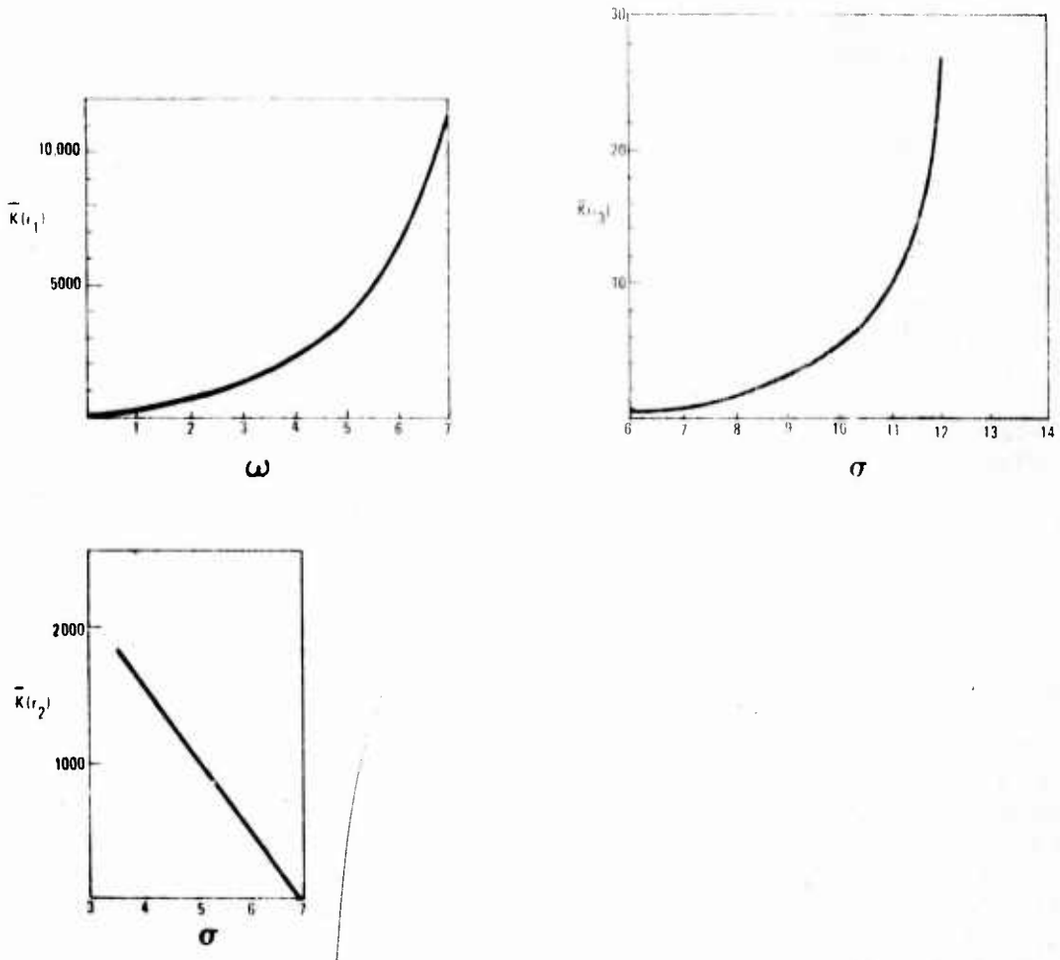

Figure 17. Root Locus for Angular Rate Compensation—Initial Autopilot (Concluded)

providing a (k's + k) expression in the guidance law of Figure 13. This would displace the root locus as illustrated qualitatively in Figure 17, resulting in a reduced stability margin.

This leads to the second problem: The r_1 branch in Figure 17 indicates a lack of good response in its present form. As soon as the r_1 branch leaves the σ axis, its damping characteristics become very poor. It will never achieve an overall response time constant greater than 4 seconds. Adding k feedback would make the situation worse by driving the r_1 branch in the direction of the ω axis more quickly.

One conceivable alternative to this problem is to substitute a k" compensation in the loop; that is, a guidance law of the form $n = k''(\ddot{LOS})$. The root locus of a k" guidance system is shown in Figure 18. At a K of 500, the system has a time constant of 1.0. The dominant root is on the real axis, so there will be no overshoot in the response of the system to $\ddot{LOS}$ correction commands. The complex root system originating at r_1 will have a secondary impact on step function response. At a K of 500, the system will have a damping ratio of 0.3. This will result in a 30 percent deviation from the first-order lag response line governed by the r_3 root branch.

The k" system, while mathematically sound, is probably not practical for this application, since $\ddot{LOS}$ is not an observable quantity. This is not an insurmountable obstacle because the guidance loops being discussed are synthetic loops. The system is not faced with stringent real-time response requirements. Since the objective is merely to transport the vehicle from one position to another, $\ddot{LOS}$ values can be synthesized or derived rather than measured. Note that the above system will have a drift proportional to the square of flight time, since there is no angle or angle rate reference. The resulting position errors can be corrected by discrete inputs during the midcourse guidance phase.

Guidance Law Derivation With Autopilot Variation

The detailed investigation of the above procedure indicates that the resulting mechanization will be unduly cumbersome; consequently, an alternative approach is presented in the following paragraphs, in which feedback gains of the autopilot are varied.

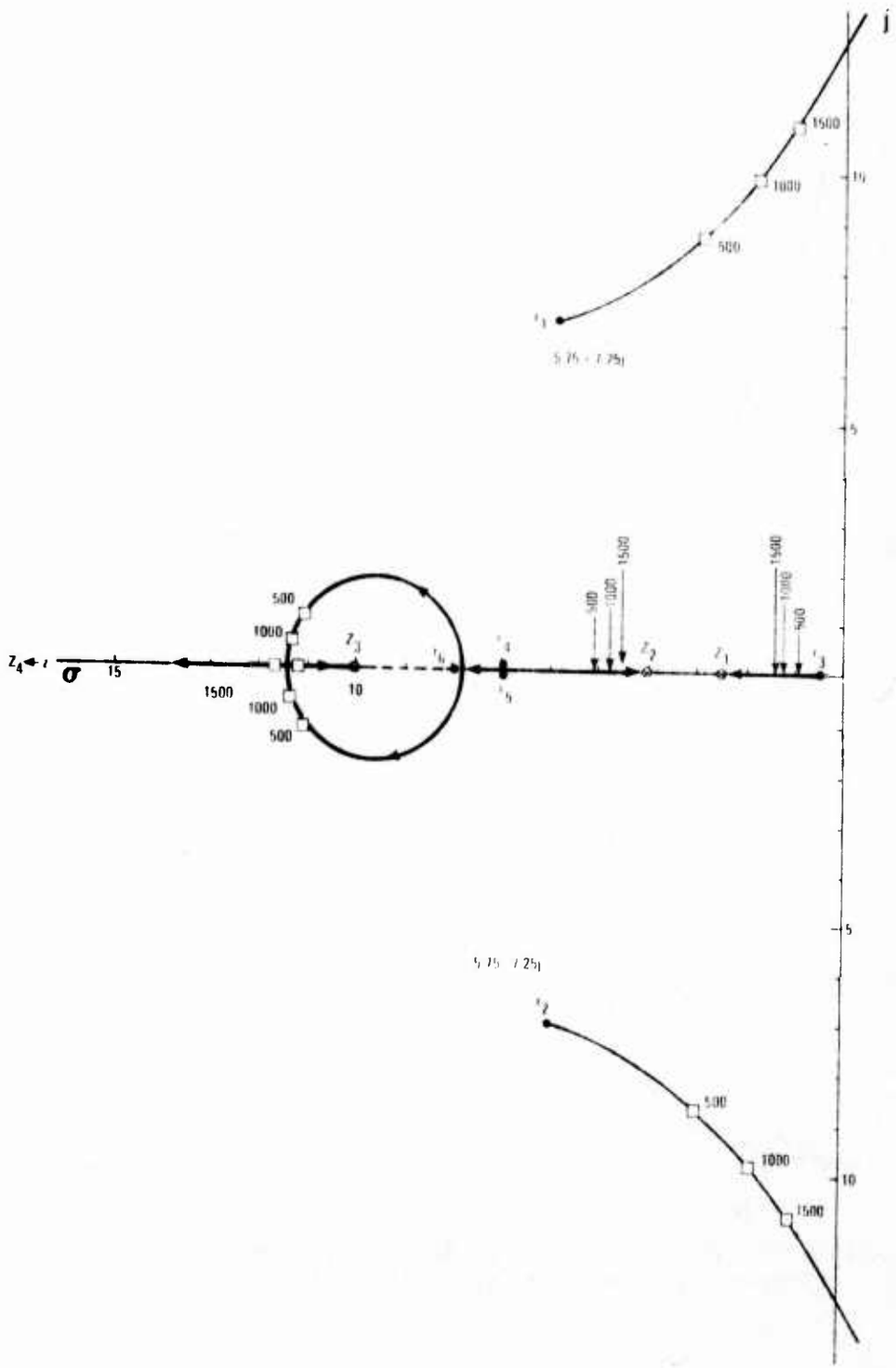

Figure 18. Root Locus for Angular Acceleration Compensation--Initial Autopilot

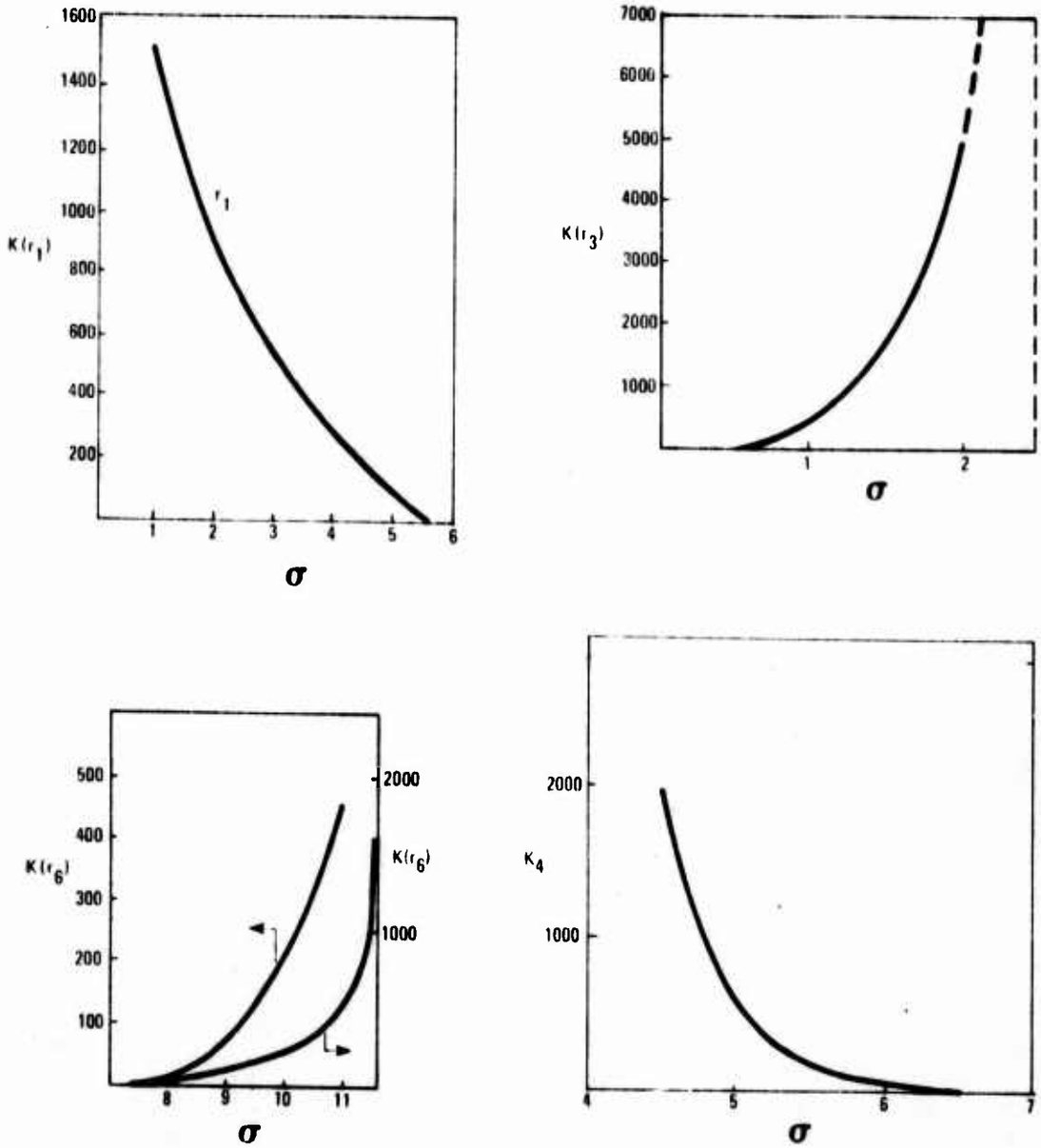

Figure 18. Root Locus for Angular Acceleration Compensation—Initial Autopilot (Concluded)

The autopilot root locus (Figure 12) was examined to assess the impact of acceleration feedback variation. A gain adjustment from 5.9 to 39 was first examined. This resulted in the following closed loop transfer function:

$$\frac{(s + 2.5)(s + 4)(s + 10)(s + 40)}{(s + 2)[(s + 5)^2 + 9^2][(s + 8.5)(s + 7)^2]}$$

The corresponding AFBGW acceleration root locus was examined for the following guidance law:

$$n_c = (L\dot{O}S)k'$$

The result is shown in Figure 19 as a function of variable guidance gain k'. The system is superior in performance to the best of the systems that employ the original autopilot transfer function (using angular acceleration compensation, Figure 18).

The system of Figure 19 gives the best mix of time constant and overshoot when the effective feedback gain is set at K = 2000. The time constant is 0.40 second, and the damping ratio for the governing root is 0.89 (resulting in a step function overshoot of less than 1 percent. The secondary root branch (r_2) is critically damped at K = 2000, and the non-critical tertiary root (r_3) has a damping ratio of 0.62. Neither r_2 nor r_3 has a material impact on system response or stability. The above system could be used for terminal as well as midcourse guidance, since a time constant of 0.4 effectively eliminates dynamic lag as a terminal error source (Reference 12). One major deficiency in the system of Figure 19 is its lack of a k term in the guidance law, which would result in angular errors being uncorrected.

Figure 20 shows the impact of implementing a guidance law of the following form:

$$n = k'\dot{\sigma} + k\sigma = (k's + k)\sigma$$

Choosing K to counteract the effect of the roots at the origin while retaining adequate corrective capability:

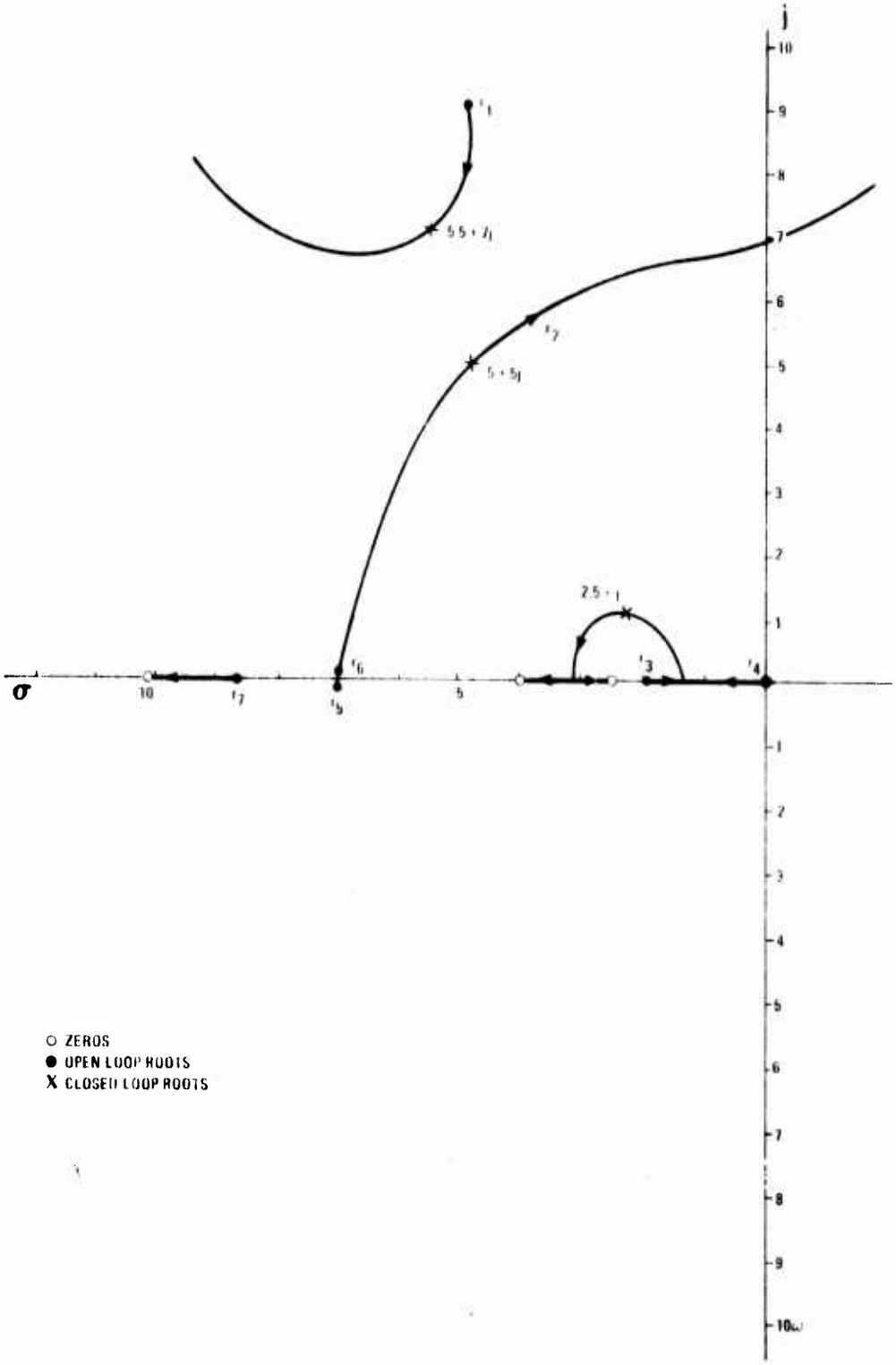

Figure 19. Root Locus for Adjusted Autopilot With Angular Rate Compensation

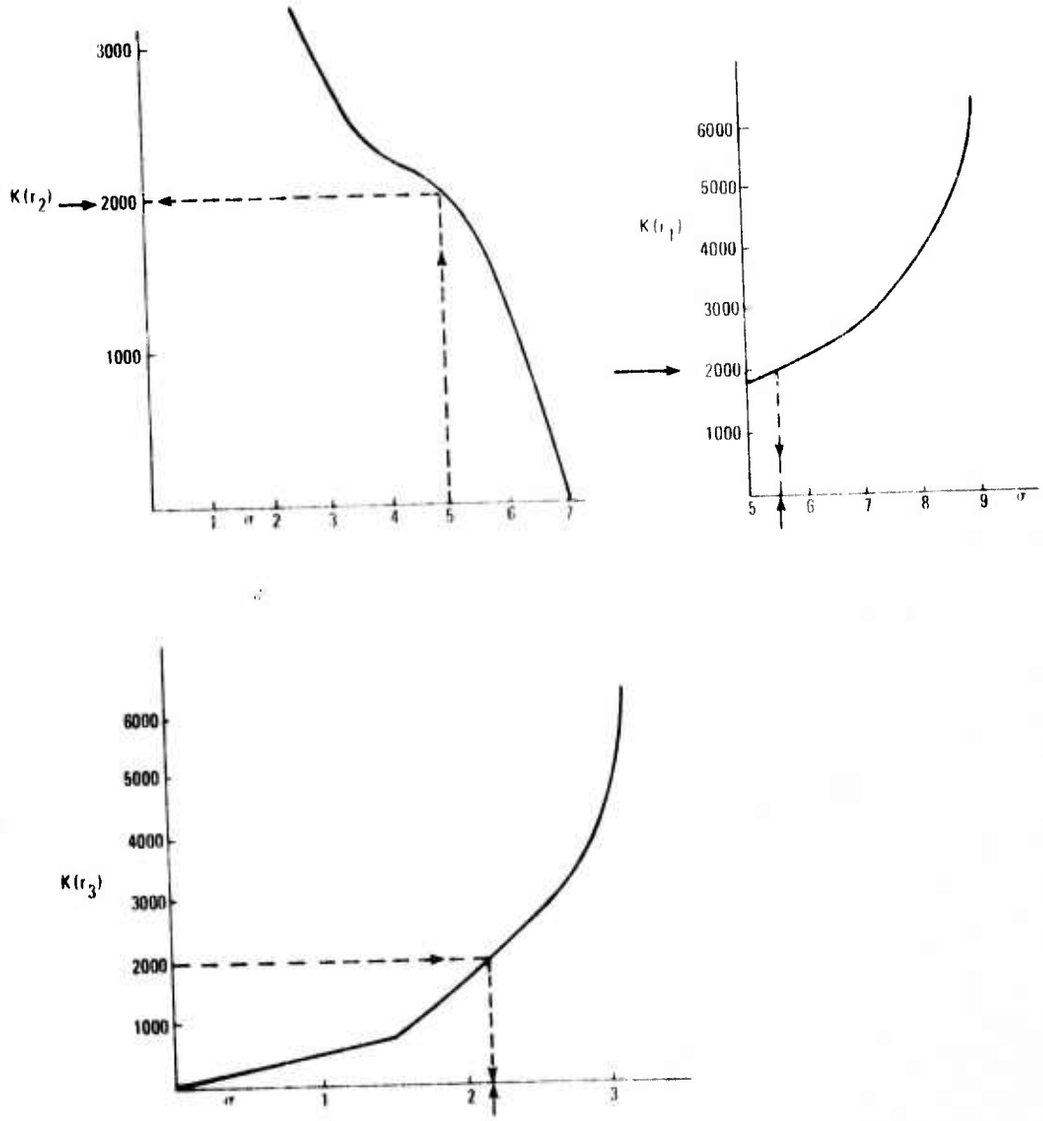

Figure 19. Root Locus for Adjusted Autopilot With Angular Rate Compensation (Concluded)

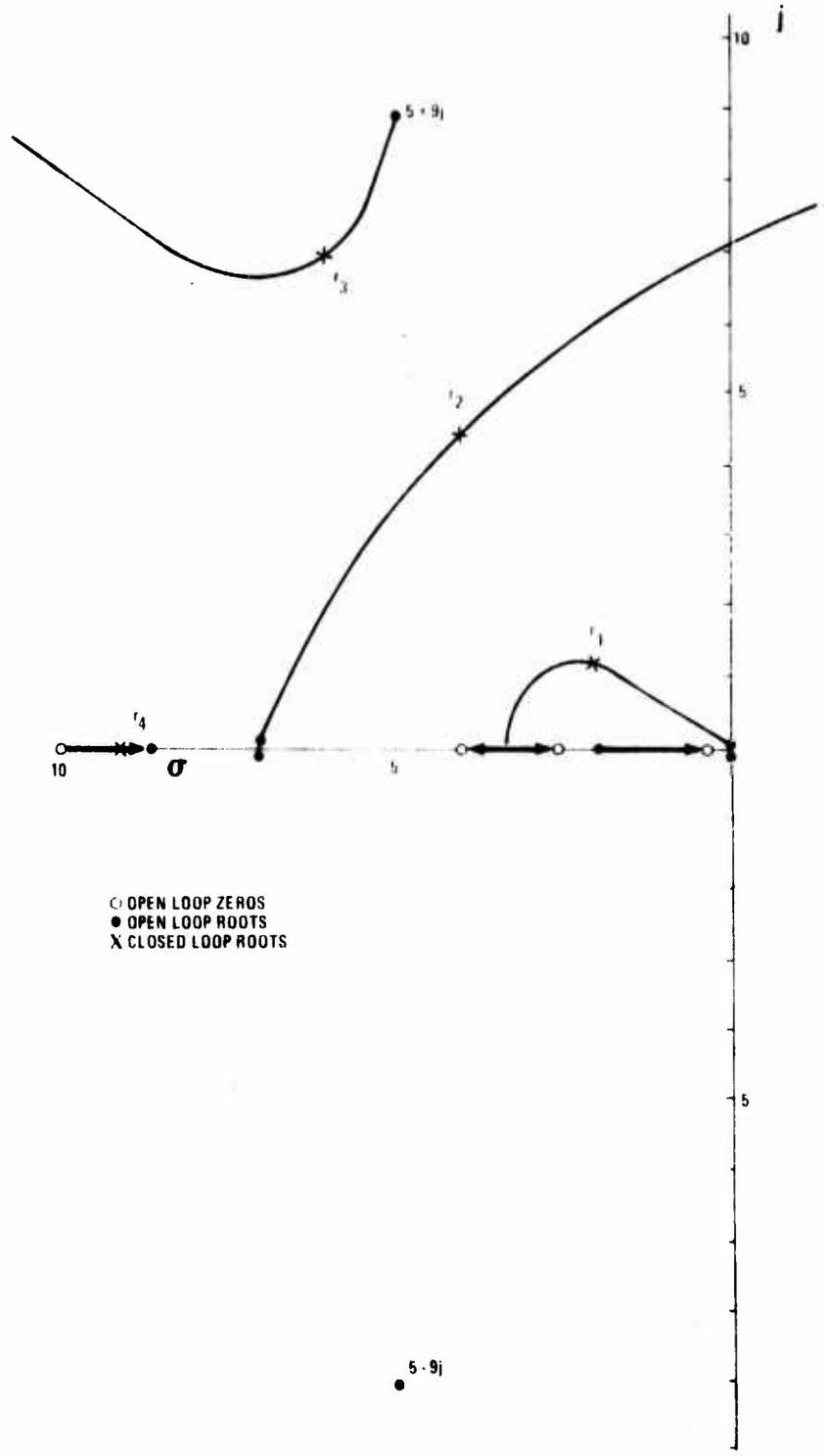

Figure 20. Root Locus for Adjusted Autopilot With Angular Rate Compensation and LOS Feedback

$$\frac{n}{\sigma} = K_x(s + 0.5)$$

This resulted in an acceptable system identified as:

$$\frac{(s + 2.5)(s + 10)(s + 4)(s + 40)(s + 0.5)}{[(s + 2)^2 + 1.2^2][(s + 4)^2 + 4.4^2][(s + 6)^2 + 7.0^2](s + 8.0)}$$

This guidance law will provide position correction. It will also give adequate response and stability. The governing parameters are:

- Governing time constant = 0.5 second
- Governing root damping ratio - 0.84
- Secondary root r_2 damping ratio - 0.64.

It should be noted that, for operations typical of the AFBGW, an autopilot with a long time constant (e.g., >1 second) precludes an effective, simply formulated guidance system that is also highly accurate. An autopilot with a short time constant (e.g., <0.5 second) is compatible with a simply formulated guidance law.

It should be emphasized that guidance law formulation may not be the primary factor in definition of the autopilot requirement for this application. For this air-to-surface missile, the guidance law is merely a convenience in the transportation of the missile from launch point to terminal acquisition point. The autopilot must, of course, be compatible with this function. It must also provide adequate terminal accuracy; it must assure economical management of kinetic energy to maximize range; and it must possess sufficient dynamic response flexibility in trajectory shaping to assure the military utility of the weapon.

The above considerations may make the autopilot that was derived in this section undesirable. If so, there are other alternatives. For example, if a very simple pursuit guidance law is desired, the Boeing virtual target steering method can be used. (This method is discussed in Appendix A, Volume II.) It allows great simplicity in guidance law formulation, but requires a digital computer capability to formulate virtual target trajectories. If this constraint is to be avoided and an autopilot with a short time constant is

considered otherwise desirable, its use can materially simplify the formulation of a guidance law.

ANALYSIS OF TRANSIT DYNAMICS—SLOW NONLINEARITIES

Up to this point in the analysis, the effect of variation of range with flight time has not been discussed. The most significant effect of this variation is that the kinematic loop of Figure 13 cannot be linearized in the general case because range (1/R) appears as a variable factor in the loop. As the (velocity) x (missile time constant) produce ($V \times \tau$) becomes significant compared to the range remaining, the loop begins to develop slow nonlinearity (that is, a change in dynamics that is slow compared to the time constant of the system and which may be corrected by gain variation).

An examination of Figure 13 indicates that it contains previously defined flight parameters, the autopilot/airframe system, and the navigation function. The complete autopilot/airframe system has been closely approximated in an earlier subsection by the following:

$$\frac{n}{n_c} = \frac{(s + 2.5)(s + 4)(s + 10)(s + 40)}{(s + 7)^2(s + 0.68)(s + 8.12)\left[(s + 5.75)^2 + 7.25^2\right]}$$

and typical guidance laws were defined including the following forms:

$$\frac{n_c}{(\overline{LOS})} = k_1 s + k_2$$

$$\frac{n_c}{(\overline{LOS})} = k'' s^2 + k' s + k$$

The k", K', and k values in general should be functions of R and $\dot{R}$. However, traditional guidance law practice involves the use of k", k', and k as constants. This approach has its origin in the design applications where range data are not available and compromises have been required. The problem is illustrated by a root locus plot of an undersea system (Figure 21) which shows the variation of performance of a system as the range to target decreases. The general transfer function of this system is approximated by the following expression:

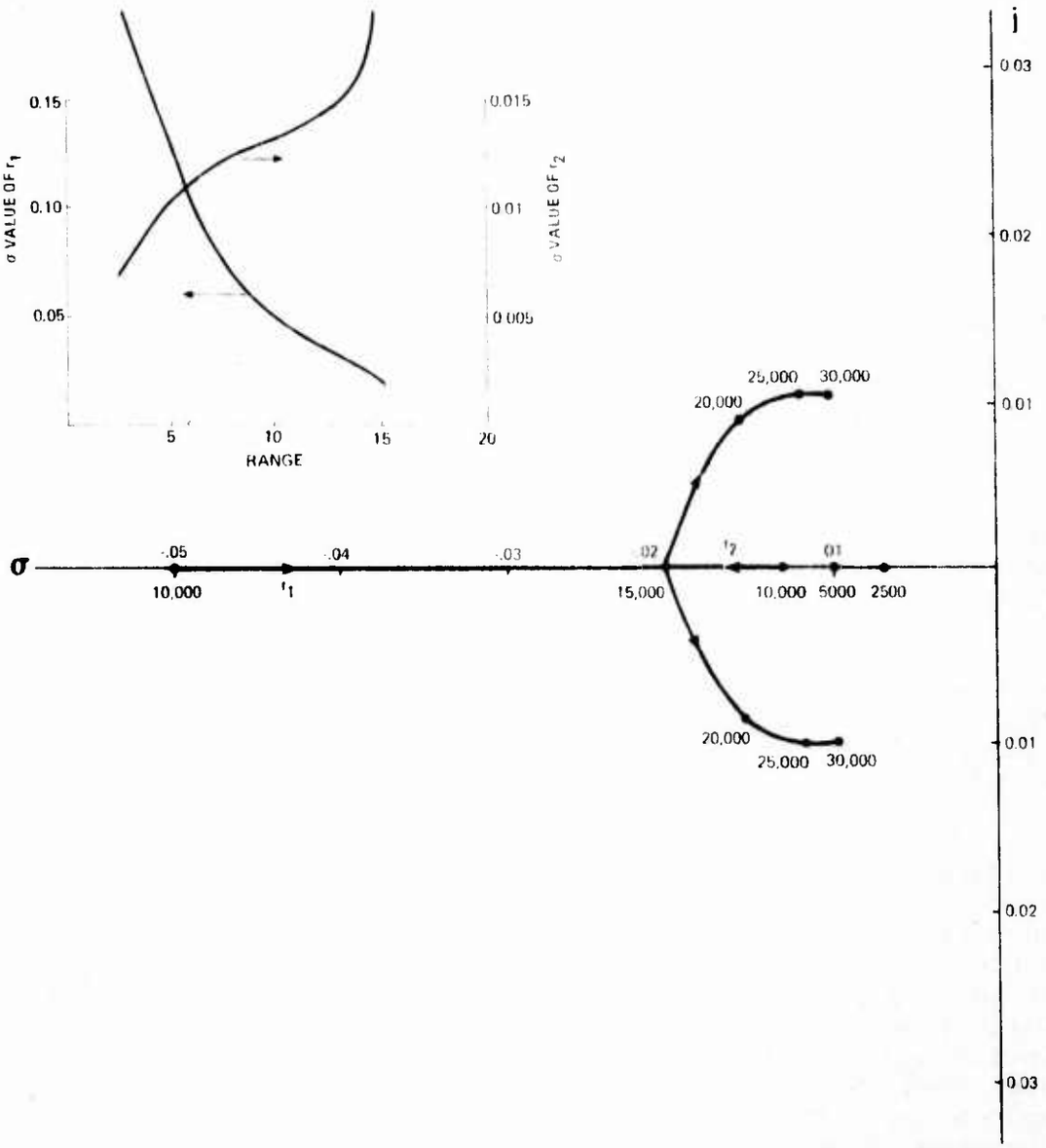

Figure 21. Root Locus Illustrating the Effect of Range Variation in an Undersea Application

$$\frac{\delta_x}{\Delta_x} = \frac{g(K_1 s + K_2)}{R(s^2)\left[(s + 0.36)^2 + 0.52^2\right] + g(K_1 s + K_2)}$$

This results in a time constant of 50 seconds. As the weapon moves in from 15,000 feet and begins to close on the target, the time constant increases. At a range of almost a mile (about 4,200 feet), the weapon is virtually committed—the time to go is less than the time constant.

One would intuitively expect that the time constant would decrease at longer ranges, since it increases at shorter ranges. This, in fact, is not the case. Figure 21 shows that the governing root intersects the real axis at 15,000 feet. At prior ranges, its time constant was smaller than at 15,000 feet.

Thus, with angle data only, there is a very slow response at very long range, an increasingly fast response to some intermediate range, and a slowing response as the missile closes on its target.

The above arrangement is not acceptable, even for an air-to-surface system with a slow moving target. It would be desirable to adjust the weapon autopilot gain to maintain a time constant in the region of 0.5 second and thus to ensure an effectively responsive weapon.

It is, therefore, illustrated that, for the system under discussion, further improvement could be achieved by changing gain with range. This would have the effect of assuring operation at the design point for all ranges, and would allow the fastest available response for a given autopilot design. It would also result in a large part of the error correction being made at long range. Systems with fixed gains (unstabilized k", k', and k) have to increasingly maneuver at high load factors to make corrections as the end of the flight approaches. This can result in control surface saturation, premature loss of missile kinetic energy, and unstable performance.

Note that a knowledge of range rate does not appreciably improve the situation except in cases in which rapidly moving targets require advance knowledge of future range.

ANALYSIS OF TRANSIT DYNAMICS—FAST NONLINEARITIES (DESCRIBING FUNCTIONS) (REFERENCE 13)

System nonlinearities are considered fast if they cause dynamic changes that cannot be compensated by gain adjustments. In real time, saturation is the principal fast nonlinearity in the kinematic loop of the AFBGW. The effect of saturation is conveniently analyzed by use of its describing function (the ratio of the fundamental of the loop response to a sinusoidal input signal) (Reference 8).

The equation of the describing function of saturation is:

$$\frac{G_x}{K_o} = \frac{2}{\pi}\left(\sin^{-1}\frac{S_o}{|M_o|} + \frac{S_o}{|M_o|}\cos\left[\sin^{-1}\frac{S_o}{|M_o|}\right]\right)$$

where S_o is input limit of linear operation, $|M_o|$ is input magnitude, and K_o is system gain under linear operation.

The describing function approach is effective in making a qualitative assessment of performance impact in the frequency domain. The approach is not an exact method, and no analyst has made a rigorous evaluation of its accuracy. The technique is usually assumed to yield results with an accuracy of about 20 percent, however.

A plot for the AFBGW of the describing function for saturation is given in Figure 22. The result of exceeding the saturation limit by a factor of two is indicated by the revised root positions shown as ρ_1, ρ_2, and ρ_3. The result is an increase of time constant from 0.5 second to 1 second. No increase in frequency response is indicated by this analysis.

ANALYSIS OF TRANSIT DYNAMICS—EFFECT OF SAMPLING RATE (REFERENCE 14)

Although it has been tacitly assumed to this point that all data are continuous, this, in fact, is not the case. The AFBGW control system may have to operate with sample data inputs. If the data rate is less than three times the AFBGW natural frequency, a detrimental performance effect will be experienced.

To examine the problem, a Bode Plot of the selected concept is shown (Figure 23). The plot shows a 5.00-db gain

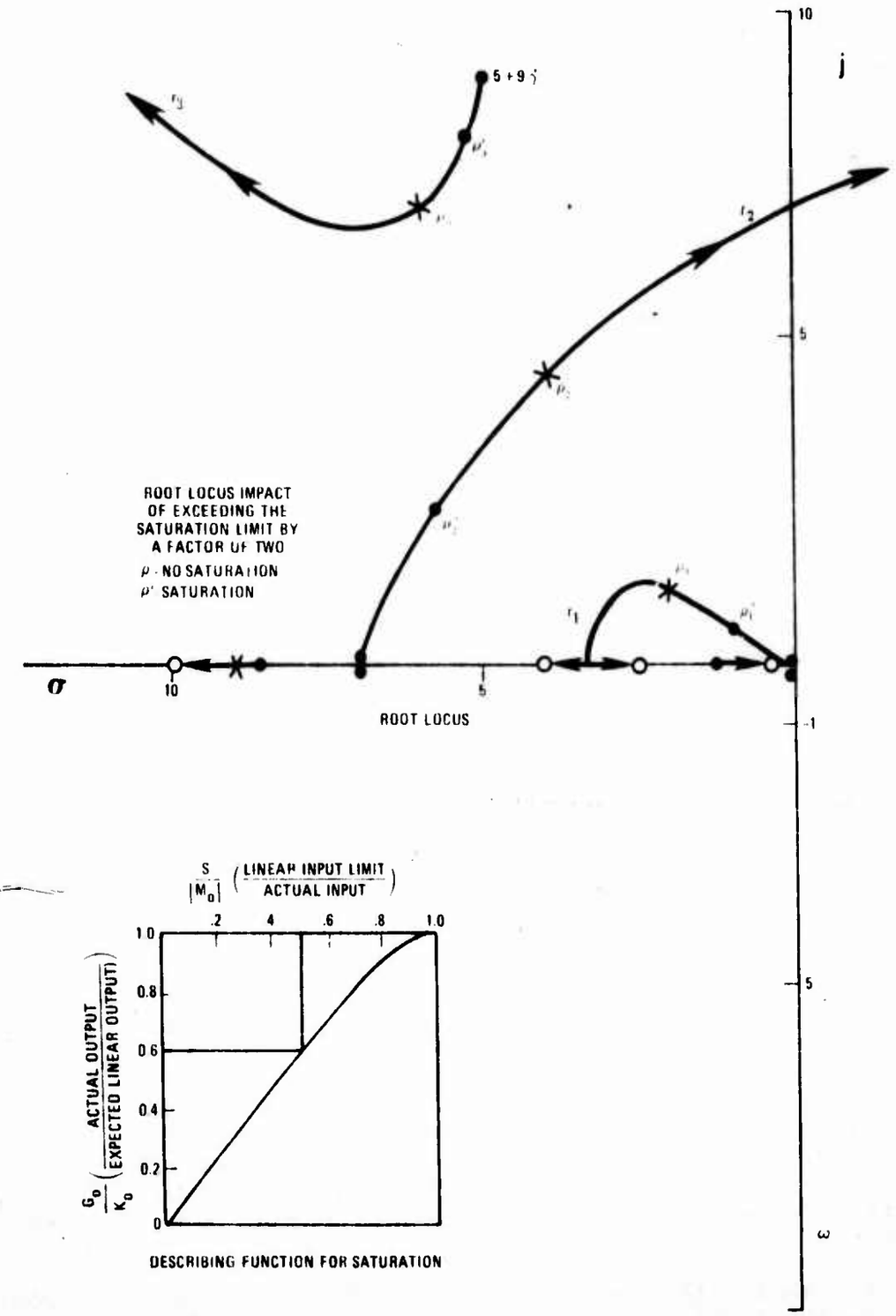

Figure 22. The Stability and Response Effect of Exceeding Saturation Limit

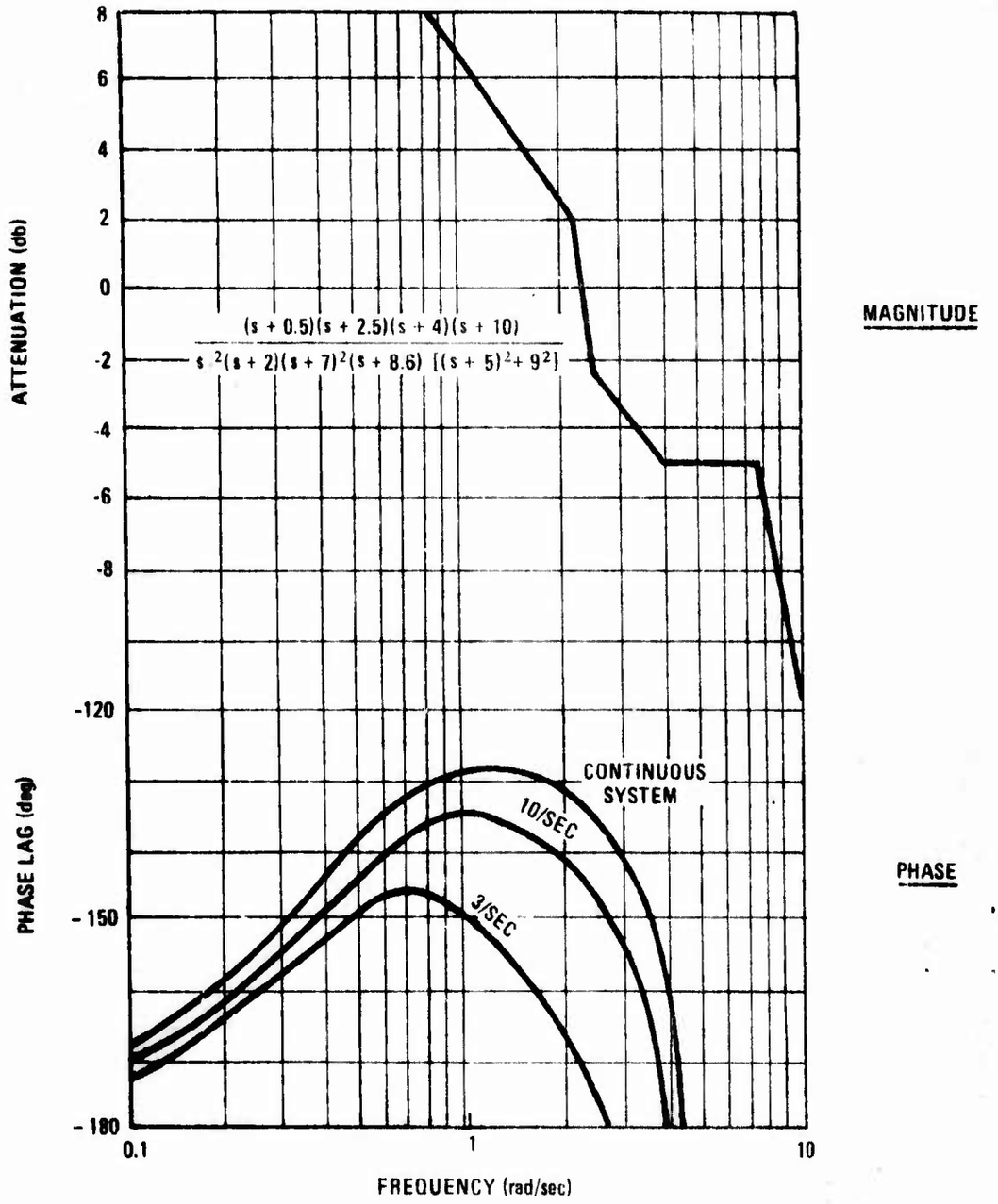

Figure 23. Bode Plot for Selected Concept With Continuous Operation (10 Samples/Second and 3 Samples/Second)

margin for a continuous system, which corresponds to the root locus plot of Figure 20. The curves also show the effect of decreasing the sampling rate to the point where a continuous system is no longer approximated. At 10 samples per second, there is almost no change in the gain margin. However, when the sampling rate is dropped to 3.0 samples per second, the gain margin drops to about 3.5 db. This situation is considered borderline, and is characterized by an overshoot to command response of about 50 percent. The frequency response is magnified by about 6 db, and the time constant of the loop is beginning to be adversely affected.

SUMMARY

A guidance law methodology was developed that involved extensive use of root locus synthesis to assess the response of the vehicle to corrective commands. It included an evaluation of such nonlinearities as range variation, saturation, and digitization.

This section resulted in the definition of two guidance laws that could be applied to the AFBGW/short range vehicle. Both would provide adequate terminal accuracy and maneuvering flexibility. One was suitable for use with the stipulated AFBGW/short range autopilot. The other required some gain adjustments to reduce the time constant. The use of the Boeing virtual target steering approach was also discussed. The effect of nonlinearities and sampling rate on the performance of a candidate guidance law was also investigated.

LIST OF SYMBOLS

SYMBOL	DEFINITION
A-I	Parameters associated with the acceleration autopilot loop.
a	f_δ.
b	$f_\delta m_{\dot{\theta}} + f_\delta m_{\dot{\alpha}} - f_\alpha m_{\dot{\delta}}$.
c	$f_\alpha m_\delta - f_\delta m_\alpha$.
D_1	Denominator of the open loop transfer function of the pitch loop $\{n/\theta_c\}$.
D_2	Denominator of the open loop transfer function for the lateral acceleration loop $\{n/n_c\}$.
d	Missile diameter.
e	$m_{\dot{\alpha}} - f_\alpha + m_{\dot{\theta}}$.
f_α	Normalized side force resulting from angle of attack.
f_δ	Normalized side force resulting from a control surface deflection.
G_o	Sinusoidal input in describing function analysis.
G_1, G_2	Transfer functions in block diagram reduction.
G_1	Open loop transfer function of the pitch loop $\{n/\dot{\theta}_c\}$.
G_2	Feedback transfer function of the pitch loop $\{n/\dot{\theta}_c\}$.
G_3	Closed loop transfer function of the pitch loop $\{n/\dot{\theta}_c\}$.
G_4	Closed loop transfer function for the lateral acceleration loop $\{n/n_c\}$.

LIST OF SYMBOLS (CONTINUED)

SYMBOL	DEFINITION
g	Gravitational acceleration constant.
h	$m_\alpha + m_{\dot{\theta}} f_\alpha$.
I_{yy}	Missile moment of inertia about the pitch or yaw.
i	$f_\delta m_{\dot{\alpha}} - m_\delta - f_\alpha m_{\dot{\delta}}$.
J	Radian to degree conversion (57.3).
j	Imaginary part of transfer function roots.
K	Equivalent airframe gain relating normal acceleration to control surface deflection.
K_o	System gain under linear operation in describing function analysis.
K'	$\frac{V}{g} K$.
$\bar{K}$	Gain constant when transfer function is of the form $G(s) = \bar{K}/s + s_2$.
$\bar{\bar{K}}$	Root locus gain constant when transfer function is of the form: $G(s) = \frac{\bar{\bar{K}}}{\frac{s}{s_2} + 1}$
K_1, K_2	Gain constants in block diagram reduction examples.
k	Gain constant for guidance law using correction signals proportional to the error in LOS.
k'	Gain constant for guidance law using correction signals proportional to the error in $\dot{LOS}$.

LIST OF SYMBOLS (CONTINUED)

SYMBOL	DEFINITION
k''	Gain constant for guidance law using correction signals proportional to the error in $\ddot{LOS}$.
L	Normal acceleration to angular rate conversion factor.
LOS	Line-of-sight error.
J	$m_{\dot{\delta}}$.
$\|M_o\|$	Input magnitude in describing function analysis.
m	Missile mass.
m_α	Normalized pitch/yaw moment resulting from an angle of attack.
$m_{\dot{\alpha}}$	Normalized pitch/yaw moment resulting from a change of angle of attack with time.
m_δ	Normalized pitch/yaw moment resulting from a control surface deflection.
$m_{\dot{\delta}}$	Normalized pitch/yaw moment resulting from a control surface angular rate.
$m_{\dot{\theta}}$	Normalized pitch/yaw moment resulting from an angular rate of the missile body.
N_1	Numerator of the open loop transfer function of the pitch loop $\{n/\dot{\theta}_\varepsilon\}$.
N_2	Numerator of the open loop transfer function for the lateral acceleration loop.
n	Normal acceleration.
n_c	Conditioned externally commanded missile normal acceleration.

LIST OF SYMBOLS (CONTINUED)

SYMBOL	DEFINITION
n_{cx}	Externally commanded missile normal acceleration.
n_ϵ	Difference between conditioned externally commanded missile normal acceleration and current missile normal acceleration.
q	Dynamic pressure $1/2\rho V^2$.
R'	Range.
r_1, r_2, r_3	Indicate specific roots on the root locus plots.
S	Missile reference area (body cross-sectional area).
S_o	Largest input magnitude that will result in a linear output in describing function analysis of the saturation effect.
s	The Laplace operator. Indicates the operation d/dt on any variable associated with it. Its inverse indicates integration. Powers of s indicate orders of differentiation. To designate specific values in this text, subscripts of s have been used; even values indicate roots, odd values indicate zeros.
V	Missile velocity.
Δx	Changes in flight path reference.
δx	Linear displacement of the missile aimpoint from the desired aimpoint.
W	Missile weight.
X_i (i = 0 to i = 3)	Composite denominator coefficients for the closed loop transfer function of the lateral acceleration loop.

LIST OF SYMBOLS (CONCLUDED)

SYMBOL	DEFINITION
$Y_i (i = 0 \text{ to } i = 3)$	Composite denominator coefficients for the open loop transfer function of the lateral acceleration loop (n/n_c).
$Z_i (i - 0 \text{ to } i - 3)$	Composite denominator coefficients for the closed loop transfer function of the pitch loop $(n/\theta_c = G_3)$.
γ	Orientation of missile velocity vector with reference axis.
δ	Control surface deflection.
δ_{EFF}	Effective control surface deflection.
ε	$q\ SD^2/2\ VI$.
ζ	Damping ratio.
η	qS/mV.
θ	Missile angular orientation.
$\dot{\theta}_c$	Equivalent commanded missile angular rate (pitch or yaw).
$\dot{\theta}_\varepsilon$	Difference between equivalent commanded missile angular rate and current missile angular rate.
μ	Acceleration-angular rate lead frequency.
ξ	qSd/I.
ρ_1, ρ_2, ρ_3	Indicates specific roots on the root locus plot.
σ	Indicates the real axis on a root locus plot.
ω	Frequency.
Dots $(\cdot)$	Dots above a variable indicate time differentiation. The number of dots indicate the order of differentiation.

SECTION V

ERROR PROPAGATION

Missile navigation is defined as the process of determining position; guidance is the process of using navigation data to steer the vehicle to its objective.

The previous section discussed the guidance analysis. The balance of this report is concerned with the accuracy of navigation.

In this section, error propagation is examined as follows:

- The design requirements that govern the magnitude of error forcing functions are stated.
- The equations that relate error forcing functions to system errors are derived.
- System position and level errors are calculated as a function of time.
- The significance of the form of system position error histories in the use of auxiliary sensors is discussed.
- The significance of computational errors in a strapdown mechanization is examined.

INERTIAL SYSTEM DESIGN REQUIREMENTS

Inertial requirements for AFBGW and RACG are established by two factors: navigation accuracy and auxiliary sensor datum needs.

In this context, navigation accuracy refers to the ability to determine horizontal position. Auxiliary sensor datum needs refer to altitude, velocity, and attitude reference parameters that are vital to the orderly operation of update sensors. For example, RACG requires an accurate vertical reference; the Global Positioning System (GPS) may require a velocity reference for counter-countermeasure operations; the doppler radar requires an independent heading reference; and terrain elevation correlation requires a means to measure distance between elevation sample points.

Navigation accuracy for the AFBGW/RACG concept depends on update acquisition capability. Target midcourse accuracy of 3,000 feet is required to assure adequate acquisition capability for the RACG correlator. In this study, it is assumed that the AFBGW must reach the 3,000-foot acquisition envelope with a 95 percent confidence level (i.e., 3,000 feet is a 2σ number. (Note that inertial component parameters are normally quoted in 1σ figures defining a 62 percent confidence level.)

RACG requires a very accurate level reference; consequently, emphasis must be given to the propagation of both position and level errors. The required baseline level accuracy for this study is 0.3 degree (1σ) (Reference 15).

The AFBGW/RACG performance objectives for the inertial system are shown in Table 22, as defined by Lockheed (Reference 15). Three classes of error sources are listed: those caused by gyroscope imperfections, those caused by accelerometer imperfections, and those caused by failure to initialize the navigation system adequately.

Gyroscope imperfections are the result of gradients in magnetic field and temperature that cause variations in the physical properties of critical components and parameters. These result in a drift of the output axis of the instrument. The day-to-day bias is a prime measure of instrument quality and is, in fact, a valid estimate of the drift rate to be expected 24 hours after calibration. Random drift is the drift that remains after thorough calibration. Mass imbalance error depends upon the intensity of the gravitational field in which the instrument is operated and is closely related to vehicle load factors. Electromechanical and laser gyroscopes differ in their sensitivity to error forcing functions.

For example, input axis variation due to random drift and mass unbalance are not applicable to ring laser gyroscope systems, but conventional (electromechanical) gyroscopes are affected by these error forcing functions in a strapdown application.

The accelerometer performance required by the parameters listed in Table 22 are of somewhat higher quality than the gyroscopes. Consequently, the total system position error is not greatly influenced by the accelerometer parameters. Alignment performance and level accuracy are the primary factors in the selection of a relatively high-grade accelerometer.

The initialization errors are determined by the accuracy of the reference sensor data and the effectiveness of the

TABLE 22. AFBGW/RACG PERFORMANCE OBJECTIVES FOR INERTIAL SENSORS

PARAMETER	CURRENT RACG	PROJECTED
Gyroscope		
Day-to-Day bias	2 degrees/ hour	1.0 to 0.5 degree/hour
Random Drift*—Output Axis Variation (OAV)	0.2 degree/ hour	0.1 degree/ hour
Random Drift*—Input Axis Variation (IAV)	0.3 degree/ hour	0.1 degree/ hour
Mass Unblanace	2 degrees/ hour/g	1 degree/ hour 4 g
Accelerometer		
Bias Stability	2×10^{-4} g	2×10^{-4} g
Random Bias	3×10^{-5} g	3×10^{-5} g
Scale Factor	0.04 percent	0.04 percent
Initialization		
Azimuth	2.0 milliradians	2.0 milliradians
Velocity	2.0 feet/ second	2.0 feet/ second
Position	1,500 feet	1,500 feet
Level	1 minute	1 minute

* 10-minute drift.

transfer process. The tabulated values represent the level of quality of an A-7 aircraft platform (AN/ASN 90).

DERIVATION OF ERROR EQUATIONS

The error equations relevant to AFBGW system performance are shown in Table 23. These equations assume a local vertical inertial mechanization, which can be attained either by use of a platform or by equivalent strapdown computation. A block diagram corresponding to a single channel representation of the system is shown below the table. This diagram represents the familiar Schuler loop with an 84-minute period. The sine and cosine functions prominent in the table reflect this characteristic oscillation. While Broxmeyer is cited as a reference, Leondes, Fernandez and MacComber, Parvin, and others all give adequate explanations of these and other error sources (see References).

The error sensitivity coefficients given in Table 23 result from a single-axis model. Error coupling terms also appear, but these are only applicable to a full three-dimensional analysis. Azimuth gyroscope drift may be omitted because of the short flight duration.

Table 24 shows the error sensitivity polynomial approximation, which may be used effectively for flights of 20 minutes or less. These expressions can be useful in short flights because error expressions are easier to model.

CALCULATION OF SYSTEM PERFORMANCE ERRORS AS A FUNCTION OF TIME

If values from Table 22 are combined with the equations from Tables 23 and 24, and time (t) is taken as an independent variable, an error propagation history can be developed.

This error propagation history is shown in Figure 24 for typical mission parameters. Flight times are approximated at 4 and 10 minutes for the short range and long range versions, respectively. The resulting error is determined from the root sum square (rss) combination of the constituents. No confidence level (1σ, 2σ, etc.) is designated; however, the input and the result must correspond in confidence level.

TABLE 23. ERROR PERFORMANCE EQUATIONS (REFERENCE 16)

ERROR SOURCE	DISTANCE ERROR	VELOCITY ERROR	LEVEL ERROR
Level Gyro Drift Rate	$\delta R\left(t - \frac{1}{\lambda}\sin \lambda t\right)$	$\delta R\,(1 - \cos \lambda t)$	$\delta \sin \lambda t/\lambda$
Mass Unbalance	$\delta' g v t^2/2$	$\delta' g v t$	$\delta' v$
Accelerometer Bias	$a\,(1 - \cos \lambda t)/\lambda^2)$	$a \sin \lambda t/\lambda$	$\frac{a}{g}\cos \lambda t$
Accelerometer Scale Factor	$K v\left(t - \frac{1}{\lambda}\sin \lambda t\right)$	$K v\,(1 - \cos \lambda t)$	$K v \sin (\lambda t)/\sqrt{g R}$
Initial Azimuth Misalignment	$\psi_o v t$	$\psi_o v$	Not applicable
Initial Level Misalignment	$\phi_o R\,(1 - \cos \lambda t)$	$\phi_o R \lambda \sin \lambda t$	$\phi_o \cos \lambda t$
Initial Velocity Error	$\Delta v_o \sin (\lambda t)/\lambda$	$\Delta v_o \cos (\lambda t)$	$\Delta v_o \sin (\lambda t)\sqrt{g R}$

δ Gyro drift rate
R= 20.6 x 10^7 ft (earth radius)
t = Time
λ = 125 x 10^{-3} rad/sec
δ'= G sensitive gyro drift rate
g= 32.2 ft/sec^2
v= Vehicle velocity

a Accelerometer bias
$\lambda^2 = g/R$
K Scale factor error
ψ_o Initial azimuth error
ϕ_o Initial level error
v_o Initial vehicle velocity

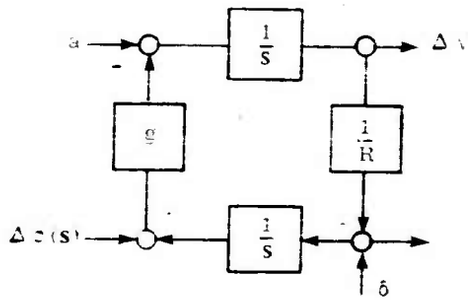

TABLE 24. ERROR POLYNOMIAL APPROXIMATIONS (REFERENCE 17)

ERROR SOURCE	DISTANCE ERROR	VELOCITY ERROR	LEVEL ERROR
Level Gyro Drift Rate	$1/6\ \delta\ g\ t^3$	$1/2\ \delta\ g\ t^2$	$\delta\ t$
Mass Unbalance	$1/2\ \delta'\ g\ v\ t^2$	$\delta'\ g\ v\ t$	$\delta'\ v$
Accelerometer Bias	$1/2\ a\ t^2$	$a\ t$	a/g
Accelerometer Scale Factor	$1/6\ K\ v\ t^3$	$1/2\ K\ v\ \omega^2\ t^2$	$Kv\omega t/\sqrt{gR}$
Initial Azimuth Misalignment	$\psi_o v\ t$	$\psi_o v$	Not applicable
Initial Level Misalignment	$1/2\ O_o g\ t^2$	$O_o\ g\ t$	O_o
Initial Velocity Error	$\Delta v_o\ t$	Δv_o	$\Delta v_o \sqrt{g R}$

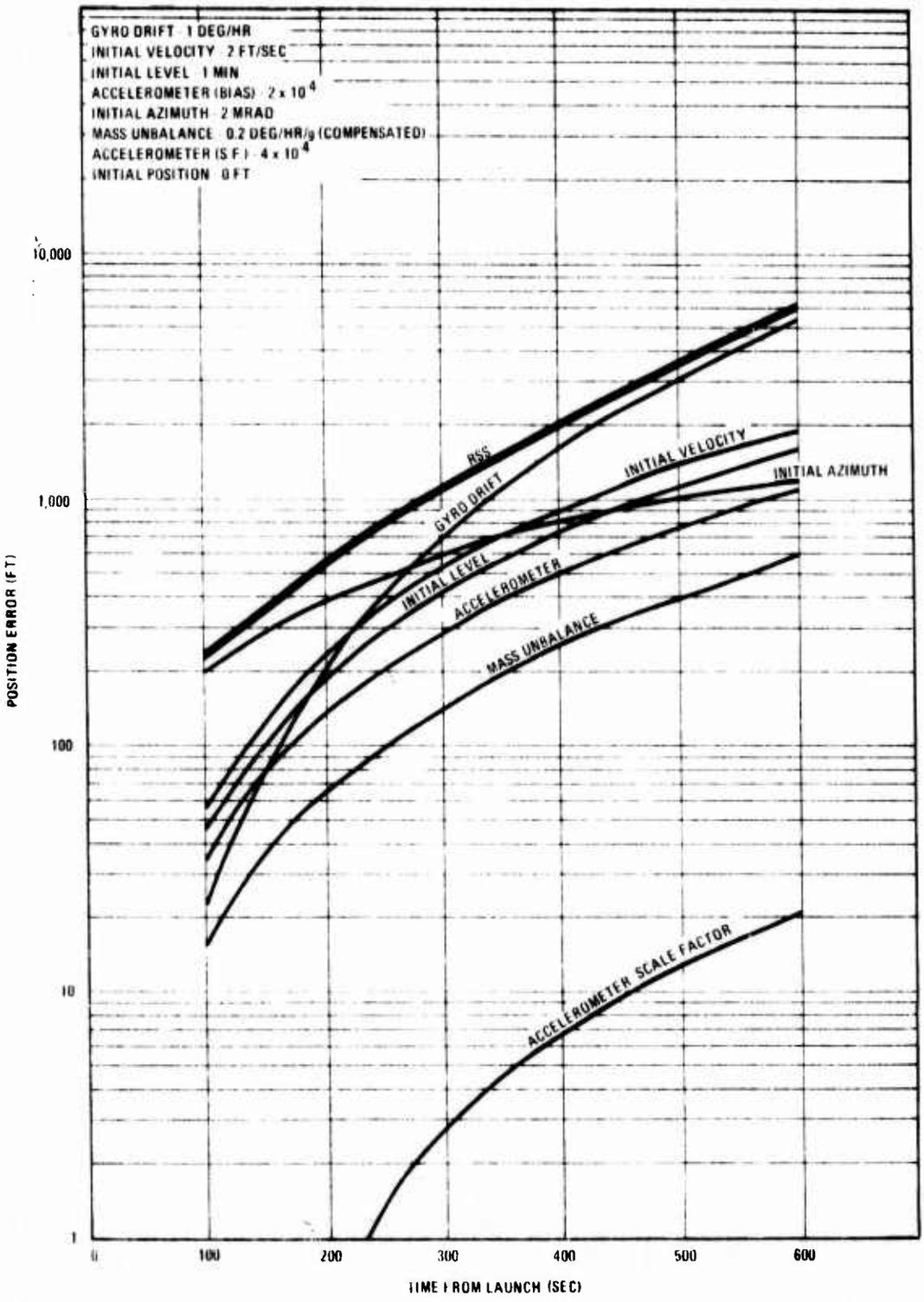

Figure 24. Position Errors as a Function of Sensor Parameters

POSITION ERROR HISTORIES AND THE USE OF AUXILIARY SENSORS

Figure 24 suggests the combination of measurements to obtain a synergistic reduction of system errors, which is emphasized by plotting gyroscope drift and initial azimuth on a linear scale (Figure 25). The result shows that, in the first 100 seconds of flight, gyroscope drift results in little error. However, as the flight proceeds, gyroscope drift becomes an overwhelming source of error compared to azimuth misalignment.

Consider a hypothetical aided system with a local vertical capability and a velocity reference. The local vertical system is based on a 1-degree/hour gyroscope, and the velocity reference has a 2-foot/second error. The system error generated by the velocity reference is coincidentally exactly equal to the error generated by a 2-milliradian initial azimuth misalignment.

A classical problem in the combination of sensors involves minimizing system error. Ideally, it is possible to calibrate the velocity reference during the first 100 seconds of flight. If the systematic biases exhibited during this time are stable, then the system error can be reduced in proportion to the gyroscope error at 100 seconds. The system can be reduced in proportion to the gyroscope error at 100 seconds. The system can use velocity dead reckoning during the last 400 seconds of the flight, and position errors will propagate along line (a). This will result in a velocity error of 0.050 foot/second, or a final position error of 150 feet.

Under practical operating conditions, complete error stability cannot be ensured. Usually, some cyclic error is associated with the bias from any error source. Assume that the position error generated by the velocity cyclic error is represented by curve (b). If the velocity sensor is calibrated at 100 seconds, dead reckoning position error propagation will proceed along line (c). Then, realistically, a 400-foot error could be expected at the end of 400 seconds. This is a great improvement over the 1,500-foot error expected from the gyroscope reference. It is also better than the 800-foot error expected from an uncalibrated velocity reference error.

In synergistic mechanisms, it is important to note that the critical factors in final system error are the stability of the velocity error and the ability to define the cyclic process rather than the original magnitude of the velocity error. The conventional and Kalman processes discussed below

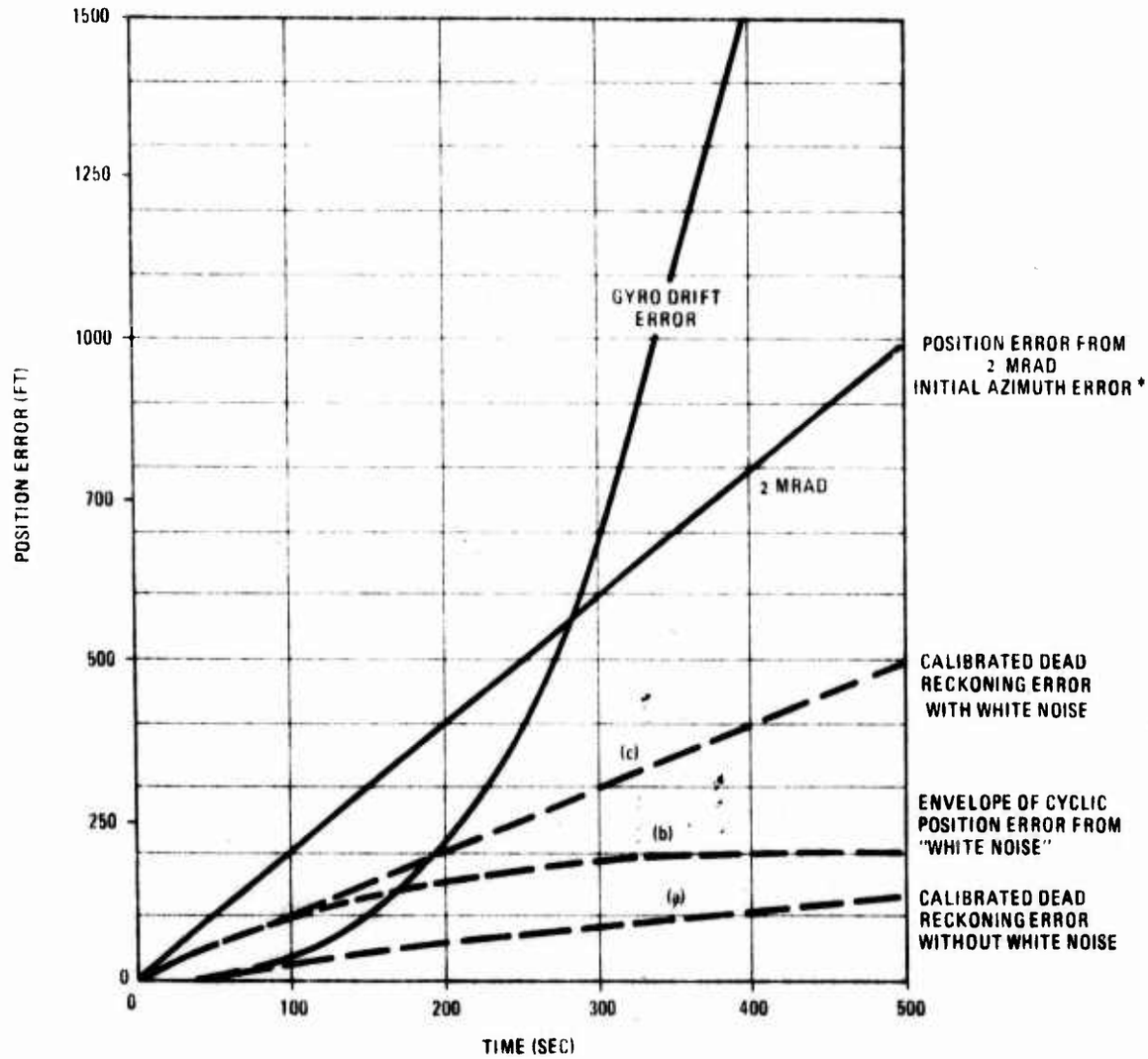

* At Mach 1.0 (~1,000 feet/second), the same cross course error propagation is produced by a 1-milliradian initial azimuth error as is produced by a 1-foot/second velocity error.

Figure 25. Position Errors as a Function of Gyroscope Drift and Initial Azimuth Error

that apply this principle are analogous but involve more sophisticated mathematical procedures (Reference 18).

LEVEL ERROR ANALYSIS

The RACG system requires the inertial navigation system to supply an accurate vertical reference (or horizontal level datum). The relationship between sensor error parameters and vertical reference accuracy is shown in Figure 26. The curve shows that an accuracy of 3 milliradians can be maintained for the 600 seconds required of the AFBGW/long range.

COMPUTATIONAL ERRORS IN A STRAPDOWN SYSTEM

The AFBGW/RACG system will employ a strapdown inertial navigation mechanization. Because of exposure to high angular rates and angular accelerations, strapdown sensors are subject to errors not experienced by conventional (gimballed) platforms. The magnitude of these errors is influenced by the character of the algorithm used in coordinate conversion and by the computational rate of the coordinate conversion computer program. Table 25 identifies typical error sources in terms of computational rate. Also noted are the types and magnitudes of motion resulting in the error forcing functions. The body of the table lists the formulas used to determine gyroscope drift caused by inadequate computational rate and missile motions. Figure 27 indicates the magnitude of gyroscope drift as a function of computational rate for three types of angular integration algorithms. The curves show that gyroscope drift resulting from environmental disturbances can be made negligible if sufficient computer resources are used. The material used in Table 25 and Figure 27 was developed from data provided by Sperry Gyroscope Company and a paper by J.J. Sullivan (Reference 19) on strapdown errors. Further data on strapdown systems and their computational requirements appears in Appendix C.

SUMMARY

This section has related the design characteristics and preflight conditioning standards to operational performance for gyroscopes and inertial platforms. The section starts with a statement of inertial specifications for AFBGW navigation. It then derives the error equations that relate sensor and platform specifications to navigation accuracy. The equations reflect the cruise glide trajectory of the

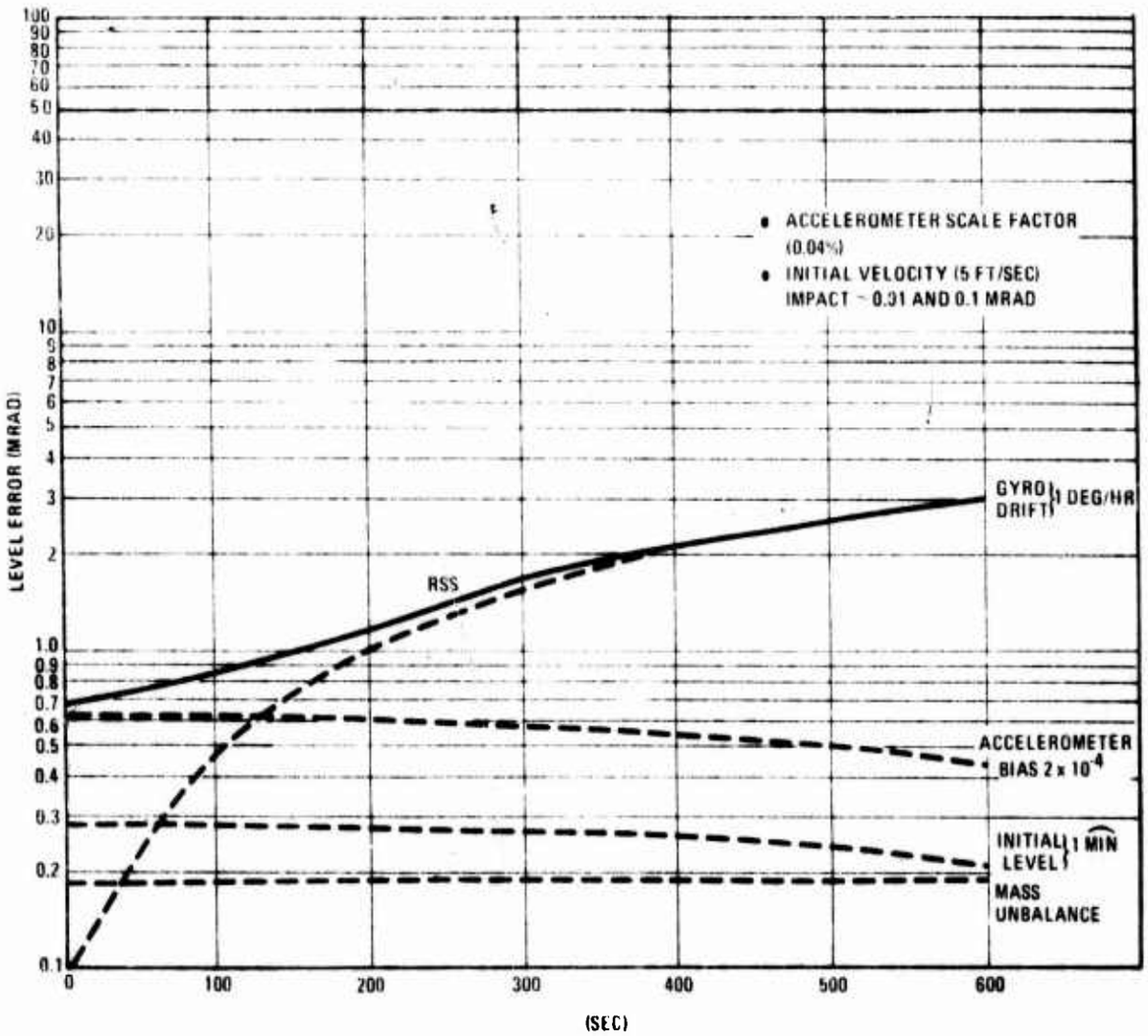

Figure 26. Level Errors as a Function of Sensor Parameters

TABLE 25. STRAPDOWN COMPUTATIONAL ERRORS (EQUIVALENT GYROSCOPE DRIFT IN DEGREES/HOUR)

Error Source	Type of Motion Responsible for Forcing Function	Rectangular Integration	Second-Order Runge Kutta Integration	Fourth-Order Runge Kutta Integration
Truncation	Constant angular rate: 134 deg/sec (max)	$35.6\left(\frac{\Omega}{N}\right)^2$	$0.133\left(\frac{\Omega}{N^2}\right)^3$	$1.62 \times 10^{-4}\left(\frac{\Omega}{N^4}\right)^5$
Truncation	Sinusoidal rates: 5-deg amplitude; 2 cps	$117\, A^2 N \left\{\sin\left(\frac{\pi\omega}{2N}\right)\right\}^2$	$0.0985\, A^4 N \left\{\sin\left(\frac{\pi\omega}{2N}\right)\right\}^4$	$0.0535\, A^4 N \left\{\sin\left(\frac{\pi\omega}{2N}\right)\right\}^6$
Truncation	Coning ($N < 1.25N$) Pitch: 20-deg half angle; 1/6 cps Yaw: 5-deg half angle; 1/2 cps	$197\, A\omega$	$197\, A\omega$	$197\, A\omega$
Truncation	Coning ($N > 1.25N$)	$327\, A^2\omega^2/N$	$406\, A^2\omega^3/N^2$	$646\, A^2\omega^5/N^4$
Quantization	Coning	$12\Delta O^2 A\omega/N$	$12\,\Delta O^2 A\omega/N$	$12\Delta O^2 A\omega/N$
Round-off	All motions	$\left(2.1 \times 10^6\right) 2^{-n} f_c$	$\left(2.1 \times 10^6\right) 2^{-n} f_c$	$\left(2.1 \times 10^6\right) 2^{-n} f_c$

ω = Frequency of missile oscillation (cps)

N = Number of calculations per second

A = Amplitude of oscillation (deg/sec)

Ω = Missile angular rate (deg/sec)

ΔO = Quantization level (arc sec)

n = Number of bits

f_c = Computation rate

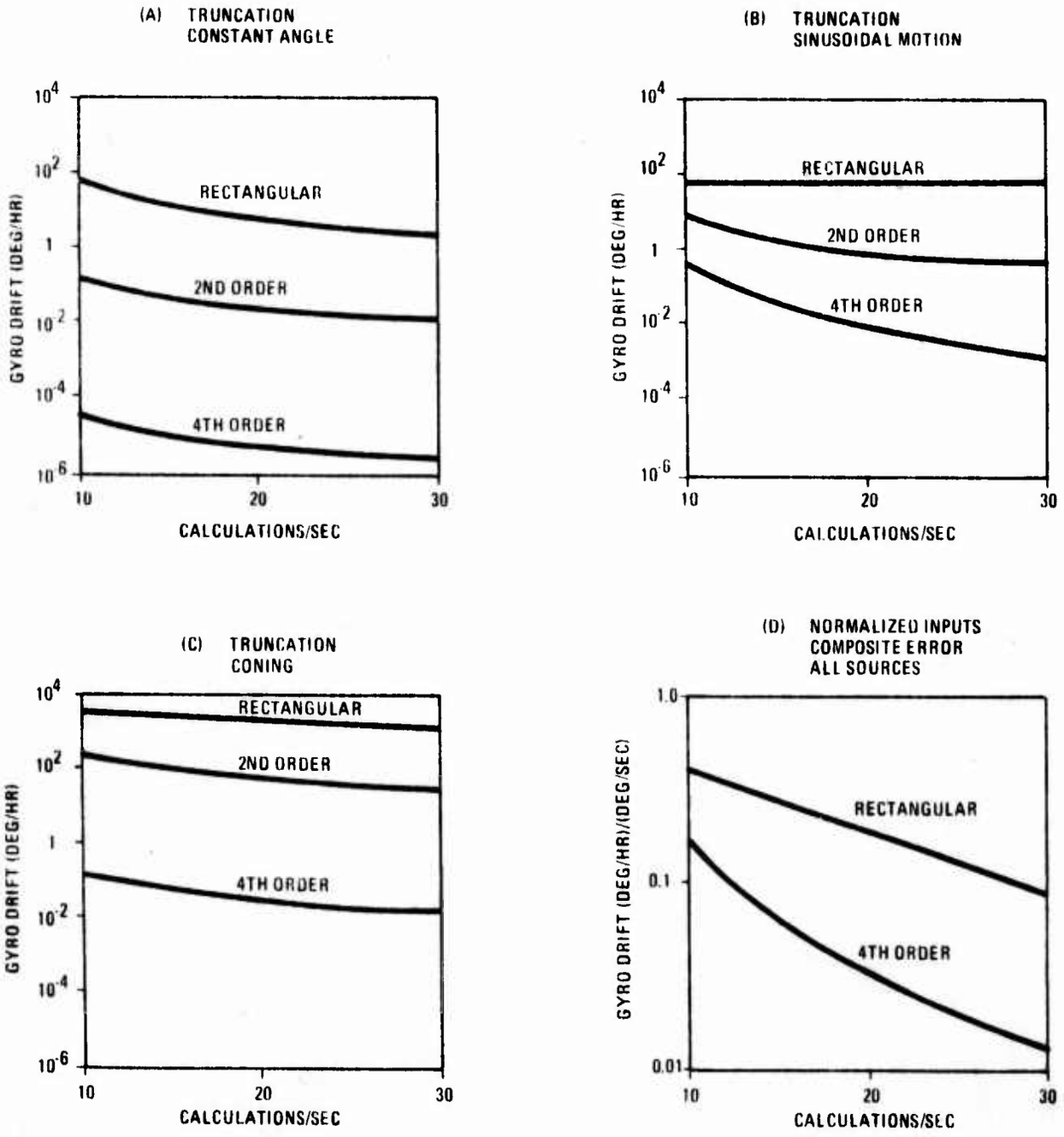

Figure 27. Gyroscope Drift Rate Induced by Strapdown Calculations

of the AFBGW but otherwise can be applied generally to all inertial navigation situations.

Calculation of system errors consists of applying the specifications parameters to the error equations to produce error time histories. This concludes the explicit assessment of error propagation.

The balance of the section is devoted to a discussion of error propagation and its relationship to updating, level error analysis, and a discussion of computational errors.

The section establishes the single axis error for the 10-minute long-range flight as 6,000 feet. It also establishes the single axis error for the 4-minute short-range flight as 600 feet. (All axis errors are 1.66 times the single axis error.) The section also shows the way in which a knowledge of error propagation profiles can be helpful in developing aiding approaches. A level error of 3 milliradians after 10 minutes of flight is established; also established are computational procedures that will avoid the gross errors that can result from the lack of isolation characteristic of the strapdown approaches.

This study has not addressed the effects of Scorsby or coning motion which may be induced into the AFBGW environment by limit cycles induced by the airframe/autopilot combination.

LIST OF SYMBOLS

SYMBOL	DEFINITION
A	Amplitude of missile oscillation.
a	Accelerometer bias.
f_c	Computational rate of algorithm.
g	Gravitational constant.
K	Accelerometer scale factor error.
N	Number of calculations per second.
n	Number of bits in computer word.
R	Earth radius.
t	Time.
V	Vehicle velocity.
V_o	Initial vehicle velocity.
δ	Gyroscope drift rate (g insensitive).
δ'	Gyroscope drift rate (g sensitive).
λ	Schuler frequency.
ϕ_o	Initial level error.
$\Delta\phi$	Angular quantization level (arc second).
ψ_o	Initial azimuth error.
Ω	Missile angular rate (degree/second).
ω	Frequency of missile oscillation (cps).

SECTION VI

ALIGNMENT AND INITIALIZATION

INTRODUCTION

This portion of the study involves the identification and evaluation of current methods for airborne alignment and initialization of strapdown and gimballed low-cost platforms. These functions may be performed in the following ways:

- At base prior to takeoff without the use of aircraft equipment.
- While the missile is attached to the aircraft, using aircraft equipment as the primary source of reference data.
- After missile launch, using onboard missile guidance and navigation equipment.

Each of the above methods has its advantages and disadvantages; they will be discussed in detail further in this section.

Alternative alignment and initialization methods are presented in Table 26 and are discussed in detail in this section under the following headings:

- Leveling and alignment
  - Gyrocompassing
  - Transfer alignment—parameter matching
  - Discrete fixtaking alignment
- Initialization
  - Missile gyroscope and accelerometer calibration
  - Initialization of missile position and velocity
  - Transfer of update sensor data to missile
  - Prelaunch environmental conditioning of sensors and support equipment.

(The Reverse of This Page is Blank.)

TABLE 26. ALTERNATIVE ALIGNMENT AN

Function	Alternative Approach	A
Alignment		
Leveling and azimuth alignment	Gyrocompassing and self-level with missile sensors	Missile can aircraft equi
	Parameter matching	High speed
		Allocates eq launch aircr
		Eliminates
	Successive discrete fixes by RACG	Requires on aircraft sen
Initialization		
Missile gyro and accelerometer calibration	Matching to aircraft sensor	Highly reliab No stringent ments
	Modulation, Modelling of environment	Performanc reference s
	Successive discrete fixes by RACG to align and calibrate sensors	Full alignm supporting s
Initialization of missile position and velocity	Transfer from master inertial navigator	Simple, dir
	Successive discrete fixes by RACG	Very accura
	Aiding devices in the aircraft employing prelaunch velocity correction and position update. GPS, ground mapping, radar fixes, radio navaids, visual fix may be applied	Best mix of can give co
Transfer of update sensor data to missile	Transfer to missile at base	No aircraft update sens
	Transfer from missile to aircraft	Target sele
		Ability to p captive fligh initializatio
Prelaunch environmental conditioning of sensors and support equipment	Environmentally immune sensors (operate from -15° to 180°F)	No launch d
	Heated sensors with a limited tolerance to temperature change	Decreased level

IVE ALIGNMENT AND INITIALIZATION APPROACHES

ch	Advantages	Disadvantages
level with	Missile can function without high cost aircraft equipment	Time consuming
		Requires long calibration period for low cost sensors to level
		Azimuth alignment not feasible with missile sensors
	High speed	Requires maneuver inflight which may form an operational constraint
	Allocates equipment requirements to launch aircraft	Requires aircraft platform
	Eliminates missile/aircraft interface	
y RACG	Requires only missile equipment, no aircraft sensors employed	Can impose stringent data storage requirements on missile
	Highly reliable, simple procedure. No stringent computational requirements	Requires aircraft sensors that are at least an order of magnitude (x 10) more precise than the calibrated sensor
viron-	Performance not dependent upon reference sensors	Can leave high residual drifts. Transfer of gimballed platform proven technologies has not been demonstrated in a strapdown situation
RACG	Full alignment/calibration without supporting systems	Limitation in observability of some sensor alignment error combinations
al	Simple, direct, high speed	Requires exceptionally high quality navigation capability on the aircraft
	Very accurate	A geometric growth of computational requirements results from loading more and more requirements on the RACG. Aircraft computer or low cost semiconductor technology may be the answer
cor- GPS, radio plied	Best mix of sensors on aircraft can give cost-effective initialization	As the required equipment list gets more complex, the task of weapon assignment becomes equally complex
	No aircraft computer requirement for update sensor	Limits operational flexibility target situation, cannot be changed from aircraft takeoff to missile launch
	Target selection flexibility in transit	Requires bulk computer memory on aircraft
	Ability to provide data to RACG during captive flight for self-alignment and initialization	
	No launch delay	Higher cost for a given accuracy level
	Decreased cost for a given accuracy level	Launch delay

(The reverse of this page is blank)

Capsule summaries of alternative alignment and initialization methods are given in the following paragraphs.

Leveling and Alignment

Gyrocompassing is a leveling and alignment process that can use low-cost sensors, but it requires a time-consuming, iterative calibration procedure. Gyrocompassing is accomplished with the use of a velocity reference while the AFBGW is still attached to the aircraft. The final azimuth error resulting from gyroscope drift rate in earth rate gyrocompassing is given by the following equation:

$$\Delta\psi = \frac{\delta}{\Omega}$$

where δ is gyroscope drift rate, Ω is earth rate, and $\Delta\psi$ is steady state azimuth error.

A 1-degree/hour gyroscope drift and an earth rate of 15 degrees/hour produce a 67-milliradian heading error, which is considerably greater than the acceptable error for the AFBGW. Therefore, the only form of gyrocompassing that can be considered for the AFBGW is one in which the launch equipment includes a gyroscope of higher quality (e.g., 0.02 degree/hour) that could be used as a continuous reference for the missileborne gyroscope. Self-level is not precluded by sensor capability, but it may require an undesirably long period of time.

Parameter matching involves a comparison of missile and aircraft sensor outputs to estimate the differences in orientation of the two platforms. The match can be made either by a direct output signal comparison (angular rate and acceleration) of all sensors, or by comparison of navigational data. The first method must overcome the problem of aircraft flexure; the second must distribute errors in navigation variable differences among the various possible sources. Some of these error sources are shown in Table 23 (Section V).

During a parameter matching operation, differences in position and velocity must be distributed among the error sources. However, this problem can be partially circumvented by using a predetermined aircraft maneuver. This eliminates many of the basic inertial system error sources and allows a relatively simple computation of relationship between navigation errors and platform misalignment.

Several investigators have examined platform alignment through successive discrete fixes and have advanced algorithms, but these algorithms have not been demonstrated operationally. This process involves determining heading error by measuring changes in position error as indicated by position fixing at predetermined intervals.

The discrete fix methods of alignment have been investigated by several specialists, including Sutherland at TASC. This technique can involve the use of the RACG sensor to obtain position data at predetermined points along the flight path (prior to launch or after launch). All of these techniques are based on the premise that, if sufficient commonly based data on position are obtained, all navigation variables (position, velocity, and attitude) can be determined. Simplistically speaking, if three position fixes are taken, nine pieces of data are provided. This should be sufficient to solve simultaneous equations to provide position errors in three coordinates (cross-track error, on-track error, and inertial error), velocity error in three coordinates (axial, transverse, and vertical), and attitude error in three coordinates (roll, pitch, and yaw—from which azimuth can be derived). Alignment by discrete fixtaking usually involves extensive digital computer utilization because of the large state vector associated with the process. (State vector includes all error parameters in all dimensions and can include a subdivision of errors into its constituent components.)

Initialization

Missile gyroscope and accelerometer calibration are critical issues. Draper laboratory specifications for the modular sensor show a 10:1 turn-on error to random error, indicating that prelaunch calibration is highly desirable to reduce the effect of the initial error to acceptable levels. Calibration by matching to the aircraft sensor can be performed either prior to the alignment process or simultaneously with it. Several investigations, including those performed by Delco and TASC, have encountered technical difficulties in perfecting algorithms that provide simultaneous alignment and calibration. Computer requirements, which otherwise are relatively simple, also become stringent in a simultaneous calibration/alignment operation, increasing by a factor of four over a simple calibration process.

Calibration by Modulation. Calibration can alternatively be achieved by modulation of the platform or gyroscope. Modulation consists of a cyclic variation of some parameter that influences gyroscope drift. It could involve the rotation of

the platform to compare indicated instantaneous velocity with indicated average velocity. It could also include a sinusoidal variation in the spin motor speed. This would cause a cyclic change in the momentum of the gyroscope wheel, which would allow the detection of drifts caused by nonuniform changes in dimension and magnetic field. (All of the above calibration techniques are required because it is desirable to calibrate as short a time as possible before launch. If calibration before takeoff of the carrier aircraft were adequate, it would be possible to simply observe the apparent velocity of the platform when the system was at rest.)

Modeling of g-sensitive errors involves a determination of the relationship between gravitational field and gyroscope drift rate. The knowledge of this relationship is used to provide drift rate compensation. The process can involve empirical analog arrangements within the instrument or explicit digital computer calculations.

Initialization of Missile Position and Velocity. The approaches to initialization of missile position and velocity listed in Table 26 include the transfer initialization method, the successive discrete fixtaking method, and the aiding sensor method. An exceptionally high quality master inertial navigation system on board the aircraft is a requirement for transfer initialization; only the LN33 or the SKN2400 systems are satisfactory for the AFBGW/RACG system.

If discrete fixtaking is employed for alignment and gyroscope calibration, it will be available for initialization of velocity and position. However, this results in a 12 state vector computational problem. Specialists estimate that simultaneous operations that involve 12 primary state vectors are about 20 times more difficult than a simple three-state operation.

Aiding devices on board the aircraft (e.g., GPS, doppler radar, LORAN, radio navaids, and radar) can also be used to initialize position and velocity. Although these can be cost effective, they present logistics problems. For example, in a large operation, it would be necessary to identify aircraft with appropriate avionic systems. This could cause problems in weapon assignment and, in critical cases, could adversely affect their operational value.

Finally, update sensor data transfer and sensor equipment prelaunch environmental conditioning are discussed. This points up an important decision in the selection of inertial sensors. If temperature control is required, a heating cycle

is necessary before launch, and this delays the initiation of the weapons flight. If design obviates the need for gyroscope heating, then a cost penalty will be incurred for a specified level of accuracy.

The alignment/initialization alternatives identified above pose a complicated problem that involves system accuracy, operational flexibility, and expendable sensor sophistication. The most cost-effective systems could result from combinations of the above alternatives for a given function (for example, it might be desirable to self-level and then align with a discrete fix). The following sections examine each of the functions in Table 26 and provide a basis for selecting preferred concepts.

ALIGNMENT—LEVELING AND GYROCOMPASSING

Leveling is the process of establishing a vertical reference to prevent the effect of the earth's gravitational field from distorting calculations that involve vehicle lateral acceleration. In a gimballed platform, the inertial block is physically aligned either to the local vertical or to the earth's center of gravity. In a strapdown system, the process is computational. Prior to the introduction of optimal alignment techniques, the leveling operation preceded the elimination of heading reference errors because the level errors coupled into the heading alignment loop and complicated the process. Using optimal estimation techniques, however, the entire level/heading error compensation procedure can be accomplished at one time.

Leveling in its basic form is done from a fixed position on earth. The magnitude of accelerometer readings when the vehicle is at rest indicates the initial angle of the system with the horizontal. The ability to level at rest depends upon the accuracy of the accelerometer (2×10^{-4} g bias corresponds to 40 arc seconds).

Since the comparatively inexpensive AFBGW gyroscopes have a relatively high drift rate, they will be leveled from the launch vehicle, close to launch, to minimize drift errors. This can be done either by using a velocity reference to account for the aircraft motion or by matching the aircraft accelerometer output to the platform output. A typical leveling mechanization using a velocity reference is shown in Figure 28. Theoretically, the loop could be leveled in an arbitrarily short time. However, there are random as well as bias errors to the loop. The equation below indicates relationship between pitch level errors and pitch sensor error sources:

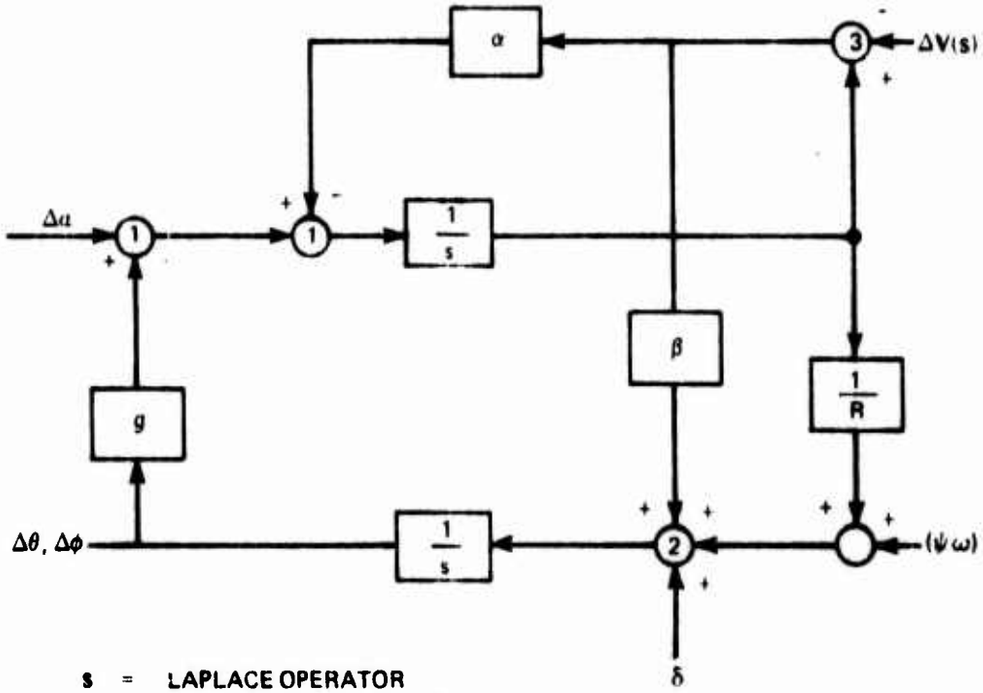

s = LAPLACE OPERATOR
α, β = LOOP GAIN
δ = GYRO DRIFT RATE
Δ a = ACCELERATION BIAS
ΔV(s) = VELOCITY REFERENCE ERROR PROCESS
ψ = INITIAL AZIMUTH ERROR
ω = MISSILE ANGULAR RATE
g = GRAVITATIONAL CONSTANT
R = EARTH RADIUS
Δφ, Δθ = LEVEL ERRORS (PITCH AND ROLL AXIS)
λ = $\sqrt{g/R}$

*NOTATION AND VALUES GIVEN IN TABLE 27.

Figure 28. Platform Leveling Diagram

$$\Delta\theta = \frac{\left(\frac{1}{R} + \beta\right)\Delta a + (s + \alpha)\delta + (s + \alpha)\omega\Delta\psi + \left(\frac{\alpha}{R} + \beta s\right)\Delta V(s)}{s^2 + \alpha s + (1 + R\beta)\lambda^2} \quad (1)$$

The steady state form of Equation (1) is:

$$\Delta\theta_{ss} = \frac{\left(\frac{1}{R} + \beta\right)\Delta a + \alpha\delta + \alpha\omega\Delta\psi + \frac{\alpha}{R}\Delta V}{(1 + R\beta)\lambda^2} \quad (2)$$

The notation is the same as that shown in Figure 28. All the above error sources may be represented by a power spectrum; however, only velocity reference $[\Delta V(s)]$ is shown as a frequency variable because its non-zero frequency dependent errors are usually critical to a velocity reference leveling system.

In specifying the gains for Figure 28 (α and β), it is important to strive for three objectives that are, to a certain extent, contradictory: (1) a loop with a fast time constant; (2) a loop that results in a minimum value for $\Delta\theta$ in Equation (2); and (3) a minimum value for the errors resulting from the term $(\alpha/R + \beta s)\Delta V(s)$ in Equation (1), which involves steady state and noise errors. The noise errors for the system are given by the following equation:

$$\overset{\omega\omega}{C^2}(t) = 2\int_0^\infty \Phi(\omega)\,|G(j\omega)|^2\,d\omega \quad (3)$$

where C(t) is error output, t is time, $\Phi(\omega)$ is noise process of the velocity reference, $|G(j\omega)|$ is magnitude of the frequency response of Equation (1), and ω is frequency. A low-cost doppler velocity system is characterized by the following noise process:

$$\Phi(\omega) = \frac{K}{\tau_c s + 1} \quad (4)$$

where K is power spectral density of the noise process (magnitude), and τ_c is correlation time.

Typical values for this mission are:

$$K = 15 \frac{(\text{foot/second})^2}{\text{radian/second}}$$

$$\tau_c = 30 \text{ seconds}$$

By a trial-and-error process, selected values of α and β were applied to Equations (1), (2), and (3) to evaluate the time constant, achieve an acceptably low value for $\Delta\theta_{ss}$, and minimize the value of $\tilde{\tilde{C}}^2(t)$. A reasonable system was defined by using the following parameters:

$$\alpha = 0.0125$$

$$\beta = 5 \times 10^{-6}$$

The time constant is derived by the following rationale:

- The denominator of Equation (1) is:

$$s^2 + \alpha s + (1 + R\beta)\lambda^2$$

- Applying the values from Table 27, the denominator becomes:

$$s^2 + 0.0125s + \left(1 + 2.06 \times 10^{7} \cdot 5 \times 10^{-6}\right)\left(1.56 \times 10^{-6}\right)$$

or:

$$s^2 + 0.0125s + 0.000162$$

- The roots of the equation are:

$$s = -0.00625 \pm 0.0106j$$

TABLE 27. VALUES OF PARAMETERS FOR GYROCOMPASSING ERRORS

PARAMETER	EXPLANATION	VALUE	ORIGIN
δ	Gyroscope Drift	1 degree/hour = 4.85×10^{-6} radians/second	Study Ground Rules
Δa	Accelerometer Bias	$2 \times 10^{-4} g$	Study Ground Rules
$\Delta\Psi$	Azimuth Error	1 degree = 0.0175 radians	Survey
ω	Inertial Turning Rate	10 degrees/hour = 48.5×10^{-6} radians/second	Mach 1.5 at 45 degrees/latitude
R	Earth Radius	20.6×10^{6} feet	At Surface
g	Gravitational Constant	32.2 feet/second	At Surface
λ	$\sqrt{g/R}$	1.25×10^{-3}	Computed

- The reciprocal of the real part of the root is 160, which is an approximation of the equivalent first order response time constant.

Table 28 shows the platform level errors for minimum noise output, assuming the terms of Equation (2).

TABLE 28. TYPICAL LEVEL ERRORS*

SENSOR SOURCE	SENSOR INPUT	ERROR CONTRIBUTION (seconds)
Gyroscope Drift (ϵ)	1 degree/hour	80
Accelerometer Bias (Δa)	$2 \times 10^{-4} g$	40
Azimuth Error Coupling (ψ)	1 degree	14
Velocity Bias (ΔV)	5 radians/second	8
Velocity Noise [$\Delta V(s)$]	15 $\frac{\text{(foot/second)}}{\text{radian/second}}$	4
COMPOSITE.		91

* See Table 29 for equations and Table 27 for values.

The results are compatible with the use of low-cost velocity reference equipment discussed in Section II. The velocity reference in Table 28 could be mounted on the aircraft or could form part of the AFBGW itself. Total leveling time to attain the above performance is estimated at 400 seconds or about 6.6 minutes.

Gyrocompassing

The process of gyrocompassing entails use of the earth's rotation and the platform gyroscopes to establish a north reference in a situation where the platform is fixed to the earth's surface. If the platform is in motion and a velocity reference exists—external to the platform being aligned—then the earth rate and the platform rate may be added vectorially, and the resulting spatial rate vector can be used to align the

TABLE 29. EQUATIONS FOR GYROCOMPASSING ERRORS

LEVEL ERROR SOURCE	EQUATION	SOURCE
Gyroscope Drift (δ)	$\frac{\frac{1}{R} + \beta}{(1 + R\beta)\lambda^2}$	Equation (2)
Accelerometer (Δa)	$\frac{\alpha\delta}{(1 + R\beta)\lambda^2}$	Equation (2)
Azimuth Error ($\Delta\psi$)	$\frac{\alpha\Delta\psi}{(1 + R\beta)\lambda^2}$	Equation (2)
Velocity Bias (ΔV)	$\frac{1}{R}\left\{\frac{\alpha\Delta V}{(1 + R\beta)\lambda^2}\right\}$	Equation (2)
Velocity Noise [$\Delta V(s)$]	Equation (3)	Reference 20

platform. Gyrocompassing applies to both gimballed and strapdown platforms. In the latter case, the alignment reference is computed rather than observed.

Gyrocompassing, the most frequently used method of aligning gimballed inertial platforms (Reference 21), was originally performed exclusively on the ground. Subsequently, an airborne velocity reference (the doppler navigator) permitted airborne gyrocompassing by compensating the aircraft motion with a reference external to the IMU. A cursory literature search on doppler inertial mechanizations that discuss gyrocompassing easily produced over 100 references. General Precision Laboratory (Singer GPL) alone has produced dozens of studies since 1960, with Frank McMahon, Heinz Buell, and Lou Marino (who wrote Appendix D) making outstanding contributions.

As was discussed earlier in this section, the limitations of the gyrocompassing method make its direct application to the AFBGW unsatisfactory. The chief objection is that it would require the inclusion of a high quality gyroscope (0.02 degree/hour) in the launch equipment. However, the

technique provides background for discussing other modes of alignment and is relevant to a possible hybrid system discussed in Section VII. The primary objection to the gyrocompassing approach is its inherent inaccuracy, which arises from the high effective drift in the eastward direction. When a strapdown system is referred to, a virtual east gyroscope drift is derived from the strapdown axial and lateral gyroscope drifts as follows:

$$\delta_e = \delta_x \sin\psi - \delta_y \cos\psi \tag{5}$$

where δ_e is east gyroscope drift, δ_x is axial gyroscope drift, δ_y is lateral gyroscope drift, and ψ is missile heading.

The application of gyrocompassing to the AFBGW/RACG would require a special pod containing a single-axis reference for launch aircraft without inertial systems. This equipment could form a part of the AFBGW launch equipment and could be provided at a fraction of the cost of an inertial pod system. However, some method is required to compensate for flexure between the reference and the missile. Alternatively, a single-axis reference could be placed at each mounting point.

Gyrocompassing is typically executed during the last 15 minutes before launch. Its errors arise from three principal sources: east gyroscope drift, reference velocity bias, and reference velocity noise. The error model is shown in Figure 29. A single x-axis representation of the errors associated with velocity reference gyrocompassing is given by the following transfer function:

$$\Delta\psi = \frac{\frac{K_3}{R} s\Delta a(s) - \frac{K_3}{R}(s^2 + \lambda^2)\Delta V(s) - K_3\lambda^2\delta_x(s) + \left[s^2 + K_1 s + (1 + K_2)\lambda^2\right]\delta_z(s)}{s^2 + K_1 s^2 + (1 + K_2)\lambda^2 s + K_3\omega_x\lambda^2}$$

$$K_3 = \frac{K_z}{\omega} \tag{6}$$

where $\Delta\psi$ is azimuth orientation error, R is earth radius (2.06×10^7), Δa is accelerometer bias (2×10^{-4}g), λ^2 is g/R (the square of the Schuler frequency) = 1.56×10^{-6}, ΔV is velocity error, δ is gyroscope drift rate, K_1, K_2, K_3, K_z are gains shown on the diagram of Figure 29, the subscripts

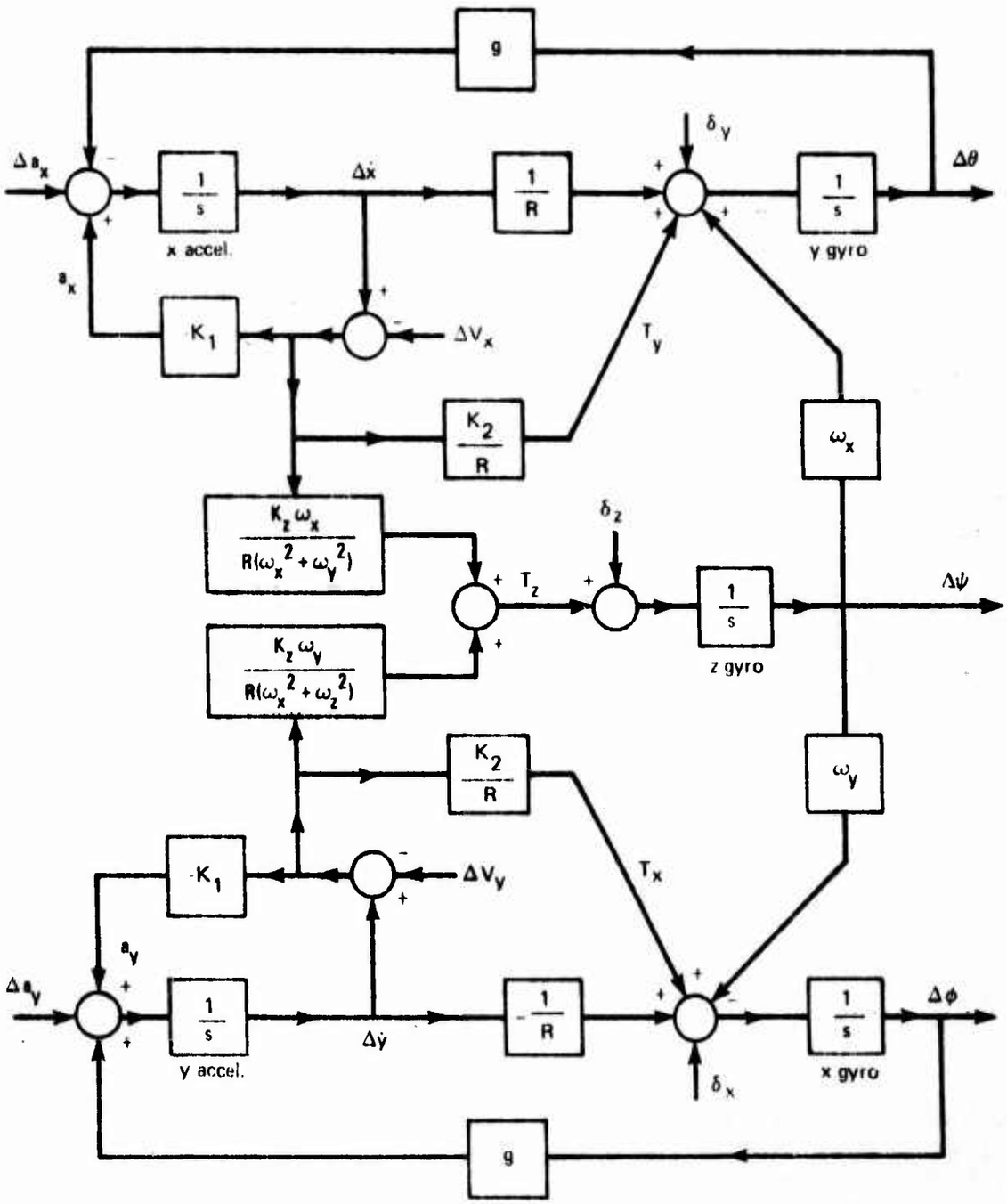

Figure 29. General Error Diagram of Spatial-Rate Gyrocompassing

x, y, and z refer to the roll, pitch, and yaw gyroscopes, respectively, and ω is the magnitude of the platform rotational rate. The steady state errors are given by the following transfer function:

$$\Delta\psi_{ss} = -\frac{\Delta V_x}{R\omega_x} - \frac{\delta_y}{\omega_x} + \frac{1 + K_z}{K_3\omega_x}\,\delta_z \qquad (7)$$

Obviously, the values of many transient and steady state errors vary with choice of K_i values, which in turn depends upon a tradeoff involving steady state errors ΔV_x, δ_y, and δ_z and the velocity noise errors (References 20 and 22).

Equivalent noise errors for doppler radars of the quality discussed here are about 1 feet/second (Reference 17). System synthesis to determine the K_i values involves a tradeoff of bias and noise errors. Bias errors for the type of doppler radar considered here are about 3 feet/second (aircraft/nonexpendable). A special nonexpendable east gyroscope for aircraft launch equipment supplement could have an accuracy of 0.02 degree/hour.

Assuming the above parameters, the portion of Equation (6) dealing with azimuth errors could be normalized to the following form:

$$\Delta\psi(s) = \frac{T^3s^2 + 3T^2s + 3T}{(Ts + 1)^3}\,\delta(s) \qquad (8)$$

The portion of Equation (6) that deals with velocity noise errors can be written as:

$$\Delta\psi(s) = \frac{T^3K_3}{R} \cdot \frac{s^2 + \lambda^2}{(Ts + 1)^3} \cdot \Delta V(s) \qquad (9)$$

The errors that result from $\Delta V(s)$ are of two types—noise and bias. The noise errors are given by the following equation, which is derived from Equation (3):

$$\overline{\Delta\psi(t)^2} = \frac{15}{R^2\omega^2{}_A{}^4T^6}\int_{-\infty}^{\infty}\frac{\left(\lambda^2 \quad \omega^2\right)^2}{2\pi\left(\omega^2 + \frac{1}{T^2}\right)^3}\,d\omega \qquad (10)$$

As the value of T increases, the effect of the bias errors increases; as the value of T decreases, the effect of noise errors increases.

It is important to determine a value of T that will provide a minimum composite value of noise and bias. This will allow the use of a T that is compatible with a near minimum value when all error sources are considered. Through a trial-and-error process that considered all of the above factors, a T value of 0.25λ was chosen (about 200 seconds). This indicated that a system could be formulated that would have an adequately fast response to meet the needs of the AFBGW launch aircraft. The steady state value of $\Delta\psi(s)/\delta(s)$ is given by allowing s in Equation (6) to go to zero, which gives a residual value of 3T. On the other hand, smaller values of T increase the values of the noise integral (James, Nichols, and Phillips [see Appendix A, Volume II]). Speed of alignment, accuracy potential, and practicality can be demonstrated. However, the concept would require the deployment of special equipment whose sole purpose is to align the platform.

Figure 30 shows the typical gyrocompassing operation as it might be applied to the AFBGW. The curves were calculated by use of Equation (6). Table 30 shows the correspondence between terms in the numerator of Equation (6), the form of the input to the equation, and the labels of the curves in Figure 30.

Table 30 shows the way in which Equation (6) is used to construct Figure 30. Column 2 of Table 30 gives the numerator term of Equation (6) that is applicable to the error source in Column 1 of Table 29. Column 3 of Table 30 indicates the value that replaces the applicable dependent variable in Equation (6). Note that there are two rows devoted to velocity errors. This occurs because velocity noise errors are significant in this analysis, while gyroscope and accelerometer noise terms are not. (If gyroscopes of lower quality, say 100 degrees/hour, were being investigated, all sources would be analyzed for noise.) The velocity noise cannot be analyzed by simply putting a transfer function into Equation (6). All noise calculations require the use of Equation (3), which was mentioned in connection with the discussion on leveling.

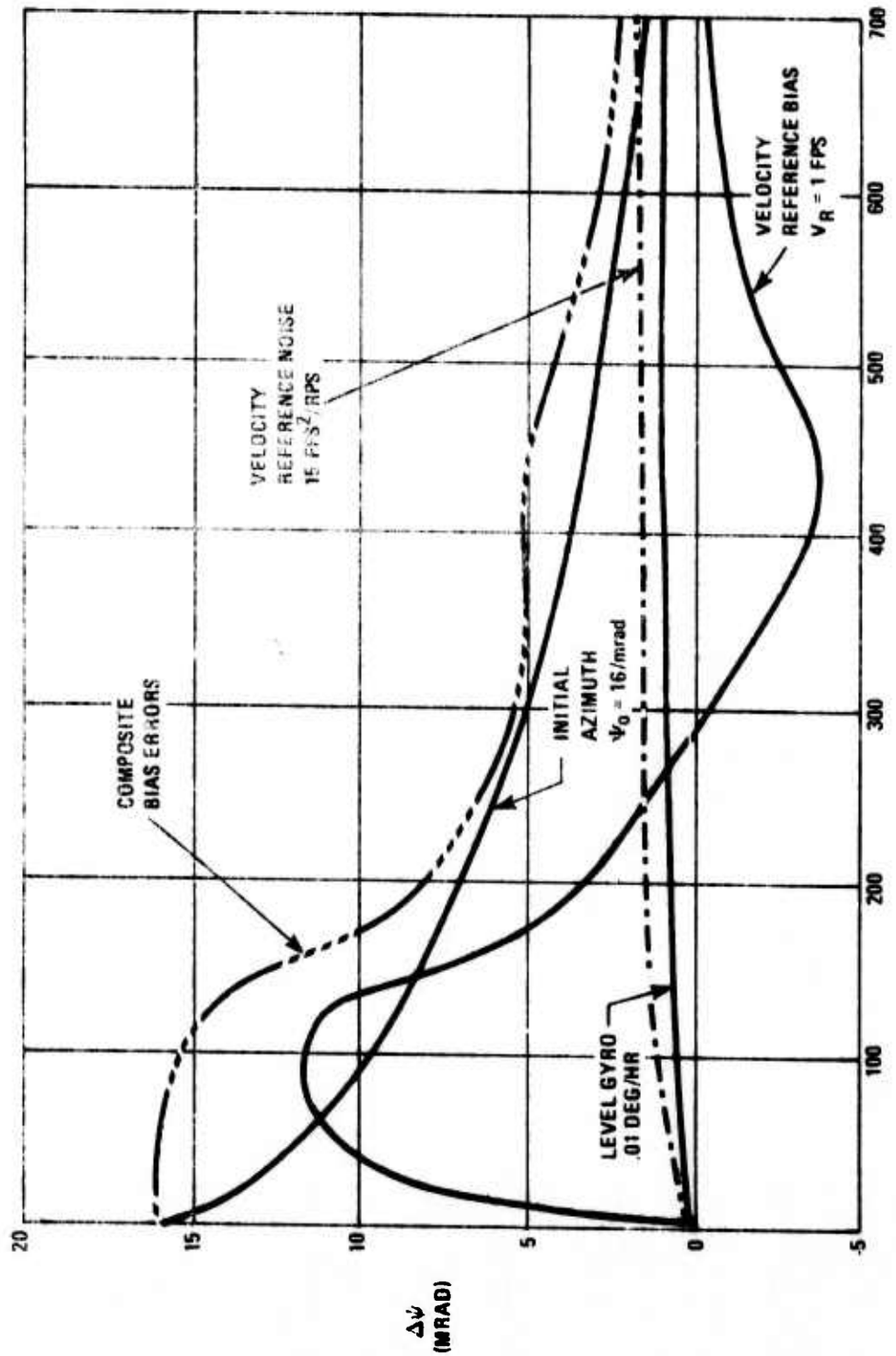

Figure 30. Air Force Baseline Guided Weapon Gyrocompassing Alignment

TABLE 30. ELEMENTS USED IN CALCULATING THE CURVES OF FIGURE 30

ERROR SOURCE (CURVE DESIGNATION)	APPLICABLE EQUATION (6) NUMERATOR TERM	FORM OF INPUT TO EQUATION (6)
Level Gyroscope	$K_3\lambda^2\delta_x(s)$	$\delta_x(s) = 0.01 \times 4.85 \times 10^{-6} \times \frac{1}{s}$
Accelerometer	$\frac{K_3}{R} s\Delta a(s)$	Not included because of negligible impact
Initial Azimuth	$\left[s^2 + K_1 s + (1 + K_2)\lambda^2\right]\delta_z(s)$	$\delta_z(s) = 0.016$
Velocity Reference Bias	$\frac{K_3}{R} (s^2 + \lambda^2) \Delta V(s)$	$\Delta V(s) = 1 \times \frac{1}{s}$
Velocity Reference Noise	$\frac{K_3}{R} (s^2 + \lambda^2) \Delta V(s)$	Equation (3) is used for this term only: $\Phi(\omega) = \frac{15}{\omega^2 + 0.030^2}$

The expressions that appear in Column 3 of Table 30 include constants and transfer functions. Where the term 1/s occurs, it indicates that the input is an impulse or instantaneous value applicable only at the instant when $t = 0$ ($s = \infty$).

The numerical values in Table 30, Column 3, have the following origins:

- For $\delta_x(s) = 0.01 \times 4.85 \times 10^{-6} \times 1/s$:
  - 0.01 is the gyroscope drift rate of the auxiliary launcher mounted gyroscope in degrees per hour.
  - 4.85×10^{-6} is a conversion factor from degrees per hour to radians per second.
- For $\delta_z(s) = 0.016$, an initial azimuth misalignment of 16 milliradians or slightly less than 1 degree is assumed. This value would be reasonably achieved with simple magnetic references.
- For $V(s) = 1 \times 1/s$, a 1 foot/second velocity reference is used for this calculation—possible with the GPS X-receiver.
- The expression $\Phi(\omega) = 15/\omega^2 + 0.030^2$ is representative of doppler noise. It is thought to be applicable to most radio-derived velocity sources, although individual classes of instruments vary in capability.

Transfer Alignment—Parameter Matching

The transfer of attitude reference from aircraft master inertial navigator to missile inertial measuring unit (IMU) may be performed by parameter matching (Reference 21). Originally called velocity matching, the process now includes acceleration and angular rate. Because of its simplicity and operational flexibility, parameter matching is considered a primary alignment candidate. The limitations of this technique include requirements for a prelaunch maneuver and for an inertial navigator on the launch aircraft; however, these are largely offset by the flexibility factor, which eliminates the need to arrive at a specified area before launch. Furthermore, allocating all requirements to nonexpendable aircraft equipment minimizes expendable equipment cost. From this viewpoint, velocity matching also seems desirable.

Table 31 outlines some of the variations of parameter matching that can be applied to the AFBGW tactical situation. Response times are relatively short, and computational requirements are reasonable. As examples of the effectiveness potential of the generic approach, Systems 6 and 7 were chosen for further examination.

System 7 evolved as a part of the Simple High Accuracy Guidance (SHAG) Program. Employing several innovations that have not been generally adopted, the system is outstanding in that it employs both acceleration and angular rate matching. This allows an unprecedented flexibility in choice of alignment maneuvers. The pilot can use a straight approach with a small roll oscillation, a 3g S maneuver, or a lateral maneuver (Reference 23).

Another unique and desirable feature of System 7 is related to the application of aircraft flexure modeling. The system employs a weighting matrix that is tied to actual aircraft flexure. In the final algorithm, one noise intensity matrix was computed by Honeywell to compensate for the aircraft bending process, and the other was tied to the gyroscope drift process. System 7 is identified by its mechanization equations, which appear in Appendix D, Volume II.

The SHAG concept (System 7) was compared to a class of algorithms developed specifically for the RACG program (Table 31, System 6). The objectives included an alignment accuracy of 15 arc minutes and a level accuracy of 50 arc seconds. Gyroscope calibration was also achieved with this algorithm. Initial drift rate was assumed to be 3 to 5 degrees/hour, and a calibrated value of 0.3 degree/hour was sought (Reference 24). Two generic concepts were included under System 6—Kalman filter and an analog mechanization.

The Kalman system is designed for minimum computational complexity within the accuracy objectives stated above. It allows 10 minutes for the alignment/compensation process, but the final system is capable of achieving its accuracy objectives within a much shorter time period. Six error states are employed in the system, and direction cosines are employed in the transformation.

The problem of coupling of misalignment into the gyroscope correction process is significant in the Kalman filter concept. It is necessary to reduce the gyroscope drift sample to 20 arc seconds in 1 minute of observation. This requires a 5- to 6-minute period of gentle maneuver with a very short iterative interval (1 to 5 seconds). The Delco RACG Kalman approach of System 6 is described in detail in Appendix D, Volume II.

TABLE 31. TRANSFER ALIGNMENT BY PARAMET

System	Data Source	Development Base	Application	Parameters	Maneuver Used
1	Vanderstoop Boeing	Jan. 1963	Strapdown to strapdown	Acceleration	2.5 g
2	MacLoon Nortronics	Jan. 1968	Gimbal system	Velocity increment	2-g turn
3	Fagan TASC	June 1969	Strapdown gimballed ref.	Acceleration	Long duration lateral turn
4	Lackowski Honeywell	July 1969	Strapdown Strapdown ref.	Angular rate	Quick response with slow maneuv. semirigid path
5	Schultz Honeywell	Oct. 1971	Strapdown Strapdown ref.	Acceleration	3-g turn
6	Wolfe Delco	June 1972	Strapdown to strapdown	Velocity change	0.5-g turn
7	Schultz Honeywell	July 1972	Strapdown Strapdown ref.	Angular rate acceleration	3-g turn

NMENT BY PARAMETER MATCHING—RECENT DEVELOPMENTS

Maneuver Used	Sensor Accuracy (Missileborne)	Time Constant Initial Error Final Error	Concepts	Remarks
2.5 g	0.5 deg/hr	Υ = 200 sec $\Delta\psi_o$ = 20 mrad $\Delta\psi_f$ = 1 mrad	Alignment test and synthesis effort	
2-g turn	GBU-15 type sensors	Compatible with AFBGW	Directed to low performance IMU	6-state Kalman filter, NAC 10 C5A computer characteristics
Long duration lateral turn	Parametric examination	13-min gyrocomp. 5-min Kalman	6-gain GC 3 and 6 state Kalman	Angular rate matching also considered
Quick response with slow maneuv. semirigid path	3 deg/hr	Υ = 3.0 sec $\Delta\psi_o$ = 9 mrad $\Delta\psi_f$ = 1 mrad	Least squares nonrecursive	Demonstrated feasibility of using angular rate
3-g turn	60 deg/hr	Υ = 19 sec $\Delta\psi_o$ = 20 mrad $\Delta\psi_f$ = 1 mrad	SHAG	Especially directed to fighter aircraft situation
0.5-g turn	3 deg/hr (day-to-day) 0.3 deg/hr (10-min drift)	Υ = 50 sec $\Delta\psi_o$ = 5 deg $\Delta\psi_f$ = 1 mrad	Analog 6-state Kalman	Simultaneous gyro drift calibration and alignment
3-g turn	60 deg/hr	Υ = 13 sec $\Delta\psi_o$ = 1 deg $\Delta\psi_f$ = 1 mrad	Angular rate matching	Modeling of aircraft flexure

(The reverse of this page is blank)

To reduce computer requirements and to increase flexibility, a similar algorithm was developed by using analog processing. This system is illustrated in Figure 31. The basic elements of the analog algorithm are two first-order leveling loops with a 1-second time constant and high accuracy. However, the process is adversely affected by the presence of high gyroscope drift rates. When the aircraft is flying in a banked turn, the bias drift in the y gyroscope cannot be distinguished from the azimuth misalignment in the horizontal plane coupled with the aircraft angular rate. Consequently, there is residual azimuth error of about 2 milliradians for an uncompensated gyroscope bias. If the bias is compensated simultaneously with alignment, zero azimuth error can be achieved in 4 minutes or less.

The analog approach of System 6 and several options for System 7 were compared during this study. This involved adjusting raw data from Delco's simulation analyses to make the data compatible. The results are shown in Figure 32. System 7 is considerably faster than either the analog or Kalman versions of System 6 when both acceleration and angular rate matching are employed. When only acceleration matching is used, Systems 6 and 7 are comparable, although System 7 maintains a performance margin. Decreasing the maneuver intensity from 3.0g to 0.5g did not have a markedly detrimental impact on the AFBGW mission requirements for either system. However, gain matrix and maneuver strategy changes were required to keep the response and accuracy at acceptable levels.

Discrete Fixtaking Alignment

Azimuth alignment, which may be achieved through a series of discrete position fixes, has the advantage of not requiring external data. For a full velocity position and attitude alignment, three position fixes are required. Fixtaking processes such as the RACG and terrain elevation correlation provide two dimensions of position. It is assumed that a third dimension of altitude can be provided by raw data from the barometric or radar altimeter in combination with the inertial accelerometer (Reference 25).

Available algorithms for discrete fixtaking alignment vary greatly in sophistication; the situation is somewhat analogous to that presented by the velocity/angular rate matching. At one extreme is a full Kalman system with many error states and multiple error models. At the other extreme is a basic solution using velocity, position, and azimuth error equations simultaneously.

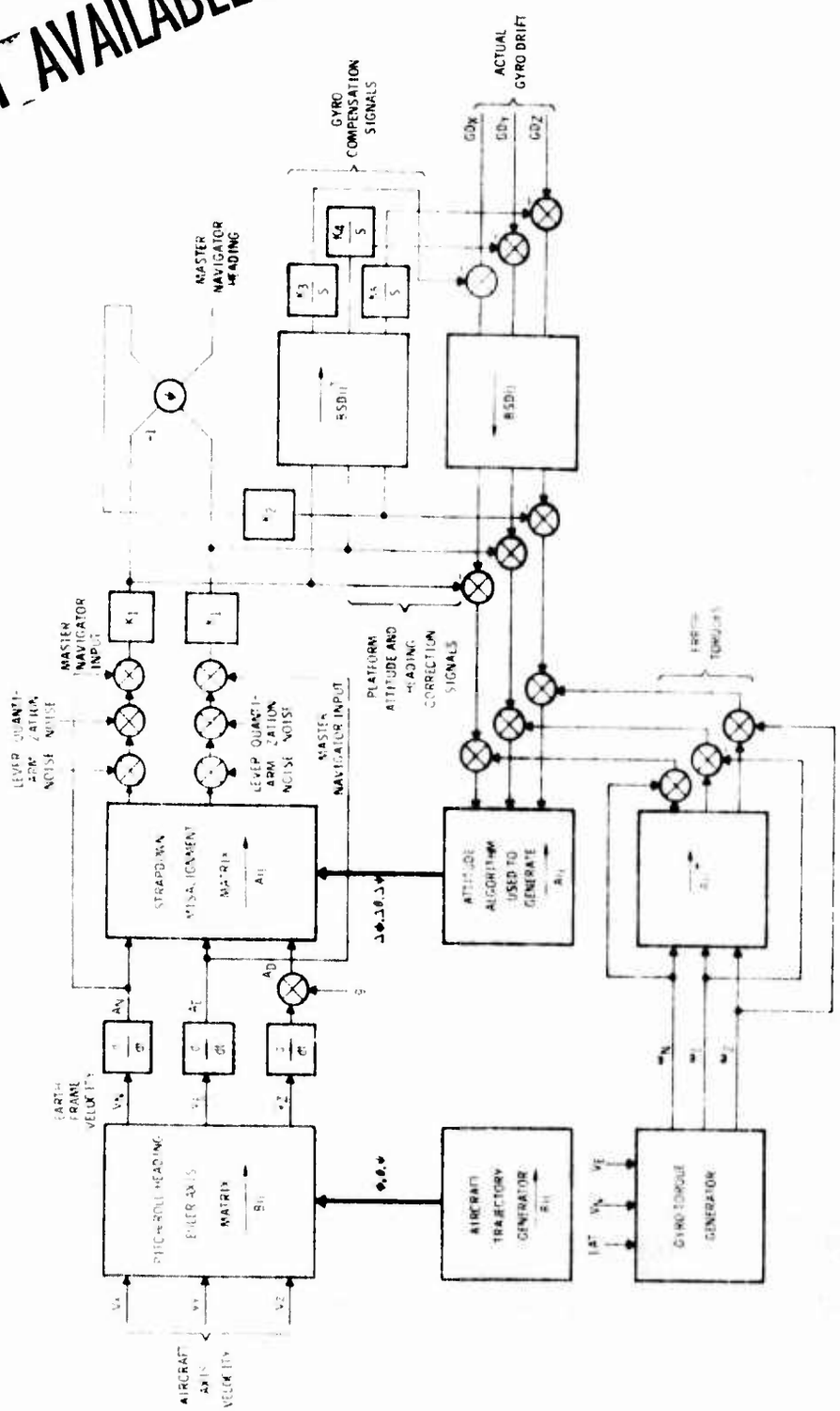

Figure 31. Simulation Block Diagram for Analog In-Air Alignment

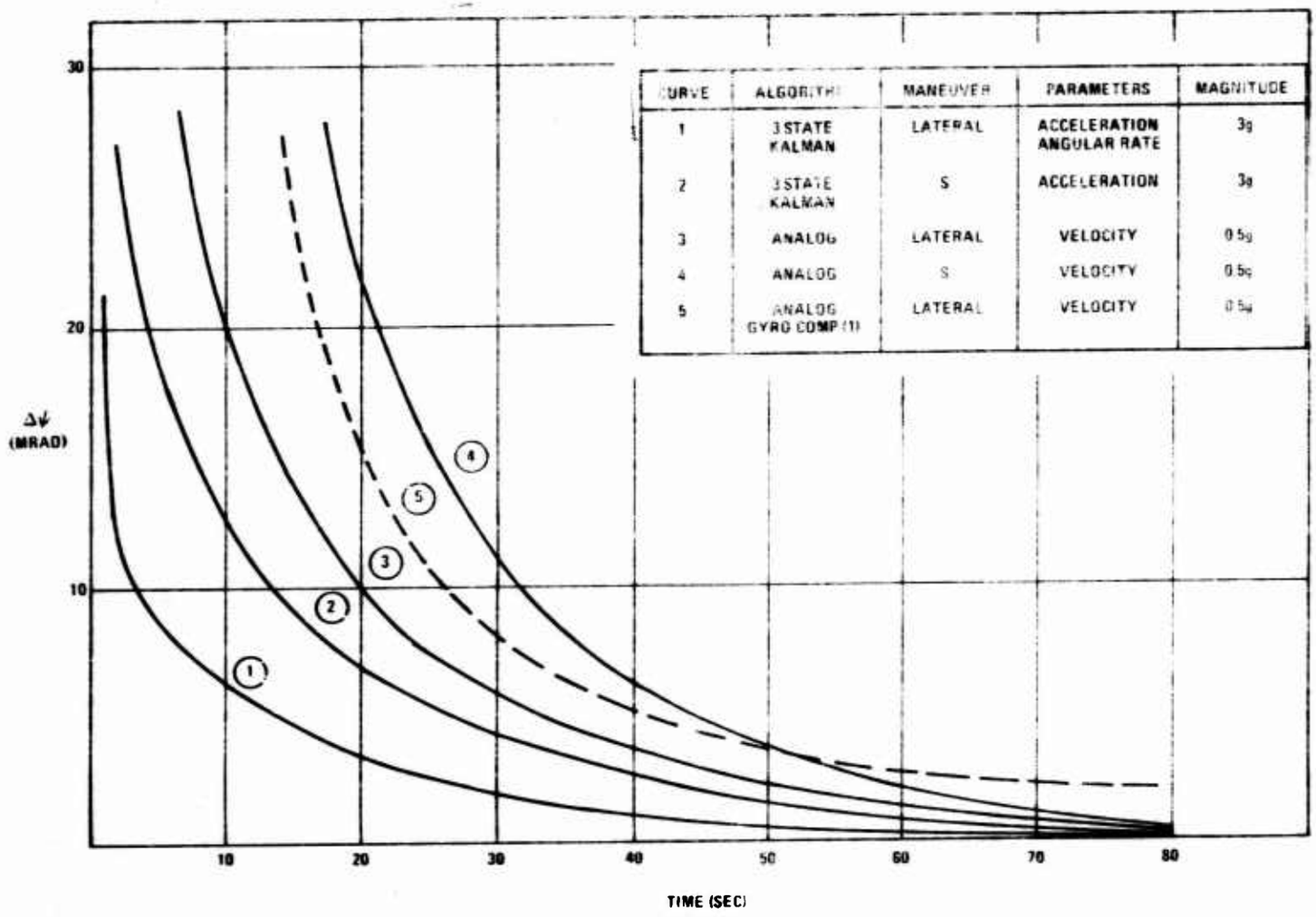

Figure 32. Comparison of Azimuth Alignment Techniques—Parametric Matching

In the basic solution, the navigation equations can be decoupled to give the following single channel relationship:

$$\Delta P_{ym} = \Delta P_x + \Delta V_x(2t)[t_1 - 2t] - \Delta\psi gt[t_1 - 2t]^2/2$$

where ΔP_{ym} is position error at the end of flight, ΔP_x is initial position error, ΔV_x is initial velocity error, t is time between fixes, t_1 is time between last fix and end of flight, $\Delta\psi$ is initial azimuth error, and g is gravitational constant.

If three position fixes are taken, the following relationship results:

$$\begin{bmatrix} 1 & -2t & -4t^2 \\ 1 & -t & t^2 \\ 1 & 0 & 0 \end{bmatrix} \begin{bmatrix} \Delta P_x \\ \Delta V_y \\ g\Delta\psi/2 \end{bmatrix} = \begin{bmatrix} P_{ym1} \\ P_{ym2} \\ P_{ym3} \end{bmatrix}$$

where P_{ym1}, P_{ym2}, and P_{ym3} are components of position error at the end of flight.

The initialization errors at the end of the fixtaking process are given by the following (Reference 26):

$$\Delta P_x = P_{ym3}$$

$$\Delta V_x = (P_{ym1} - 4\ P_{ym2} + 3\ P_{ym3})/(2t)$$

$$\Delta\psi = -\ (P_{ym1} - 2\ P_{ym2} + P_{ym3})/gt^2$$

The total error in initialization can be expressed as a function of errors in the fixtaking technique by the following:

$$\Delta P_x = \delta P$$

$$\Delta V_x = 2.066\delta P/t$$

$$\Delta\psi = 0.076\delta P/t^2$$

where δP is the error in the fixtaking process.

The errors in azimuth are shown in Figure 33 as a function of discrete fixtaking error. They show that multiple fixtaking is a practical approach to the alignment problem. However, the curves do not convey the disadvantages of constrained approach and severe computer requirements.

Alignment Methods—Comparative Summary

The alternative methods of heading error elimination are summarized in Table 32. The following order of preference is suggested: (1) prelaunch transfer alignment; (2) prelaunch alignment by successive position fixing; (3) postlaunch alignment by successive position fixing; (4) prelaunch analog gyrocompassing; and (5) postlaunch analog gyrocompassing. Items (1), (2), and (4) require precision reference equipment on the aircraft. These approaches are desirable for controlling the cost of expendable equipment; however, a lack of flexibility in the choice of launch aircraft is an associated penalty. Items (3) and (5) involve a relatively high missile investment cost but offer the ability to launch from any attack aircraft without regard to navigation avionics.

Transfer alignment was chosen as the preferred mode of heading error elimination on the basis of its accuracy, flexibility, and economy of missileborne equipment. All of these methods are valid for application where the missile and aircraft platforms do not share a common rigid physical structural interface. They apply to situations where the missile is wing mounted or located in a bomb bay that is remote from the aircraft inertial navigation system (INS) location. Under these circumstances, differences in angular position of the missile and aircraft reference structure can approach 3 degrees. Since the differences in angular orientation are a function of random forces, it is impossible to predict or compensate for position. For the level of accuracy sought in transfer alignment, the motions of the aircraft and missile are virtually uncorrelated in straight and level flight periods of less than 10 minutes.

It is important to note that accurate transfer alignment is possible at rest by direct comparison on the ground, or on

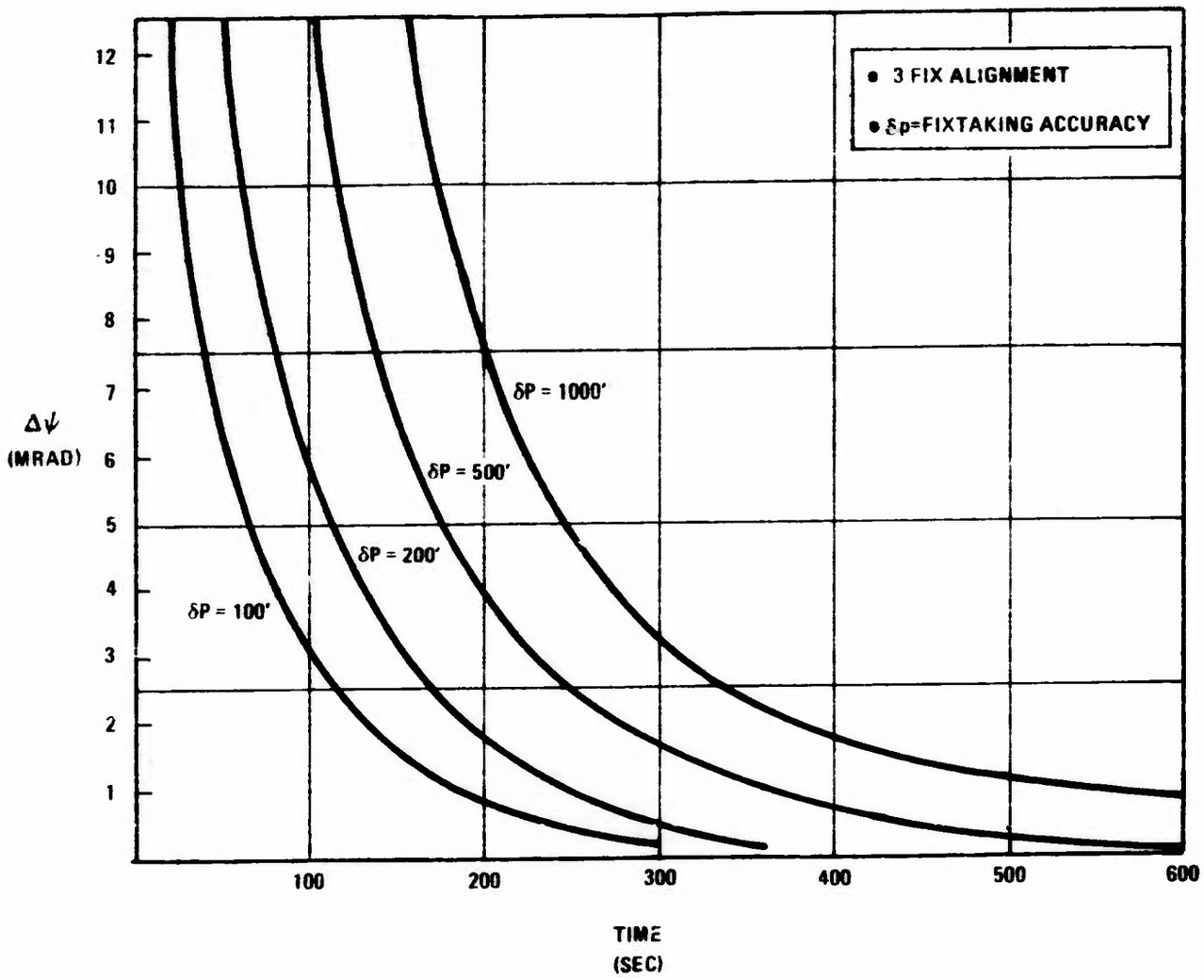

Figure 33. Discrete Alignment of Strapdown System

TABLE 32. ALIGNMENT ALT

Alignment Approach	Aircraft Equipment	Missile Equipment	Sensor Requirements	Software
Prelaunch transfer (navigation parameter matching)	Inertial platform required	Strapdown IGS of 1 deg/hr to 10 deg/hr quality (absolute value)	Aircraft Velocity reference . Doppler radar navigator . GPS receiver	Aircraft Depends on equipment, goals, and c Minimum 100 words/(adds Maximum 10 state Kal 2000 words
Prelaunch successive position fixes	Position fix device	Strapdown IGS	Aircraft Group A . Radiometer . TERCOM . Ground mapping radar Group B . LORAN . OMEGA . GPS	Aircraft 10 state Kal 2000 word a Group A ca an additiona 5000-10,00
Postlaunch successive position fixes	None	Position fix device Strapdown IGS	Above aircraft equipment must be placed on missile. Add missile	Above airbor ware must be on missile. Stringent com requirements
Prelaunch analog gyrocompassing	Inertial platform velocity reference	Strapdown IGS	Aircraft . Doppler radar . IGS	None attributi alignment
Postlaunch analog gyrocompassing	None	Strapdown Velocity reference	Missile . Doppler radar . IGS	None attribut alignment

2. ALIGNMENT ALTERNATIVES MATRIX

	Software	Constraints	References
ator	Aircraft Depends on quality of equipment, accuracy goals, and constraints Minimum 100 words/600 equiv. adds Maximum 10 state Kalman 2000 words	Time/maneuver/sensor accuracy tradeoff Example Point . 5 minutes . 28 deg bank angle maneuver . 5 deg/hr gyro drift Produces about 1 mrad accuracy	Lear Siegler, Inc., An Investigation of an Augmented Strapdown Inertial Guidance System, by Alan Bronkhorst, Rodney D. Wierenga, and Wayne D. Bard, GRR-005-0669, June 1960.
ar	Aircraft 10 state Kalman 2000 word average. Group A can require an additional 5000-10,000 words	Group A Must fly over preselected points Group B Must be within the effective operating envelope of the device	Analytic Sciences Corporation, MPMS/AIRS Calibration and Alignment Study, by Edward M. Duiven and Bard S. Crawford, September 1973.
must	Above airborne software must be placed on missile. Stringent computer requirements	Above constraints apply to missile	
	None attributable to alignment	5-10 minute preflight. Gyro drift rate an error source	Earl R. Norman and Donald J. Hafner, A Timed Cut-Off Technique for Fast Inertial System Alignment on an Accelerating Base, The National Aerospace Electronics Conference, Dayton, Ohio, 1962.
	None attributable to alignment	5-10 minute postflight. Gyro drift rate an error source	Massachusetts Institute of Technology, In-Flight Alignment of Inertial Navigation Systems by Means of Radio Aids, by Walter Tanner, R-720, June 1972.

(The reverse of this page is blank)

an aircraft when a rigid structural load path exists between the missile and aircraft INS. Under these circumstances, the orientation of the missile may be entered by direct transfer of digital, analog, or synchro data.

It is also possible to instrument the aircraft between missile and aircraft INS. This provides a real-time deterministic measure and allows compensation for differences in orientation angular rates and angular acceleration that are caused by aircraft flexure. Compensations may be accomplished by systems employing strain gauges, optical references, or mechanical sensors. Examination of these approaches was not pursued because they impose particular requirements on the aircraft prime and support equipment.

The type of transfer alignment schemes that were evaluated here involve the use of a maneuver to match the state variables of the missile system with those of the aircraft system. This was formerly called velocity matching, but subsequent use of position acceleration has led to a more general designation. The physical effect of the maneuver is to produce a sufficient monatonic change in a navigation parameter to overwhelm the random effects induced by aircraft flexure. The measured changes in navigation parameters are used to compensate sine alignment gyroscope drift and other error forcing functions.

Figure 34 compares typical examples of alignment technique that could be applied to the AFBGW concept. Curves 1 and 2 both provide the accuracy and response that are required. Curve 3 represents a marginal capability.

INITIALIZATION

Steps in initialization are discussed in the following paragraphs.

Missile Gyroscope and Accelerometer Calibration

The extreme importance of gyroscope calibration was emphasized in Section V. Draper Laboratory (Reference 5) indicates that their low-cost modular rate-integrating gyroscope (RIG) may have a day-to-day drift of 1.0 degree/hour and a random drift of 0.1 degree/hour. This indicates an excellent opportunity to reduce cost or improve performance at cost by adequate gyroscope calibration.

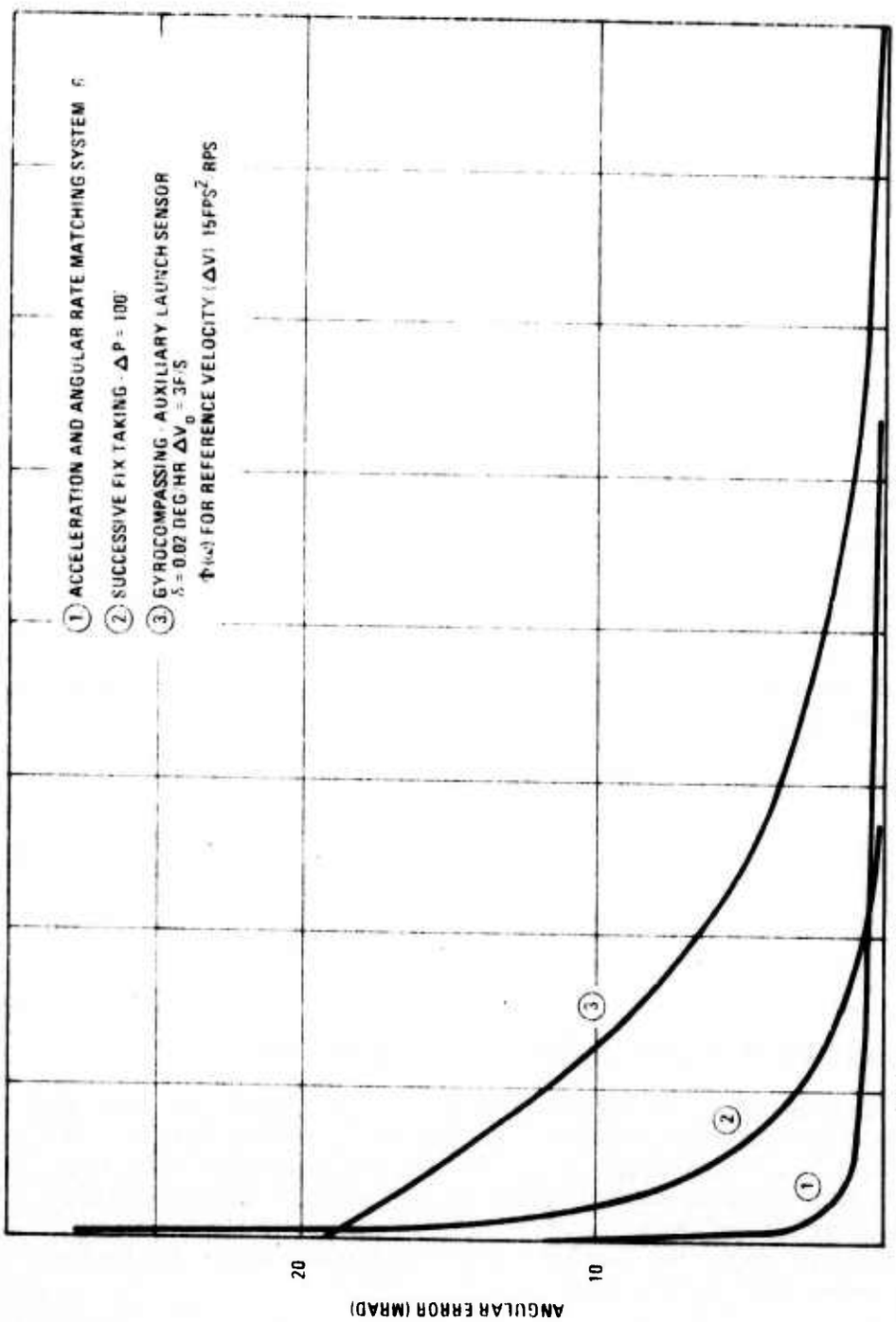

Figure 34. Comparison of Alignment Techniques

Three options for gyroscope calibration are well suited to the AFBGW/RACG application: (1) velocity matching; (2) calibration by modulation; and (3) discrete fixtaking. The Delco alignment study shows the feasibility of simultaneous attitude alignment and gyroscope calibration by acceleration matching. The gyroscope calibration process under this mechanization is much more time consuming than is the attitude alignment process.

The Kalman approach with an S maneuver and an iteration rate of 1 second provides the best performance for calibration of gyroscope drift. The ability to null level gyroscope drift to about 0.12 degree/hour (8 meru)* in about 250 seconds is possible. In all simulation runs, the azimuth gyroscope calibrated more slowly than did the level gyroscopes. Z-axis azimuth gyroscopes typically calibrated from 5 degrees/hour to 1.5 degrees/hour in 250 seconds, ultimately reaching 0.12 degree/hour in 600 seconds. (Azimuth gyroscope drift is not a critical error source for flights of short duration.) Representative drift profiles for velocity matching are shown in Figure 35.

Performance improvement through gyroscope output modulation has been pursued extensively in the inertial navigation industry. As discussed in Section V, gyroscopes are subject to three principal types of errors: uncompensated drift; torquer scale factor instability; and misalignment of the input axes. Gyroscope drift is caused by changes in the physical and mechanical environment of the gyroscope. Temperature distortion, electromagnetic field variations, and small pressure differentials can cause minute variations in the geometry of critical components. These, in turn, can cause significant errors in navigation. For example, a shift in position of the gyroscope's spinning wheel element of 1μ inch can cause a 200-foot increase in navigation error for the long-range mission.

Scale factor errors generally result from variation in torquing current. These error processes are not stationary and, consequently, cannot be modeled. Scale factor error causes an error in computed platform rotation that is proportional to the rate of rotation. Imperfect alignment of the gyroscope input axis causes the gyroscope to detect a

---

* One meru (milli-earth rotational unit) is equal to 0.015 degree/hour.

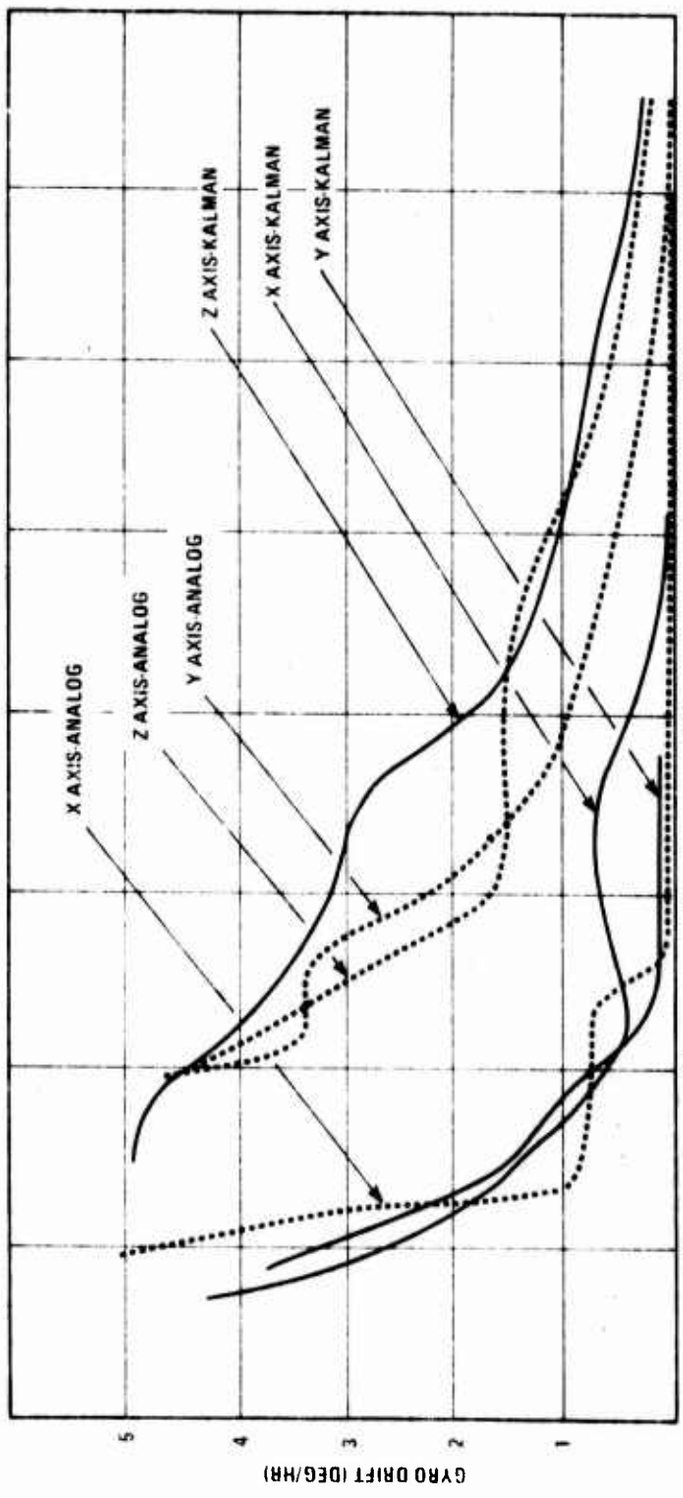

Figure 35. Gyroscope Drift Calibration Performance Potential

small part of the angular rate about another axis. The result is an apparent gyroscope drift that is proportional to the rate of the other input axis.

Correction of the above errors can be attempted in a variety of ways. An example is rotation of the IMU sensor block. The most successful and significant application of this practice is found in the use of the Carousel platform (Reference 27). Although the technique has not yet been applied to strapdown systems, there seems to be no physical reason why this cannot be done. The suggestion frequently arose in discussions with experts during the survey. The point is significant because Carousel achieves an accuracy factor of 80 when compared with nominal expected performance (i.e., Carousel can modulate a 0.8-degree/hour gyroscope and achieve a 1-nautical mile/hour performance). This is much greater leverage than can be obtained from simple drift compensation. It is well beyond the performance expected from the random drift performance of the instrument.

Another modulation approach involves variation of the spin motor speed. Experience with this approach is found primarily in the area of low-cost, rate-integrating gyroscopes. A performance level somewhat below the potential of velocity matching has been achieved by this technique.

The simultaneous modeling of gyroscope drift and attitude error while making discrete measurements of position has not been developed in a manner that allows direct application to the AFBGW/RACG. The correction of velocity, position, and attitude with successive fixes accomplishes a similar result, however. Extension of this effort into identification of individual error sources would be required for a true calibration model.

Initialization of Missile Position and Velocity

The transfer of initial position and velocity from the launch aircraft to the AFBGW may be accomplished in the following ways: (1) direct data transfer from the aircraft master inertial navigator; (2) use of the RACG to secure position and velocity data; and (3) use of alternative aircraft sensors.

With the first option, master inertial navigator transfer, the adequacy of the reference is critical. Table 33 indicates the types of aircraft IMU performance that can be expected for the deployment of the AFBGW/RACG system; it also shows that

TABLE 33. MASTER INERTIAL NAVIGATION SYSTEM—COST AND PERFORMANCE

MISSION TYPE	COST ($K)	POSITION ACCURACY (nautical miles)	DURATION (hours)	ACCURACY VELOCITY (feet/second)
Air Defense/Superiority	60 - 100	3 - 4	1 - 2	8
Attack/Close Air Support	75 - 125	1 - 2	1 - 2	4
Attack/Strike	100 - 200	0.5 - 1.0	10	2
Strategic	100 - 200	0.5 - 1.0	10	2

aircraft IMU initialization is probably not feasible. Even the expensive systems are not capable of satisfying the initial conditions and requirements.

The second option, use of the RACG for initialization, was shown to be feasible in the discussion of discrete fixtaking alignment. The position fix potential of the system is unquestionably adequate. Velocity is given as 2.06 P_{ym}/t. This indicates a 100-second interval between fixes for each 100-foot error (2σ) anticipated by the fixtaking device.

Transfer of Update Sensor Data to Missile

Airborne auxiliary equipment sensors and computer memory offer the greatest flexibility for cost-effective initialization. There is clearly a need for position update after extended flight. Radar, LORAN, differential Omega, DME, and GPS all are adequate to provide velocity and/or position update to the required accuracy. An RACG bulk storage capability onboard the aircraft with adequate interfaces with the missile would allow position velocity and azimuth to be determined in captive flight.

Prelaunch Environmental Conditioning of Sensors and Support Equipment

In many applications, it is considered appropriate to bring the temperature of the gyroscope to a specified level and to stabilize temperature differentials before system activation. In the low-cost gyroscopes emphasized in this study (Section IV), temperature control is not required. However, the final decision concerning heating requires a tradeoff involving cost, performance, and operational constraints. Aircraft launch equipment requirements constitute a critical aspect of this tradeoff.

Temperature stabilization detracts from operational flexibility because it requires a certain heating period. It also requires appropriate power regulation and precise temperature measurement. Temperature control is attractive because it allows the gyroscope to operate at the temperature design point without elaborate compensation arrangements. A few of the more obvious advantages are neutral stabilization buoyance, maintenance of tolerances, uniform friction coefficients, and predictability of fluid properties.

SUMMARY

The purpose of the effort reported in Section VI was to identify and evaluate known alignment techniques. This phase of the investigation showed that gyrocompassing is a marginal technique for the AFBGW. It also showed that a series of discrete fixes can be used to align the system to the required accuracy within a reasonable period of time.

The alignment investigation included a comparative analysis of several techniques that employed velocity and angular rate matching. The results showed a progressive increase in sophistication, alignment speed, and accuracy as these systems are improved and tested.

The investigation indicated a general parity of the prelaunch discrete fixtaking approach and the parameter matching approach. The prelaunch discrete fixtaking approach has not been subjected to as extensive a series of tests as has the parameter matching approach. However, the discrete fixtaking approach will not require that the launch aircraft have an inertial platform—as will the parameter matching approach. Both techniques will constrain the aircraft, but in different ways. The prelaunch discrete fixtaking method will require that the aircraft fly over a designated fixtaking zone. The parameter matching technique will require a prelaunch maneuver.

The above considerations do not indicate a clear advantage for either system. The major factor in selection involves the requirement of a master navigator for the transfer alignment process. If the AFBGW were to be launched only from aircraft with a third-generation inertial platform, transfer alignment is recommended. If the AFBGW were to be launched from aircraft with no inertial platform, discrete fixtaking is preferred.

LIST OF SYMBOLS

SYMBOL	DEFINITION
Δa	Acceleration bias (2 x 10-4g).
$\overbrace{C^2(t)}$	RMS error due to a cyclic error forcing function (any variable may be substituted for C).
$\|G(j\omega)\|$	Magnitude of system frequency response.
g	Gravitational constant (32.2 feet/second^2).
K	Power spectral density magnitude.
K_z	$\omega_x K_3$.
K_1, K_2, K_3	System gains in gyrocompassing mechanization.
ΔP_x	Initial position error.
δP	Error in the fixtaking process.
ΔP_{ym}	Position error at the end of flight (total system).
P_{ym1}, P_{ym2}, P_{ym3}	Components of position error at the end of flight.
R	Earth radius (2.06 x 10^7 feet).
T	Time constant of the gyrocompassing loop ($T = 3/K_1$).
T_x, T_y, T_z	Torquing rates.
t	Time.
t_1, t_0	Time between last fix and end of flight; time between fixes.
ΔV	Velocity reference error.
ΔV_x, ΔV_y	Initial velocity errors.

LIST OF SYMBOLS (CONCLUDED)

SYMBOL	DEFINITION
ΔX, ΔY, ΔZ	Errors in inertially derived position.
α	Feedback loop gain (analog leveling).
β	Forward loop gain (analog leveling).
δ	Gyroscope drift rate (level gyroscope).
δ_ε	Virtual east gyroscope drift.
$\Phi(\omega)$	Error process (power spectral density).
δ_x, δ_y, δ_z	Gyroscope drift.
$\Delta\theta$, $\Delta\phi$	Level error; orthogonal quasi-level axes.
$\Delta\theta_{ss}$	Steady state heading error.
λ	$\sqrt{g/R}$ (1.25×10^{-3}).
τ_c	Correlation time.
$\Delta\psi$	Heading error.
$\overbrace{\Delta\psi(t)^2}$	RMS azimuth alignment error.
Ω	Earth rate (15 degrees/hour).
ω	Magnitude of the vehicle angular rate vector; frequency.
ω_x, ω_y	Vehicle angular rates; quasi-level axes.
Subscripts x, y, z	Quasi-level orthogonal axes and computational vertical axes.
ψ	Missile heading.

SECTION VII

AIDING

This section deals with the way in which information from navigational aids and the IMU are combined. Its content is somewhat theoretical in that it deals with mechanization equations rather than specific update hardware. This was done intentionally to preserve the general applicability of the equations and algorithms discussed. Equipment descriptions and descriptions of the mathematical processes that occur before combination appear in Section VIII.

Selection of an approach to inertial aiding is influenced by the error process of the aiding system and by the availability of data from the aiding sensor. The error process may be considered to consist of either a bias-type component and a noise-type component, or a spectrum in which the zero frequency point represents the bias. The availability of data may be influenced by tactical or geographic considerations or by the nature of the aiding device. Currently available devices (discussed in Section VIII) may be classified by data availability into two groups: (1) those providing discrete inputs; and (2) those providing continuous inputs.

This aiding analysis was organized, as shown in Figure 36. Discrete mechanizations were addressed first and are covered in the initial part of the section. The conventional systems are then examined, and the analytical methods of establishing system gains are demonstrated for the AFBGW parameters. Relevant Kalman filter experience in weapon system guidance is reviewed. Synergistic systems are then discussed and the relative performance of selected candidates is defined.

DISCRETE AIDING SYSTEMS

The discrete systems include the RACG, film drum scanner, and terrain correlation matching. In discrete mechanizations, the fixtaking process, which can realign the system as well as provide initialization information, is important because an enroute alignment can reduce the error accumulation rate as well as instantaneous position offset. The following parameters affect the propagation of errors in discrete aiding mechanizations:

- Measurement error

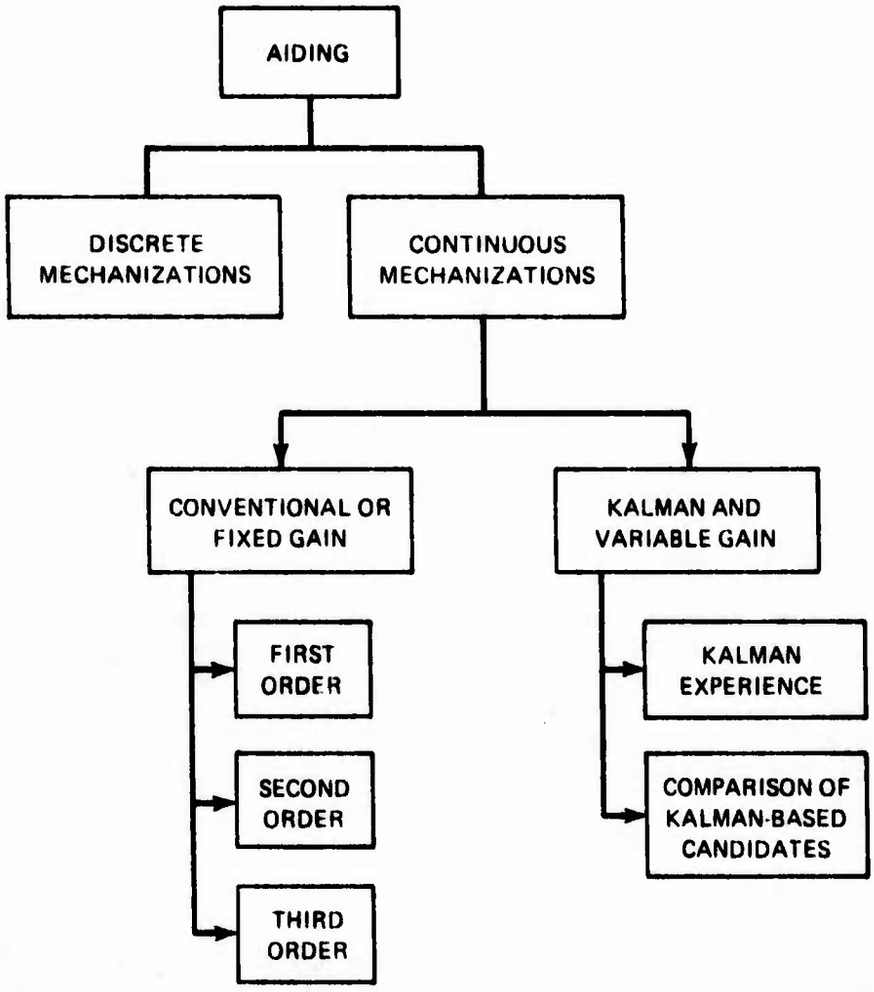

Figure 36. Organization of the Aiding Analysis Guidance Study

- Time between measurements
- Number of measurements taken
- The time between the instant that the last measurement was taken and terminal acquisition.

Figure 37 shows the relationship between discrete fixtaking accuracy and system error for selected fixtaking intervals (Reference 28). The curves indicate that it is highly desirable to distribute the fixpoints of a discrete system as broadly as possible over the approach course. Accordingly, fixes taken in the first minute of flight would require high accuracy—allowing only 4 feet of error. On the other hand, if the fixtaking process consumes 3 minutes of a 10-minute flight, a fixtaking process with as much as a 100-foot error could be used. The more fixes that are taken in a given series, the greater the accuracy of the system for a given fixtaking capability. Figure 38 shows the effect of increasing the number of fixes from three to five. The result indicates a drastic decrease in fixtaking accuracy requirements.

The above curves represent the performance of a Kalman filter modeling velocity and position in two axes and attitude in three axes. The approach is illustrated in Figure 39. Similar results can be obtained from any method of solving the error equation. Simple one-time inversion is adequate for the three-fix situation. For the five-fix situation, distribution of redundant data may be accomplished by least squares or maximum likelihood. (With this limited number of observations, there is little opportunity for system improvement.)

CONTINUOUS SYSTEMS

The continuous systems form the heart of the effort from the point of view of applying classical aiding techniques to the improvement of inertial sensors (Reference 29). The three generic candidates are DME/TOA, GPS, and doppler radar. This effort will first examine the aiding potential of these parametrically—working up from the most basic approach to the more sophisticated. Topics to be discussed are as follows:

- First-order conventional velocity aiding
- Second-order conventional velocity aiding
- Third-order conventional velocity and position aiding

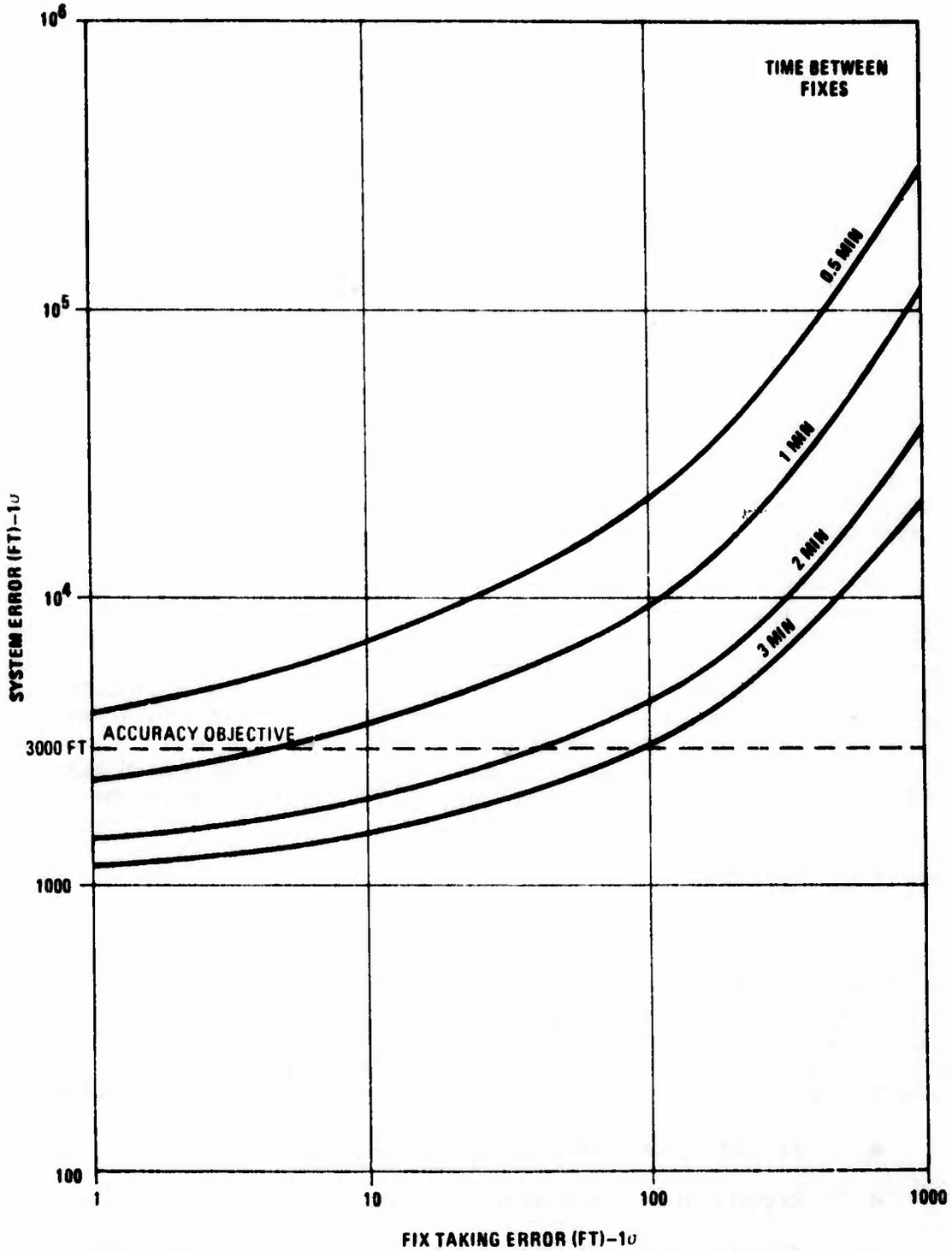

Figure 37. System Error Versus Fixtaking Error—Three Discrete Fixes

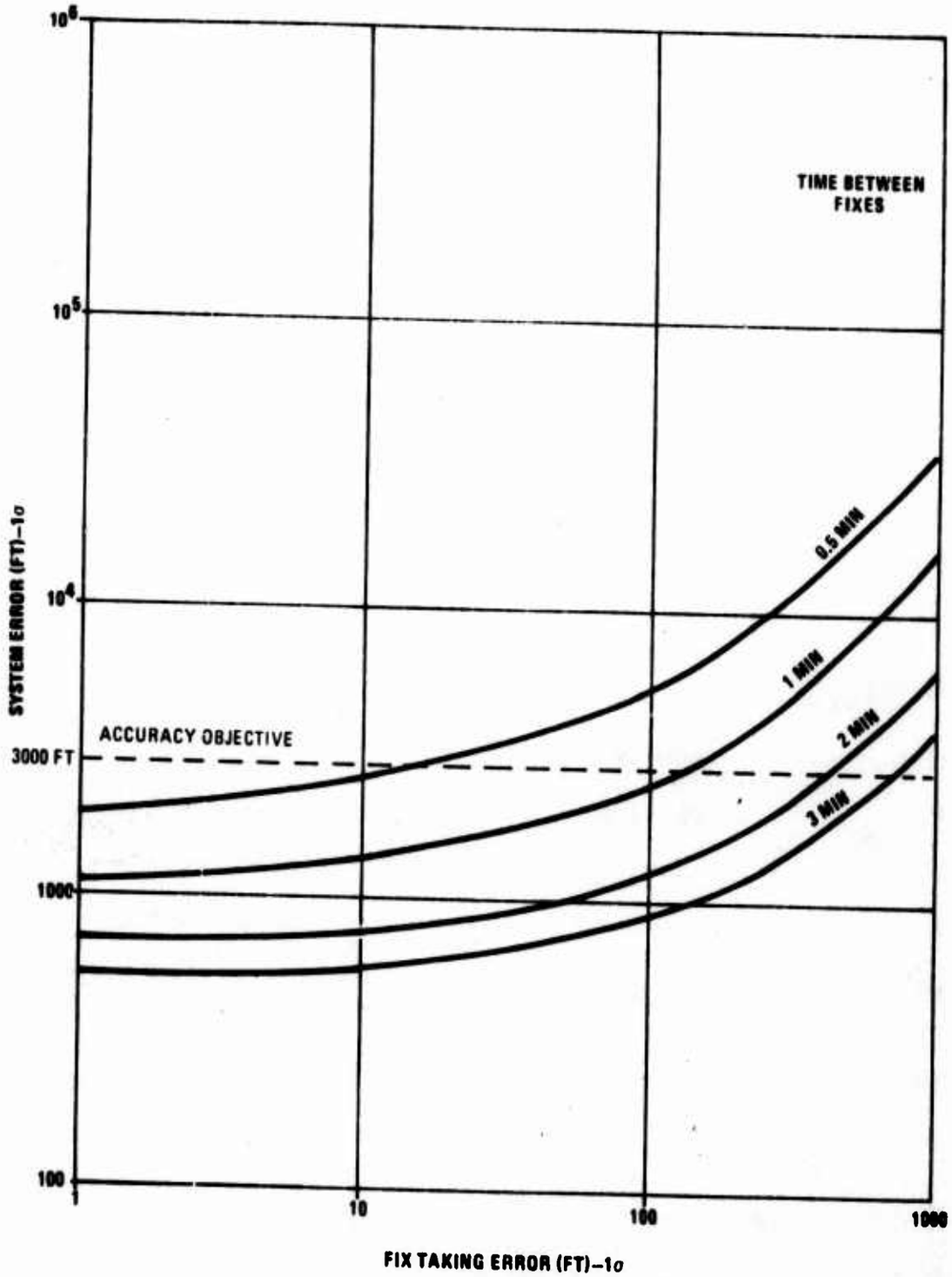

Figure 38. System Error Versus Fixtaking Error—Five Discrete Fixes

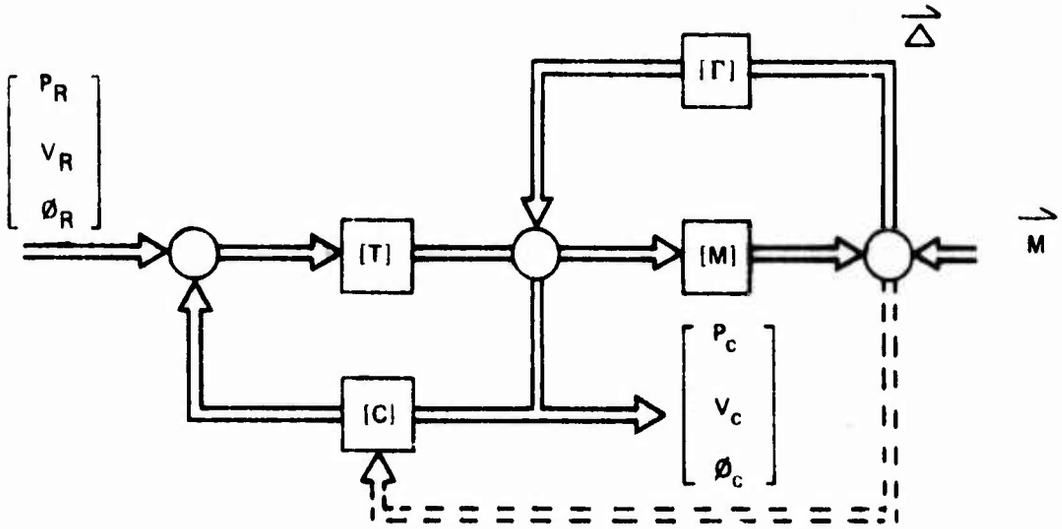

FUNCTIONS AND VARIABLES OF THE KALMAN PROCESS

SYMBOL	IDENTITY	FUNCTION
P	Position	State Vector
V	Velocity	State Vector
ϕ	Attitude	State Vector
[M]	Measurement Matrix	Convert From State Vector to Measured Quantity
[C]	Covariance Matrix	Weights Measured Data; Reflects Correlation
$\vec{\Delta}$	Measurement Error Vector	Reflects Measurement Errors
$\vec{M}$	Measured Values	Aiding Parameters
[T]	Transition Matrix	Updates State Vector
Γ	Correction Matrix	Reconcile Derived Data and Measured Data

Figure 39. Kalman Filter Model

- The role of the Kalman filter in the AFBGW mechanization.

There are certain strategies in aiding that are common to all approaches. All involve the attempt to use the accuracy of the most cost-effective sensors (inertial or RF, etc.); and all attempt to minimize bias-type errors while controlling the noise-type errors.

First-Order Conventional Velocity Aiding

A diagram of a basic first-order system is shown in Figure 40.

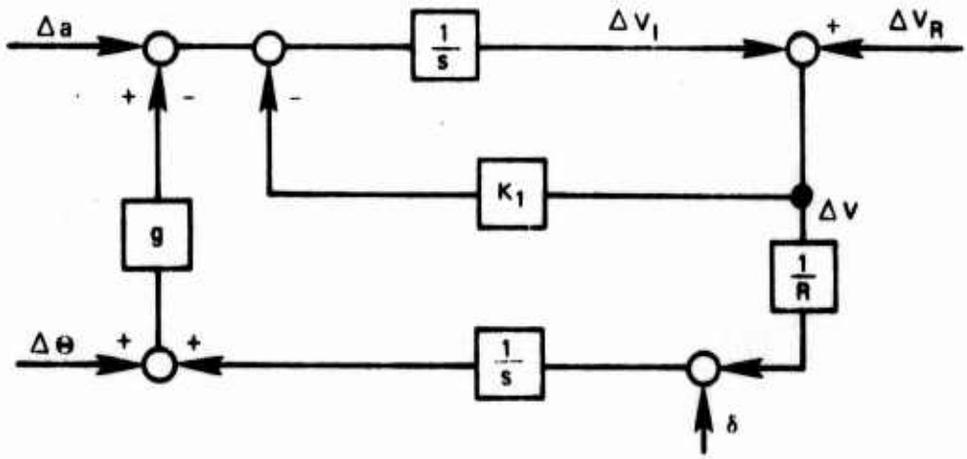

Figure 40. First-Order Conventional Aiding

The transfer function for error propagation from three major error sources is given by the following:

$$\Delta P = \frac{1}{s}\left\{\frac{\frac{\delta}{R} + s(\Delta a) + K_1 s\ (\Delta V_R)}{s^2 + K_1 s + \lambda^2}\right\}$$

where Δa is accelerometer bias, ΔV_I is velocity error in inertial equipment, ΔV_R is velocity error in aiding sensor, ΔV is error difference in inertial and aiding sensor, K_1 is first-order loop gain ($\gamma = K_1/\lambda$), g is gravitational constant

(32.2 feet/second^2), s is Laplace operator (d/dt), δ is gyroscope drift rate, $\Delta\theta$ is level error, and R is earth radius (3,440 nautical miles).

The corresponding time domain errors are as follows:

$$\Delta P_1 = \frac{\Delta a}{\lambda^2}\left\{1 - \frac{e^{-\gamma\lambda t}}{\sqrt{1-\gamma^2}}\sin\left(\sqrt{1-\gamma^2}\cdot\lambda t + \phi\right)\right\}$$

where:

$$\gamma = \frac{K_1}{\lambda} \qquad \tan\phi = \sqrt{\lambda^2 - K_1^2}/K_1^2$$

$$\Delta P_2 = \frac{2\Delta V_R}{\lambda}\left\{1 - \frac{e^{-\gamma\lambda t}}{\sqrt{1-\gamma^2}}\sin\left(\sqrt{1-\gamma^2}\,\lambda t + \phi\right)\right\}$$

$$\Delta P_3 = -\frac{R\delta}{\lambda}\left\{\lambda t - 2\lambda + \frac{e^{-\gamma\lambda t}}{\sqrt{1+\gamma^2}}\sin\left(\sqrt{1-\gamma^2}\lambda t + \phi\right)\right\}$$

where ΔP_1 is position error resulting from an accelerometer bias, ΔP_2 is position error resulting from a velocity reference error, and ΔP_3 is position error resulting from a gyroscope drift rate.

The above equation is, of course, dependent upon random values of Δa, ΔV_R and δ; consequently, they will not cancel out. A 1σ value of the error total corresponds to the root sum squares of the constituent errors, which is to say $\{\Delta P_1^2 + \Delta P_2^2 + \Delta P_3^2\} = \Delta P^2$ (total position error).

The purpose of this exercise is to minimize the sum of the squares by varying γ (that is, K_1). The result is shown in Figure 41; it is indicated that, with a first-order system, one can reduce the errors dramatically, even though the value of the error sources may themselves be rather high.

This arrangement could result in a low-cost-effective operation. There is a constraint on the above system, in that it must be accurately designed. A variation of 10 percent in the value of K_1 could cause the error to go from a nominal 3,000 feet to over 5,000 feet.

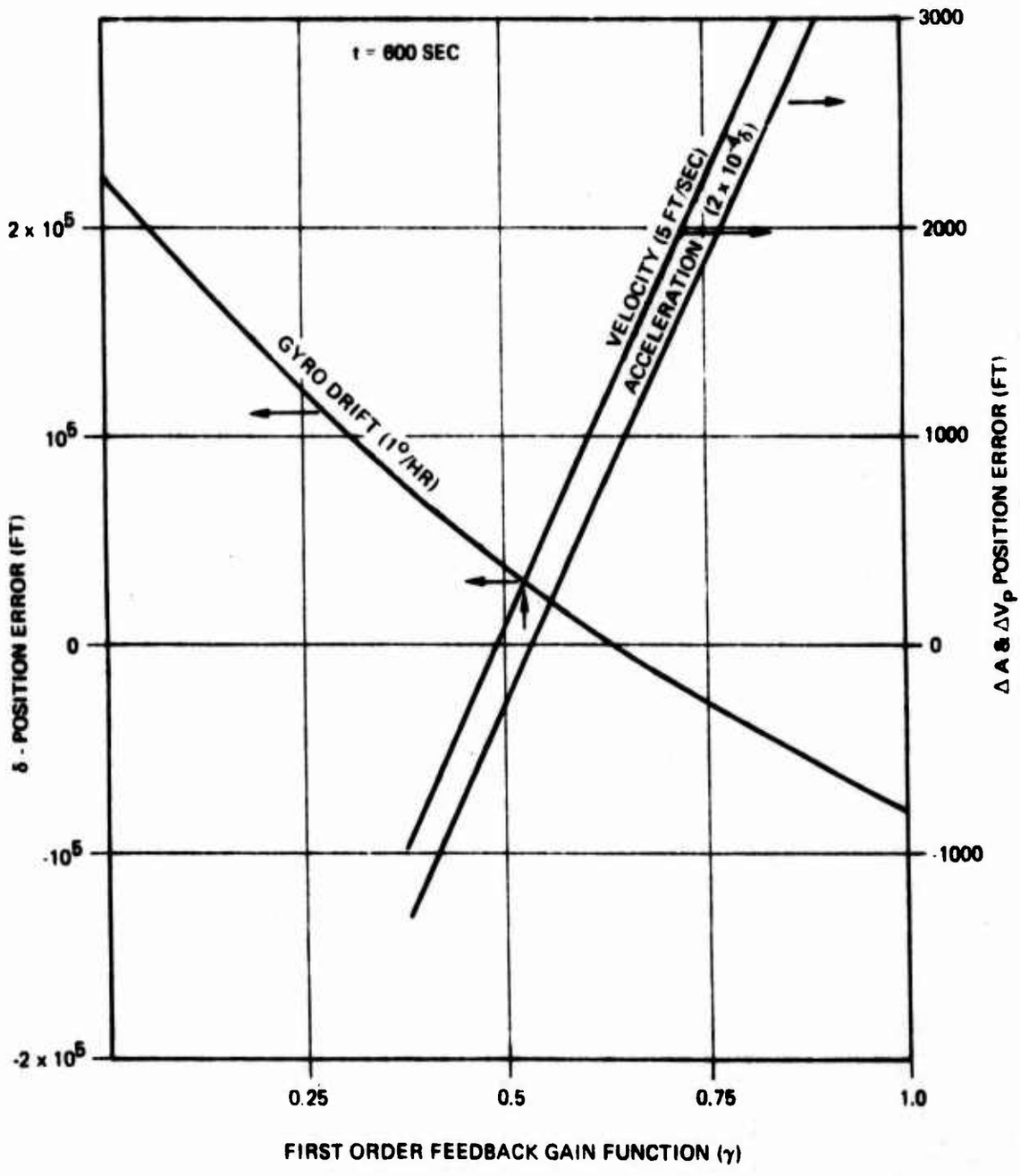

Figure 41. First-Order Doppler Inertial Conventional Optimization

Second-Order Conventional Velocity Aiding

The error block diagram is now expended and generalized in Figure 42. Bias error transfer functions, bias error final values, and white noise error transfer functions are shown in Tables 34 to 36. With these data, a continuous tuned and damped inertial system will be derived.

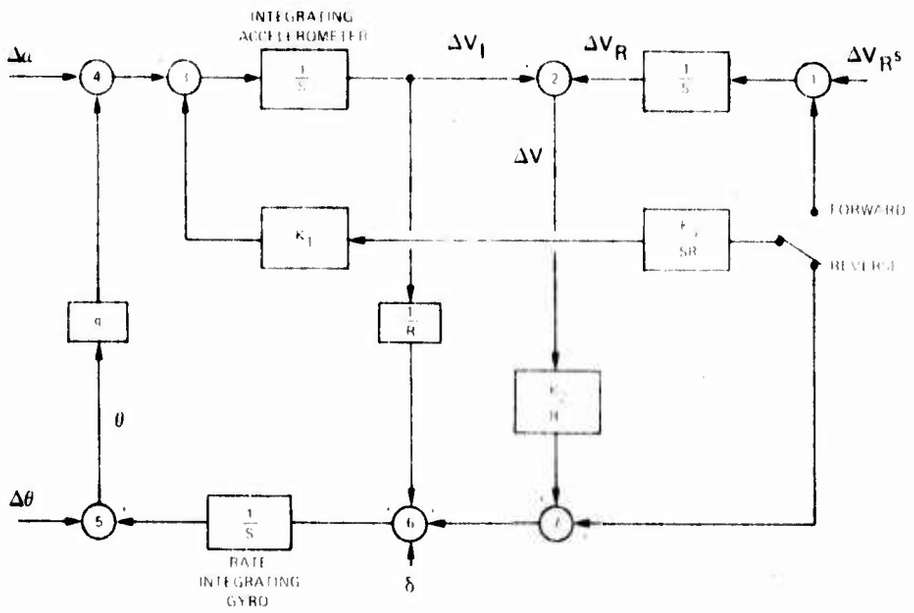

δ LEVEL GYRO DRIFT RATE
$\Delta\alpha$ ACCELEROMETER BIAS
$\Delta\theta$ PLATFORM ATTITUDE ERROR
ΔV_I SINGLE CHANNEL VELOCITY ERROR (INERTIAL)
ΔV_R REFERENCE ERROR

Figure 42. Conventional Mechanization Alternatives

The strategy in this case will be to reduce the criticality of gain settings so that changes in constants (g and K_1) will not adversely affect performance. The required K_1 varies with the variations in the actual error processes as opposed to the assumed error process; g varies as load factor of the missile varies. The system will still require a velocity reference source (GPS, DME/TOA, doppler, etc.). However, the overall error will now be reduced by having reduced the sensitivity of system error to gyroscope drift bias and doppler radar bias.

Figure 43 indicates the response of second-order systems for a range of fixed gains to 0.01 radian/second. The curves

TABLE 34. BIAS ERROR TRANSFER FUNCTION

	System 1 Untuned 2nd Order $K_2 = K_3 = 0$	System 2 Tuned 2nd Order $K_3 = 0$	System 3 Forward 3rd Order	System 4 Reverse 3rd Order
$\frac{\Delta\xi}{\delta}$	$\frac{S - K_1}{S^2 - K_1 S - \lambda^2}$	$\frac{S - K_1}{S^2 - K_1 S - \lambda^2 (1 - K_2)}$	$\frac{S (S - K_1)}{S^3 - K_1 S^2 - \lambda^2 (1 - K_2) S - \lambda^2 K_3}$	$\frac{S (S - K_1 - K_3)}{S^3 - (K_1 - K_3) S^2 - \lambda^2 (1 - K_2) S - K_3 \lambda^2}$
$\frac{\Delta\xi}{\Delta a}$	$\frac{1/R}{S^2 - K_1 S - \lambda^2}$	$\frac{(1 - K_2)/R}{S^2 - K_1 S - \lambda^2 (1 - K_2)}$	$\frac{S (1 - K_2)/R - K_3/R}{S^3 - K_1 S^2 - \lambda^2 (1 - K_2) S - \lambda^2 K_3}$	$\frac{S (1 - K_2)/R - K_3/R}{S^3 - (K_1 - K_3) S^2 - \lambda^2 (1 - K_2) S - K_3 \lambda^2}$
$\frac{\Delta\xi}{\Delta V_R}$	$\frac{K_1/R}{S^2 - K_1 S - \lambda^2}$	$\frac{(K_1 - S K_2)/R}{S^2 - K_1 S - \lambda^2 (1 - K_2)}$	$\frac{S (K_1 - K_3 - K_2 S)/R}{S^3 - K_1 S^2 - \lambda^2 (1 - K_2) S - \lambda^2 K_3}$	$\frac{S (K_1 - K_2 S)/R}{S^3 - (K_1 - K_3) S^2 - \lambda^2 (1 - K_2) S - K_3 \lambda^2}$
$\frac{\Delta V}{\delta}$	$\frac{- g}{S^2 - K_1 S - \lambda^2}$	$\frac{- g}{S^2 - K_1 S - \lambda^2 (1 - K_2)}$	$\frac{- g S}{S^3 - K_1 S^2 - \lambda^2 (1 - K_2) S - \lambda^2 K_3}$	$\frac{- g (S - K_3)}{S^3 - (K_1 - K_3) S^2 - \lambda^2 (1 - K_2) S - K_3 \lambda^2}$
$\frac{\Delta V}{\Delta a}$	$\frac{S}{S^2 + K_1 S + \lambda^2}$	$\frac{S}{S^2 - K_1 S - \lambda^2 (1 - K_2)}$	$\frac{S^2}{S^3 - K_1 S^2 - \lambda^2 (1 - K_2) S - \lambda^2 K_3}$	$\frac{S (S - K_3)}{S^3 - (K_1 - K_3) S^2 - \lambda^2 (1 - K_2) S - K_3 \lambda^2}$
$\frac{\Delta V}{\Delta V_R}$	$\frac{K_1 S}{S^2 + K_1 S + \lambda^2}$	$\frac{K_1 S - \lambda^2 K_2}{S^2 + K_1 S + \lambda^2 (1 - K_2)}$	$\frac{S^2 K_1 - \lambda^2 K_2 S + \lambda^2 K_3}{S^3 + K_1 S^2 - \lambda^2 (1 - K_2) S + \lambda^2 K_3}$	$\frac{S (K_1 S - K_2 \lambda^2)}{S^3 - (K_1 + K_3) S^2 + \lambda^2 (1 - K_2) S + K_3 \lambda^2}$

TABLE 35. BIAS ERROR FINAL VALUES

	System 1	System 2	System 3	System 4
$\frac{\Delta\theta}{\delta}$	$\frac{K_1}{\lambda^2}$	$\frac{K_1}{\lambda^2 (1 + K_2)}$	0	0
$\frac{\Delta\theta}{\Delta a}$	$\frac{1}{g}$	$\frac{1}{g}$	$\frac{1}{g}$	$\frac{1}{g}$
$\frac{\Delta\theta}{\Delta V_R}$	$\frac{K_1}{g}$	$\frac{K_1}{g (1 - K_2)}$	0	0
$\frac{\Delta V}{\delta}$	R	$\frac{R}{1 - K_2}$	0	R
$\frac{\Delta V}{\Delta a}$	0	0	0	0
$\frac{\Delta V}{\Delta V_R}$	0	$\frac{K_2}{1 + K_2}$	-1	0

TABLE 36. WHITE NOISE ERROR TRANSFER FUNCTIONS

	Reference Noise	Accelerometer Noise
System 3	$\left\{\frac{P_{NR}\left[(1+K_2)K_1^2+\lambda^2K_2^2\right]}{2\left[K_3-(K_1+K_3)(1+K_2)\right]}\right\}^{1/2}$	$\left\{\frac{P_{Na}\left[\lambda^2(1+K_2)+K_3^2\right]}{2\lambda^2\left[K_3-(K_1+K_3)(1+K_2)\right]}\right\}^{1/2}$
System 4	$\left\{\frac{P_{NR}\left[K_1^2(1+K_2)+\lambda^2K_2-K_1K_3\right]}{2\left[K_3-K_1(1+K_2)\right]}\right\}^{1/2}$	$\left\{\frac{P_{Na}(1+K_2)}{2\left[K_3-K_1(1+K_2)\right]}\right\}^{1/2}$
	Gyro Drift Rate Noise	
System 3	$\left\{\frac{P_{N\delta}\left[g^2(1+K_3/\lambda^2)(K_1+K_3)\right]}{2\lambda^2\left[K_3-(K_1+K_3)(1+K_2)\right]}\right\}^{1/2}$	
System 4	$\left\{\frac{P_{N\delta}R^2\lambda^2}{2\left[K_3-K_1(1+K_2)\right]}\right\}^{1/2}$	

P_{NR} = Noise power spectral density of velocity reference

$P_{N\delta}$ = Noise power spectral density of gyro

P_{Na} = Noise power spectral density of accelerometer

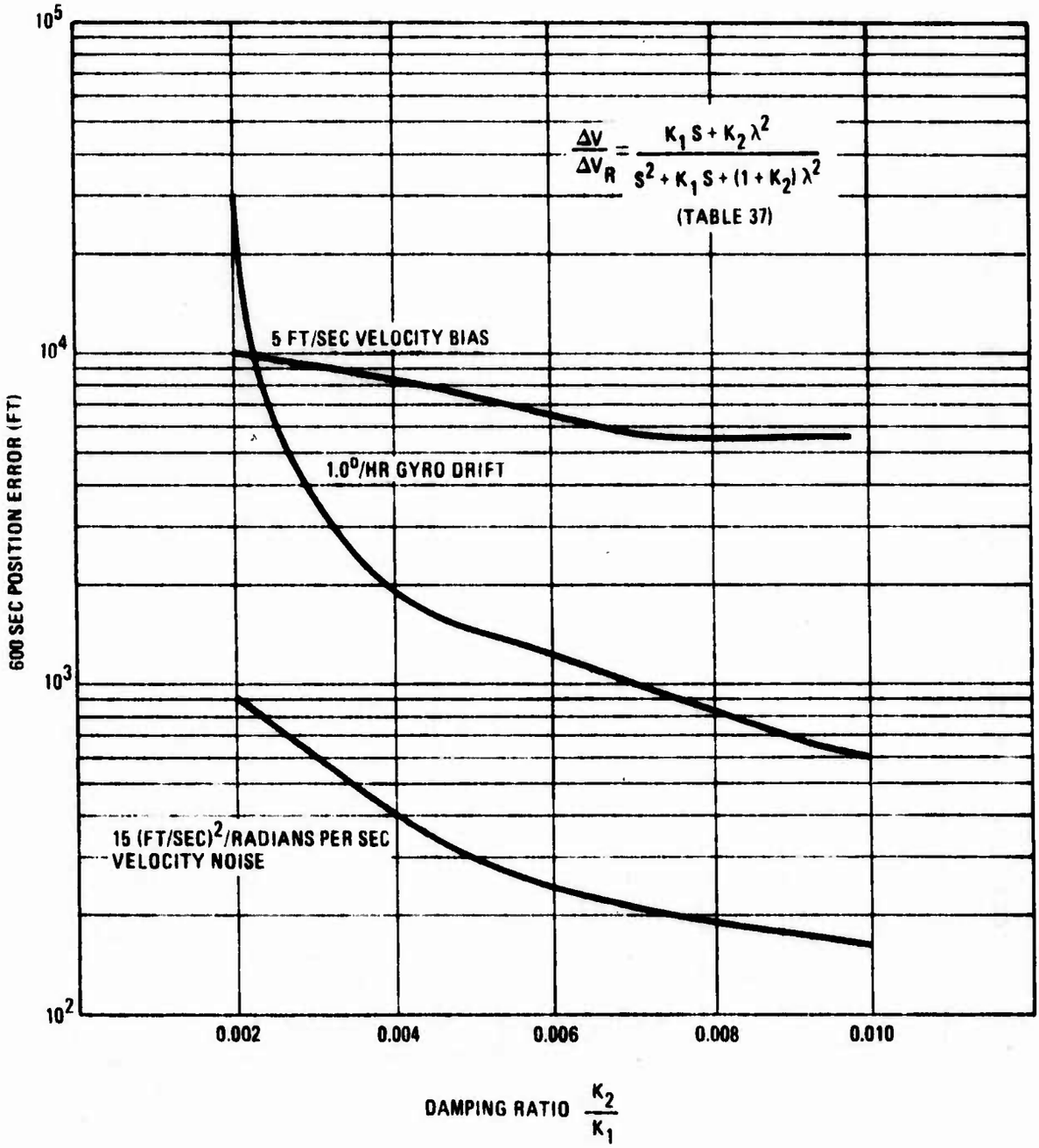

Figure 43. Response of Second-Order Systems for Range of Fixed Gains

indicate an error of about 1,000 feet at 0.010 radian/second. The velocity noise curve represents residual error at 160 feet at the same frequency. Theoretically, a step gain mutually calibrative system could achieve this performance level. Ability to realize this potential depends upon the stability of the velocity bias errors. A certain portion of the nominally labeled bias errors are exponentially correlative at less than an hour. In a 10-minute flight, these errors must also be classified as noise errors. Our investigation did not produce conclusive results regarding the portion of the spectrum below 0.278×10^{-3}. However, the survey indicated that a 2,000-foot error represents a realistic target.

The bias error curves in Figure 43 were developed by evaluating the inverse transforms of the appropriate error equations of Table 35 (Reference 30).

Noise curves are commonly evaluated in the frequency domain by the use of the following relationship(s):

$$\tilde{e}^2(t) = \frac{1}{2\pi} \int_{-\infty}^{\infty} \Phi(\omega) \left| G(j\omega) \right|^2 d\omega$$

where $\tilde{e}$ is root mean square error in position, $\Phi(\omega)$ is power spectral density of noise process, and $|G(j\omega)|$ is mechanization frequency response function.

In this case, θ has a value of 15 (feet/second)^2/radians per second and has a band limit of 0.003 radian/second.* The transfer function for position error is given by the following: (a is a generalization of λ allowing for variations in g.)

$$G(s) = \frac{\Delta P}{\Delta V_R} = \frac{K_1 s + \lambda^2 K_2}{s(s^2 + 2a\gamma s + a^2)}$$

where a^2 is $\lambda^2(1 + K_2)$, $2a\gamma$ is K_1, and ΔP is position error.

* As indicated by suppliers of velocity sensors, particularly Singer Kearfott (GPL).

If the above expression is bounded, the integral expression can be evaluated by residue summation, Nichols procedure, or numerical integration. In this case, G(s) is unbounded, and impulse integral squaring is used (Reference 9). The following expression applies:

$$\tilde{e}^2(t) = \int_0^t \mathcal{L}^{-1}\left(\frac{K_1 s + K_2\lambda^2}{s(s^2 + 2a\gamma s + a^2)}\right)^2 dt$$

The resulting integral is given by the following:

$$\tilde{e}^2(t) = \frac{A}{a^2}\,t + \frac{A}{2a^3}\left(1 - e^{-2at}\right) + 2\left[\frac{A(A-a)}{4a^5}\right]\left[1 - e^{-2at}(2at + 1)\right]$$

$$+ \left(\frac{A-a}{2a^2}\right)^2\left[1 - e^{-2at}(2at + 1) + 2at^2\, e^{-2at}\right]$$

$$+ \frac{2A(A-a)}{A^4}\left[1 - e^{-at}\,(at + 1)\right] + 2\,\frac{A^2}{a^5}\,e^{-at}$$

where $A = \lambda^2 K_2$ and $\lambda^2 = g/R$.

Third-Order Conventional Velocity and Position Aiding

If a greater flexibility is desired, a third-order mechanization can be adapted to the problem. A third-order system can employ a continuous position reference or integrate velocity. Position data can be derived through angular observations, range observations, or a combination of the two. Systems that rely on angular data alone can employ celestial or terrestrial measurements. Celestial measurements provide data in a spherical coordinate/earth geometric reference system. These can provide a level reference and a gyroscope drift correction only if an adequate ephemeris and time base are provided. Terrestrial references, whether based on angular or distance measurement, provide position data without the need for a precision time reference.

Reference to Table 34 indicates that there is much greater scope for varying error sensitivity than there was in a second-order system. Consider the following equations from Table 34 (System 4):

$$\frac{\Delta V}{\delta} = \frac{-g(S + K_3)}{S^3 + (K_1 + K_3)S^2 + \lambda^2(1 + K_2)S + \lambda^2 K_3}$$

$$\frac{\Delta V}{\Delta V_R} = \frac{S(K_1 S + K_2 \lambda^2)}{S^3 + (K_1 + K_3)S^2 + \lambda^2 (1 + K_2)S + K_3\lambda^2}$$

K_1 and K_3 may be assigned an arbitrary range of values, increasing and decreasing the time constant of the system. The objective is to find gain settings that minimize bias errors without having the noise process become an error factor. This depends on two items: system stability and control of K_2. The position error for the above system is bounded and is given by the following:

$$\left\{\frac{P_{NR}\ (1 + K_2)K_1^2 + \lambda^2 K_2^2}{2[K_3 - (K_1 + K_3)(1 + K_2)]}\right\}^{1/2}$$

The above type of equation may be derived by using the method outlined in Grabbe, pages 24-11 to 24-15 (Reference 9). There are many compilations of these formulations in Air Force documents. Reference 31 is a good example.

Kalman Filter

An extensive investigation was made to determine the adaptability of existing Kalman filter mechanizations (as shown in Figure 39) to the RACG midcourse guidance approach. The distinguishing characteristics of the most appropriate candidates are shown in Table 37. The consensus of specialists in this field indicated a preference for step-gain Kalman-derived filters for a short-term flight.

Sperry's P gain optimal filter has break points at 5, 9, and 15 minutes. This corresponds to the AFBGW inertial error sensitivities of 0.115 nautical mile/degree/hour, 0.68

TABLE 37. SUBOPTIMAL KALMAN FILTER ADAPTATION CANDIDATES

AGENCY	DEVELOPER	CONCEPT	APPROACH	UNIQUE FEATURE	GAINS	STATES	RELATIVE PERFORMANCE (Error)	POTENTIAL APPLICATIONS
Sperry	B. Schwartz	LORAN inertial	Step gain (P gain) suboptimal	Break at 5, 9, 15 minutes	15	30	1.1 Kalman	Light aircraft
Army Electronics Command	W. Light	LORAN inertial	Fixed gain	Simulation of flight patterns	22	---	1.5 x Kalman	Light aircraft
Boeing	G.H. Yamomoto	STAMP	Quasi-discrete	Calculation of miss distance directly	[a]	10	Comparable to conventional (continuous) systems	SCRAM
Litton	J.R. Huddle	Omega inertial	Simplified error model	Process approximated by single noise source	[a]	5, 12, 16	---	Light aircraft missiles
Lockheed	L. Goe	RACG inertial	Quasi-discrete	Models channel error only - no azimuth	[a]	4	10 percent more range 33 percent less error	RACG
Lear Siegler	L. Warenga	DME inertial	Minimization of states/ high accuracy	Noise compensation for unmodeled states	[a]	14	Comparable performance	Tactical missiles

[a] Not applicable.

nautical miles/degree/hour, and 3 nautical miles/degrees/hour, respectively. The mechanization weights inertial sensor measurements more highly in the initial flight period than in subsequent phases. The Army Electronics Command concept achieves good results by matching simulated flight performance to actual performance and by setting gains accordingly.

The Boeing STAMP concept obtains a performance approaching continuous aiding by use of discrete data projections. This could present an opportunity for anti-gain margin enhancement in systems like the GPS and DME/TOA.

Litton has developed a large number of Kalman and Kalman-based systems. In a particularly applicable Omega-inertial concept, good results were attained by using a unified noise model to reduce the number of states required. It is significant that the performances of optimal, suboptimal, and conventional systems were very close in one phase of this study. The RACG and DME/inertial mechanizations were also reviewed. Both indicated improved performance by Kalman mechanizations when compared to conventional mechanizations. However, both studies indicated that the use of Kalman-derived data in a modified conventional configuration could improve conventional performance significantly.

The survey indicates that the AFBGW performance could be improved by application of mutual calibration. Literature indicated, however, that rapid growth of computational requirements is a problem; this is illustrated in Figure 44. If 20 states are modeled, a memory requirement of 6,000 is indicated for the Kalman filter operation alone (Curve 1). If the quality of the measurements is relatively predictable, certain shortcuts can be made, and a somewhat less accurate system results (Curve 2). If a preselected, scheduled gain system was selected, still greater memory economy could be achieved.

In view of the above problems and the recommendations of those experienced in the use of optimal processes, emphasis was on the application of Kalman concepts to scheduled gain variations.

Accuracy Potential of Candidates

The accuracy potential of several generic classes of continuous aiding concepts was evaluated. These included: (1) a second-order fixed gain model; (2) a second-order scheduled gain model; and (3) a second-order adaptive gain system. For

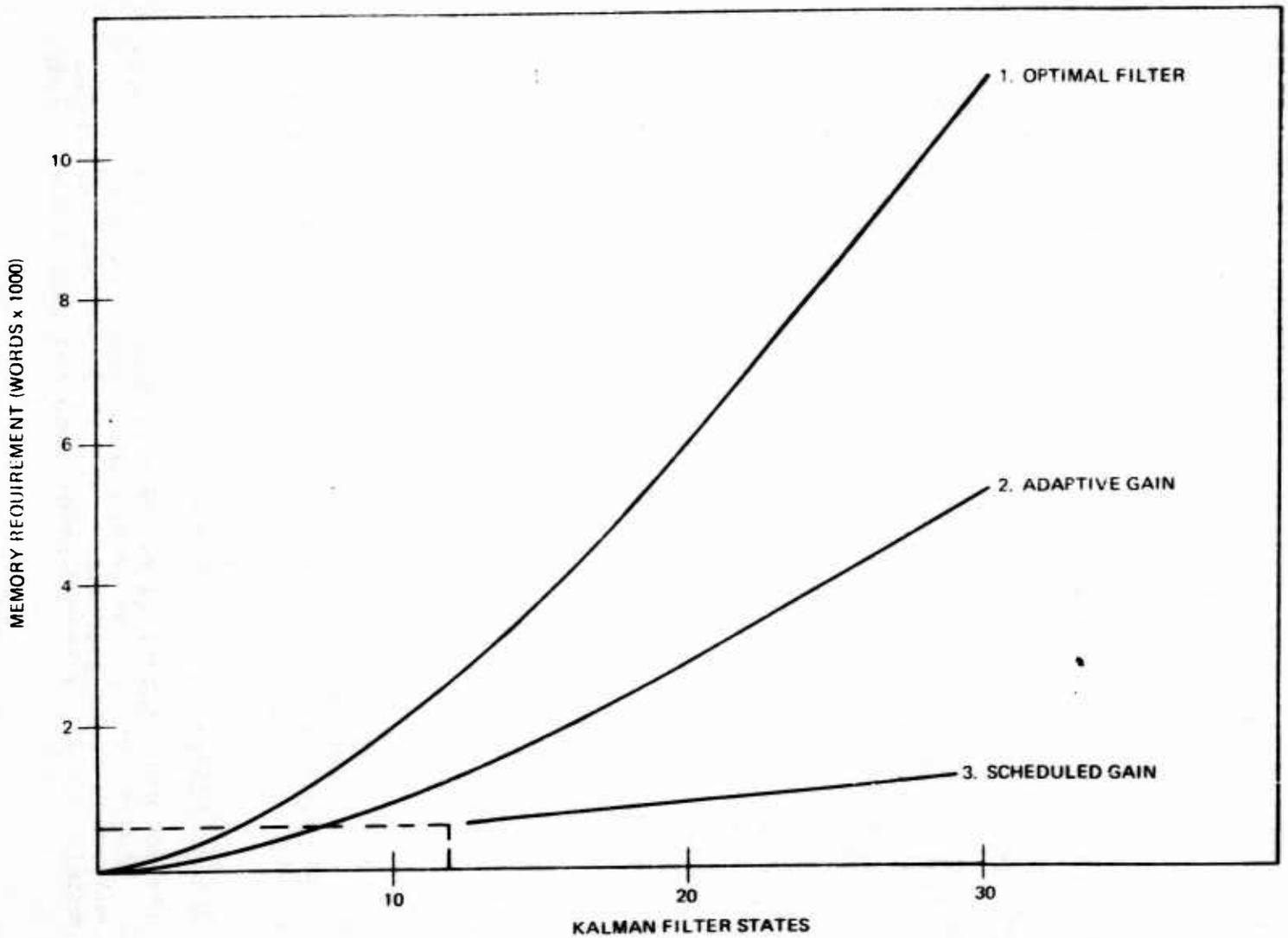

Figure 44. Computer Memory Requirements for Selected Mechanizations

the fixed gain system, a combination of parameters was chosen from Figure 43 that permitted a damping ratio A value of 0.008.

For the second-order scheduled gain option, a mechanization defined by Table 34 was used. In referring to System 2 ($\Delta V/\delta$ and $\Delta V/\Delta V_R$), it is seen that a variation in K_2 from ∞ to 0 can cause the final value of $\Delta V/\delta$ to go from zero to g/λ. K_1 variations were examined, and position errors proved relatively insensitive to these variations for the AFBGW parameters. The corresponding values of $\Delta V/\Delta V_R$ are to 1 to 0. These values were varied to produce high gyroscope drift rate sensitivity early in the flight and high velocity reference error sensitivity in the latter part of the flight.

The concept of adaptive aiding is illustrated in Figure 45. The gains are adjusted by ρ, the gain adjustment parameter. ρ is derived by operating on the observed difference in inertially derived velocity and the reference velocity. When ρ is negative, the system essentially operates on inertial information and calibrates the reference sensor. (The function Γ represents this calibrative operation and includes adaptation and weighting.) When ρ is positive, the system operates on calibrated ΔV_R data.

The above approach allows the use of inertial data when these are the most accurate. The approach also provides the opportunity to compare reference data to inertial data when the latter is extremely accurate. The comparison is superior to a prelaunch calibration because it better approximates the operational environment of the portion of the flight during which navigation data will be derived from the reference sensor.

One of the problems associated with adaptive systems, such as the one just mentioned, is that the uncalibrated error process is not stationary. Errors that appear to be bias-type errors under a 5-minute observation period may, in fact, be cyclic (cosine type) errors with a 1-hour period.

The manner in which errors vary has a critical impact on the practicality of the type of concept illustrated in Figure 45. It is absolutely essential that the major portion of the error either be virtually stationary over the time of flight or that its variations be sufficiently high in frequency so that they are self-cancelling (using the inertial sensor as an averaging device).

The potential of the adaptive approach is illustrated in Figure 46. The curves present a comparison of the three types

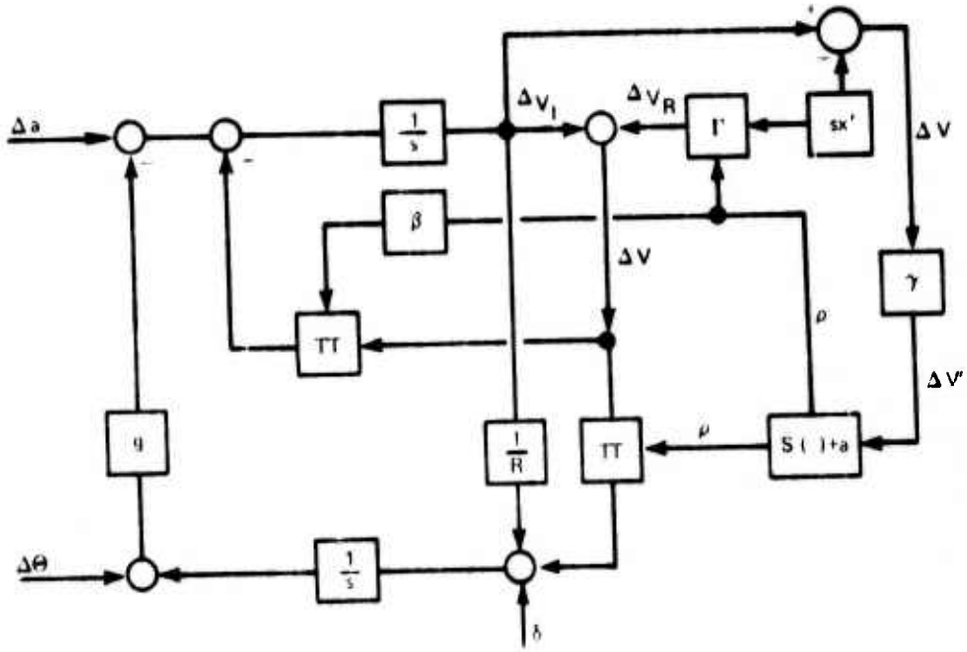

Δa - ACCELEROMETER BIAS

ΔV - DIFFERENCE BETWEEN OBSERVED AIDING AND INERTIALLY DERIVED VELOCITY

I - INERTIAL (SUBSCRIPT)

R - REFERENCE (SUBSCRIPT)

[Γ] - CALIBRATION, ADAPTATION, AND WEIGHTING

sx' - OBSERVED AIDING VELOCITY

β, γ - SYSTEM GAINS

[S( )+a] - GAIN ADJUSTOR - DEPENDS UPON THE DIFFERENCE IN SENSOR RATE DIVERGENCE (INERTIAL AND AIDING)

ρ - GAIN ADJUSTMENT SIGNAL

δ - GYRO DRIFT

[TT] - MULTIPLIER

R - EARTH RADIUS

g - GRAVITY CONSTANT

Figure 45. Adaptive Aiding Concept

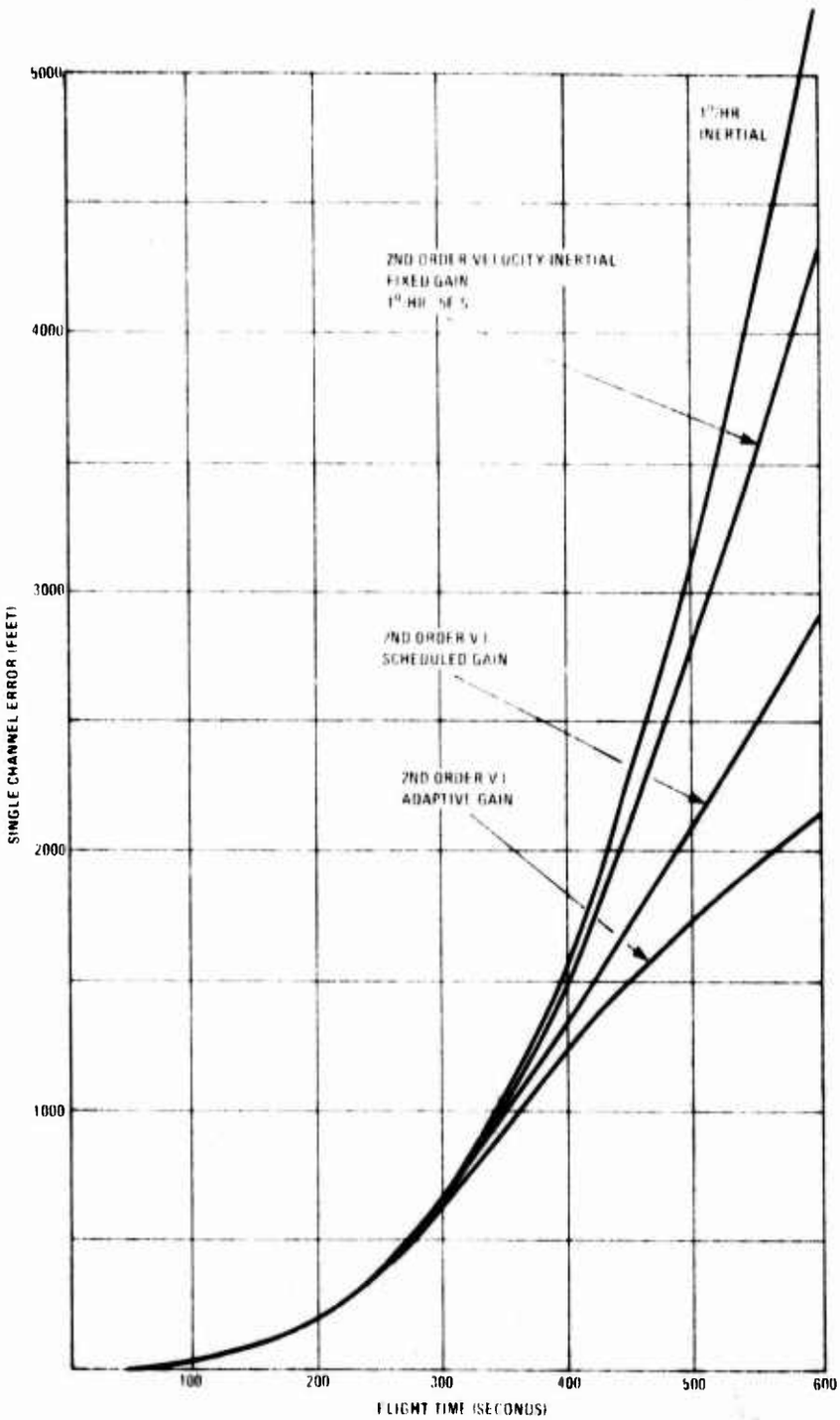

Figure 46. System Performance for Selected Aiding Networks

of continuous aiding that were discussed in this section with pure inertial operation. Pure inertial operation gives an error of about 6,000 feet (single-channel gyroscope drift effect only). A second-order fixed gain velocity inertial system can show some improvement on a statistical basis (4,300 feet). A scheduled gain system can reduce the error to 2,800 feet by allowing the system to operate on inertial data during the first phase of flight.

The adaptive system performance shown in Figure 46 indicates a 2,000-foot error. The construction of the curve that shows the accuracy was based on the assumption that half of the error that appeared to be bias was actually noncompensatable cyclic error. A check of industry specialists was made to confirm this estimate. No exception was taken to the estimate, but the consensus indicated that background data in this area were fragmentary and inconclusive.

SUMMARY

This section examined the methods of combining navigation data from diverse sensors to derive the best available estimate of position, velocity, and attitude (state vector). Both discrete and continuous update procedures were investigated. The discrete update investigation showed that three fixes at the midpoint of flight can provide an overall accuracy of 3,000 feet for the 600-second long-range mission.

In the continuous aiding portion of the investigation, fixed gain, variable gain, and adaptive gain concepts were studied. The fixed gain concept was marginally better than pure inertial operation, while variable (prescheduled) gains produced an accuracy within the AFBGW requirements for navigation performance.

Performance of an adaptive concept was evaluated by using an estimate of reference error characteristics. A more rigorous analysis of adaptive gain systems is desired. This will depend on a more highly developed error process data base than is now available. The investigation showed that the systems discussed in this report had an ultimate potential of 160-foot accuracy with a reference noise of 15 (feet/second)^2/radians per second.

LIST OF SYMBOLS

SYMBOL	DEFINITION
A	$\lambda^2 K_2$—Constant used in calculating unbounded noise response.
a	$\lambda\sqrt{1 + K_2}$—Constant used in calculating unbounded noise response.
$[C]$	Covariance matrix.
e	Exponential base.
$\tilde{e}_2$	RMS error resulting from noise process.
$G\lvert j\omega\rvert$	Absolute value of system output in response to unit oscillatory disturbance.
g	Gravitational constant.
K_1	First-order loop gain—velocity feedback.
K_2	Second-order loop gain—velocity feed forward.
K_3	Third-order loop gain—velocity feed forward.
$[M]$	Measurement matrix.
$\vec{M}$	Measured values.
$\vec{P}$	Position state vector elements.
P_{NR}	Noise power spectral density of velocity reference.
$P_{N\delta}$	Noise power spectral density of gyroscope drift.
P_{Na}	Noise power spectral density of accelerometer bias.
ΔP	Position error.
ΔP_1	Position error resulting from an accelerometer bias.
ΔP_2	Position error resulting from a velocity reference error.
ΔP_3	Position error resulting from a gyroscope drift rate.

LIST OF SYMBOLS (CONCLUDED)

SYMBOL	DEFINITION
R	Earth radius.
s	Laplace operator.
t	Time.
ΔV	Error in velocity ($\Delta V_I - \Delta V_R$).
ΔV_I	Error in inertially derived velocity.
ΔV_R	Error in reference velocity.
$[T]$	Correction matrix.
γ	$K_{1/\lambda}$ parameter used in calculating gains for first-order system.
$\vec{\Delta}$	Measurement error matrix.
δ	Gyroscope drift rate.
$\Delta\theta$	Level error.
λ	Schuler frequency.
Φ	Power spectral density of noise process.
$\vec{\phi}$	Attitude vector.
ϕ	$\tan^{-1}\sqrt{\lambda^2 - K_1^2}$.
$\mathcal{L}$	Laplace transformation symbol.

SECTION VIII

UPDATE TECHNIQUES

The purpose of this study is to provide adequate mid-course guidance for the AFBGW system to acquire its target after 100 nautical miles of flight. As was demonstrated in earlier sections, the baseline inertial navigation system is not sufficiently accurate to provide this capability. It is, therefore, desirable to use updating techniques to supplement this marginal inertial capability.

This section examines performance and cost aspects of the sensors and methods that can be used as alternatives or supplements to the inertial navigation system. Emphasized here are the capabilities of several updating techniques to operate independently and to provide position, velocity, and attitude information.

Updating techniques are investigated in two steps. First, the capabilities and requirements of two discrete navigation techniques are developed: the Radiometric Correlation Guidance (RACG) process currently under development for the AFBGW, and the terrain elevation correlation process. Second, continuous navigation update techniques that provide an economical alternative to the discrete systems are described. These include doppler radar, GPS, Distance Measuring Equipment (DME), and LORAN. The organization of this section is summarized in Figure 47 for ease of reference. The objectives of the update investigation are summarized in Table 38.

This section differs from Section VII in that it treats equipment and techniques that provide navigation data to the system; Section VII treats computational approaches that employ inertial and updating data to produce navigation performance that is more accurate that could be expected from the independent use of either inertial or updating techniques. This section deals with the use of sensors and with their performance in the updating process, while Section VII deals with the use of mathematical equations and algorithms.

DISCRETE UPDATE SYSTEMS—RADIOMETRIC CORRELATION GUIDANCE

This discussion of the RACG concept is based on on-site interviews held with George Clancy, John Rarich, and Larry Goe of Lockheed Missile and Space Division. Additional data were obtained from a recent report on the RACG concept (Reference 15).

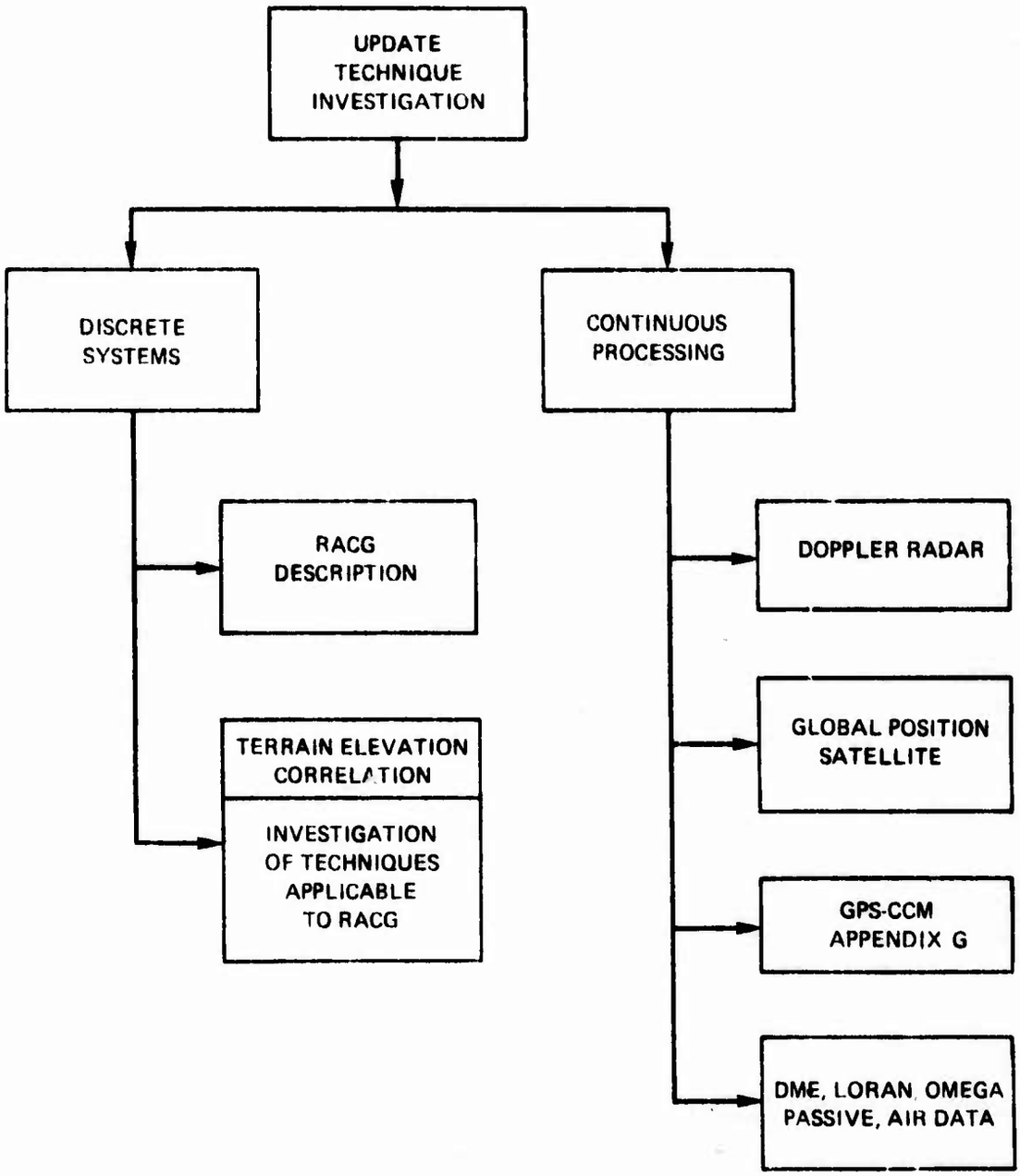

Figure 47. Organization of Work Flow for Update Techniques Investigation

TABLE 38. OBJECTIVES OF UPDATE INVESTIGATION

SYSTEM	ASSESS PERFORMANCE	ASSESS COST	COMPARE COSTS FOR A GIVEN PERFORMANCE LEVEL
A. Inertial System	Error analysis to assess the impact of flight, instrument design, and computational structure	Equipment cost today for 3,000-foot (2σ) accuracy	Is equipment differential less than computational costs in B or sensor costs in C?
B. Inertial System with Discrete Update	Relation of navigation errors to update accuracy and flight parameters	Cost of sensor, computer hardware, and software on missile	Are sensor and computation costs less than equipment differential in A or sensor costs in C?
C. Inertial System with Continuous Update	Evaluation of accuracy of alternative available equipment and techniques	Cost of additional sensors	Are sensor costs less than equipment differential in A or computational costs in B?

A block diagram of the RACG system is shown in Figure 48. The system, which requires an accurate vertical reference (10 arc minutes of vertical error), provides discrete navigation updates with relatively high accuracy and can provide a velocity correction through successive RACG updates. The accuracy of this process is estimated at 2 feet/second. About half of the velocity error is attributed to inertial drift during measurement, and half is caused by errors in the correlation process. This accuracy in velocity data requires a minimum of two position fixes, and improvement in this accuracy can be achieved by using up to five fixes. As shown in Figure 49, typical RACG performance has been determined by Lockheed. The results assume flight within a 3,000-foot acquisition corridor. The curves show: (1) that a range of 32 nautical miles can be achieved with a single fix for the baseline configuration; and (2) that improving the quality of the inertial system does not produce a large improvement in the range that may be flown within the 3,000-foot corridor.

The RACG system antenna is 1 foot in diameter and operates in the 35 GHz region with a 2-degree beam. System accuracy is designated in an angular rather than a positional reference; current angular accuracy is between 5 and 6 milliradians. Because of this angular rather than linear error dependency, it is desirable to take the last fix at as low an altitude as possible.

Specialists in the field of passive terrestrial measurements (George Clancy, for example) compare the 35 GHz RF earth mapping operation to IR earth mapping. This comparison is included to demonstrate the effectiveness of the concept in the competitive situations encountered in midcourse updating.

The 35 GHz spectral region resembles IR in that noncoherent natural energy is sensed. However, 35 GHz experiences a first-power variation of power with temperature rather than the fourth-power variation of IR. There are no inversions (changes in the intensity magnitude sequence of an observed set of emission elements) with 35 GHz RF, and in the temperature range from 0 to 100 degrees Fahrenheit, there is little change in emission level and less in relative intensity. Since there is no K_a band energy in the sun, no day/night effect occurs. There is also very little tendency for the RACG system to make a false match (or false fix), although this could occur theoretically if random readings of radiometric intensity correlated with position source data.

The RACG system has three advantages: (1) the reference does not require special measurement; (2) the angle of observation is not a problem; and (3) the system is not altitude

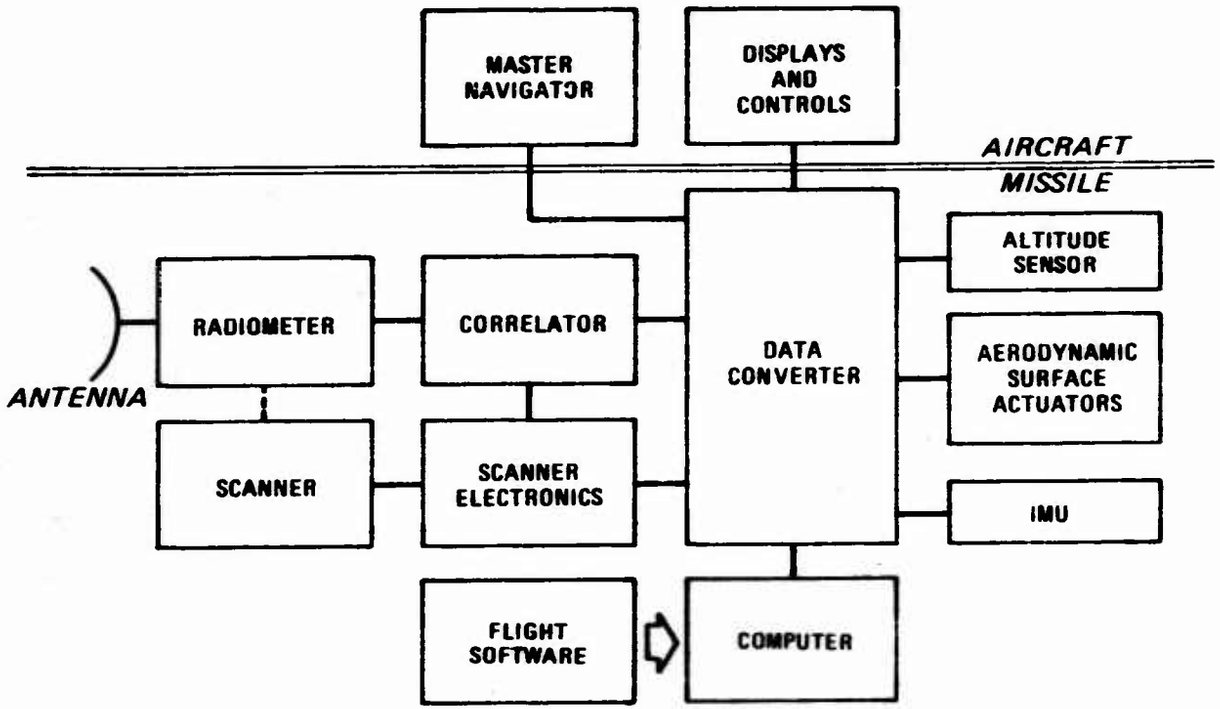

Figure 48. RACG System Diagram

IMU CHARACTERISTICS		IMU QUALITY				
CHARACTERISTIC	UNITS	2	5*	8	15	50
GYRO DRIFT	10^{-6} RAD/SEC	2.0	5.0	8.0	15.0	50
GYRO RANDOM DRIFT	10^{-6} RAD/SEC	0.8	2.0	3.2	6.0	20
ACCELEROMETER RANDOM DRIFT	10^{-3} g	0.2	0.5	0.8	1.5	5
INITIAL TILT ANGLE	10^{-3} RAD	0.2	0.5	0.8	1.5	5

*BASELINE (1 DEG/HR GYRO DRIFT)

QUALITY LEVELS FOR RESET/QUALITY TRADEOFF

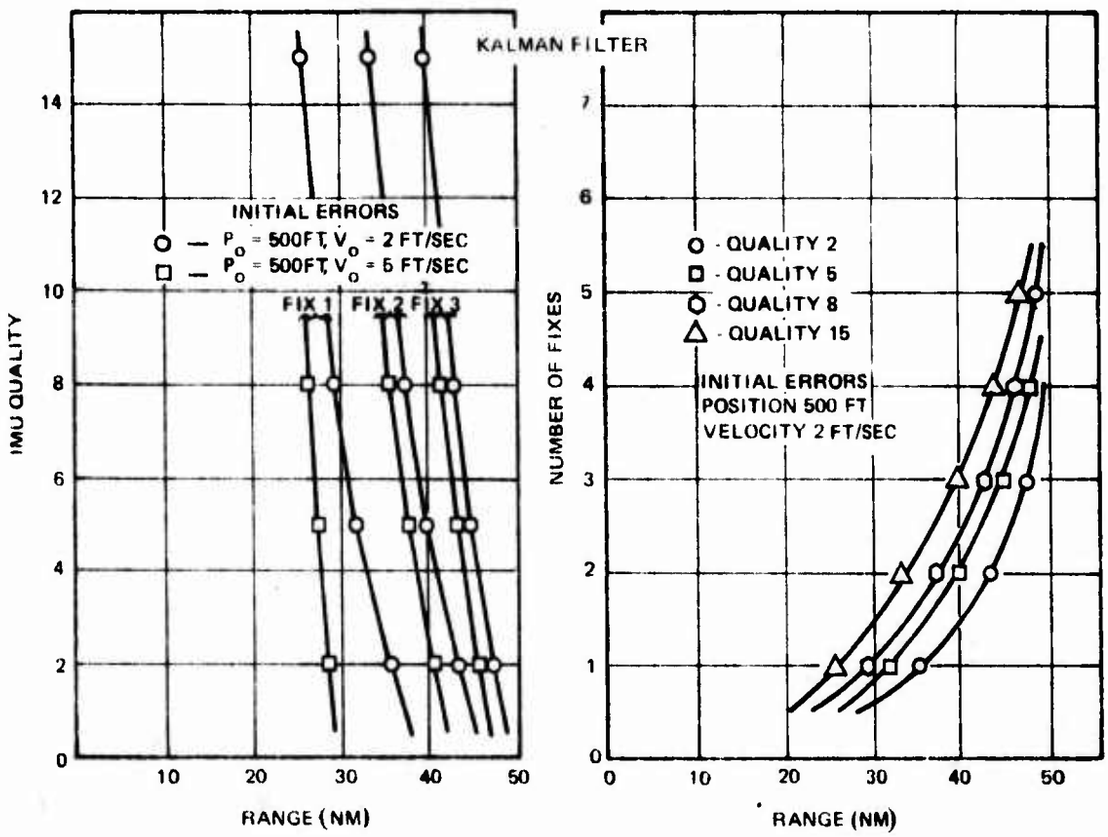

Figure 49. Lockheed Calculations for Single-Fix Update

limited. Photographs associated with this program are readily available at the Defense Mapping Agency. The system is intended for use with pre-briefed strike, but can be used with existing reconnaissance data. It is also feasible to construct new references in a van near the strike operations center using recently acquired data since only 10 to 20 minutes are required to convert images from photographic material. (It is not desirable to build reference matrices on site since the intensity and urgency of the operation require massive amounts of reference data to be acquired and processed. However, data control at the organization level would be an important consideration.) The device is not influenced by the look angle of the terrain; furthermore, acquisition at the low depression angles is as easy as overhead acquisition providing that the relevant terms of the radar range equation are equivalent.

The system, as configured for demonstration purposes, has a Delco MAGIC 362 computer and a special purpose computer of equivalent memory capability. The memory is divided functionally as follows:

- System program - 4,000 words
- Scratch pad - 4,000 words
- Mission data - 8,000 words.

Cognizant RACG project specialists (who supplied the above data) indicate that both a midcourse fix and a terminal fix can be made without difficulty.

The RACG system was assumed to be the discrete update sensor for AFBGW guidance. Its application as a midcourse correction device forms a major element in this study. The next paragraphs present a description of a similar discrete update system, Terrain Elevation Correlation. The purpose of presenting subsequent material is to document the adaptation to RACG of applicable update techniques associated with Terrain Elevation Correlation.

DISCRETE UPDATE SYSTEMS—TERRAIN ELEVATION CORRELATION

Midcourse navigation by the terrain elevation correlation process, illustrated in Figure 50, is similar to the RACG in that it involves the matching of source data. Both techniques employ data secured from the Defense Mapping Agency. Other similarities indicate parallel processes and an opportunity to adapt updating techniques.

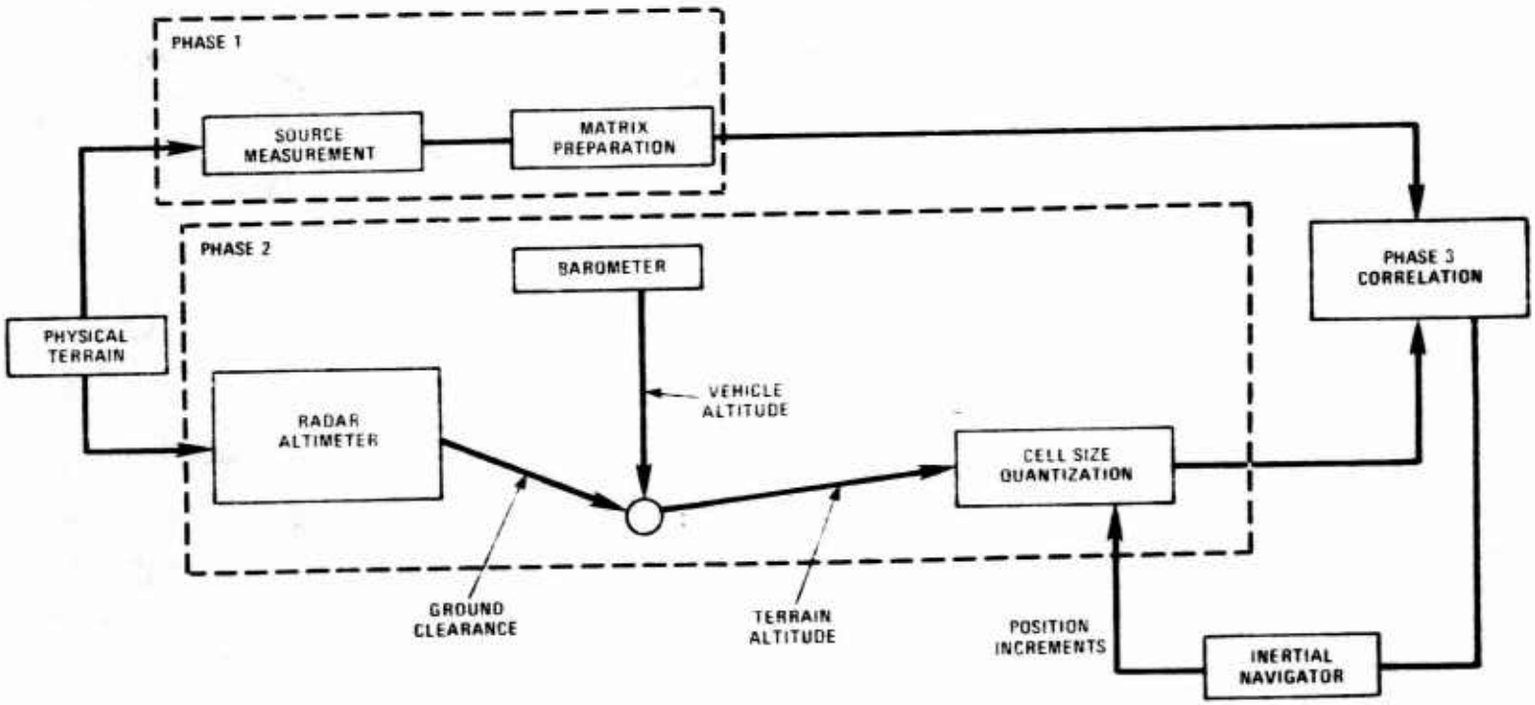

Figure 50. Typical Terrain Elevation Correlation Process

Three distinct phases are associated with terrain elevation correlation: source preparation, data acquisition, and data correlation. Source preparation involves the collection and reduction of terrain elevation measurements into a matrix of appropriate intervals (50 to 400 feet). The data acquisition phase involves the measurement and temporary storage of altitude measurements by the missile's radar altimeter at equidistant position intervals. The correlation phase involves matching acquired data with source data.

Figure 51 shows the use of terrain elevation correlation in making a midcourse correction. The air-to-surface missile is launched at any point along the launch perimeter, and update is accomplished anywhere between the 34- and 40-nautical mile circles. This method has been used for some time with air-to-surface missiles equipped with a 1-degree/hour inertial systems. Its usefulness to the AFBGW depends on its cost and complexity, which, in turn, depend mainly on the required computer loading (the computer memory required to perform the calculations in a given arithmetic operation).

The size of the computer memory needed for the midcourse update scheme shown in Figure 51 is reported in studies by E-Systems, Inc. (References 36 and 37). An 8-bit data element is required for every area cell of 400 square feet over which the vehicle will pass.

Consequently, if the missile can navigate with sufficient accuracy to assure its ability to fly directly over a specified cell, the computer needs to store only one piece of data. Alternatively, if it can navigate with sufficient accuracy to pass over an area containing 100 cells, only 100 pieces of data need to be stored. If the missile's mission must be flexible enough to pass over an entire circular band with a 40-nautical mile outside radius and a 34-nautical mile inside radius, a large amount of data is required. If, as indicated in Figure 51, the approach is restricted to ½ radian, the area to be covered is 111 square nautical miles (Figure 51). If, as References 36 and 37 indicate, a data element is needed for each 400-square-foot element, about 174 data elements are needed for each square nautical mile of area to be covered. Consequently, 19,371 8-bit data words are needed in computer memory to cover this ½-radian segment.

Investigations of the terrain elevation correlation effort (References 36 and 37) have evaluated the use of the aircraft data processing equipment to initialize the missileborne fix-taking system. For example, using an aircraft computer to load source data on missiles during flight adds mission flexibility. However, loading missile source data on the ground

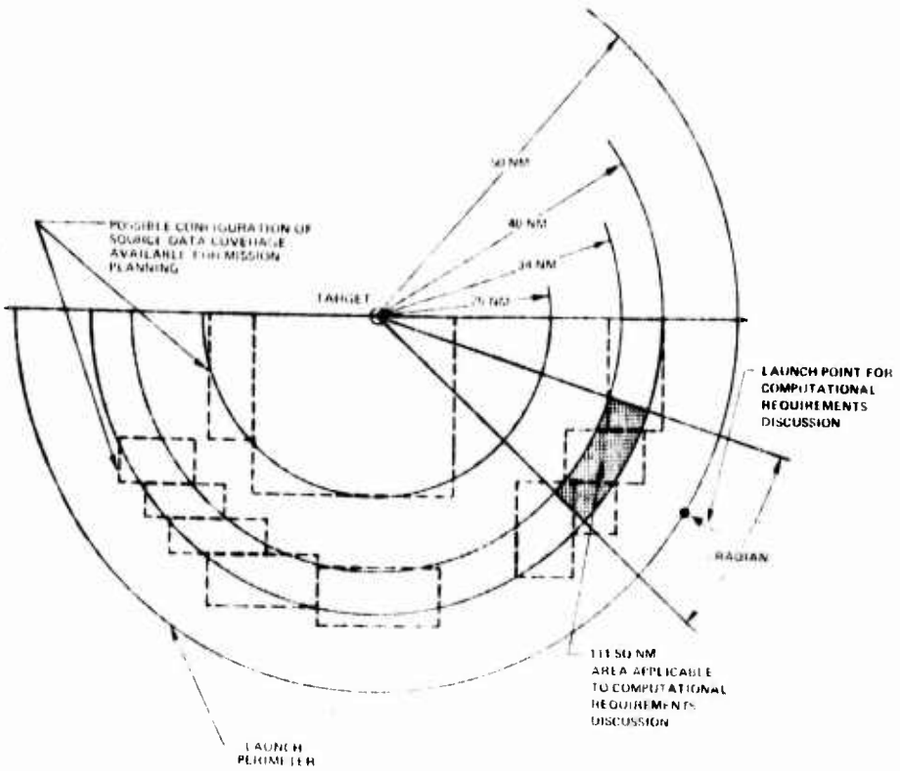

Figure 51. Illustration of Source Data Coverage

avoids an aircraft/missile exchange of source data and reduces system complexity. References 36 and 37 recommend a 2 percent velocity accuracy and 10 milliradians azimuth reference as inertial navigation system requirements associated with the midcourse update scheme shown in Figure 51. These are less stringent than the requirements associated with other update approaches investigated in this study (RACG, doppler radar, GPS, DME, ALSS, LORAN, and passive concepts). Consequently, the critical issue associated with the use of terrain elevation correlation for update is that of increased computational requirements versus minimal sensor requirements.

The developers of discrete update techniques provided neither realistic cost data nor a rigorous computational analysis for the discrete correlation fixtaking process. Therefore, the following rough estimates must suffice. Computer requirements were previously estimated to be in the neighborhood of 4,000 to 10,000 16-bit words per fix. For three fixes, 12,000 to 30,000 words of memory are required. The cost of stable computer memories is estimated at $0.20 to $0.40 per word, resulting in a cost of $2,400 to $4,800 for three additional fixes, assuming minimal area coverage. (Semiconductor memories available at lower cost lack stability.) Consequently, a price of $5,000 for additional update capability for midcourse guidance seems probable.

Previous discussions indicated that there are three alternatives open in the AFBGW/inertial navigation system design. They are: (1) use a fully inertial system with a 0.15 degree/hour (1σ) drift rate; (2) use a 1.0 degree/hour inertial system and a continuous update device with a velocity bias of 5 feet/second (2σ); or (3) use a 1.0 degree/hour (1σ) inertial system and an intermediate discrete fix with the radiometric area correlation guidance (RACG) equipment on board.

The costs of alternatives (1) and (2) have been discussed previously in this section. It is now necessary to establish the cost of alternative (2) in competition with (3) to establish a cost criterion for the selection of alternative (2).

CONTINUOUS UPDATE PROCESSES

Continuous update processes were examined primarily because the computational requirements for a discrete RACG update system seem high. In examining continuous update systems, a capability in the $5,000 range was sought, for the following reasons:

- The 0.15 degree/hour (3,000 feet-2σ) inertial systems cost $25,000 to $30,000 apiece at this time for 2,000 to 6,000 units.

- A 1-degree/hour (10,000 feet-1σ) capability through inertial capability alone costs $17,500 at this time.

- If a $17,500 platform with a $5,000 auxiliary sensor (total cost $22,500) could perform the required mission, it would probably be competitive despite decreased system reliability and the additional expense of mechanization, and would provide an effective ceiling on the additional cost that could be justified for an improved inertial system.

It is shown in Section V that a system with a 1-degree/hour gyroscope produces a total error of approximately 10,000 feet at the end of the AFBGW/long-range mission. This indicates that an accuracy of about 0.3 degree/hour is required to perform the mission with an unaided inertial capability, assuming that the 3,000-foot baseline system specification is quoted in 1σ numbers. It is more reasonable to assume that a 3,000-foot accuracy is desired 95 percent of the time. In this case, a 0.15-degree/hour (1σ) system is required. The cost of a continuous aiding device or the cost of the sensor and additional computer capability required for a discrete update also must be less than the difference in price between a 0.15-degree/hour system and a 1σ-degree/hour system. The examination of continuous update systems also considers their counter-countermeasure potential and flexibility. Jamming immunity was not considered mandatory, but the cost and complexity associated with a specified counter-countermeasure was addressed.

The following candidates were examined on the basis of cost, counter-countermeasure, and performance:

- Passive interferometer

- Air data processor

- Doppler radar

- Single/dual channel Global Positioning Satellite (GPS)

- Distance measuring equipment (DME)/ALSS and equipment.

Of the above concepts, the first two are undesirable. The passive interferometer requires two fixed ground installations that would be expensive and high risk in the 1980 to 1985 time period. They would also lie below the radar horizon when the AFBGW descends below 10,000 feet.

The air data processor depends heavily on the availability of meteorological data. The air data processing computer must be calibrated in the early phases of flight at altitudes from 50,000 to 30,000 feet and between 0 and 40 nautical miles from the launch point. The system would then operate in a zone below the 30,000-foot altitude and between 40 to 100 nautical miles from the launch point, conditions in which the calibration may not be applicable. Experience shows that, even with these factors, a 10-foot/second accuracy is possible with the air data processor. However, widespread use of the device will require collection, examination, and correlation of substantial quantities of meteorological data before the commitment of development resources to the testing of the air data concept can be recommended.

The doppler radar and the GPS are of interest with regard to cost, counter-countermeasure, and performance. The doppler radar is available at the $5,000 cost level, is almost immune to ECM, and can meet the 3,000-foot accuracy objective with a 100-nautical mile flight. The GPS can be configured to provide adequate counter-countermeasure capability, and its cost potential with counter-countermeasure is within the guidelines. Its performance is satisfactory for the 100-nautical mile mission. Both of these concepts are discussed in greater detail subsequently in this section.

The ALSS may be applicable from a performance and cost point of view. However, the counter-countermeasure capability cannot be positively assessed because it is a highly classified program and because a competition was in progress among several contractors that restricted the flow of information during the course of this study.

CONTINUOUS UPDATE PROCESSES—DOPPLER RADAR (REFERENCE 38)

Two doppler radar systems were examined; the doppler radar velocity system (DRVS) and the 727D system. Their characteristics are quire similar, as is indicated in Table 39. Either of these systems can provide the horizontal velocity accuracy required for the mission (3,000 feet-2σ at 100 nautical miles). The inertial sensor group provides the necessary azimuth accuracy. Appendix E provides a detailed

TABLE 39. DOPPLER RADAR CHARACTERISTICS

PARAMETER	DRVS	727D
Horizontal Velocity (Bias)	0.32 percent + 0.24 kt (1σ)*	0.25 percent (1σ)
Vertical Velocity (Bias)	0.14 percent + 0.12 kt (1σ)*	0.5 percent (1σ)
Horizontal Velocity (Noise)	0.0033 $(kt)^2$/RPS (1σ)	0.0024 $(kt)^2$/ RPS (1σ)
Size ($Inches^3$)	6 x 5 x 5	Transceiver Antenna: 9.5 x 6.2 x 2.0 Signal Data Converter: 7.5 x 6.2 x 4.0
Weight (Pounds)	7.5	Transceiver Antenna: 2.7 Signal Data Converter: 4.9
Power (W)	30	25
Environment	MIL E 5400-1	MIL E 5400-2
Power Out (mW/GHz)	100 mW/13.325 GHz	50 mW/13.325 GHz
Cost ($)	5,000 - 7,000 (Large Quantity Production)	5,000 (2,000-6,000 Units)

* Velocity bias is expressed in terms of percent of vehicle velocity. The total error is also equivalent to the total distance traveled multiplied by the bias percentage terms. (In the case of DRVS, the time of flight must also be calculated and multiplied by the constant velocity terms and added to the percentage derived terms.)

description of the DRVS system that was prepared by Lou Marino of GPS Singer. The configuration described in Appendix E was specifically planned for the AFBGW, as performance and packaging are directed to particular requirements.

Either the DRVS or the 727D can absorb the entire error allowance. In an actual operational situation, it might be desirable to derive position data from the 1-degree/hour gyroscope system during the early part of the flight and from the doppler system later in the flight. This would reduce system error sufficiently to allow provision in the error budget for the azimuth misalignment.

The cost estimates in Table 39 are derived from production experience. The 727D system was designed for drone and remotely piloted vehicle (RPV) application and is currently production rated for a CANADAIR system. The DRVS technology is based on large-scale existing production. Consequently, the estimated costs carry a high confidence level. Cost reduction through relaxation of performance specifications might be appropriate if a doppler inertial mechanization is designed on the basis of the principles illustrated in the section on aiding. As an indication of the state-of-the-art, note that of the five doppler suppliers contacted, three expressed interest in sensors below the 0.62 percent (1σ) performance level and $5,000 cost level. (Doppler error performance is normally expressed in terms of percent of distance traveled.)

The DRVS installations and configuration for the AFBGW/long-range are shown in Figure 52. The microstrip antenna is conformal and has the same radius as the guidance adapter. The antenna is flush mounted to the skin of the vehicle, with cutouts required only for the antenna coaxial connectors, which are about 0.25 inch in diameter. Coaxial lines connect the antenna to the receiver/transmitter box mounted in the vehicle. The receiver/transmitter would be powered by the vehicle's battery supply. The beam pattern of the DRVS is shown in Figure 53.

There is extensive electronic warfare (EW) experience with the implied gain pattern involving emission power levels below 0.1 mW. The general consensus of the specialists in the EW community contacted during the survey was that this type of emitter is not detectable in a realistic scenario, and that both doppler systems are virtually immune to countermeasures.

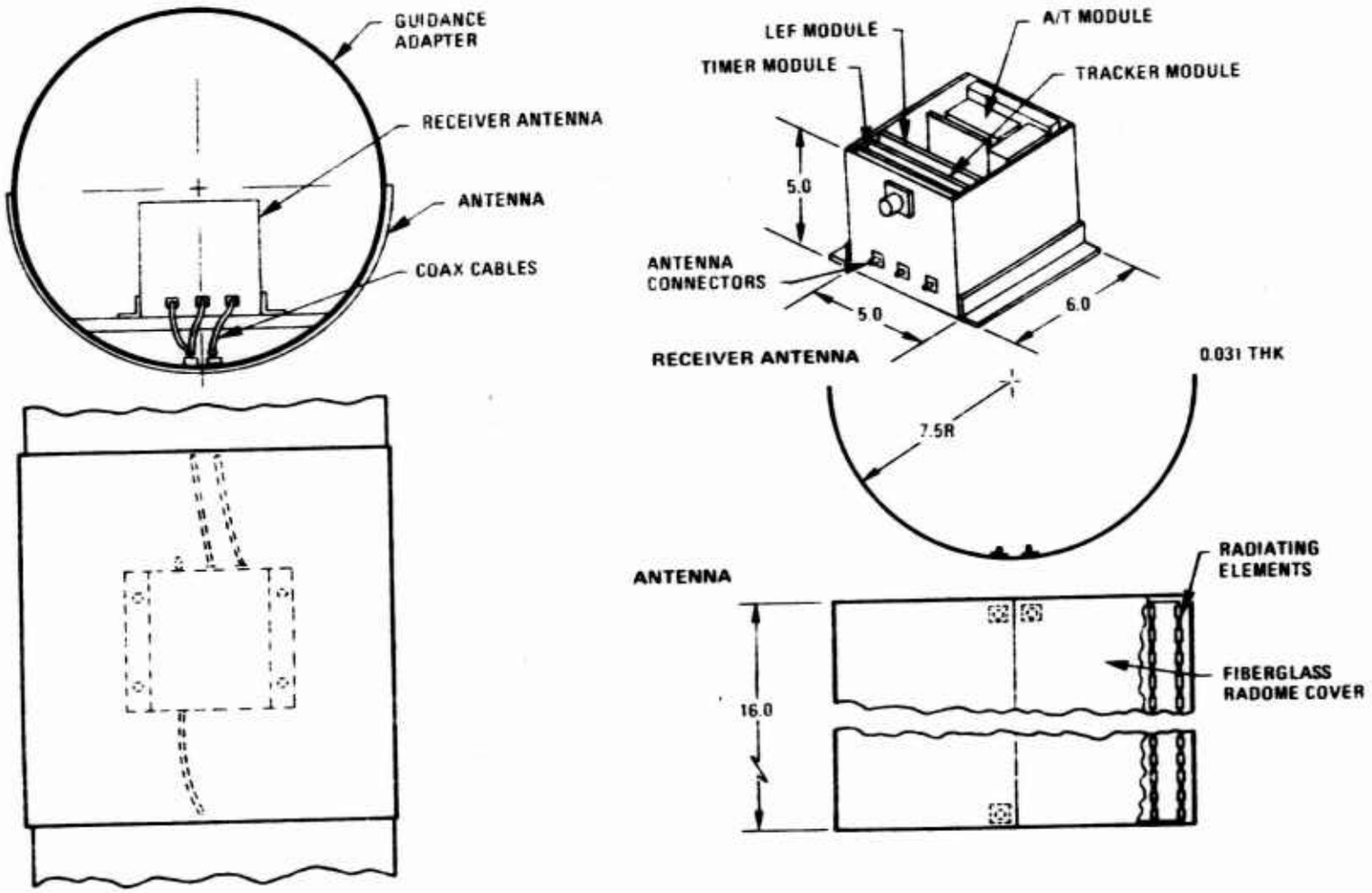

Figure 52. DRVS Doppler Radar Installation and Configuration for the AFBGW

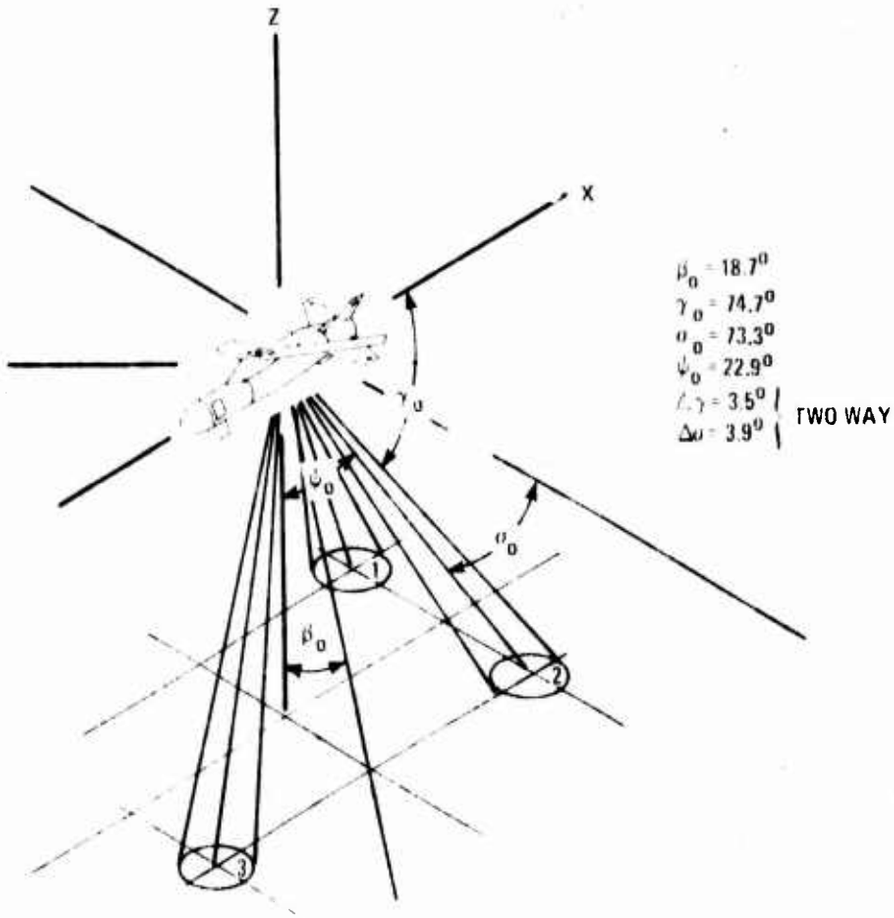

NOTE 1: $\Delta\gamma$ IS THE BEAM WIDTH OF THE BEAMS 1, 2, AND 3 IN THE γ DIRECTION AND $\Delta\sigma$ IS THE BEAM WIDTH OF BEAMS 1, 2, AND 3 IN THE σ DIRECTION.

NOTE 2: THE BEAMS ARE FIXED IN THE POSITION SHOWN AND DOPPLER RETURNS ARE COMPARED TO DETERMINE HORIZONTAL VELOCITY

NOTE 3: FOR FURTHER EXPLANATION OF THIS SYSTEM SEE APPENDIX F. FURTHER DATA CAN BE PROVIDED ON THE THEORY OF DOPPLER RADAR NAVIGATION FROM REFERENCE 38.

Figure 53. DRVS Antenna Beam Pattern

CONTINUOUS UPDATE PROCESSES—GLOBAL POSITIONING SATELLITE (GPS) (REFERENCE 39)

This section discusses the possible role of a GPS receiver and antenna system for the AFBGW/long-range midcourse guidance.

Table 40 addresses the impact of critical design options on the accuracy, cost, counter-countermeasure, and flexibility of a GPS receiver and antenna system for midcourse guidance. The capabilities and requirements associated with the options of Table 40 were discussed during the survey, particularly with personnel from Hazeltine, Inc., and several system guidelines evolved.

A cursory review of the position accuracy requirements suggests that a continuous velocity update capability is adequate for the AFBGW/long-range mission. To assess the most economical method of providing this capability, several support and design alternatives were examined. It may be economical and practical to rely as much as possible on an aircraft (x) GPS receiver to initialize the AFBGW missile (m) receiver. The x system transmits the error biases to the m system, stabilizes the m oscillator, and transfers the appropriate constants to the missile system before launch. This eliminates the need for a synchronizing circuit in the m system and offers potential for a low-cost m system.

The missile system for the AFBGW would include the following elements:

- Low noise front end
- Oscillator
- Superheterodyne converter
- Amplifier
- Code generator
- Timing control loop (two integrated chips)
- Doppler processor (two integrated circuit chips).

The objective of a system based on the above equipment is to provide range rate information with reference to one satellite at an accuracy of 1 foot/second (1σ). The knowledge of range rate to a single satellite, together with an adequately

TABLE 40. AFBGW GPS RE

Design Options	Accuracy	Cost
Single-channel receiver	Would depend upon IMU Requires 1.0-5.0 mrad azimuth reference	Low cost compatible $2000 target
Four-channel receiver	Accuracy would be independent of IMU	High cost $10,000 target
Narrow noise bandwidth	Lag in velocity data and position data would adversely affect system response	Can escalate cost under conditions
Continuous position update capability	Level of accuracy an order of magnitude above the requirement	Well above the $5000 li
Continuous velocity update	Potential accuracy more than adequate	Possible to realize cap bility in the low thousa
Antenna directionality	No impact	Computer and/or electr mechanical equipment
Jammer suppression techniques	No impact on accuracy	Requires additional ant and processing hardwa
Initialization with x receiver system	No impact on accuracy	Could eliminate the ne 10^{-10}/SLO short term Possible $2000 target

SLO = System local oscillator
x Receiver = Aircraft GPS receiver

• AFBGW GPS RECEIVER OPTIONS

Cost	CCM	Flexibility
ow cost compatible 2000 target	Could be highly susceptible Single look direction	Not inherently inflexible. If sequential satellite reception was desired, antijam margin would be reduced. Continuous tracking would result in constraints on satellite-trajectory combinations. IMU-inertial combinations would be limited.
igh cost 10,000 target	Could be selective in choice of satellite	Continuous operation insured. Tradeoff between effectiveness and IMU accuracy
n escalate cost under extreme nditions	Can provide over 50 db antijam margin	Can impose tracking loop stability requirement. Alternately, could limit missile lateral acceleration level
ell above the $5000 limit	Requires interpretation of coded input data. Reduces antijam margin	Requires clock on missile to determine satellite pseudo range
ossible to realize capability in the low thousands	High antijam margin potential—no data reduction required	No time reference required
mputer and/or electro-echanical equipment cost	Beam could be directed to place the null on emission source	Requires beam pointing, continuous signal processing
quires additional antennas d processing hardware	Could provide 40 db antijam margin	
uld eliminate the need for -10/SLO short term stability ssible $2000 target cost	No impact on CCM	Could limit operation to aircraft with x receiver

(The reverse of this page is blank)

aligned platform (3 milliradians-1σ), allows the resolution of velocity data along the missile axes. The target price of a system based on the above approach is $2,000.

This arrangement affects system flexibility in several ways. The selection of launch aircraft is limited to those carrying an x receiver. An inertial alignment system must be provided for the missile independent of the GPS sensor. There are also operational blind spots, or singularities, in the navigation process. For example, the missile cannot fly perpendicular to the satellite/missile line-of-sight (LOS) without significant velocity error magnification in the GPS derived data.

GPS counter-countermeasure potential and design capability are more serious issues than system flexibility. The GPS approach offers opportunities to hostile jammers. Consequently, the focal point of successful operation of the system is reliable counter-countermeasure capability.

For this reason, the following approaches were investigated:

- High-gain antenna design and beam shaping
- Sidelobe suppression (adaptive beam shaping)
- Adaptive noise cancellation
- Delay lock loop filtering with inertial velocity stabilization.

Table 41 summarizes selected counter-countermeasure options and indicates the associated cost and performance impact. A thorough discussion of the counter-countermeasure approaches outlined in Table 41 is given in Appendix F.

CONTINUOUS UPDATE PROCESSES—DME

Several forms of DME were examined, including a ground-based commercial system and the ALSS. The ground-based system is adapted from a DME/VOR aircraft navigation upgrade (Reference 40).

If the system is located near the launch line but displaced 25 nautical miles laterally from the launch position, a 4,000-foot error occurs for a range of 100 nautical miles and an average missile speed of 1,000 feet/second.

TABLE 41. SELECTED GPS COUNTER-COUNTERMEASURE OPTIONS

Concept	Approach	Performance Objective (db)	Cost Goal ($)	Reference
High gain antenna design	Use the fuselage and wings to gain antenna aperture. Planar arrays, conformal arrays, phase interference reinforcement	15	Less than 500	
Beam shaping	Locate the jammer and set phase shifters to create a null in the gain pattern	10 in addition to high gain capability	Possibly 100 in addition to the antenna cost	
Adaptive beam shaping	Place auxiliary loops in the GPS antenna array elements to suppress jammer. No need to determine angular location of jammer explicitly	16. One jammer per loop. Systems now in operation. Packaged in a few cubic inches	400 per jammer (estimate)	Mr. Al Cooper General Electric Utica, N.Y.
Adaptive sidelobe suppression	Use of auxiliary antenna to receive jamming signal. Sidelobe suppression network nulls the jammer noise that is present in the output of the GPS antenna	50	Low thousands, possibly 2000, for volume production	Mr. Al Cooper General Electric Utica, N.Y.
Delay lock loop	Use of narrow bandwidth to enhance signal-to-jammer noise ratio. Employs inertial stabilization	30-50 potential	Estimated cost 2000 Could be packaged in a 8x4x2-in. envelope. 5 lb additional weight	

Effective counter-countermeasure operations with this system are prevented by adverse geometry and lack of system adaptability to secure transmission techniques.

The ALSS is a prime DME candidate, since it is already applied to the AFBGW system; however, its highly classified nature prevents a detailed discussion in this study. The operational concept and missile equipment block diagram are shown in Figure 54 (Reference 41).

If the baseline inertial system is combined with the ALSS for the first 140 seconds of flight, the AFBGW can achieve the required 3,000-foot midcourse guidance performance after 600 seconds of flight.

The ALSS system provides similar support for the AFBGW midcourse guidance, as does the discrete update function. However, the ALSS system requires external systems, data decoding, and retransmission. It is also subject to hostile counter-countermeasure.

CONTINUOUS UPDATE PROCESSES—OTHER SENSORS

LORAN

The accuracy of the LORAN permits the type of capability provided by the ALSS system and has been applied to glide bomb weapons (KMU-353A/B, etc.) in the past. LORAN is subject to wideband noise disturbances which can be addressed by phase-locked loop designs and can be improved by the use of inertial reference data. However, stability of wideband noise has a potential impact on ability to reduce errors through adaptive LORAN inertial networks.

Omega

Omega is not well adapted to the AFBGW because of the basic instability of its error process. The present system consists of eight stations transmitting on selected frequencies, and it is possible to track with a -10 to -20 db signal-to-noise ratio (difficult to achieve with a tactical missile).

The baseline accuracy of Omega is 0.7 to 1.0 nautical mile (1σ). With an airborne relay station, this would probably be improved to 0.2 nautical mile (1σ). The basic process

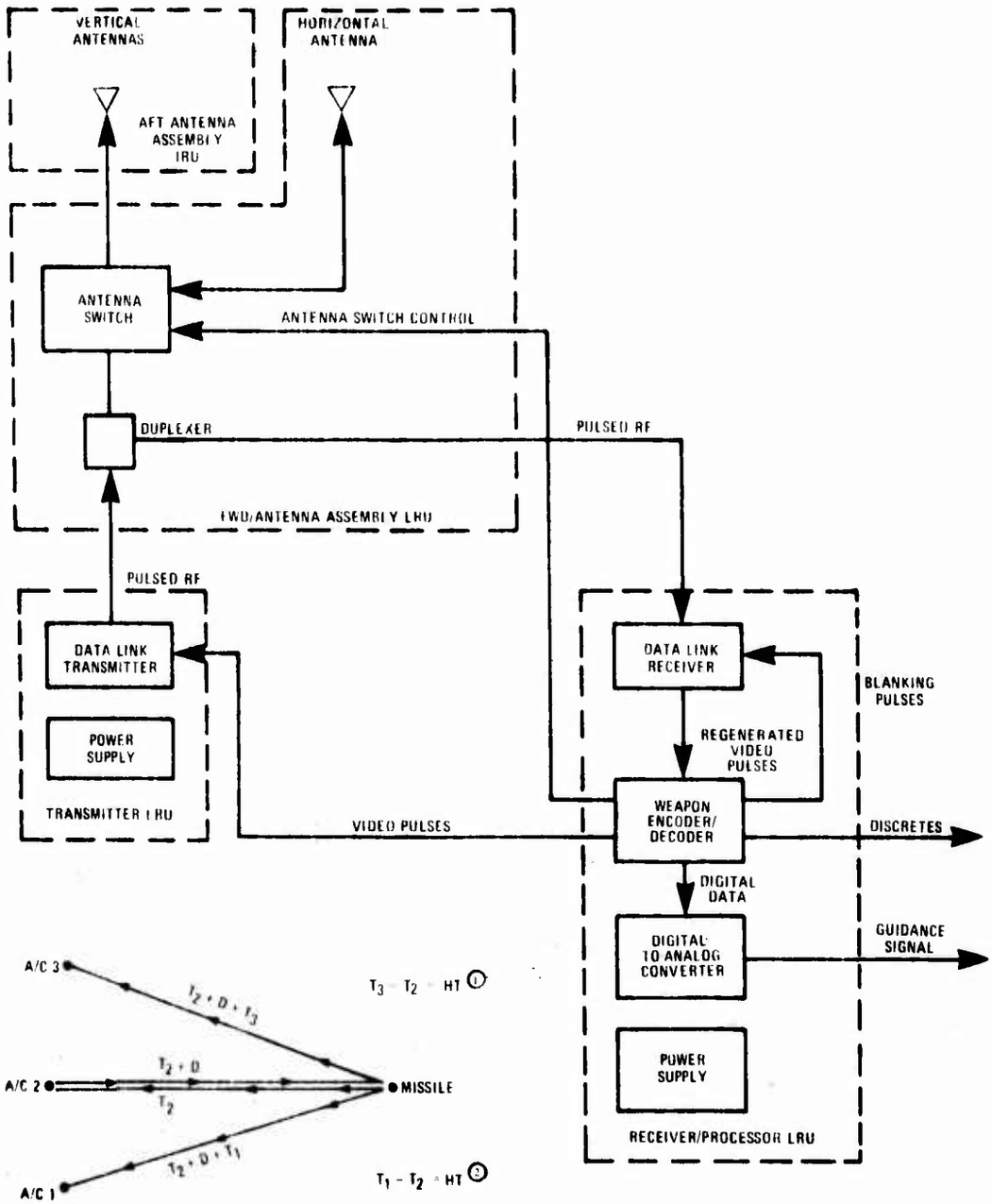

Figure 54. Advanced Location Strike System Guidance System Concept and Operational Diagram

has a 3,000- to 4,000-foot position noise, and there is a significant lag (1 minute) in velocity data. There is also a 36-nautical mile theoretical wavelength in the smallest band.

Passive RF Guidance

The application of passive electronic warfare techniques to the AFBGW midcourse guidance effort was also investigated, and system components were defined as follows:

- Ground support equipment: two retrodirective, high-power, moderate gain transmitters that are positioned prior to launch.
- Missileborne equipment: one single-axis reference and two body-mounted chain interferometers.

The ground transmitters amplify hostile transmissions and beam them to the AFBGW. The chain interferometers determine the vertical plane that contains the launch point and the target. The AFBGW flies in this vertical plane throughout the mission. The missile also carries a single-axis reference with a gyroscope, one level accelerometer, and one vertical accelerometer. This allows two-dimensional precision navigation. The system is inherently low cost, and it is difficult to detect because the energy transmitted by the ground emitters is already present in the atmosphere.

This concept was conceived by T.E. Yee of Honeywell, Inc., during an earlier program. Further data is available on the components from the following sources:

- Ground support equipment: Threat Handbook (Reference 42)
- Single-axis references: Appendix C, Volume II, of this report
- Body-mounted chain interferometers: Mr. W.A. Bishop of Litton Amecom Division, College Park, Maryland.

CONTINUOUS UPDATE SUMMARY

The above discussion has established the adequacy of several velocity references. The guidelines for adequacy are: accuracy of 5 feet/second (2σ); a cost of $5,000 (2,000 to 6,000 units); counter-countermeasure effectiveness; and

operational flexibility. The doppler radar is ideally suited to the performance, cost, counter-countermeasure, and support requirements associated with the AFBGW missile.

The GPS can also be used. Its cost and performance are even more attractive than those of the doppler radar. However, it is subject to ECM, and the counter-countermeasure approaches that were defined to correct this situation are cumbersome and add to the complexity of the concept. The GPS is not a self-contained system, and it depends upon the availability of both aircraft and space equipment.

The ALSS is also an applicable system; however, no positive conclusions can be made at this time on its relative merit in this situation because insufficient data are available.

The LORAN can be classed with the GPS in many respects. It has the accuracy and the low-cost potential required for the AFBGW application. However, its counter-countermeasure performance is inferior to the GPS because it will be receiving signals in the horizontal plane. Jammers can compete quite effectively under these circumstances. Support transmitters will also have to be charged against the system (which is not the case with the GPS). Consequently, system cost may be somewhat higher than system costs for comparable wideband noise problems.

In general, the continuous update process investigation established a large number of techniques and components that can be used to augment the inertial navigation sensors. While the doppler radar is preferred, many others would be adequate in their present form, and all that were examined have potential. Some, however, require further study and adaptation.

UPDATE TECHNIQUE SUMMARY

The data developed in both the discrete update study and the continuous update study are summarized in Table 42. The table shows that when both continuous and discrete systems are compared, the RACG and doppler radar are roughly comparable in accuracy, counter-countermeasure, and cost. The table also indicates that there is greater certainty about the probable cost of the doppler radar than of the RACG. Although the RACG updating costs are estimated to be lower, the RACG requires an external function, source data processing, while the doppler radar does not.

TABLE 42. UPDATE SYSTE

Update Technique Or Equipment	Accuracy	ECM Susceptibility	Cost
RACG	Classified, see Reference 15. Acceptable	K_a band jammers can interfere, must be located near fix point	The cost of the RACG ceiver, antenna, and estimated at about $50 quantities of 2000 to 6
Terrain Elevation Correlation	Examined for potential spinoff of techniques to RACG This and RACG are parallel concepts, they would not be used in combin		
Doppler Radar	0.5% or 5 ft/sec (2σ) adequate to replace inertial navigator as prime position	Virtually immune to ECM	$5000 in quantity
Global Position Satellite	1.0 ft/sec (estimate) More than adequate	Susceptible to ECM Extensive CCM examined	$2000 without CCM $4000 to $7000 with CC
ALSS	More than adequate Classified	Performance classified, system geometry less favorable than GPS	Missile equipment cost able Extensive support requ
Passive Techniques	Adequate in combination with a nonbaseline inertial concept	Retrodirective emitters masked by environment Highly resistant to ECM	Missile equipment $50 support requirement
Air Data	10-40 ft/sec Improvement depends upon synergistic approach	Immune to ECM	$160 to $500

UPDATE SYSTEM SUMMARY

Cost	System Requirement External to Missile	Conclusion
ost of the RACG sensor re-, antenna, and gimbals is ated at about $5000 in ties of 2000 to 6000 items.	Source data required from defense map agency	RACG discrete update feasible and could be cost-effective More definitive computational analysis required
e used in combination		Duplicate RACG capability rather than supplementary
in quantity	None required	Could provide excellent supplement to 1.0 deg/hr inertial platform
without CCM to $7000 with CCM	Satellite and ground transmitter required; system elements used for other purposes Cost impact not assignable to GPS	Effectiveness depends upon reliability and simplicity of CCM approaches
e equipment cost not avail- ive support requirement	Three aircraft required	Insufficient data available CCM could be a problem
e equipment $5000, extensive ort requirement	Ground transmitters required	Requires further study
o $500	No requirement, although meteorological data may be an element in synergistic operations	Requires further study

(The reverse of this page is blank)

The GPS must be placed after both the RACG and the doppler radar because of the counter-countermeasure question and because of questions concerning availability of external systems (Table 40). Terrain elevation correlation is not considered a candidate; it was examined to determine what processes and techniques might be adapted to the RACG.

The ALSS cannot be evaluated because essential data are not available. Passive techniques and air data processing are not competitive.

SECTION IX

CONCLUSIONS AND RECOMMENDATIONS

The conclusions and recommendations of this report reflect the objective and scope of the study, which were described in the introduction. As indicated in the introduction, the objective of the study is to identify analytical methods and guidance techniques for the AFBGW concept. Consequently, the following conclusions and recommendations will be directed to the application of available technologies, the appropriate action for support of the AFBGW cost and performance goals, and the application of synthesis techniques.

Where appropriate, these conclusions and recommendations will relate to the AFBGW project and the RACG development effort. However, most of the material in this section deals with the need for new analytical techniques and the need to develop supporting data.

This section is organized into six subsections—each corresponding to a previous section of this report (Sections III to VIII).

SECTION III

Section III presented a review of candidate inertial equipment. These were selected from diverse applications. Investigation of currently operational inertial systems led to an assessment of the potential of the following types of gyroscopes: rate-integrating gyroscopes, rate gyroscopes, tuned flexure gyroscopes (gyroflex), and laser gyroscopes. It also involved the estimate of the performance and cost of strapdown platforms constructed from these gyroscopes.

The following conclusions and recommendations resulted from activities associated with Section III:

- Rate-integrating gyroscope (RIG) technology offers an excellent potential for achieving the cost and performance objectives of the AFBGW concept. Examples of instruments that are very close to the baseline requirement are Northrop GI-G6-S and GI-G6-B, Honeywell G1111-LC, Lear Siegler 1903, and Hamilton Standard Mini-RIG 30. The following positive factors are cited with regard to the RIG approach: extreme flexibility of cost and performance objectives,

extensive history of application, and evidence of a large group of potential suppliers realistically seeking to address the AFBGW requirement.

- Rate gyroscopes do not address the performance objectives of the baseline requirement. Applications that were reviewed indicated that aiding a rate gyroscope mechanization may present problems not associated with a RIG application.

- Tuned flexure gyroscopes have the performance potential for the AFBGW concept. Pricing objectives were seen to be somewhat above the baseline target cost ($15,000 rather than $10,000 for a three-axis platform without computer). Interest is limited with only one supplier claiming an active development program.

- Laser gyroscopes have the performance potential with at least two suppliers directing effort to the AFBGW requirement. However, experience in this technology area is measured in tens of units delivered—compared to tens of thousands in the RIG technology area.

- The platform cost goal of $10,000 for a 1-degree/hour performance with a 2×10^{-4} g accelerometer may be difficult to achieve with off-the-shelf equipment.

- The platforms reviewed all have prior association with ongoing programs. Their cost is influenced by requirements that are not applicable to the AFBGW concept. Cost estimates are also influenced by existing contracts and contracts to be negotiated in the near future. Consequently, there is ample ground for exploring the requirements that are tailored to the AFBGW. Special consideration is warranted in the operating life, reliability, and compensation of applicable designs.

- The operational and support constraints in the system will profoundly affect the design objectives of a AFBGW gyroscope. Calibration cycle, aircraft support requirements, and environmental control are prime related examples. Well-defined objectives relating operational flexibility, support requirements, and performance are required.

- Innovative techniques for improving performance at cost without prelaunch calibration cycles may be

available. Applicability of portions of the Carousel technology to strapdown systems and calibration through spin motor modulation are pertinent related issues. The use of auxiliary sensors is also to be considered.

SECTION IV

Section IV illustrated the application of classical system synthesis in the development of a guidance law. It also indicated the impact of a guidance policy on range and available energy. This work led to the following conclusions and recommendations:

- The problem of transit of an air-to-surface missile from launch to target has been successfully solved in many previous missile system developments. The choice of approach for the AFBGW depends on the computational resources to be allocated to this function. If ample resources are available, the SRAM virtual target approach is indicated. If limited computational resources are available, an acceleration loop mechanization is indicated; however, this approach may impose undesirable autopilot requirements and provide reduced flexibility.

- Error propagation will not impose a serious range penalty on the AFBGW. Cross-course errors of as much as 5 miles can be tolerated even when the missile is within 20 miles of the target. (This situation results in a range penalty of less than 2 percent.)

- A successful synthesis of the guidance loop can be conducted by use of classical linear techniques. The predominance of linear constraints in the missile guidance situation tends to make the linear phase of analysis a critical one. Nonlinear analysis and the investigation of the role of nonlinear control approaches are also important.

SECTION V

Section V derived the error equations for the baseline inertial guidance equipment and presented the error propagation history. This effort led to the following conclusions and recommendations:

- The AFBGW/long range can navigate to within 600 feet of the target with a 1-degree/hour inertial guidance unit, assuming a nominal 240 seconds of flight (Mach 1.0 with 40-nautical mile range).

- The AFBGW/long range can navigate to within 10,000 feet of the target with a 1-degree/hour inertial guidance unit, assuming a nominal 600 seconds of flight (Mach 1.0 with a 100-nautical mile range).

- The AFBGW/long range can maintain a vertical reference of 3 milliradians with the baseline (1.0-degree/hour system).

- At the end of 600 seconds of flight, a 1-degree/hour system will experience a velocity error of 24 feet/second (dual channel).

- The first two items indicate the desirability of using different approaches for the AFBGW/long range and AFBGW/short range systems. The use of two different gyroscopes that are mutually compatible has been suggested by several sources.

- The critical requirement for level accuracy for RACG tends to support the use of high-quality sensors of the use of a velocity reference to reduce level error.

- The high rate of platform divergence (velocity error) after 600 seconds places emphasis on a velocity reference. A representative velocity reference has a fixed bias at 5 feet/second. A comparable inertial guidance unit has a 24-foot/second error that increases with the square of flight time. Use of a velocity reference with the long range version and common short range/long range inertial systems is a logical alternative.

- The AFBGW concepts are not subject to the type of environment that causes high computational errors in strapdown equipment. First- or second-order algorithms are appropriate for evaluation in this context. This study has not addressed the effects of Scorsby or coning motion which may be present in the AFBGW environment.

SECTION VI

Section VI explored the available methods of aligning the AFBGW strapdown platform. Successive discrete update alignments and transfer alignments were reviewed, and gyrocompassing was discussed. The following conclusions and recommendations are associated with alignment.

- The choice between transfer alignment and discrete update alignment can be based entirely on support and operational considerations, since either technique will provide the required accuracy.

- Alignment accuracy of 1 milliradian (600 feet for the long-range mission) will essentially remove azimuth misalignment as an error source. The upper error limit is 3 milliradians in azimuth misalignment (1,800 feet).

- If successive discrete update is selected, no aircraft navigation equipment is required. It may be desirable to store the source data for fixes in an aircraft computer for transfer to the missile computer. Alternatively, it may be desirable to make successive fixes before launch.

- Transfer alignment will require a full inertial platform on the aircraft and require a maneuver before launch. If the maneuver is found objectionable, the aircraft can be instrumented to compensate for aircraft flexure.

- Transfer alignment is the fastest method of alignment, requiring from 13 to 16 seconds. Discrete alignment time can consume from 60 to 180 seconds, depending on the heading accuracy desired and the accuracy of the fixtaking mechanization.

SECTION VII

The following conclusions and recommendations resulted from work related to Section VII.

- Discrete update using three requested fixes at the midway point can provide the necessary accuracy to perform the 600-second long range mission within a 3,000-foot accuracy goal.

- A velocity reference with a fixed bias of 5 feet/second in combination with a 1.0-degree/hour inertial system can provide the necessary accuracy. This accuracy requires a scheduled variable gain operation with inertial errors being emphasized in the beginning of the flight and velocity reference errors being emphasized toward the end of the flight.

- An evaluation of the potential of adaptive gain systems (optimal estimate) depends on a knowledge of the error process of the continuous update sensors, which is not highly organized and readily available in a form necessary for tradeoff evaluation.

- Adaptive system effectiveness is limited by the power in the error spectrum beyond 0.278×10^{-3} radians/second. Ultimate potential is estimated at 160 feet for the systems discussed in this report.

SECTION VIII

Section VIII documented selected update techniques that were found to have merit during the course of the study. The emphasis of the documentation effort for individual devices depended on the nature of the technique associated with each device. For example, the GPS presentation emphasized counter-countermeasure capability because the accuracy of the system was far above the AFBGW requirement. On the other hand, the doppler radar section emphasized performance.

The work associated with Section IV was divided into two categories; the first involved discrete updates, and the second involved continuous updates. Relevant conclusions and recommendations are categorized accordingly.

Discrete Updating of Inertial Platform

Three or more discrete updates can provide the necessary data to correct attitudes, velocity, and position. The ultimate error in a system using discrete updates depends on the accuracy of the update process, the length of time taken to make sequential updates, and the time of flight after the updates are taken.

Classification of data prohibits precise accuracy in discussing update systems. However, the discrete techniques described in Section IV provide adequate accuracy.

Storage of source data may be an issue in the use of discrete fixes for updating an inertial system. Preliminary examination of several alternatives indicated a maximum possible requirement of 10,000 words per fix. Tradeoff analysis is required to identify possible economies in fixtaking procedures.

The cost of memory storage for source data involved in the fixtaking process is highly dependent upon operational constraints. At $0.10 per word (NCR-EARCOM technology), a cost of $3,000 for a discrete update process would be imposed. Ultimately, the use of semiconductor memory technology could reduce memory cost to $1,000. The latter alternative could impose stability problems in certain electromagnetic environments.

The update function could be provided before launch, allocating the memory requirement to the aircraft computer. This policy would prolong post-update flight time for the missile and constrain aircraft flight during the period of update.

Continuous Update of the Inertial Platforms

At present, there is no highly organized and readily available data base that describes the error processes of candidate velocity references. This type of data is essential for evaluation of the in-flight calibration potential of such equipment.

The doppler radar can provide adequate position accuracy for the long-range (600 seconds) mission. The concept is also cost competitive with inertial sensors.

The GPS can provide a highly accurate continuous velocity reference. A cost-effective version of the GPS would probably be based on a single-channel design with velocity measurement capability (no position). The ECM susceptibility problems can be addressed by a combination of approaches. These include a high gain antenna, null shaping, adaptive sidelobe suppression, sidelobe cancellation, and delay loop suppression with inertial stabilization.

The LORAN, VOR/DME, DME/TOA, and passive approaches are also effective as continuous update velocity references.

Omega and air data computation require adaptation and development of supplementary techniques for application as velocity references.

REFERENCES

1. Inertial Navigation—A Report Bibliography, DDC Search No 034919, Defense Documentation Center (prepared for Booz, Allen Applied Research), September 1975, (300 entries).

2. Witting, J.H. and J.W. Jorr, Virtual Target Steering, The Boeing Company, August 1972.

3. Harpoon Weapon System, McDonnell Douglas Astronautics, May 1973.

4. AGM-65A Maverick Missile Segment, Hughes Aircraft Company, September 1972.

5. Bloodworth, J.E. and P.B. Huntress, Development and Optimization of the SRAM Guidance and Control Software, The Boeing Company, Seattle, Washington, August 1972.

6. Feldman, J., Standardized Strapdown Inertial Component Modularity Study, R-826, Charles Stark Draper Laboratory, Massachusetts Institute Technology, July 1974.

7. Chin, S.S., Missile Configuration Design, McGraw-Hill Book Company, Inc., New York, 1963.

8. Bailey, J.L., et al., Aerodynamic Characteristics of the Mark 84 GBU-15 CWM Guided Weapon, Rockwell International, Columbus, Ohio, July 1975.

9. Grabbe, E.M., S. Ramo, and D.E. Wooldridge, Ed., Handbook of Automation, Computation, and Control, Volume I: Control Fundamentals, John Wiley & Sons, Inc., New York, 1958.

10. Truxal, J.G., Automatic Feedback Control System Synthesis, McGraw-Hill Book Company, Inc., New York, 1955.

11. Whitcombe, D.W., Present and Advanced Guidance Techniques, TR-0073(3115)-1, Aerospace Corporation, November 1972.

12. Leistenhow, L., et al., Optimum Control of Air-to-Surface Missiles, AFFDL TR 66-64, R&T Division, USAF Flight Dynamics Laboratory, Wright-Patterson Air Force Base, Ohio, p. 89.

13. Thaler, G.H. and R.G. Brown, Analysis and Design of Feedback Control Systems, McGraw-Hill Book Company, Inc., 1960.

14. James, H.M., N.B. Nichols, and R.S. Phillips, Ed., Theory of Servomechanisms, Boston Technical Lithographers, Inc., Lexington, Massachusetts, 1963.

15. Carpenter, T.A., J.M. Dodd, and J.K. Matsuaza, Radiometric Correlation Evaluation, AFATL-TR-73-78, LMSC, Inc., Sunnyvale, California, May 1973.

16. Broxmeyer, C., Inertial Navigation Systems, McGraw-Hill Bock Company, New York, 1964.

17. Parvin, R.H., Inertial Navigation, D Van Nostrand Co., Inc., Princeton, N.J., 1955.

18. Leondes, C.T., Ed., Guidance and Control of Aerospace Vehicles, McGraw-Hill Book Company, Inc., New York, 1963.

19. Sullivan, J.J., Evaluation of the Computational Errors of Strapdown Navigation Systems, United Aircraft Corporation, February 1968.

20. Pitman, G.R., Inertial Guidance, John Wiley & Sons, Inc., 1962.

21. Cannon, R.H., Jr., "Alignment of Inertial Guidance Systems by Gyrocompassing-Linear Theory," Journal of the Aerospace Sciences, Volume 28, November 1961.

22. McMurray, L.R., "Alignment of an Inertial Autonavigator," ARS Journal, January 1960.

23. Schultz, R.L., C.L. Keyes, and E.E. Fisher, "Simple High Accuracy Guidance Flight Test Program—IRP-to-IRP Alignment Study," Addendum to Report No. SHAG-PR-2005, and to Honeywell Report No. 14575-1R1, prepared for Air Force Avionics Laboratory, AFAL/NVA-698DF, Air Force Systems Command, Wright-Patterson Air Force Base, Ohio, June 1972.

24. Alignment Study for the Radiometric Area Correlation Guidance System, Delco Electronics (General Motors Corporation), prepared for Advanced Program, Missile System Division, Lockheed Missiles and Space Company, Incorporated.

25. Sutherland, A.A., Jr. and C.D. Bayne, Jr., Aided Inertial Guidance for Air-to-Surface Missiles In-Flight Alignment, TR-145, Analytic Sciences Corporation, January 1960.

26. Sutherland, A.A., Jr. and A. Gelb, The Kalman Filter in Transfer Alignment of Airborne Inertial Guidance Systems, NNC TP 4653, The Analytical Sciences Corporation, for the Weapons Development Department, October 1968.

27. Carousel IV and IV-A Inertial Navigation Systems, Delcon Electronics (General Motors Corporation), March 1974.

28. Klein, D.W. and A.A. Sutherland, Jr., Handbook Summary of Inertial Guidance for Air-to-Surface Missiles, TR-245-1-2, Analytic Sciences Corporation, August 1973.

29. Danik, B., Hybrid-Inertial Navigation With Range Updates in a Relative Grid, Kearfott Division, The Singer Company, August 1973.

30. Nixon, F.E., Handbook of Laplace Transforms—Fundamentals, Applications, Tables, and Examples, Prentice Hall, New York, 1960.

31. Primary Data Processing for Douglas C-8A Program, Honeywell Aero Document R-ED-24250, Honeywell Military Products Division, March 1965, pp. 5-56 to 5-65. This document was prepared under the concept definition phase of the C-5A program and is consequently available to the Air Force.

32. Schwartz, B., Step Grain Suboptimal Filtering Applied to LORAN-Inertial Systems, Sperry Gyroscope, August 1974.

33. Light, W.R., et al., Design of a Kalman-Derived, Fixed-Gain, Hybrid Navigation System, AD 754 548, Army Electronics Command, Fort Monmouth, New Jersey, November 1972.

34. Yamamoto, G.H. and J.I. Brown, Design, Simulation, and Evaluation of the Kalman Filter Used to Align the SRAM Missile, AIAA 71-948, The Boeing Company, Seattle, Washington, August 1971.

35. Huddle, J.R., The Application of Kalman Filter Theory to the Design of an Integrated Omega-Inertial Navigation System, Litton Systems, Inc., Woodland Hills, California, October 1974.

36. Bowden, R.L., et al., Tactical TERCOM Guidance System Study (U), E-Systems, Inc., Dallas, Texas, July 1975.

37. Webber, W.F., Guidance Systems, Technical Note GS-75-1, E-Systems, Inc., Dallas, Texas, June 1975.

38. Lightweight Doppler Navigation Systems (LDNS), ETO-1201A, Kearfott Division, the Singer Company, Little Falls, New Jersey, March 1976.

39. Hevert, H.W., et al., ARPA Workshop on GPS/Missile Guidance (U), ARPA Order No. 2554, Program Code No. 5G10, R&D Associates, Santa Monica, California, January 1975.

40. Bobick, J.C. and A.E. Bryson, Sr., Improved Navigation by Combining VOR/DME Information With Air Data or Inertial Data, USAF Avionics Laboratory, Stanford University, May 1972.

41. Advanced Location Strike System Technical Manual, IBM CD No. 3-075-006, IBM Federal Systems Division, for AFSC, Aeronautical Systems Division, January 1975.

INITIAL DISTRIBUTION

Hq USAF/SAMI	1
AFIS/INTA	1
Hq TAC/DRA	1
Hq USAFE/DOO	1
Hq PACAF/DOO	1
Hq AFSC/XRLW	1
Ogden ALC/MMSM	2
ASD/ENFEA	1
ASD SD-65	1
DDC	2
AUL (AUL/LSE-70-239)	1
ADTC:	
SD-7	1
SD-15E	1
XRO	1
AFATL/DLMA	25
AFATL/DLIM	4
AFATL/DL	1
AFATL/DLOSL	9
AFATL/DLMT	1
TAWC/TRADOCLO	1
TAC/INA	1
ASD/XRP	1

(The reverse of this page is blank.)

ADTC
EGLIN AFB, FLA. 32542

OFFICIAL BUSINESS
PENALTY FOR PRIVATE USE $300

THIRD CLASS